Study Report SR474 [2024]

# Fire-safe use of timber construction II – partial timber linings

George Hare, Kevin Frank, Anna Walsh, Kai Li, Greg Baker and Colleen Wade


BRANZ
1222 Moonshine Rd, RD1, Porirua 5381
Private Bag 50 908, Porirua 5240
New Zealand
branz.nz

© BRANZ 2024
ISSN: 1179-6197

# Preface

A research project has been undertaken entitled *Fire Safe Use of Timber Construction II*. The project had two streams of work. The first part deals with the fire behaviour of exposed timber-based materials that line walls and ceilings within typical New Zealand buildings. The second part of the project deals with a number of different aspects of the performance of mass timber construction in fire:

- External Report ER67 *Pyrolysis model for mass timber: B-RISK theory* (Wade, 2021).
- External Report ER68 *Passive fire protection of cross-laminated timber* (OFR Consultants, 2020).
- Fire performance of mass timber connections, a PhD thesis by Paul Horne to be released when available.

This report presents data and analysis in support of the first part of this project addressing the use of partial coverage of internal walls and ceilings with timber linings in order to meet the performance objective of the New Zealand Building Code clause C3.4(a).

This report includes experimental data and analysis previously reported by Peel (2016) and Baker et al. (2017) as well as experiments carried out as part of this project between 2019 and 2020.

Experiments carried out as part of this project included ISO 9705 room-scale testing using products identified from a clustering analysis based on small-scale cone calorimeter test data for a variety of engineered wood products that might be used to line internal walls and ceilings in buildings.

The ability of current fire safety modelling tools (FDS and B-RISK) to accurately predict performance was also investigated.

# Acknowledgements

We would like to thank:

- BRANZ Fire Lab technicians Rik Engel, Brett Millin and Aman Kumar for supporting all the testing activities undertaken during the project
- Jon Clarke from Prestige Ceilings for the installation of the test specimens for the ISO 9705 testing
- the project advisory group – Danny Hopkin and Michael Spearpoint from OFR Consultants, Anthony Abu and Charles Fleischmann from the University of Canterbury and Hans Gerlich from Winstone Wall Boards Ltd
- BRANZ Inc for funding this research through the Building Research Levy.

# Fire-safe use of timber construction II – Partial timber linings

## BRANZ Study Report SR474


## Authors

George Hare, Kevin Frank, Anna Walsh, Kai Li, Greg Baker and Colleen Wade



## Reference

Hare, G., Frank, K., Walsh, A., Li, K., Baker, G. & Wade, C. (2024). *Fire-safe use of timber construction II – partial timber linings*. BRANZ Study Report SR474. BRANZ Ltd.



## Abstract

A variety of New Zealand made *Pinus radiata* engineered wood products were tested in a cone calorimeter to determine key combustion properties, including time to ignition and heat release rate at different incident heat fluxes as well as heat of combustion and critical heat flux.

A clustering analysis was then undertaken to group similar products based on their fire performance in small-scale testing.

A series of ISO 9705 room corner experiments were then conducted using two of the products. The results of these experiments were combined with previous experimental data gathered by others and were then used to determine the limiting factors influencing their contribution to fire growth in compartments where timber linings are used for partial coverage of the internal surfaces.



## Keywords

Engineered wood products, timber, partial linings, fire hazard, fire growth, compartment fire dynamics, reaction to fire, Material Group Number, heat release rate.

# Contents

# Figures

# Tables

# Executive summary

A variety of engineered wood products (EWPs) manufactured from New Zealand grown *Pinus radiata* were tested in a cone calorimeter to determine key combustion properties, including heat release rate at different incident heat fluxes, heat of combustion and critical heat flux.

A clustering analysis was undertaken grouping the products into a thermally thick group and a thermally thin group.

A series of ISO 9705 room corner experiments were then conducted using 9 mm and 18 mm MDF taken from each of the thermally thin and thick groups respectively. The results of these experiments were then combined with previous and similar datasets collected by Peel (2016) and Baker et al. (2017), and these were then used to determine the limiting factors to achieve the equivalent of a Material Group 2 or better in a partially lined compartment.

EWP type and thickness were not found to be major contributors to product performance. Coverage area was found to be the most important factor. With coverage of less than 37% of the room surfaces, equivalent to Material Group 1 or 2 performance could be achieved.

Further to the experimental work, modelling was undertaken using both FDS and B-RISK to determine if such models could be used to predict the performance of particular materials and lining configurations.

FDS was found to be unsuitable for modelling this type of scenario without further work. B-RISK was found to be able to predict performance reasonably well and was conservative. However, where deviations occurred, some tuning of the minimum temperature for flame spread was required to achieve this.

A risk model based on fuel area and location in the compartment, initially developed by Baker et al. (2017), was also updated with the new data and applied. This was carried out to see if the performance of different configurations could be predicted.

The updated risk model was able to reasonably predict the performance of different configurations. Risk scores between 1.5 and 3.0 were predicted for those configurations with equivalent Material Group 3 performance and risk scores below 1.37 for equivalent Material Groups 1 and 2. The model was less selective with the equivalent Material Group 1 and 2 configurations, with three configurations predicted to perform at Material Group 1, which experimentally resulted in an equivalent to Material Group 2 performance.

Further work is required to validate results at larger scale before the methods described in this report can be recommended for demonstrating compliance.

# 1. Introduction

## 1.1 Research objective

This report forms part of the outputs from the BRANZ research project QR01810 *Fire Safe Use of Timber Construction II*. This project addresses several areas of research around the fire performance of timber used in construction, including:

- protection of mass timber structures
- performance of unprotected mass timber joints
- reaction to fire behaviour of partial internal timber linings.

This report deals exclusively with the topic of reaction to fire behaviour of surface timber linings and details a series of associated experiments and modelling. This research on current reaction to fire behaviour of timber surface linings builds upon previous research conducted at BRANZ (Baker et al.) and the University of Canterbury (Peel, 2016).

Reaction to fire properties of internal surface linings are regulated to ensure that surface spread of flame across combustible surfaces and the associated heat release does not unduly contribute to unacceptable fire safety outcomes. Clause 3.4(a) of the New Zealand Building Code (NZBC) (New Zealand Government, 2023) specifies requirements that allow (or not) the use of exposed combustible materials on walls and ceilings in different occupancies and locations within buildings, but these only consider full linings of a single material. There is currently little flexibility to mix materials with different performance levels or to propose alternative strategies to demonstrate safety. The project has developed a methodology for evaluating the impact of varying amounts of exposed wood surface linings to demonstrate NZBC compliance. The methodology will have application to performance-based design and will assist the Ministry of Business, Innovation and Employment (MBIE) in evaluating potential changes to Acceptable Solutions for the use of exposed wood surfaces in buildings.

The specific objective of the research described in this report is to develop a methodology for analysing varying amounts of exposed wood surface linings so as to demonstrate NZBC compliance.

## 1.2 Current reaction to fire provisions

A number of fires internationally (BBC News, 2015; The Telegraph, 2015; Grosshandler et al., 2005) have highlighted the risk of combustible surface finishes within public spaces where a large number of people are gathered without supervision and are unfamiliar with the building and its escape routes. These fires resulted in a significant number of fatalities, and the incidents highlight the importance of using appropriate materials for surface finishes.

The C clauses in the NZBC, including clause C3.4, were amended in 2012 to set a clear quantifiable measure of performance for the fire reaction of materials in buildings. Combustible materials used for surface linings needed to be restricted in buildings where there is risk to occupants due to mobility, the number of people and familiarity with the building and its fire exits. The reaction to fire restriction on surface finishes is important for the safe use of buildings. The NZBC is a performance-based building code. However, the fire behaviour of different materials used for surface finishes cannot be easily quantified.

Clause C3 of the NZBC relates to fire affecting areas beyond the fire source. Clause C3.4 is a performance clause within clause C3, and it prescribes the fire performance of materials that can be used on walls, ceilings and floors. Fire properties of internal surface linings for walls and ceilings are characterised using the Material Group Numbers depending on their location in the building as summarised in Figure 1 (DBH, 2012, p. 4).

| **Area of *building*** | **Performance determined under conditions described in ISO 9705: 1993** | |
|---|---|---|
| | ***Buildings* not protected with an automatic *fire* sprinkler system** | ***Buildings* protected with an automatic *fire* sprinkler system** |
| Wall/ceiling materials in sleeping areas where care or detention is provided | Material Group Number 1-S | Material Group Number 1 or 2 |
| Wall/ceiling materials in exitways | Material Group Number 1-S | Material Group Number 1 or 2 |
| Wall/ceiling materials in all *occupied spaces* in importance level 4 *buildings* | Material Group Number 1-S | Material Group Number 1 or 2 |
| Internal surfaces of ducts for *HVAC systems* | Material Group Number 1-S | Material Group Number 1 or 2 |
| Ceiling materials in crowd and sleeping uses except *household units* and where care or detention is provided | Material Group Number 1-S or 2-S | Material Group Number 1 or 2 |
| Wall materials in crowd and sleeping uses except *household units* and where care or detention is provided | Material Group Number 1-S or 2-S | Material Group Number 1, 2, or 3 |
| Wall/ceiling materials in occupied spaces in all other locations in *buildings*, including *household units* | Material Group Number 1, 2, or 3 | Material Group Number 1, 2, or 3 |
| External surfaces of ducts for *HVAC systems* | Material Group Number 1, 2, or 3 | Material Group Number 1, 2, or 3 |
| Acoustic treatment and pipe insulation within airhandling plenums in sleeping uses | Material Group Number 1, 2, or 3 | Material Group Number 1, 2, or 3 |

**Figure 1. Group Number performance requirements for NZBC clause C3.4(a).**

Currently, the use of exposed timber linings (typically a Group 3 material) is not permitted (unless fire-retardant treated) in those parts of unsprinklered buildings defined as crowd activity spaces, exitways and some sleeping uses. The definition of crowd activity (Risk Group CA) includes a wide range of occupancies, including shops, malls, libraries, public halls, cinemas, cafés, bars, restaurants and similar (MBIE, 2019). In these spaces, a minimum Group 2 specification is required under NZBC clause C3.4(a). Exceptions to this exist for timber joinery, trim, heavy structural timber members and small areas of non-conforming product (<5 m² in area). If fire sprinklers are installed, exposed timber may be used on walls only in crowd and most sleeping uses, but this is not extended to exitways and higher-risk sleeping uses (such as hospitals and aged care).

Architects and specifiers have found the requirements provide little flexibility and are especially quite restrictive for small spaces meeting the crowd definition. There is a

need for more experimental data to be gathered and investigations to be undertaken to support a more flexible approach to specifying linings. An engineering approach would better account for the potential impact that high ceilings and the amount and location of combustible material within the space have on the rate at which untenable conditions develop.

The current NZBC requirements comprise a significant impediment to the use of exposed timber in buildings. They do not encourage innovation or flexibility to use timber without fire-retardant treatment or installation of sprinklers. For environmental reasons, the unnecessary use of fire-retardant chemicals should be avoided. However, it is also essential that any engineering or calculation approach be well founded and be supported by experimental data and that this results in buildings that are safe in the event of fire.

### 1.2.1 Material Group Numbers

Material Group Numbers provide a way to categorise materials by their fire performance. Appendix A of Verification Method C/VM2, Appendix A (MBIE, 2017a) sets out the methods for assigning these Material Group Numbers, including testing to either ISO 9705 (ISO, 1993) or ISO 5660-1 (ISO, 2015).

For materials tested to ISO 9705, Group Numbers are determined as follows:

- Group Number 1 – material has a heat release rate not greater than 1 MW following exposure to 100 kW for 10 minutes then 300 kW for a further 10 minutes.
- Group Number 1-S – as per Group Number 1 and the average smoke production rate of the period 0–20 minutes is not greater than 5.0 m²/s.
- Group Number 2 – material has a heat release rate not greater than 1 MW following exposure to 100 kW for 10 minutes.
- Group Number 2-S – as per Group Number 2 and the average smoke production rate of the period 0–20 minutes is not greater than 5.0 m²/s.
- Group Number 3 – material has a heat release rate not greater than 1 MW following exposure to 100 kW for 2 minutes.
- Group Number 4 – material has a heat release rate greater than 1 MW following exposure to 100 kW for 2 minutes.

The rate of heat release determined when tested to ISO 9705 includes the contribution from both the internal lining and the exposure source, i.e. the gas burner.

## 1.3 Earlier reaction to fire provisions

Prior to 2012, the NZBC C clauses for protection from fire had performance objectives for fire safety of surface finishes. This meant that any test method or fire engineering approach was allowed in order to determine the fire properties of surface finishes and AS 1530.3 was cited in Acceptable Solution C/AS1 as the main method for meeting the performance requirements. In addition, at the time, Acceptable Solution C/AS1 provided an exemption for the requirements for wall finishes where sprinklers were provided (DBH, 2011). During the 2009 Building Code Review, it was noted that the fire safety performance requirements were not well defined and allowed too much flexibility. This resulted in situations where combustible materials were being used as surface finishes in high-risk areas.

As a result, in 2012, prescriptive requirements for surface finishes were introduced through the addition of Material Group Numbers to NZBC clause C3. At the same time, a change was made to the test method with the introduction of ISO 9705.

After these changes came into effect, stakeholders raised significant concerns that the requirements for internal surface finishes were at Code level and that alternative tests or fire engineering methods were no longer able to be applied. There was also a supply issue due to a lack of material tested to the new standards. This was especially problematic for existing buildings applying the as near as reasonably practicable (ANARP) test to material tested under a different standard. However, in the last few years, products have come to market that allow treated timber to achieve a Group 1-S rating.

The timber industry was particularly affected by the change. An unintended effect of the changes was a restriction on the use of exposed timber within all buildings open to the public. The changes also effectively ruled out applying an alternative fire engineering methodology to assess buildings according to risk.

## 1.4 Proposed amendments to NZBC clause C3.4

In March 2015, two determinations were issued by MBIE that permitted the use of timber linings in small crowd use buildings. In each case, additional measures were applied to mitigate the risk posed by the use of a Group 3 material rather than the Group 2 required by clause C3.4(a) (MBIE, 2015a, 2015b). This again highlighted the issue of having quantitative regulatory settings for combustible surface finishes at Code level.

In July 2015, MBIE launched the Fire Programme, which sought to define adjustments to the consenting system to provide an effectively functioning fire regulatory system. One of the projects under the Fire Programme was a review of the fire safety requirements for surface finishes.

In May 2017, MBIE published a proposal for changes to NZBC clause 3.4 regarding internal surface finishes (MBIE, 2017b). At Code level, the proposed changes included removing the current version of clauses 3.4(a), (b) and (c) and replacing them with qualitative performance requirements for internal surface finishes, flooring and suspended fabrics. In Acceptable Solutions C/AS2–C/AS7 (now just C/AS2) and Verification Method C/VM2, changes included:

- defining a new term 'internal surface finishes' to reduce the current ambiguity of application
- defining a new term 'place of assembly', to refine the level of risk in public spaces
- updating the requirements for the maximum permitted Group Numbers for walls and ceilings with the new term 'place of assembly'
- defining a new table for requirements for pipes and ducts, separate to internal surface finishes
- rewriting the design scenario (IS) for internal surface finishes in C/VM2, creating a fire engineering method for assessment of the contribution of internal surface finishes.

This approach would provide the intent of the 2012 changes while providing flexibility for smaller buildings and allowed for Alternative Solution designs, commensurate with the level of risk.

### 1.4.1 Proposed new definition for internal surface finishes

The MBIE proposal for changes to clause C3.4 regarding internal surface finishes included a new definition for internal surface finishes. One aspect of this proposed new definition was to permit up to 25% of the total wall area to consist of exposed structural timber building elements (solid timber, glulam, laminated veneer lumber).

### 1.4.2 Proposed new definition for place of assembly

The MBIE proposal for changes to clause C3.4 regarding internal surface finishes also included a new definition for place of assembly to replace the current term 'crowd'. It was defined as "occupied spaces where people gather for a common activity, interest or purpose where escape routes are likely to be unfamiliar to the occupants".

The change in definition was proposed to refine the CA risk group profile to reflect the risk of exposure to fire and the vulnerability of this risk group. The term 'crowd' and its current application classifies a small hairdressing salon in the same risk profile as a large sporting arena.

### 1.4.3 Proposed calculation method for IS scenario in C/VM2

MBIE also proposed that a fire engineering design method be provided to allow Group Number 3 materials to be used as internal surface linings in all buildings that included storage with a stack height of less than 3.0 m but excluding exitways, household units, marae buildings or sleeping spaces where care or detention is provided and car parks with stacking systems. Specifically, MBIE proposed that the current C/VM2 Design scenario (IS) *Rapid fire spread involving internal surface linings* have a calculation option in addition to the current tabulated values method, as detailed in Figure 1. The design fire characteristics for this proposed calculation method included a proposed fire growth rate of $0.188t^2$ – i.e. an ultra-fast t-squared fire compared to the fast t-squared fire ($0.0469t^2$) that C/VM2 currently stipulates for all buildings including storage with a stack height of less than 3.0 m. The choice of the ultra-fast fire growth rate is intended to simulate the influence of wall linings contributing to fire growth in addition to the combustible contents of a compartment that are simulated by a fast t-squared fire growth rate.

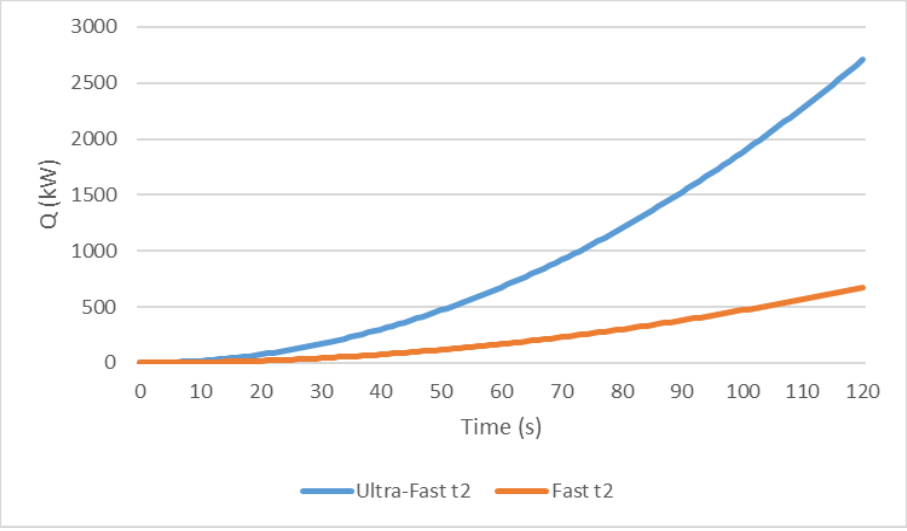


**Figure 2. Ultra-fast vs fast t-squared growth comparison.**

As can be seen from

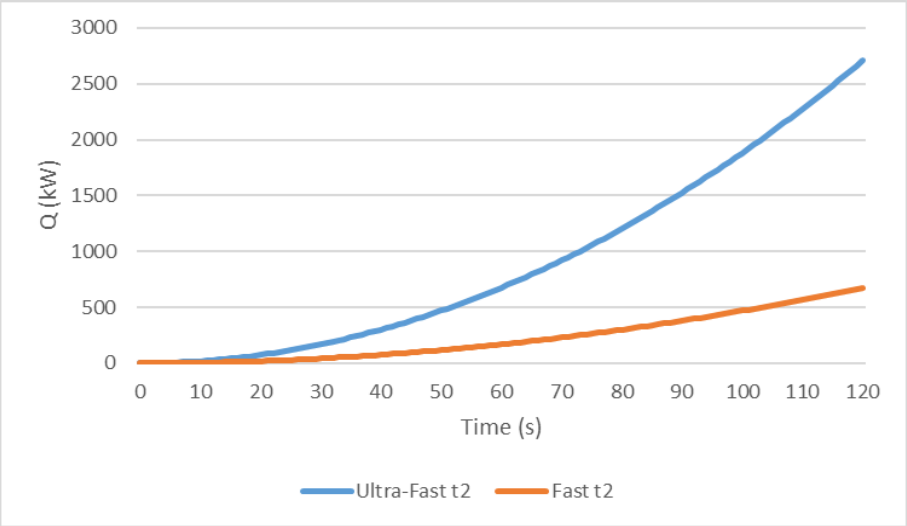


Figure 2, the boundary between a Group 3 and a Group 4 material is 120 s. A fast ($0.0469t^2$) growth rate does not exceed the 1 MW threshold within the 120 s, whereas the ultra-fast ($0.188t^2$) growth rate exceeds this threshold at 73 s. At 120 s, the fire size is more than 2 MW greater than a fast $t^2$ fire.

In the explanation given, MBIE stated:

> At present, there is not enough research to provide an accurate assessment of fire spread on internal surface finishes. In the meantime, as a conservative assumption, a faster fire growth (i.e. ultra-fast fire) simulates the influence of wall linings contributing to fire growth. (MBIE, 2017b, p. 32)

Changes in priority resulted in the proposed changes not progressing further. However, MBIE has indicated that it is still a goal to dequantify the NZBC where possible, and this research is intended to fill some of the gaps identified in the MBIE proposal document.

# 2. Prior research

## 2.1 Peel

In 2015 and 2016, a University of Canterbury postgraduate research project investigated fire development over combustible linings (Peel, 2016; Peel et al. 2016). The research consisted of a series of cone calorimeter experiments that generated input data for subsequent combustible surface lining modelling in B-RISK plus a series of ISO 9705 room experiments to validate the B-RISK output predictions against.

### 2.1.1 Cone testing

Peel conducted a series of cone calorimeter experiments where three replicates of 7 mm thick 3-ply untreated D-grade plywood were subjected to five different levels of heat flux exposure, namely 20, 30, 40, 50 and 60 kW/m². The average density of the plywood specimens was 521 kg/ m³ (range 493–545 kg/m³) after conditioning to a constant mass at 23 ±2°C with relative humidity 50 ±5% in accordance with ISO 5660-1. A substrate of 15 mm calcium silicate board was used for all experiments corresponding to the lining that would be used for the subsequent ISO 9705 room experiments (see section 2.1.2). The sample and substrate for each experiment was covered on the bottom and sides with aluminium foil and positioned so that the top face was 25 mm from below the cone element. The cone calorimeter experiments were generally conducted in accordance with ISO 5660-1 in the horizontal orientation and the piloted-ignition mode, with the spark igniter approximately 13 mm above the specimen surface. For each experiment, the time to ignition, $t_{ig}$, was recorded along with specimen mass loss rate. Heat release rate (HRR) data was calculated using the principle of oxygen consumption calorimetry.

#### 2.1.1.1 Time-to-ignition data

The time-to-ignition data recorded by Peel in the 15 cone calorimeter experiments is summarised in Table 1.

**Table 1. Peel's time-to-ignition data from cone calorimeter experiments.**

| Test | Heat flux (kW/m²) | Time to ignition (s) | Mean (s) | Standard deviation (s) |
|---|---|---|---|---|
| 1 | 20 | 366 | 288 | 70 |
| 2 | | 197 | | |
| 3 | | 301 | | |
| 4 | 30 | 66 | 76 | 8 |
| 5 | | 84 | | |
| 6 | | 79 | | |
| 7 | 40 | 33 | 38 | 9 |
| 8 | | 50 | | |
| 9 | | 30 | | |
| 10 | 50 | 18 | 21 | 2 |
| 11 | | 22 | | |
| 12 | | 22 | | |
| 13 | 60 | 14 | 11 | 2 |
| 14 | | 10 | | |
| 15 | | 10 | | |

Peel also used the time-to-ignition data to determine the flux time product (FTP) (Shields et al.; Silcock & Shields, 1995).

The FTP method involves plotting transformed time versus irradiance, in the form of Eqn. 2-1.

$$\dot{q}''_{inc} = \left(FTP/t_{ig}\right)^{1/n} + \dot{q}''_{cr} \qquad \textbf{Eqn. 2-1}$$

Where:

$\dot{q}''_{inc}$ cone calorimeter irradiance (kW/m²)

$FTP$ flux time product value for material (kW$^n$s)

$t_{ig}$ time to ignition (s)

$n$ flux time product index which reflects the thermal thickness of the material

$\dot{q}''_{cr}$ critical irradiance (kW/m²).

The data pairs $\left(1/t_{ig}\right)^{1/n}$ vs. $\dot{q}''_{inc}$ are plotted in the generic form $y = ax + b$, and the value for the flux time product index, $n$, is varied by trial and error between 1.0 and 2.0 to give the best linear trendline fit (i.e. coefficient of determination R² closest to 1.0). Having determined the optimal value for $n$, the value for the $FTP$ parameter is then derived from the gradient of the linear trendline, and the x-axis intercept gives a value for $\dot{q}''_{cr}$.

Accordingly, Peel derived an FTP dataset for the 7 mm plywood of $\frac{1}{n} = 0.56$, $FTP = 11642$ s(kW/m²)$^{1.79}$, and $q''_{cr} = 13.1$ kW/m², as depicted in Figure 3 (Peel, 2016, p. 74).

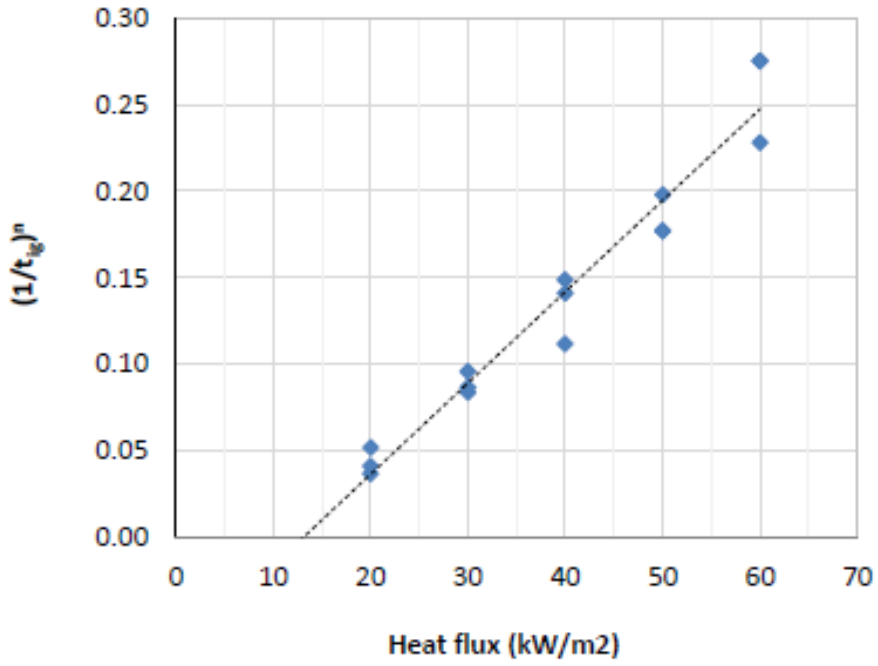


**Figure 3. FTP analysis conducted by Peel.**

#### 2.1.1.2 Heat release rate data

A summary of the HRR data collected by Peel is provided in Table 2. It should be noted that the HRRPUA data from the original source (Peel, 2016) has been adjusted for an exposure area in the standard cone calorimeter specimen holder of 94 × 94 mm².

**Table 2. Summary of Peel's 7 mm thick plywood HRR data.**

| Test | Heat flux (kW/m²) | Time to ignition (s) | HRRPUA – 1st peak (kW/m²) | Time to 1st peak after ignition (s) | HRRPUA – 2nd peak (kW/m²) | Time to 2nd peak after ignition (s) |
|---|---|---|---|---|---|---|
| 1 | 20 | 366 | 123 | 28 | 79 | 248 |
| 2 | | 197 | 124 | 31 | 88 | 267 |
| 3 | | 301 | 142 | 35 | 164 | 174 |
| 4 | 30 | 66 | 145 | 50 | 140 | 238 |
| 5 | | 84 | 137 | 36 | 128 | 265 |
| 6 | | 79 | 137 | 49 | 95 | 171 |
| 7 | 40 | 33 | 196 | 14 | 196 | 170 |
| 8 | | 50 | 187 | 15 | 172 | 135 |
| 9 | | 30 | 179 | 13 | 169 | 152 |
| 10 | 50 | 18 | 190 | 15 | 287 | 142 |
| 11 | | 22 | 212 | 12 | 190 | 176 |
| 12 | | 22 | 196 | 43 | 230 | 177 |
| 13 | 60 | 14 | 217 | 15 | 250 | 134 |
| 14 | | 10 | 213 | 17 | 302 | 129 |
| 15 | | 10 | 201 | 63 | 302 | 165 |

In Figure 4, a graph of the HRRPUA data for each of the three replicate experiments, at each of the five heat flux settings is provided. It should be noted that the time to ignition for each experiment has been set as $t = 0$ s to facilitate the comparison between both the replicates and the different heat fluxes.

In addition, in Figure 4, Peel's 'raw' data from Table 2 has been smoothed to eliminate some of the fluctuations by averaging the three adjacent values at the i$^{th}$ time step as follows:

$$Q_{i,Sm} = \frac{Q_{i-1} + Q_i + Q_{i+1}}{3}$$

As a consequence of the smoothing, the data presented in Table 2 does not visually match what is presented in Figure 4.

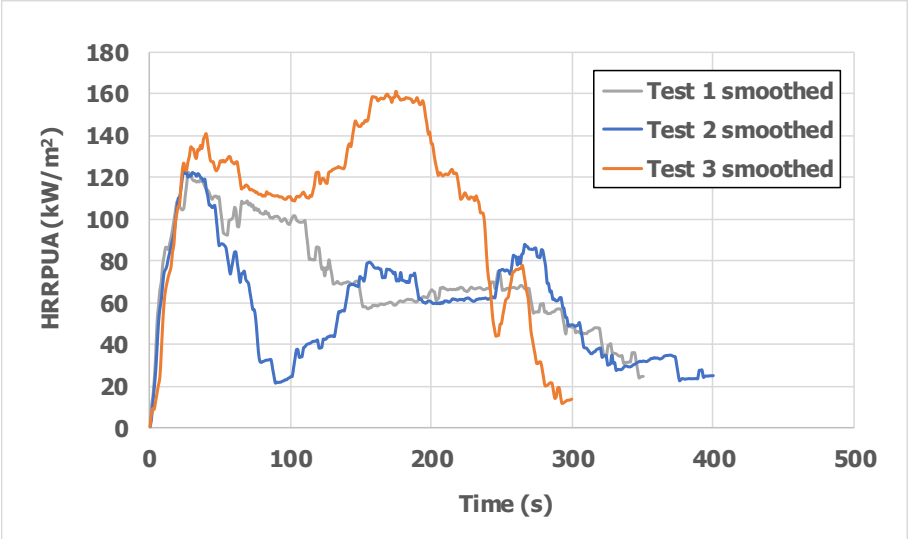


**(a) 20 kW/m²**

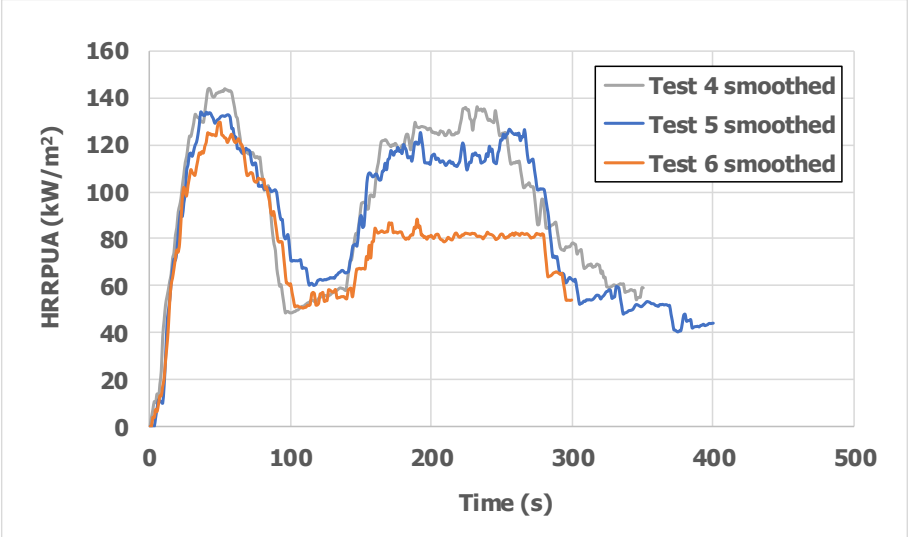


**(b) 30 kW/m²**

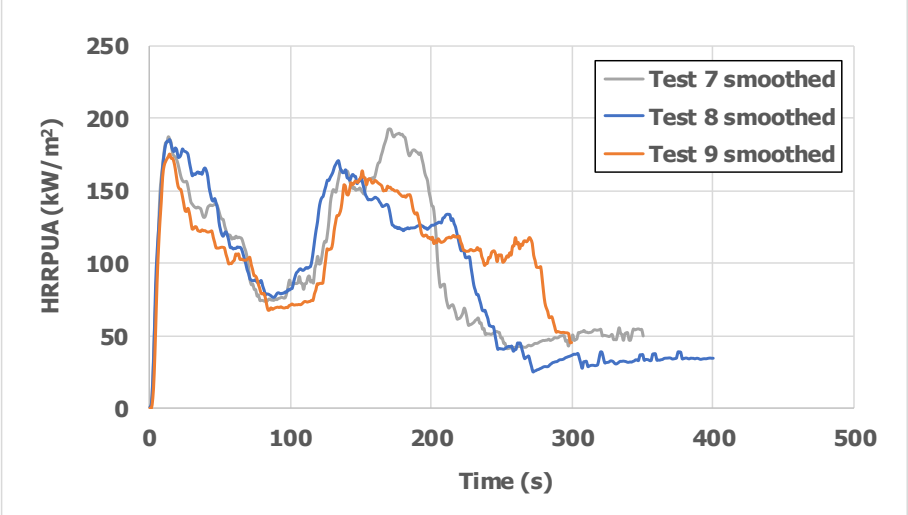


**(c) 40 kW/m²**

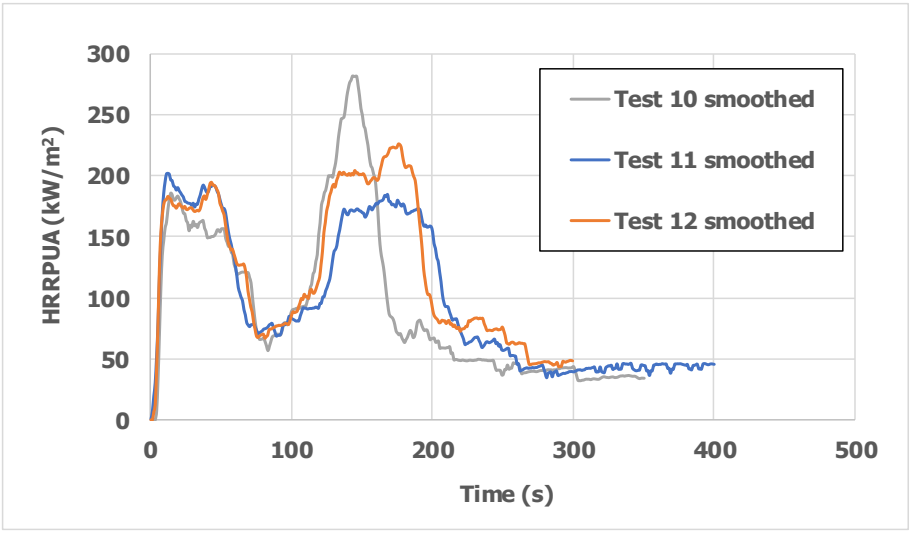


**(d) 50 kW/m²**

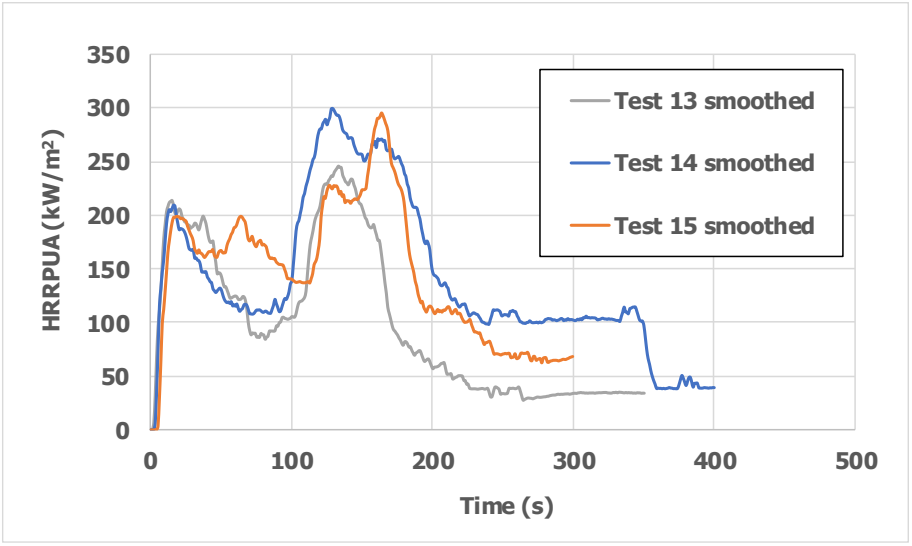


**(e) 60 kW/m²**

**Figure 4. HRRPUA curves.**

#### 2.1.1.3 Mass loss data

Peel also collected mass loss data, which was used as the basis to derive the effective heat of combustion as the sum of the heat released at each time step over the test duration divided by the overall mass loss over the test duration. This data is summarised in Table 3.

**Table 3. Peel's effective heat of combustion data.**

| Test | Heat flux (kW/m²) | Density (kg/m³) | Effective heat of combustion (MJ/kg) | Average (MJ/kg) | Standard deviation (MJ/kg) |
|---|---|---|---|---|---|
| 1 | 20 | 545.2 | 9.75 | 10.16 | 0.37 |
| 2 | | 493.3 | 10.08 | | |
| 3 | | 531.0 | 10.65 | | |
| 4 | 30 | 526.3 | 12.47 | 12.02 | 2.11 |
| 5 | | 530.0 | 14.35 | | |
| 6 | | 496.4 | 9.23 | | |
| 7 | 40 | 519.3 | 13.34 | 12.95 | 0.28 |
| 8 | | 535.5 | 12.82 | | |
| 9 | | 545.3 | 12.7 | | |
| 10 | 50 | 497.0 | 12.76 | 14.21 | 1.50 |
| 11 | | 514.5 | 13.6 | | |
| 12 | | 519.3 | 16.28 | | |
| 13 | 60 | 518.6 | 13.54 | 16.32 | 1.97 |
| 14 | | 504.5 | 17.48 | | |
| 15 | | 537.8 | 17.93 | | |

### 2.1.2 ISO 9705 room-scale testing

Peel conducted a series of seven ISO 9705 room experiments where the walls and ceiling of the test enclosure were partially lined in seven different configurations with 7 mm thick non-fire retarded plywood directly fixed to 15 mm thick calcium silicate board.

The seven different configurations were as follows:

- Experiment 1 – plywood to ceiling and three wall – standard lining configuration.
- Experiment 2 – plywood to ceiling only.
- Experiment 3 – plywood to lower half of walls extending 3.6 m in both directions from the burner corner, no plywood on ceiling.
- Experiment 4 – plywood to upper half of walls extending 3.6 m in both directions from the burner corner, no plywood on ceiling.
- Experiment 5 – plywood full height of walls extending 2.4 m in both directions from burner corner, no plywood on ceiling.
- Experiment 6 – plywood full height of walls extending 3.6 m in both directions from burner corner, no plywood on ceiling.
- Experiment 7 – plywood full height of walls extending 1.2 m in both directions from burner corner, plywood on ceiling.

The experimental configurations are summarised in Table 4, with the areas of lining material classified as lower wall below 1.2 m height (L), upper wall above 1.2 m height (U) and ceiling (C).

**Table 4. Peel's ISO 9705 room lining configurations.**

| Experiment | Location of timber wall linings | Ceiling linings | Ply thickness (mm) | Burner location | Lower wall L ($m^2$) | Upper wall U ($m^2$) | Ceiling C ($m^2$) | (Nominal) total ply area ($m^2$) |
|---|---|---|---|---|---|---|---|---|
| 1 | 3 walls (standard ISO 9705 room configuration) | Fully lined | 7 | Corner | 11.5 | 11.5 | 8.6 | 31.7 |
| 2 | None | Fully lined | 7 | Corner | - | - | 8.6 | 8.6 |
| 3 | Lower half of walls extending 3.6 m from burner corner | None | 7 | Corner | 8.6 | - | - | 8.6 |
| 4 | Upper half of walls extending 3.6 from burner corner | None | 7 | Corner | - | 8.6 | - | 8.6 |
| 5 | Full height of walls extending 2.4 m from burner corner | None | 7 | Corner | 5.8 | 5.8 | - | 11.5 |
| 6 | Full height of walls extending 3.6 m from burner corner | None | 7 | Corner | 8.6 | 8.6 | - | 17.3 |
| 7 | Full height of walls extending 1.2 m from burner corner | Fully lined | 7 | Corner | 2.9 | 2.9 | 8.6 | 14.4 |

#### 2.1.2.1 Experimental results

In accordance with the standard ISO 9705 room test procedure, a propane gas burner was placed in the corner of the enclosure against the surface of the combustible lining material, and the plywood lining was exposed to a burner with 100 kW output for 600 s and then 300 kW for a further 600 s.

Heat release rate and gas temperature measurements were collected during the experiments. Photographs were taken during each experiment to determine the flame spread rate.

Figure 5 shows the HRR curve for each of the seven plywood configurations. In some of the experiments, the gas flow to the burner was terminated prematurely, which is reflected in the duration of the HRR curve depicted in Figure 5.

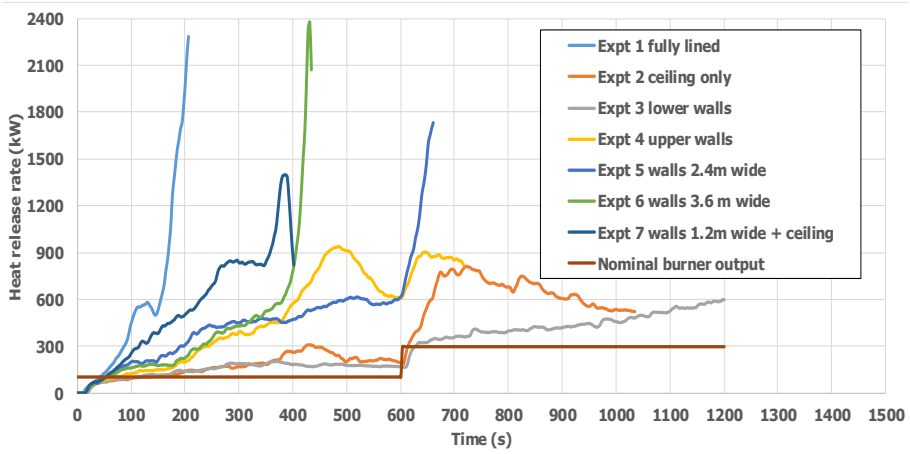


**Figure 5. HRR curves from seven lining configurations.**

#### 2.1.2.2 Ranking of results

The threshold for classification of materials is a combined (material plus burner) HRR of 1 MW, which is deemed to be the HRR at flashover in the ISO 9705 test method. Based on the data for Experiment 1 shown in Figure 5, the 7 mm thick plywood that was tested by Peel is classified as Material Group 3 with a time to exceed the flashover criterion of $120 < t_{fo} < 600$ s (see section 1.2.1).

The relative performance of the different configurations can be assessed both by ranking the time to reach the flashover criterion or the peak HRR (where the flashover criterion was not reached) and by using the $FIGRA_{RC}$ method. The $FIGRA_{RC}$ parameter (Sundström, 2007) is calculated as either the flashover criterion HRR (i.e. 1,000 kW) or the peak HRR (whichever is the least) less the burner contribution divided by the time at that point:

$$FIGRA_{RC} = \frac{1000 - Q_{burner}}{t_{fo}} \text{ or } FIGRA_{RC} = \frac{Q_{peak} - Q_{burner}}{t_{peak}} \qquad \textbf{Eqn. 2-2}$$

Table 5 provides a summary of the ranking the seven experiments conducted by Peel using both the time to flashover/peak and the $FIGRA_{RC}$ method.

**Table 5. Ranking of experiments.**

| Expt | Flashover (Y/N) | Time to flashover, $t_{fo}$ (s) | Peak HRR, $Q_{peak}$ (kW) | Time to peak, $t_{peak}$ (s) | $Rank_{peak}$ | $Q_{burner}$ (kW) | $FIGRA_{RC}$ (kW/s) | $Rank_{FIGRA}$ |
|---|---|---|---|---|---|---|---|---|
| 1 | Y | 172 | - | - | 1 | 100 | 5.2 | 1 |
| 2 | N | - | 809 | 723 | 6 | 300 | 0.7 | 6 |
| 3 | N | - | 600 | 1,197 | 7 | 300 | 0.3 | 7 |
| 4 | N | - | 942 | 486 | 4 | 100 | 1.7 | 4 |
| 5 | Y | 627 | - | - | 5 | 300 | 1.1 | 5 |
| 6 | Y | 410 | - | - | 3 | 100 | 2.2 | 3 |
| 7 | Y | 366 | - | - | 2 | 100 | 2.5 | 2 |

It should be noted that Peel reversed the ranking for Experiment 4 and 5 shown in Table 5 (shaded grey) by ranking Experiment 5 higher than Experiment 4 since Experiment 5 reached the flashover criterion and Experiment 4 did not. In Table 5, however, Experiment 4 is ranked above Experiment 5 since Experiment 4 reached its peak HRR prior to Experiment 5 reaching the flashover criterion.

### 2.1.3 B-RISK modelling

In addition to experiments, Peel also used B-RISK (Wade, 2000) to predict the HRR where varying quantities of combustible surface linings were present. However, in the context of this present research, the standard functionality of the B-RISK combustible linings fire growth submodel is for a compartment that is fully lined with combustible material.

#### 2.1.3.1 Overview of combustible linings fire growth submodel in B-RISK

B-RISK predicts ignition, flame spread and the resultant heat released by combustible wall and ceiling materials. Two modes of flame spread are considered:

- Upward flame spread includes flame spread up the walls, beneath the ceiling and along the wall/ceiling intersection on the wall in the region of the ceiling jet.
- Opposed flame spread includes lateral flame spread on the wall originating at the burner location and downward spread on the wall from the ceiling jet region.

The burner width for the standard ISO 9705 propane burner is $b_w = 0.17$ m. When the burner is located in the room corner, the height of the burner flame, $L$, is determined from the correlation $l = 5.9 b_w \sqrt{Q^*}$, where $Q^* = \dot{Q}_b \Big/ 1110 b_w^{5/2}$ and $\dot{Q}_b$ is the heat output from the burner.

There are two cases to consider when determining the pyrolysis area, $A_p$. For the first case, shown in Figure 6, the wall adjacent to the burner has ignited and is pyrolysing, while the pyrolysis front has not yet reached the ceiling.

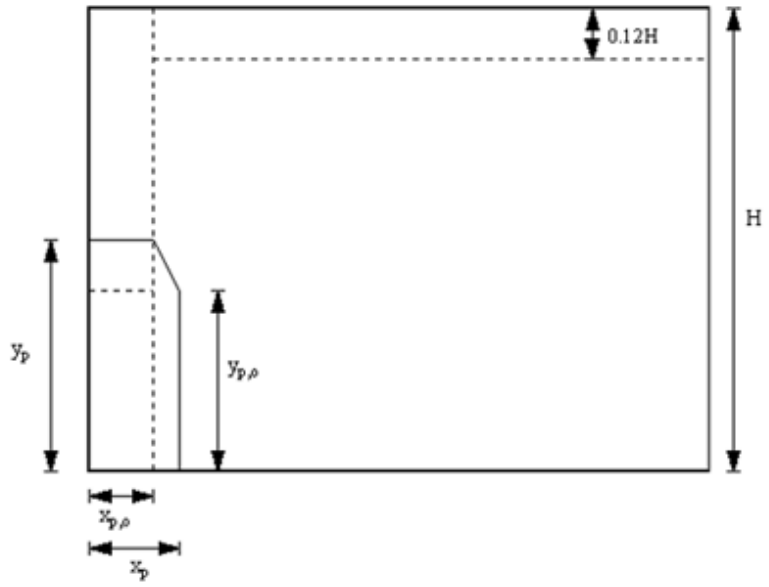


**Figure 6. Compartment cross-section showing pyrolysis area calculation – wall ignited but pyrolysis front has not reached ceiling.**

The region initially adjacent to the burner is defined by the dimensions $x_{p,o}$ and $y_{p,o}$ with initial values of $b_w$ and $0.4L$ respectively. The pyrolysis area in this case is given by $A_p = 2\left[y_p x_{p,o} + \left(x_p - x_{p,o}\right)y_{p,o} + 0.5(y_p - y_{p,o})(x_p - x_{p,o})\right]$.

The second case is shown in Figure 7 where the wall area adjacent to the burner has ignited and is pyrolysing and the pyrolysis front has reached the ceiling.

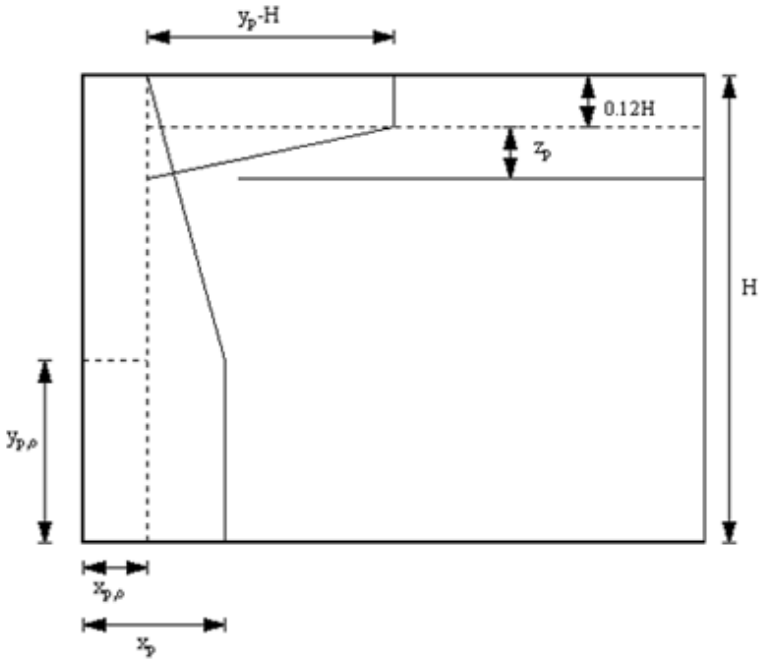


**Figure 7. Compartment cross-section showing pyrolysis area calculation – wall ignited and pyrolysis front has reached ceiling.**

The total pyrolysis area in this case has three components – the wall area, the ceiling jet area and the ceiling area (a quarter circle where the radius extends from the corner to the edge of the circle based on the flame extension under the ceiling).

#### 2.1.3.2 Modelling partially lined enclosures

The source code for B-RISK was modified by Wade for Peel's research to allow for partial linings. Two methods were used to include the contribution from wall linings:

- Specify the maximum percentage of wall lining that could contribute to the fire with the remaining portion considered non-combustible. This is the most conservative case as all wall linings within the pyrolysis area are considered to contribute up to the maximum percentage permitted regardless of location on the wall.
- Specify a maximum coverage distance from the burner in the X and Y directions. These set the upper limit for $\mathrm{Xp}$ and $\mathrm{Yp}$ of the pyrolysis area shown in Figure 6 and Figure 7.

The contribution from the ceiling linings was calculated in the same way for both methods using the percentage coverage as an upper limit on the contribution and the remaining portion being considered non-combustible.

### 2.1.4 Results

B-RISK consistently predicted flashover earlier than the experimental results, including predicting flashover in cases where this did not happen in practice. From an engineering perspective, this is a conservative result.

Peel calculated $\mathrm{FIGRA_{RC}}$ values from the B-RISK results and, although generally higher than the experimental results, when ranked, they gave a reasonably good correlation. The main difference was that Experiment 7 (with less fuel available) had a higher $\mathrm{FIGRA_{RC}}$ value than Experiment 1 where the room was fully lined.

Layer height was consistently modelled lower than that observed in the experiments, largely attributed to the model underestimating the plume entrainment. Again, this is considered conservative as visibility and FED criteria would be exceeded earlier.

## 2.2 Baker, Wade and Frank

Following the work by Peel, further research was conducted by Baker, Wade and Frank (2017), with the aim of developing a risk model based on lining material coverage. For consistency, a similar approach was adopted from Peel – material characterisation was done using cone calorimetry testing followed by ISO 9705 room-scale testing.

### 2.2.1 Cone testing

Two material thicknesses were selected for testing, 7 mm plywood and 12 mm plywood. Although the 7 mm plywood was nominally identical to that used by Peel (untreated D-grade plywood), due to the high likelihood of material variability, it was decided to conduct a full repeat series of cone calorimeter experiments on the (new) 7 mm plywood and the corresponding full series for the 12 mm material. Three replicates of each material were subjected to the five different levels of heat flux exposure – 20, 30, 40, 50 and 60 kW/m². A substrate of 15 mm calcium silicate board was used for all experiments (corresponding to the lining that would be used for the subsequent ISO 9705 room experiments). The cone calorimeter experiments were conducted in accordance with ISO 5660-1, with each experiment running for the full 1,920 s exposure after ignition in the horizontal orientation and the piloted-ignition mode. For each experiment, the time to ignition, $t_{ig}$, was recorded along with specimen mass loss rate, and heat release rate data was generated using the principle of oxygen consumption calorimetry.

#### 2.2.1.1 Time-to-ignition data

As noted in section 2.1.1.1, Peel derived a FTP dataset for the 7 mm plywood of $\frac{1}{n} = 0.56$, $q''_{cr} = 13.1$ kW/m² and $FTP = 11642$ s(kW/m²)$^{1/0.56}$ with a coefficient of determination of $R^2 = 0.96$. Baker identified a small discrepancy in Peel's analysis of the time-to-ignition data. A reanalysis of the data indicated that the best fit for the linear regression analysis using the FTP correlation procedure occurs when $\frac{1}{n} = 0.5$, i.e. $n = 2$ rather than $\frac{1}{n} = 0.56$ as suggested by Peel. This revised analysis gives an FTP dataset of $\frac{1}{n} = 0.5$, $q''_{cr} = 11.6$ kW/m² and $FTP = 27073$ s(kW/m²)$^{1/0.5}$ with a coefficient of determination of $R^2 = 0.9623$, as depicted in Figure 8.

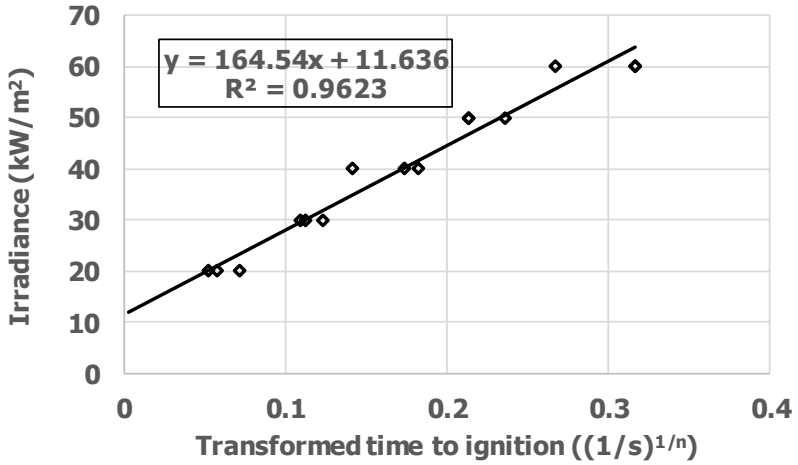


**Figure 8. Revised FTP analysis of Peel's time-to-ignition-data.**

The analysis over the full flux time product index range is shown in Table 6.

**Table 6. Complete FTP correlation analysis of Peel's data.**

| *n* | $R^2$ | $q''_{cr}$ | *FTP* |
|---|---|---|---|
| 1 | 0.8755 | 24.6 | 419 |
| 1.1 | 0.8954 | 23.2 | 625 |
| 1.2 | 0.911 | 21.9 | 936 |
| 1.3 | 0.9234 | 20.6 | 1407 |
| 1.4 | 0.9333 | 19.3 | 2123 |
| 1.5 | 0.9411 | 18 | 3215 |
| 1.6 | 0.9474 | 16.7 | 4887 |
| 1.7 | 0.9524 | 15.4 | 7456 |
| 1.8 | 0.9564 | 14.2 | 11419 |
| 1.9 | 0.9597 | 12.9 | 17550 |
| 2 | 0.9623 | 11.6 | 27073 |

It is also possible to conduct the analysis based on average time-to-ignition values, i.e. the average of the multiple values at each heat flux setting. This further analysis is presented in Figure 9 and Table 7.

A comparison of the data in Figure 8, Figure 9, Table 6 and Table 7 indicates that there is only a minimal difference when the average time-to-ignition values are used.

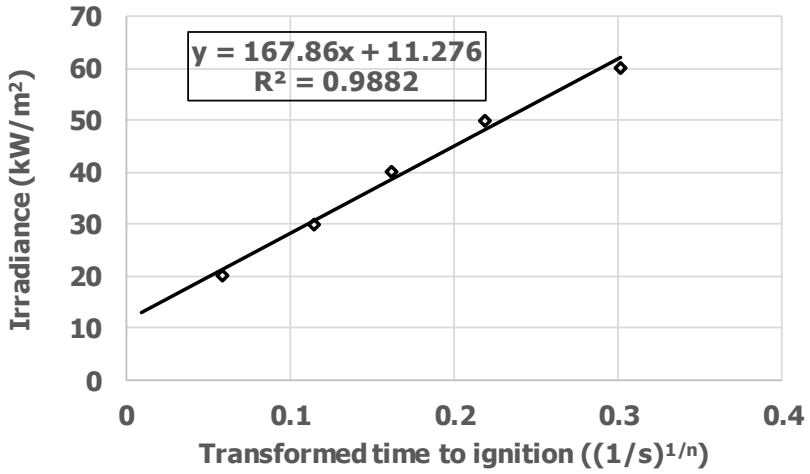


**Figure 9. Revised FTP analysis of Peel's average time-to-ignition values.**

**Table 7. FTP correlation analysis of Peel's average time-to-ignition values.**

| *n* | $R^2$ | $q''_{cr}$ | *FTP* |
|---|---|---|---|
| 1 | 0.9086 | 24.3 | 434 |
| 1.1 | 0.9266 | 22.9 | 648 |
| 1.2 | 0.941 | 21.6 | 970 |
| 1.3 | 0.9524 | 20.3 | 1458 |
| 1.4 | 0.9615 | 19 | 2200 |
| 1.5 | 0.9687 | 17.7 | 3333 |
| 1.6 | 0.9745 | 16.4 | 5069 |
| 1.7 | 0.9791 | 15.1 | 7740 |
| 1.8 | 0.9828 | 13.8 | 11862 |
| 1.9 | 0.9858 | 12.5 | 18250 |
| 2 | 0.9882 | 11.3 | 28177 |

Another important aspect to be conscious of when using the FPT correlation procedure is that the FTP dataset that is ultimately selected, in this case for modelling in B-RISK, should be physically meaningful. In this regard, it is also possible to determine an experimental minimum value at which ignition does not occur, defined as $\dot{q}''_{min}$. The cone calorimeter irradiance can be reduced, for example, in 2 kW/m² increments to determine the level at which ignition does not occur after 1,800 s exposure, with $\dot{q}''_{min}$ being calculated as the midpoint between the minimum irradiance level at which ignition did occur and the maximum value at which ignition did not occur. While $\dot{q}''_{min}$ is determined experimentally, $\dot{q}''_{cr}$ is a theoretical value at which ignition will occur after an infinite period of exposure to incident radiation. Shields et al.(1994) note that the conditions $\dot{q}''_{min} > \dot{q}''_{cr}$ should always be satisfied and that $\dot{q}''_{cr}$ should be approximately in the range $1.0 \times \dot{q}''_{min} > \dot{q}''_{cr} > 0.8 \times \dot{q}''_{min}$.

In this context, Baker et al. (2011) indicate that the value for the coefficient of determination not be the sole criteria for selecting the FTP dataset but rather the dataset selection be based on a meaningful value for $\dot{q}''_{cr}$, and that this be done by determining $\dot{q}''_{min}$ and then ensuring that an appropriate relativity for $\dot{q}''_{cr}$ is achieved.

Table 8 provides a summary of the time-to-ignition data generated by Baker et al. (2011) for the 7 mm plywood specimens. It should be noted that the numbering for the test specimens is in the format thickness-irradiance-sample number.

**Table 8. Time-to-ignition data – cone calorimeter experiments – 7 mm plywood.**

| Test number | Heat flux (kW/m²) | Time to ignition (s) | Mean (s) | Standard deviation (s) |
|---|---|---|---|---|
| 7-20-1 | 20 | 233 | 211 | 20 |
| 7-20-2 | | 217 | | |
| 7-20-3 | | 184 | | |
| 7-30-1 | 30 | 65 | 65 | 4 |
| 7-30-2 | | 70 | | |
| 7-30-3 | | 60 | | |
| 7-40-1 | 40 | 39 | 35 | 5 |
| 7-40-3 | | 38 | | |
| 7-40-4 | | 29 | | |
| 7-50-1 | 50 | 14 | 17 | 2 |
| 7-50-2 | | 18 | | |
| 7-50-3 | | 18 | | |
| 7-60-1 | 60 | 14 | 16<br>13* | 5<br>2* |
| 7-60-2 | | 11 | | |
| 7-60-3 | | 23* | | |

* 23 s is a longer time to ignition than any other replicate at 50 or 60 kW/m² and is therefore likely an outlier. Removing the outlier reduces the mean time to ignition to 12.5 s and the standard deviation to 1.5 s.

Table 9 provides the time-to-ignition data for the 12 mm plywood cone testing.

**Table 9. Time-to-ignition data – cone calorimeter experiments – 12 mm plywood.**

| Test number | Heat flux (kW/m²) | Time to ignition (s) | Mean (s) | Standard deviation (s) |
|---|---|---|---|---|
| 12-20-1 | 20 | 519* | 318<br>218* | 141<br>6* |
| 12-20-2 | | 212 | | |
| 12-20-3 | | 224 | | |
| 12-30-1 | 30 | 55 | 65 | 8 |
| 12-30-2 | | 74 | | |
| 12-30-3 | | 65 | | |
| 12-40-3 | 40 | 29 | 29 | 2 |
| 12-40-4 | | 26 | | |
| 12-40-5 | | 31 | | |
| 12-50-1 | 50 | 12 | 12 | 1 |
| 12-50-2 | | 11 | | |
| 12-50-3 | | 13 | | |
| 12-60-1 | 60 | 10 | 9 | 1 |
| 12-60-2 | | 8 | | |
| 12-60-3 | | 10 | | |

* 519 s is significantly longer than any other replicate. This would indicate it is either an outlier, or more replicates are required to gain a better understanding of the likely distribution. With it removed as an outlier, the mean is significantly reduced to 218 s and standard deviation to 6 s.

#### 2.2.1.2 FTP analysis

An FTP correlation analysis was carried out. For both plywood thicknesses, the linear regression analysis procedure gave a best fit for an FTP index value of $n = 2.0$, which is depicted in Figure 10.

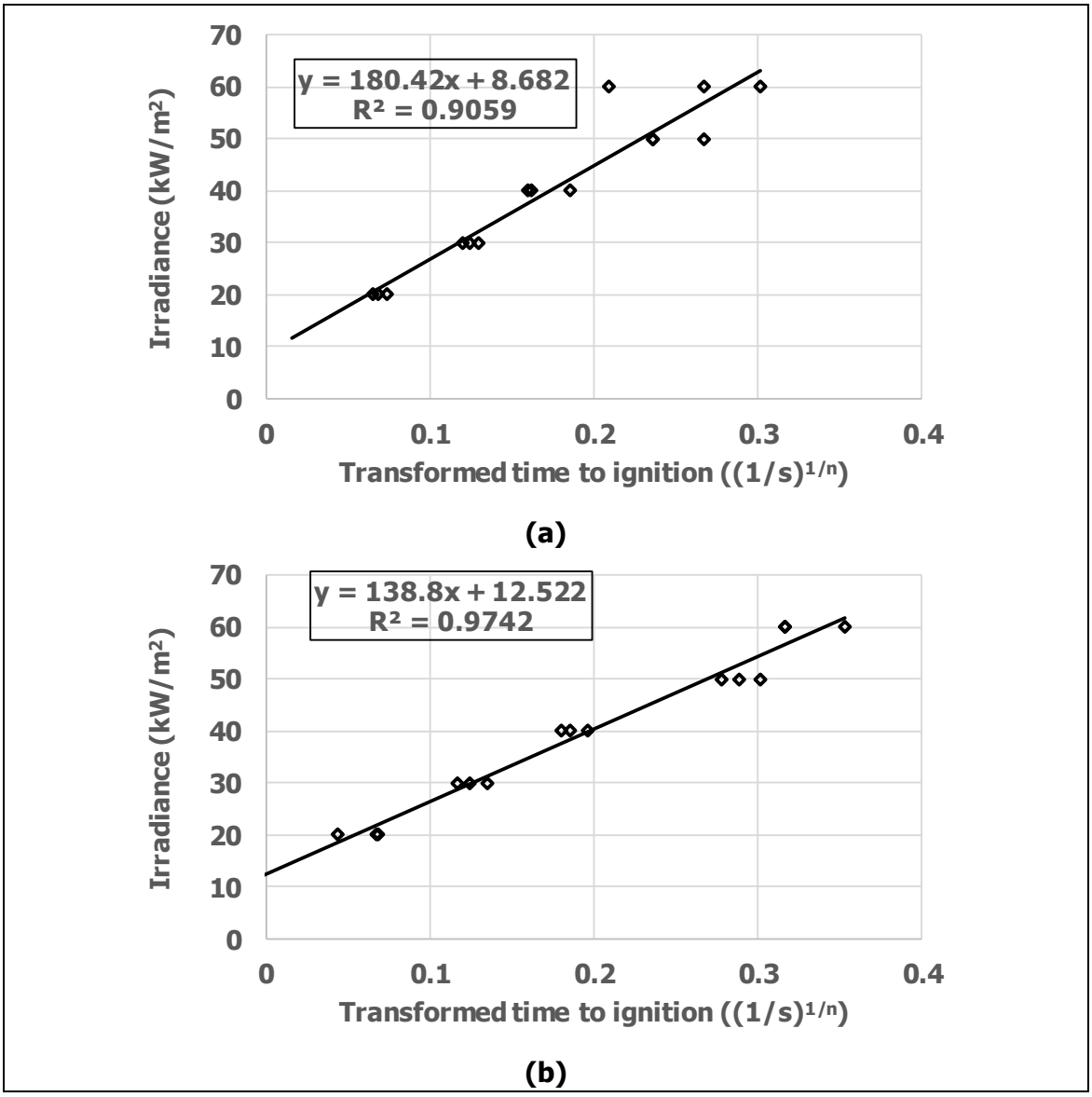


**Figure 10. FTP analysis: (a) 7 mm plywood; (b) 12 mm plywood.**

The FTP analysis over the full flux time product index range is presented in Table 10 (7 mm plywood) and Table 11 (12 mm plywood).

**Table 10. Complete FTP correlation analysis – 7 mm plywood.**

| *n* | $R^2$ | $q''_{cr}$ | *FTP* |
|---|---|---|---|
| 1 | 0.8363 | 22.8 | 483 |
| 1.1 | 0.8522 | 21.3 | 722 |
| 1.2 | 0.8646 | 19.9 | 1083 |
| 1.3 | 0.8744 | 18.4 | 1632 |
| 1.4 | 0.8823 | 17 | 2470 |
| 1.5 | 0.8885 | 15.6 | 3755 |
| 1.6 | 0.8936 | 14.2 | 5735 |
| 1.7 | 0.8976 | 12.8 | 8797 |
| 1.8 | 0.901 | 11.5 | 13550 |
| 1.9 | 0.9037 | 10.1 | 20960 |
| 2 | 0.9059 | 8.7 | 32551 |

**Table 11. Complete FTP correlation analysis – 12 mm plywood.**

| *n* | $R^2$ | $q''_{cr}$ | *FTP* |
|---|---|---|---|
| 1 | 0.9304 | 23.5 | 336 |
| 1.1 | 0.9416 | 22.3 | 494 |
| 1.2 | 0.9503 | 21.2 | 731 |
| 1.3 | 0.957 | 20.1 | 1086 |
| 1.4 | 0.9621 | 19 | 1619 |
| 1.5 | 0.9659 | 17.9 | 2423 |
| 1.6 | 0.9688 | 16.9 | 3641 |
| 1.7 | 0.971 | 15.8 | 5491 |
| 1.8 | 0.9725 | 14.7 | 8313 |
| 1.9 | 0.9736 | 13.6 | 12632 |
| 2 | 0.9742 | 12.5 | 19265 |

### 2.2.2 Minimum heat flux for ignition

Further to the discussion presented in section 2.3.2 about minimum heat flux at which ignition does not occur, an additional series of ignition-only experiments were conducted in the cone calorimeter in order to have a physical basis for the selection of the FTP dataset (values for $n$, $FTP$ and $\dot{q}''_{cr}$) for use in subsequent B-RISK modelling.

The procedure used for each plywood thickness was to reduce the irradiance in 2 kW/m² increments and subject initially a single sample for up to 1,800 s at this exposure level. If during the 1,800 s exposure period the specimen ignited, the process was repeated at the next lower exposure setting (i.e. 2 kW/m² less than the current setting). If the specimen did not ignite, a second (and if needs be a third) specimen was tested to either determine that this was the maximum irradiance level at which ignition did not occur for three replicates or to test at the next lower setting. A value for $\dot{q}''_{min}$ was then calculated as the midpoint between the minimum level at which ignition occurred and the maximum level at which ignition did not occur after 1,800 s of exposure.

Table 12 and Table 13 summarise the minimum heat flux experiments and the derivation of the $\dot{q}''_{min}$ value for both plywood thicknesses.

**Table 12. Minimum heat flux data – 7 mm plywood.**

| Test number | Heat flux (kW/m²) | Time to ignition (s) | $\dot{q}''_{min}$ (kW/m²) |
|---|---|---|---|
| 7-18-1 | 18 | 245 | 13 |
| 7-16-1 | 16 | 376 | |
| 7-14-1 | 14 | 852 | |
| 7-12-1 | 12 | NI | |
| 7-12-2 | | NI | |
| 7-12-3 | | NI | |

NI = no ignition after 1,800 s exposure.

**Table 13. Minimum heat flux data – 12 mm plywood.**

| Test number | Heat flux (kW/m²) | Time to ignition (s) | $\dot{q}''_{min}$(kW/m²) |
|---|---|---|---|
| 12-18-1 | 18 | 792 | 15 |
| 12-16-1 | 16 | 1,012 | |
| 12-14-1 | 14 | NI | |
| 12-14-2 | | NI | |
| 12-14-3 | | NI | |

NI = no ignition after 1,800 s exposure.

During the testing of the three 7 mm samples at the 12 kW/m² irradiance level, glowing ignition/combustion occurred, but this did not transition to flaming combustion during the 1,800 s exposure duration. Figure 1 shows a post-test photograph of the three specimens, with evidence of the glowing combustion clearly visible in Figure 1(a) and (b) in the region of the grey/white ash residue.

(a) (b) (c)

**Figure 1. Post-test photographs of 7 mm thick specimens at 12 kW/m² irradiance level: (a) Specimen 7-12-1, (b) Specimen 7-12-2, (c) Specimen 7-12-3.**

For Specimen 7-12-1 shown in Figure 1(a), the glowing combustion was observed to occur from approximately 24 minutes (1,440 s) onwards, and for Specimen 7-12-2 in Figure 1(b), from approximately 22 minutes (1,320 s) onwards. In contrast, no combustion occurred with Specimen 7-12-3, which is apparent in Figure 1(c) due to the absence of any obvious ash residue.

### 2.2.3 ISO 9705 room-scale testing

A series of ISO 9705 room experiments were conducted by Baker et al. (2011) that built on the series of seven experiments that had been conducted previously by Peel. Baker et al. identified the following parameters for further study:

- Surface lining coverage and location.
- Fuel load (lining thickness).
- Location of the ignition source.

#### 2.2.3.1 Coverage and location

One objective of Baker et al.'s research was to develop a predictive model for varying amounts (surface area) and locations of fuel, i.e. timber lining material. An analysis of the experiments conducted by Peel indicated the range of combinations of C: U: L that were performed and hence the gaps. Of the seven possible C: U: L combinations (ignoring an eighth combination of no lining material), Peel covered five out of seven possibilities as shown in Table 14.

**Table 14. Range of configurations tested by Peel.**

| Peel's experiment | Ceiling (C) | Upper walls (U) | Lower walls (L) |
|---|---|---|---|
| 1, 7 | Y | Y | Y |
| 5, 6 | N | Y | Y |
| | Y | N | Y |
| | Y | Y | N |
| 2 | Y | N | N |
| 4 | N | Y | N |
| 3 | N | N | Y |

To contribute to further development of the generality of the prototype predictive model described in section 2.2.5, additional experiments to cover the C : L and C : U combinations were added, providing useful extra data points.

#### 2.2.3.2 Fuel load

In relation to the fuel load, Baker et al. identified (by inspection of the HRR curves) from Peel's Experiments 2 and 4 (refer to Figure 5) that the combustion was limited by the available fuel. In Experiment 4, this is indicated by the HRR reducing from approximately 480 s during the 100 kW burner exposure and then again from approximately 700 s during the 300 kW exposure. A similar trend was apparent for Experiment 2 where the HRR steadily decreases from approximately 700 s. To investigate this aspect further, Experiments 2 and 4 were repeated with 12 mm thick plywood, giving a 71% increase in fuel load with the same coverage.

#### 2.2.3.3 Ignition source

The standard location for the gas burner in an ISO 9705 room test is in the corner as close to the intersecting wall linings as possible. One impact of proximity to the compartment walls is to reduce entrainment of air into the fire plume, which can impact the plume temperature and flame height (Karlsson & Quintiere, 2000; Drysdale, 1998). In the standard corner location, entrainment is only possible from one quadrant, while positioning the burner at the mid-point of a wall allows for entrainment from two quadrants and positioning the burner in the middle of the room allows entrainment from all four quadrants. To investigate this aspect further, an experiment was conducted where the burner was moved away from the standard corner location to the mid-point of the short wall.

#### 2.2.3.4 Experimental series

Table 15 lists the experiments carried out by Baker et al. with consideration of the experimental variables described in 2.2.3.1 to 2.2.3.3.

**Table 15. Baker et al. experimental test plan.**

| Test | Location of timber wall linings | Ceiling linings | Ply thickness (mm) | Burner location | Lower wall L ($m^2$) | Upper wall U ($m^2$) | Ceiling C ($m^2$) | (Nominal) total ply area ($m^2$) |
|---|---|---|---|---|---|---|---|---|
| 2B | None | Fully lined | 12 | Corner | - | - | 8.6 | 8.6 |
| 4B | Upper half of walls extending 3.6 from burner corner | None | 12 | Corner | - | 8.6 | - | 8.6 |
| 7B | Upper wall extending 2.4 m from burner corner, lower wall extending 1.2 m from burner corner | Fully lined | 7 | Corner | 2.9 | 5.8 | 8.6 | 17.3 |
| 7C | Upper wall extending 3.6 m from burner corner, lower wall extending 1.2 m from burner corner | Fully lined | 7 | Corner | 2.9 | 8.6 | 8.6 | 20.2 |
| 7D | Upper wall extending 3.6 m from burner corner | Fully lined | 7 | Corner | - | 8.6 | 8.6 | 17.3 |
| 7E | Full height wall extending 1.2 m from burner (symmetric about middle of end wall) | Fully lined | 7 | Middle of end wall, against face | 2.9 | 2.9 | 8.6 | 14.4 |
| 7F | Lower wall extending 3.6 m from burner corner | Fully lined | 7 | Corner | 8.6 | - | 8.6 | 17.3 |
| 7G | Full-height wall extending 1.2 m from burner corner | Partial lining extending 1.2 m from end wall | 7 | Corner | 2.9 | 2.9 | 2.9 | 8.6 |
| 7H | Full-height wall extending 1.2 m from burner corner | Partial lining extending 2.4 m from end wall | 7 | Corner | 2.9 | 2.9 | 5.8 | 11.5 |
| 7I | Full-height wall extending 1.2 m from burner corner | Partial lining 1.2 × 1.2 m above burner corner | 7 | Corner | 2.9 | 2.9 | 1.4 | 7.2 |
| 8A | Full-height walls extending 1.2 m from burner corner | None | 7 | Corner | 2.9 | 2.9 | - | 5.8 |

## 2.2.4 Results

### 2.2.4.1 Lining location

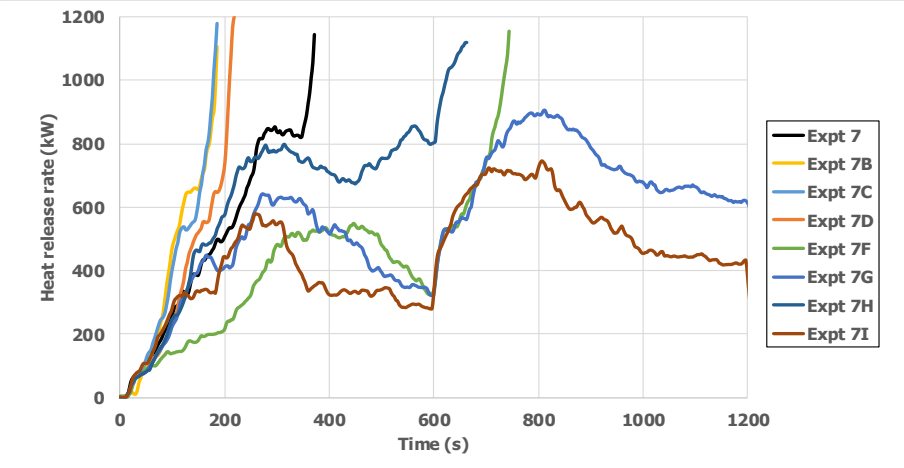


**Figure 11. HRR curves for fuel location experiments.**

**Table 16. Flashover, peak HRR and FIGRA$_{RC}$ data – fuel location experiments.**

| Expt | Flashover (Y/N) | Time to flashover, $t_{fo}$ (s) | Peak HRR, $Q_{peak}$ (kW) | Time to peak, $t_{peak}$ (s) | $Q_{burner}$ at test *termination* (kW) | FIGRA$_{RC}$ (kW/s) |
|---|---|---|---|---|---|---|
| 7B | Y | 184* | - | - | 100 | 4.9 |
| 7C | Y | 179 | - | - | 100 | 5.0 |
| 7D | Y | 210 | - | - | 100 | 4.3 |
| 7F | Y | 734 | - | - | 300 | 1.0 |
| 7G | N | - | 905 | 813 | 300 | 0.7 |
| 7H | Y | 624 | - | - | 300 | 1.1 |
| 7I | N | - | 746 | 807 | 300 | 0.6 |

* Adjusted due to interruption to gas flow for 72 s period.

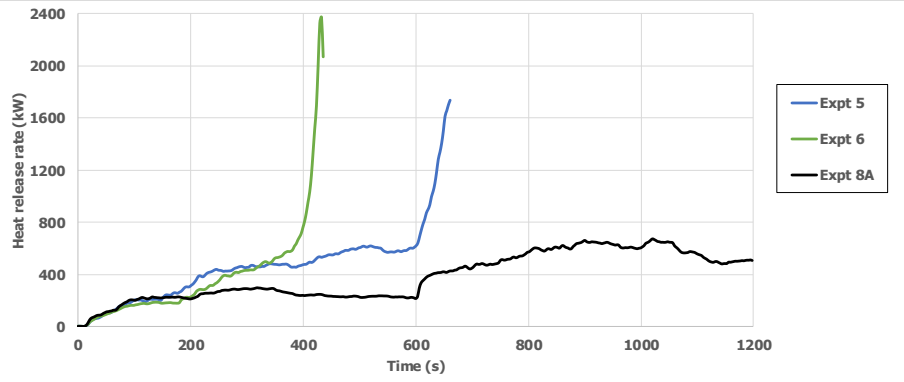


**Figure 12. HRR curves for fuel location experiments – wall only linings.**

**Table 17. Flashover, peak HRR and FIGRA$_{RC}$ data – fuel location experiments.**

| Expt | Flashover (Y/N) | Time to flashover, $t_{fo}$ (s) | Peak HRR, $Q_{peak}$ (kW) | Time to peak, $t_{peak}$ (s) | $Q_{burner}$ (kW) | FIGRA$_{RC}$ (kW/s) |
|---|---|---|---|---|---|---|
| 5 | Y | 627 | - | - | 300 | 1.1 |
| 6 | Y | 410 | - | - | 100 | 2.2 |
| 8A | N | - | 671 | 1,020 | 300 | 0.4 |

### 2.2.4.2 Fuel load

Heat release data from Experiments 2B and 4B were compared against Peel's Experiments 2 and 4 respectively.

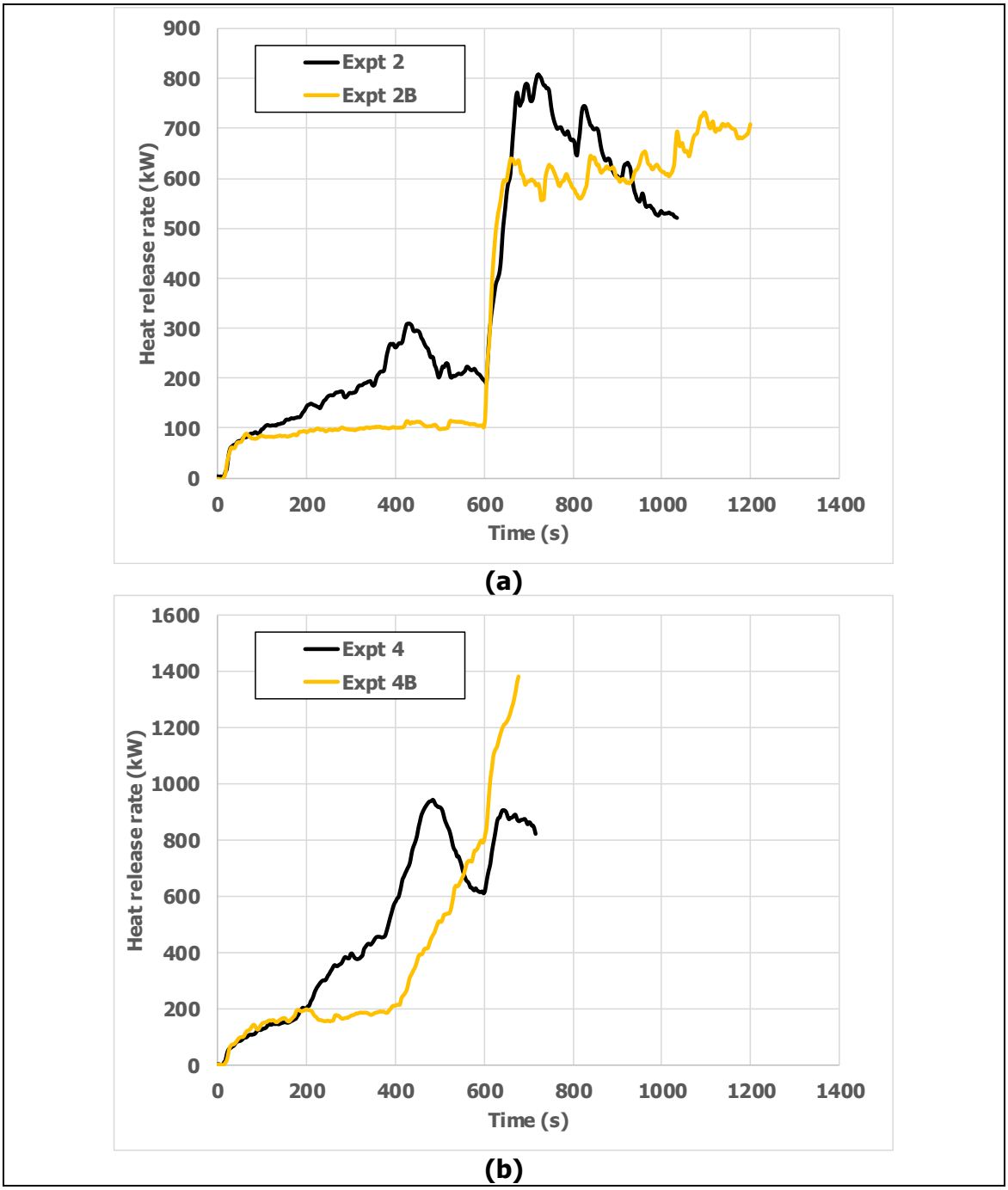


**Figure 13. HRR curves for fuel load experiments: (a) Expt 2 vs 2B, (b) Expt 4 vs 4B.**

**Table 18. Flashover, peak HRR and $FIGRA_{RC}$ data – fuel load experiments.**

| Expt | Flashover (Y/N) | Time to flashover, $t_{fo}$ (s) | Peak HRR, $Q_{peak}$ (kW) | Time to peak, $t_{peak}$ (s) | $Q_{burner}$ (kW) | $FIGRA_{RC}$ (kW/s) |
|---|---|---|---|---|---|---|
| 2B | N | - | 730 | 1,098 | 300 | 0.4 |
| 4B | Y | 614 | - | - | 300 | 1.1 |

### 2.2.4.3 Heat release rate data – burner location

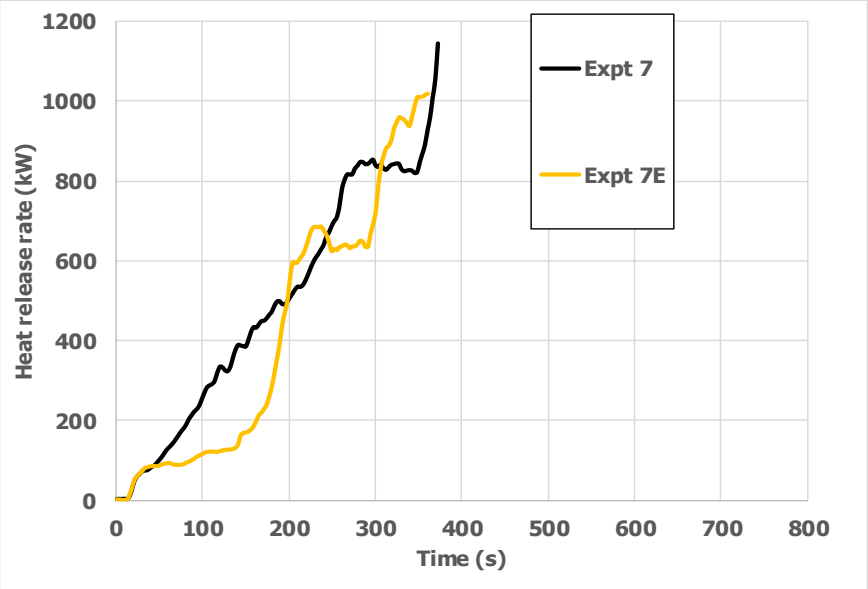


**Figure 14. HRR curves for burner location experiments.**

**Table 19. Flashover, peak HRR and FIGRA$_{RC}$ data – burner location experiment.**

| Expt | Flashover (Y/N) | Time to flashover, $t_{fo}$ (s) | Peak HRR, $Q_{peak}$ (kW) | Time to peak, $t_{peak}$ (s) | $Q_{burner}$ (kW) | FIGRA$_{RC}$ (kW/s) |
|---|---|---|---|---|---|---|
| 7 | Y | 366 | - | - | 100 | 2 |
| 7E | Y | 347 | - | - | 100 | 2.6 |

## 2.2.5 Risk model

Baker et al. (2017) proposed a risk ranking model using Peel's data and the subsequent additional test data collected (Table 20).

**Table 20. Predictive risk ranking model – initial prototype.**

| Predictive parametric risk ranking model | | | | | | FIGRA$_{RC}$ | | |
|---|---|---|---|---|---|---|---|---|
| $w_x$ | 1.00 | 0.75 | 0.25 | Risk Score | Rank | $FIGRA_{RC}$ | $FIGRA_{RC,Norm}$ | Rank |
| Expt | $A_x$ (m$^2$) | | | | | | | |
| | ceiling | upper walls | lower walls | | | | | |
| 1 | 8.64 | 11.52 | 11.52 | 100.0 | 1 | 5.2 | 100.0 | 1 |
| 2 | 8.64 | | | 42.9 | 7 | 0.7 | 13.5 | 12 |
| 3 | | | 8.64 | 10.7 | 15 | 0.3 | 5.8 | 15 |
| 4 | | 8.64 | | 32.1 | 10 | 1.7 | 32.7 | 7 |
| 5 | | 5.76 | 5.76 | 28.6 | 11 | 1.116 | 21.5 | 9 |
| 6 | | 8.64 | 8.64 | 42.9 | 7 | 2.2 | 42.3 | 6 |
| 7 | 8.64 | 2.88 | 2.88 | 57.1 | 5 | 2.5 | 48.1 | 5 |
| 7B | 8.64 | 5.76 | 2.88 | 67.9 | 4 | 4.9 | 94.2 | 3 |
| 7C | 8.64 | 8.64 | 2.88 | 78.6 | 2 | 5 | 96.2 | 2 |
| 7D | 8.64 | 8.64 | | 75.0 | 3 | 4.3 | 82.7 | 4 |
| 7F | 8.64 | | 8.64 | 53.6 | 6 | 1 | 19.2 | 10 |
| 7G | 2.88 | 2.88 | 2.88 | 28.6 | 11 | 0.74 | 14.2 | 11 |
| 7H | 5.76 | 2.88 | 2.88 | 42.9 | 7 | 1.122 | 21.6 | 8 |
| 7I | 1.44 | 2.88 | 2.88 | 21.4 | 13 | 0.6 | 11.5 | 13 |
| 8A | | 2.88 | 2.88 | 14.3 | 14 | 0.4 | 7.7 | 14 |

The initial prototype assigned weightings to the ceiling, upper and lower wall coverings, nominally assuming that the higher up in the compartment, the greater the contribution to the fire growth.

The area of coverage in each region, multiplied by the weighting factor for that region was summed together. A fully lined room being the baseline, the remaining experiments were calculated as a percentage of the baseline.

For example: Baseline = (1.00 x 8.64) + (0.75 x 11.52) + (0.25 x 11.52) = 20.16

Expt 2 = (1.00 x 8.64) + (0.75 x 0) + (0.25 x 0) = 8.64

Expt 2 Risk Score = (8.64 / 20.16) x 100 = 42.86

The results from the initial prototype gave agreement in less than half of the cases. Baker proceeded to optimise the model by adjusting the weightings assigned to the different areas, giving an improved correlation between the model ranking and the $FIGRA_{RC}$ ranking (Table 21).

**Table 21. Predictive risk ranking model – optimised version.**

| Predictive parametric risk ranking model | | | | | | $FIGRA_{RC}$ | | |
|---|---|---|---|---|---|---|---|---|
| $w_x$ | 1.00 | 1.42 | 0.00 | *Risk Score* | Rank | $FIGRA_{RC}$ | $FIGRA_{RC, Norm}$ | Rank |
| Expt | $A_x$ ($m^2$) | | | | | | | |
| | ceiling | upper walls | lower walls | | | | | |
| 1 | 8.64 | 11.52 | 11.52 | 100.0 | 1 | 5.2 | 100.0 | 1 |
| 2 | 8.64 | | | 34.6 | 9 | 0.7 | 13.5 | 12 |
| 3 | | | 8.64 | 0.0 | 15 | 0.3 | 5.8 | 15 |
| 4 | | 8.64 | | 49.1 | 6 | 1.7 | 32.7 | 7 |
| 5 | | 5.76 | 5.76 | 32.7 | 11 | 1.116 | 21.5 | 9 |
| 6 | | 8.64 | 8.64 | 49.1 | 6 | 2.2 | 42.3 | 6 |
| 7 | 8.64 | 2.88 | 2.88 | 50.9 | 5 | 2.5 | 48.1 | 5 |
| 7B | 8.64 | 5.76 | 2.88 | 67.3 | 4 | 4.9 | 94.2 | 3 |
| 7C | 8.64 | 8.64 | 2.88 | 83.6 | 2 | 5 | 96.2 | 2 |
| 7D | 8.64 | 8.64 | | 83.6 | 2 | 4.3 | 82.7 | 4 |
| 7F | 8.64 | | 8.64 | 34.6 | 9 | 1 | 19.2 | 10 |
| 7G | 2.88 | 2.88 | 2.88 | 27.9 | 12 | 0.74 | 14.2 | 11 |
| 7H | 5.76 | 2.88 | 2.88 | 39.4 | 8 | 1.122 | 21.6 | 8 |
| 7I | 1.44 | 2.88 | 2.88 | 22.1 | 13 | 0.6 | 11.5 | 13 |
| 8A | | 2.88 | 2.88 | 16.4 | 14 | 0.4 | 7.7 | 14 |

This bias towards the upper wall area rather than the ceiling is suggested to be a result of oxygen depletion in the gases directly below the ceiling whereas the upper wall region is able to access oxygen via entrainment from the lower layer more easily.

## 2.3 Discussion

### 2.3.1 Time-to-ignition data

With only three replicates at each irradiance, Peel's time-to-ignition data at 20 kW/m² showed a wide spread of times. The lower the heat flux, the more variability is expected (possibly magnified by variability in the sample itself). At first sight, one of the values would appear to be significantly different to the remaining two and inclusion of this data point shifts the mean value up accordingly. However, with only three data points, it is not possible to validate this supposition.

### 2.3.2 Minimum and critical heat fluxes

As discussed in section 2.2.1.1, Shields et al. (1994) suggest that $\dot{q}''_{cr}$ should fall between 0.8 $\dot{q}''_{min}$ and $\dot{q}''_{min}$. Table 22 shows that the critical heat flux calculated from the time to ignition in section 2.2.1.2 is outside the bounds for the 7 mm plywood and towards the bottom end of the range for the 12 mm plywood. The fact that two out of three of the 7 mm specimens reached the point of glowing combustion at 12 kW/m² would indicate that $\dot{q}''_{min}$ was likely closer to 12 kW/m² than 13 kW/m². This would change the expected range for $\dot{q}''_{cr}$ to between 9.6 and 12 kW/m². The calculated value for $\dot{q}''_{cr}$ still falls outside this range and may indicate that the FTP dataset may be overly pessimistic. It may also indicate that, at the higher heat fluxes, a reasonably repeatable time to ignition can be measured, but more replicates are required at lower heat fluxes to give a better indication of the likely distribution.

**Table 22. Minimum and critical heat flux.**

| Plywood thickness | 0.8 $\dot{q}''_{min}$ (kW/m²) | $\dot{q}''_{min}$ (kW/m²) | $\dot{q}''_{cr}$ (kW/m²) |
|---|---|---|---|
| 7 mm | 10.4 | 13 | 8.7 |
| 12 mm | 12 | 15 | 12.5 |

Although nominally the same, due to natural material variability, Peel and Baker et al. are reported separately in Table 23. Additionally, one of Baker et al.'s 7 mm thick plywood replicates at 60 kW/m² had a recorded time to ignition of 23 s, which was longer than any of the replicates at 50 kW/m². This would indicate that it was an outlier and should have been excluded when calculating the mean time to ignition.

**Table 23. Mean time to ignition repeatability.**

| Plywood thickness | Heat flux (kW/m²) | Number of replicates | Range (s) | Mean (s) | Standard deviation (s) | Percentage of mean |
|---|---|---|---|---|---|---|
| 7 mm (Peel) | 60 | 3 | 10–14 | 11.33 | 1.88 | 16.6% |
| 7 mm (Baker et al.) | 60 | 2* | 11–14* | 12.5* | 1.5* | 12% |
| 12 mm (Baker et al.) | 60 | 3 | 8–10 | 9.33 | 0.94 | 10.1% |
| 7 mm (Peel) | 20 | 3 | 197–366 | 288 | 69.6 | 24.2% |
| 7 mm (Baker et al.) | 20 | 3 | 184–233 | 211.33 | 20.4 | 9.7% |
| 12 mm (Baker et al.) | 20 | 3 | 212–519 | 318.33 | 141.97 | 44.6% |

* Outlier removed.

### 2.3.3 Fuel location

The optimised risk model proposed by Baker et al. suggested that fuel in the lower region was not contributing to flashover. However, it is noted that, even at 100 kW, the flame height of the burner was above the boundary between the upper and lower wall fuel regions so any fuel in the upper region near the burner flame was likely to be ignited irrespective of any vertical flame spread from the lower region.

It is also noted that the only difference between Experiment 2 and Experiment 7F was the addition of fuel in the lower wall area. Where Experiment 7F reached flashover at 734 s, equivalent to a Group 2 material, Experiment 2 did not flashover for the 1,200 s duration of the test, equivalent to a Group 1 material. Fuel in the lower wall area therefore must be considered to provide some contribution to the likely risk of flashover by providing a path for flame spread to the upper wall area.

### 2.3.4 Fuel load

Comparison of Peel's Experiments 2 and 4 and Experiments 2B and 4B of Baker et al. would indicate that material thickness (and therefore fuel load) does play a part.

Whereas the 7 mm thick ply used by Peel in Experiment 2 appeared to reach a peak HRR shortly after the burner was increased to 300 kW, it then began to drop as the fuel was quickly consumed, failing to reach flashover. In Experiment 2B by Baker et al., although the thicker 12 mm ply appears to take longer to become involved, once hot enough in the upper layer, the ply continued to provide fuel for an extended duration. The experiment was concluded at 1,200 s as per the ISO 9705 test standard but it can be seen from the HRR output graph that the fire was still growing, and if it had been left to run longer, it may have reached flashover.

Further, in Peel's Experiment 4, the room failed to reach flashover, consuming the fuel in close proximity to the corner of the room at 100 kW before reducing again. When the burner ramped up to 300 kW (at 600 s), the total HRR increased again for a short period before dropping off again, indicating that all of the available fuel in the room corner had been consumed. In Experiment 4B, the thicker 12 mm ply took longer to become involved (~400 s compared to ~200 s for the 7 mm ply used by Peel), but once involved, the additional fuel allowed the room to reach flashover shortly after the burner was increased to 300 kW and would likely have reached flashover even if the burner had been left at 100 kW.

### 2.3.5 Burner location

With the burner located in the middle of the end wall, the growth rate was initially slower. This is attributed to the increased entrainment available, as hypothesised by Baker et al., and the reduced radiation feedback from a corner detail. However, the rate of growth increased rapidly after 150s and eventually reached flashover earlier than the test with the burner in the corner. It is hypothesised that this could be a result of the additional fuel available at the ceiling. In the corner, only one quadrant of ceiling fuel is exposed, while in the middle of the wall, two quadrants of fuel are available. This might indicate that the corner may not always be the most severe fire location.

# 3. Cone calorimetry testing

As summarised in section 2, Peel and Baker et al. conducted experiments using 7 mm thick plywood with 15 mm thick calcium silicate backing. Baker et al. also used some 12 mm thick plywood (again with 15 mm thick calcium silicate backing) for fuel load comparison experiments.

The new research described in this report was to look at a wider range of different engineered wood products (EWPs), including thin sheet products that might be used as internal linings as well as structural EWP products where the exposed surface is equivalent to a lining and to determine the difference in performance in terms of ignition and flame spread. The EWPs included plywood, medium-density fibreboard (MDF), cross-laminated timber (CLT) and laminated veneer lumber (LVL) with 13 products sourced from five different New Zealand manufacturers. Some companies supplied a single product, while others supplied multiple products and/or the same product in different thicknesses. A summary of the products tested is given in Table 24. The wood species used in all the products was New Zealand-grown *Pinus radiata*.

**Table 24. Engineered wood products tested.**

| Sample reference | Product | Thickness (mm) | Density (kg/m³) | Adhesive type | Notes |
|---|---|---|---|---|---|
| A1 | LVL | 63 | 577±9 | Phenol formaldehyde | |
| B1 | Plywood | 7 | 525±15 | Type A phenolic | |
| B2 | Plywood | 9 | 552±7 | Type A phenolic | |
| C1 | CLT | 50 | 458±9 | Polyurethane | Two veneers of nominal 40mm and one veneer of nominal 23mm cut approximately in half |
| D1 | MDF | 9 | 729±3 | Urea/formaldehyde | |
| D2 | MDF | 18 | 721±5 | Urea/formaldehyde | |
| D3 | MDF | 18 | 745±3 | Urea/formaldehyde | |
| F1 | Plywood | 7 | 515±9 | Phenolic (PF) resin | |
| F2 | Plywood | 12 | 479±11 | Phenolic (PF) resin | |
| F3 | Plywood | 17 | 503±4 | Phenolic (PF) resin | |
| F4 | Plywood | 12 | 457±10 | Phenolic (PF) resin | |
| F5 | Plywood | 12 | 457±10 | | |
| F6 | Plywood | 12 | 508±14 | | |

Before being tested, samples were conditioned at 23±2 ˚C and 50±5% RH until their mass had stabilised. Constant mass was considered to be reached when two successive weight measurements taken at an interval of 24 hours did not differ by more than 0.1% of the mass of the sample or 0.1 g, whichever was greatest. Three specimens of each product were exposed to five different irradiance settings (20, 30, 40, 50 and 60 kW/m²). Standard oxygen depletion calorimetry data was collected generally in accordance with ISO 5660-1.

In addition to the test data required to be collected by the standard, ignition times were recorded with a hand-held stopwatch as well as by analysing a video recording of each experiment, rounded to the nearest tenth of a second.

The specimen construction and preparation varied in part from the requirements of the standard. In cases where specimens greater than 50 mm thickness (to be representative of the thickness of the EWP used in buildings) were tested, clearance to the heater base plate was adjusted to maintain the standard 25 mm separation between the heater and the sample surface. Where thinner sheet materials (up to 20 mm maximum nominal thickness) were tested, a wire mesh spacer of 30 mm nominal thickness was used to provide clearance between the back face of the specimen and the base of the specimen holder, representing a wall cavity behind the product under test.

In addition, the critical irradiance, $\dot{q}''_{cr,exp}$, was determined experimentally by reducing the irradiance in the cone calorimeter in 1 kW/m² increments to the point where three consecutive specimens did not ignite at the same irradiance level after 1,800 s exposure (deemed $\dot{q}''_{min}$). The experimental critical irradiance is then derived as being half the increment more than the minimum, i.e. $\dot{q}''_{cr,exp} = \dot{q}''_{min} + 0.5$ kW/m².

## 3.1 Cone calorimetry results

The calorimetry results are split into three parts – time to ignition ($t_{ig}$), HRR vs time and the minimum heat flux required for ignition ($\dot{q}''_{cr}$). Three replicates of each product were tested in the cone calorimeter.

### 3.1.1 Time to ignition

For each product, the time to ignition ($t_{ig}$) was recorded for each incident heat flux, rounded to the nearest second.

**Table 25. Time to ignition**

| | Time to ignition (s) | | | | | | | | | | | | | | |
|---|---|---|---|---|---|---|---|---|---|---|---|---|---|---|---|
| | @ 20 kW/m² | | | @ 30 kW/m² | | | @ 40 kW/m² | | | @ 50 kW/m² | | | @ 60 kW/m² | | |
| | Min | Max | Mean | Min | Max | Mean | Min | Max | Mean | Min | Max | Mean | Min | Max | Mean |
| **A1** | 310 | 475 | **421** | 69 | 118 | **96** | 30 | 56 | **46** | 18 | 27 | **23** | 16 | 29 | **20** |
| **B1** | 219 | 277 | **242** | 83 | 97 | **91** | 35 | 60 | **47** | 28 | 32 | **30** | 14 | 15 | **15** |
| **B2** | 230 | 315 | **273** | 77 | 89 | **82** | 41 | 47 | **45** | 23 | 27 | **25** | 14 | 18 | **15** |
| **C1** | 375 | 445 | **414** | 45 | 60 | **54** | 27 | 40 | **34** | 21 | 23 | **22** | 11 | 14 | **12** |
| **D1** | 188 | 277 | **232** | 100 | 115 | **106** | 58 | 61 | **58** | 36 | 40 | **38** | 26 | 27 | **27** |
| **D2** | 190 | 209 | **199** | 77 | 82 | **79** | 43 | 46 | **44** | 28 | 30 | **29** | 18 | 20 | **19** |
| **D3** | 222 | 232 | **227** | 86 | 91 | **89** | 48 | 52 | **49** | 32 | 34 | **33** | 18 | 20 | **20** |
| **F1** | 201 | 229 | **212** | 77 | 92 | **84** | 42 | 51 | **49** | 19 | 29 | **24** | 15 | 16 | **15** |
| **F2** | 203 | 216 | **208** | 62 | 97 | **66** | 32 | 43 | **38** | 21 | 27 | **26** | 14 | 24 | **19** |
| **F3** | 231 | 340 | **236** | 82 | 93 | **86** | 32 | 39 | **36** | 24 | 29 | **26** | 16 | 17 | **17** |
| **F4** | 217 | 244 | **231** | 84 | 102 | **95** | 37 | 43 | **40** | 19 | 27 | **22** | 17 | 19 | **18** |
| **F5** | 200 | 262 | **228** | 69 | 82 | **74** | 31 | 40 | **34** | 19 | 24 | **22** | 11 | 16 | **14** |
| **F6** | 175 | 226 | **205** | 56 | 84 | **64** | 34 | 40 | **37** | 18 | 26 | **20** | 16 | 21 | **18** |

### 3.1.2 Heat release rate

The heat release rate for each sample was taken from the point of ignition. The mean from each set of three replicates at each incident heat flux was calculated (Figures 16–28). Full results can be found in Appendix A.

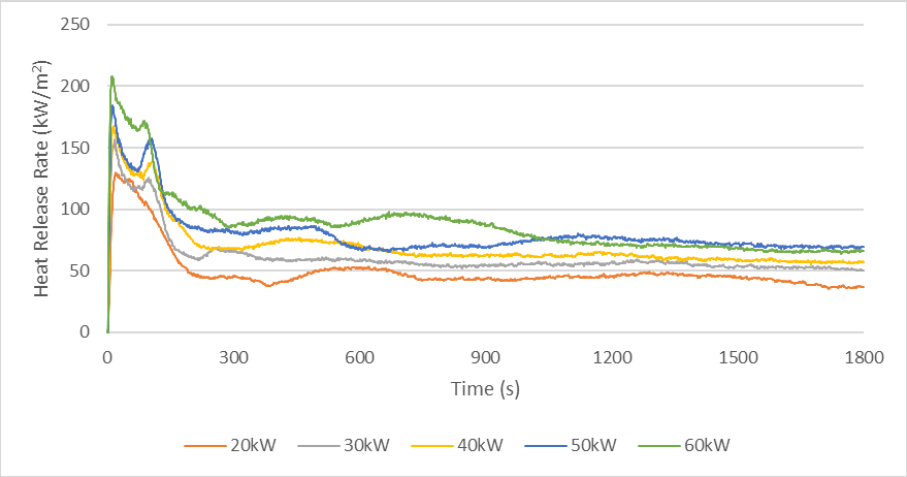


**Figure 15. Product A1 (LVL) mean HRR.**

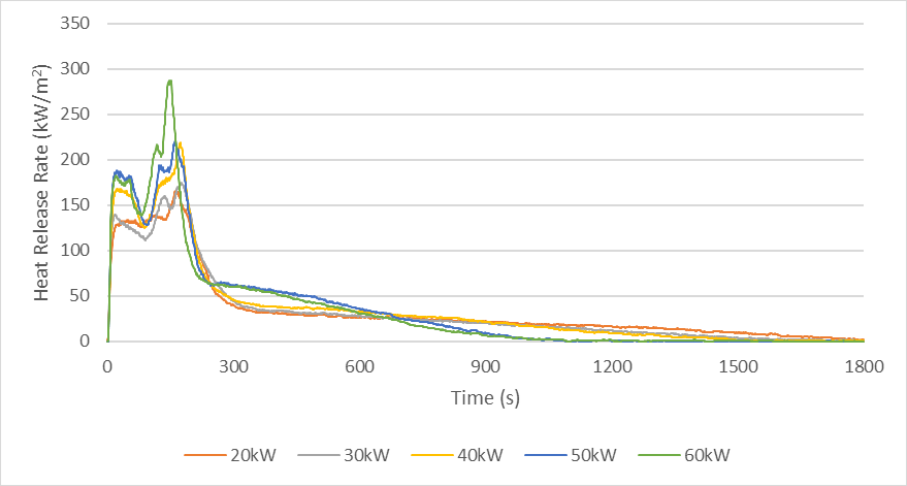


**Figure 16. Product B1 (7 mm plywood) mean HRR.**

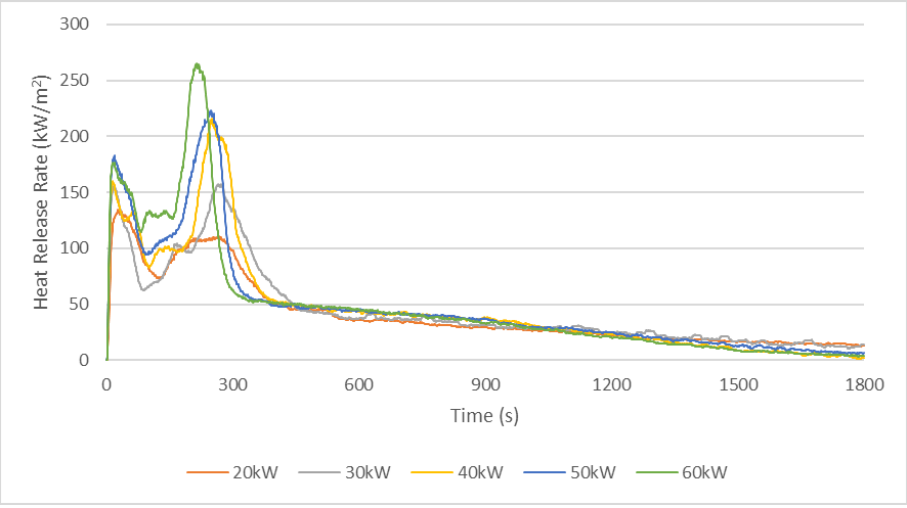


**Figure 17. Product B2 (9 mm plywood) mean HRR.**

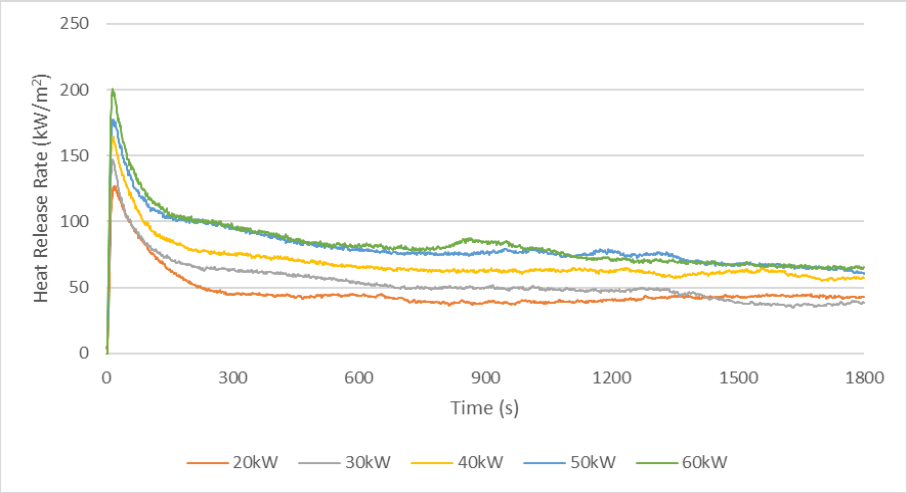


**Figure 18. Product C1 (CLT) mean HRR.**

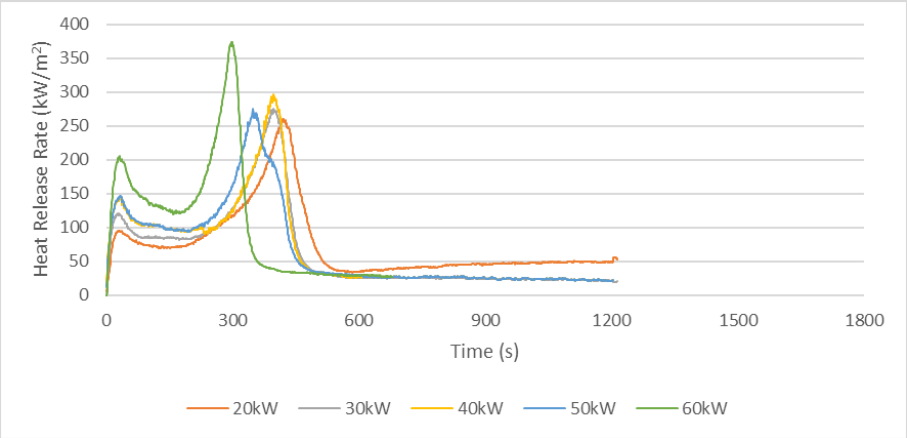


**Figure 19. Product D1 (9 mm MDF) mean HRR.**

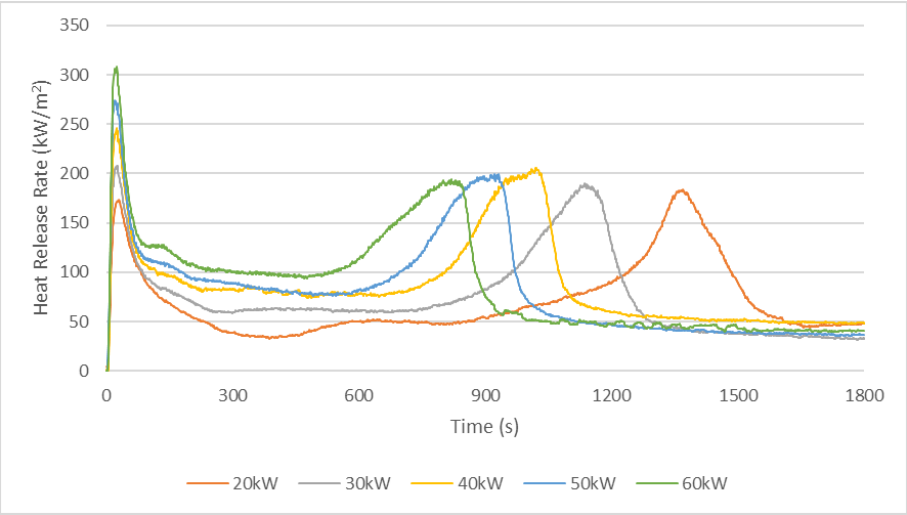


**Figure 20. Product D2 (18 mm MDF) mean HRR.**

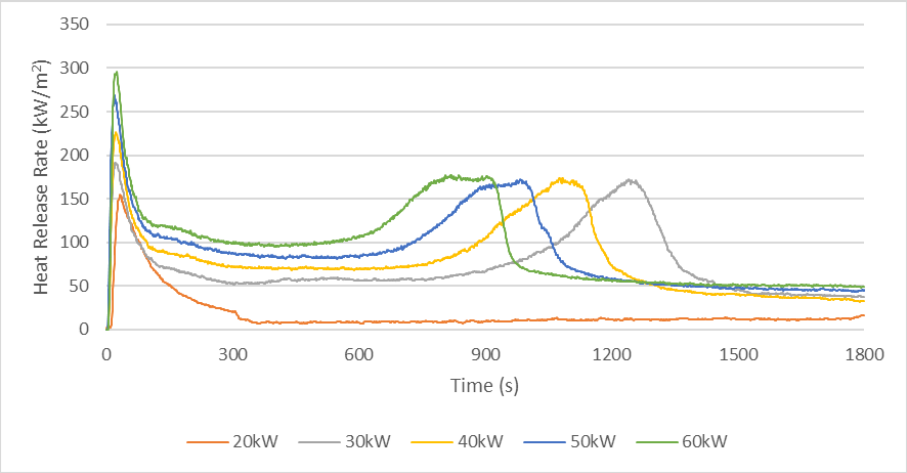


**Figure 21. Product D3 (18 mm MDF) mean HRR.**

Based on the results for products D1 and D2, the result for D3 @ 20kW appears incomplete after 300 s. The HRR drops to around 8 kW, where the output of the heater is 20 kW. Also, based on the other experimental samples, a second peak would be expected between 1,200 and 1,500 s.

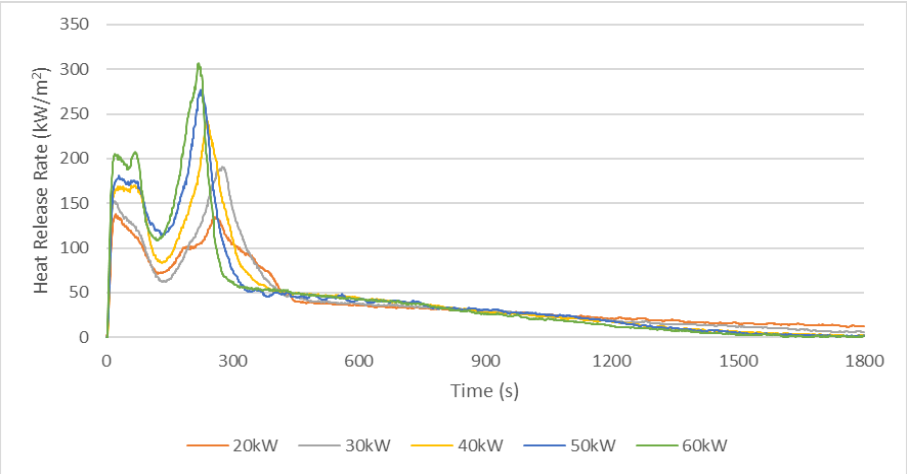


**Figure 22. Product F1 (7 mm plywood) mean HRR.**

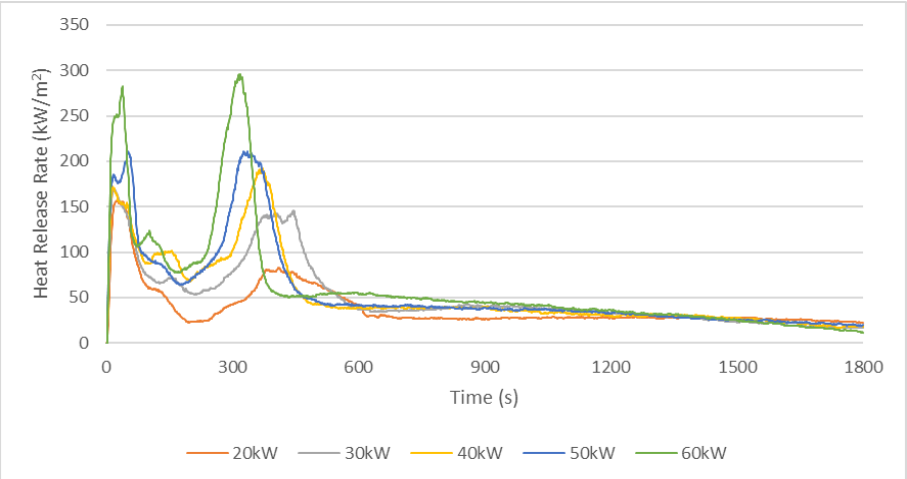


**Figure 23. Product F2 (12 mm plywood) mean HRR.**

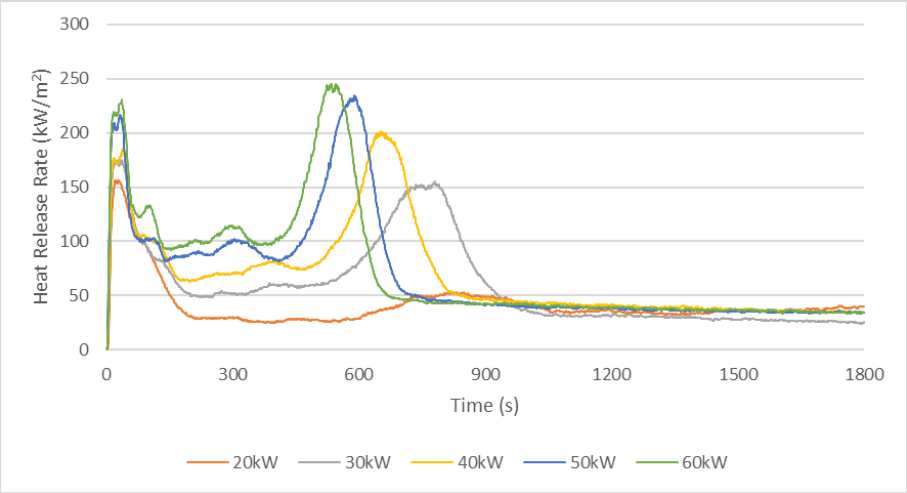


**Figure 24. Product F3 (17 mm plywood) mean HRR.**

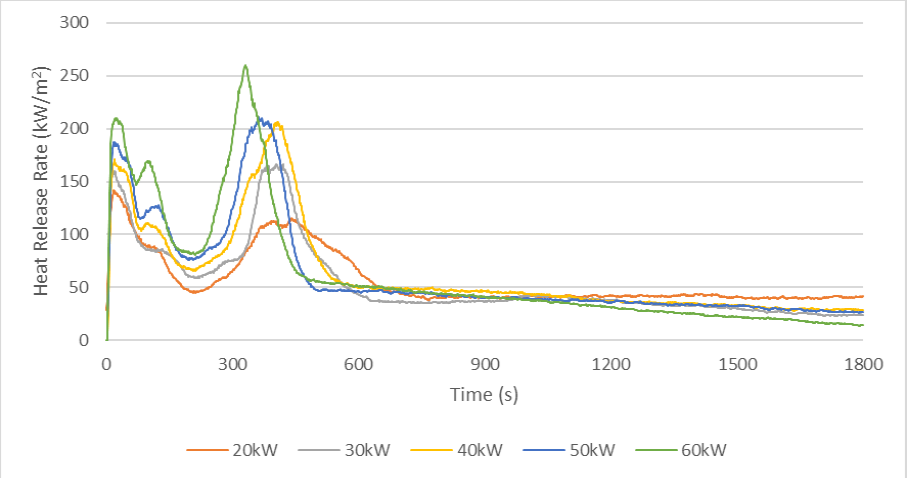


**Figure 25. Product F4 (12 mm plywood) mean HRR.**

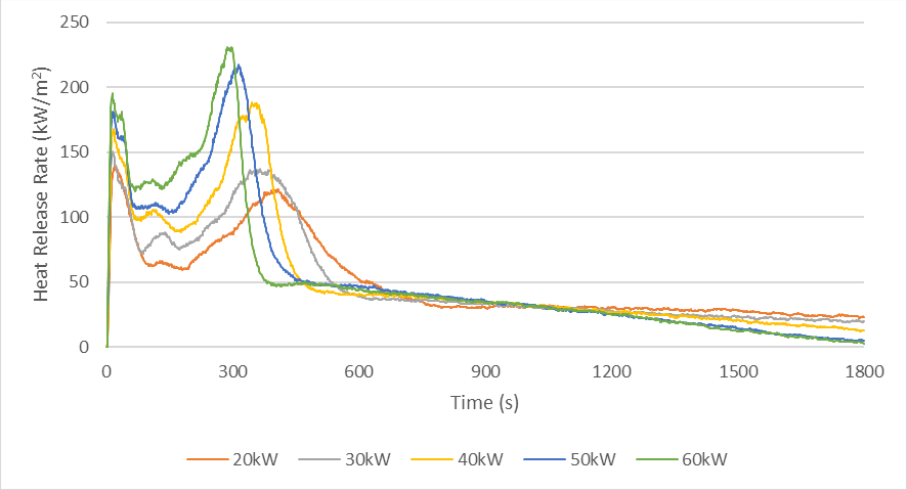


**Figure 26. Product F5 (12 mm plywood) mean HRR.**

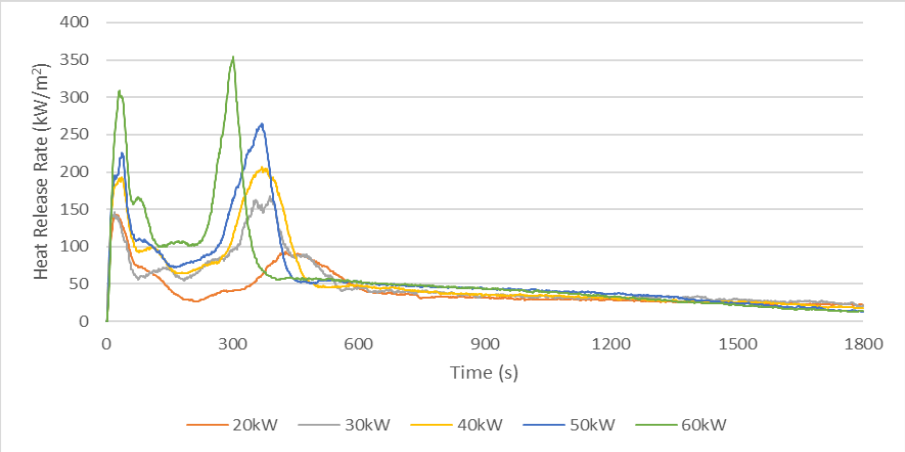


**Figure 27. Product F6 (12 mm plywood) mean HRR.**

### 3.1.3 Minimum heat flux for ignition

Minimum heat flux for ignition was determined in a similar manner to Baker et al. by reducing the incident heat flux from the cone to the point where the sample did not ignite within 30 minutes of exposure. Baker et al. proposed the actual minimum heat flux required for ignition would fall somewhere between the heat flux that failed to result in ignition and the minimum heat flux at which ignition did occur and taking the mid-point of the two, with the inherent assumption that the error was plus or minus half the interval. Baker et al. used 2 kW/m² steps whereas this research used 1 kW/m² steps. Minimum heat flux data for each product is contained in Appendix B. No minimum heat flux data was recorded for products A1 or D1.

**Table 26. Minimum heat flux for ignition.**

| Product | Critical heat flux -$\dot{q}''_{min}$ (kW/m²) |
|---|---|
| B1 | 9.5 |
| B2 | 9.5 |
| C1 | 13.5 |
| D2 | 12.5 |
| D3 | 17.5 |
| F1 | 9.5 |
| F2 | 10.5 |
| F3 | 12.5 |
| F4 | 9.5 |
| F5 | 9.5 |
| F6 | 9.5 |

### 3.1.4 Clustering analysis

The results from the cone calorimeter experiments were analysed to determine if they could be clustered into similar-performing materials. The goal of the clustering analysis at small-scale was to reduce the number of materials required to be tested at room-scale. Five different methods were assessed.

#### 3.1.4.1 Flux time product method

The first method used to attempt to cluster the materials was by calculating the FTP used by both Peel and Baker et al. using Eqn. 2-1.

Where Peel and Baker et al. used the method to calculate the critical flux, this clustering method used the FTP itself to see if the materials could be grouped.

#### 3.1.4.2 FIGRA method

The Single Burning Item (SBI) test method (EN 13823) is the basis for the FIGRA parameter (short for **Fi**re **G**rowth **Ra**te). Data from the SBI was compared to the ISO 9705 room corner test where an HRR of 1 MW is deemed to be the HRR at flashover, regardless of material, as the fire is ventilation limited (Sundström, 2007). From this, the $FIGRA_{RC}$ parameter (where $_{RC}$ signifies the room corner test method ISO 9705) was calculated as either the flashover criterion HRR (i.e. 1,000 kW) or the peak HRR (if flashover is not reached) less the burner contribution divided by the time at that point:

$$FIGRA_{RC} = \frac{1000 - Q_{burner}}{t_{fo}} \text{ or } FIGRA_{RC} = \frac{Q_{peak} - Q_{burner}}{t_{peak}} \qquad \textbf{Eqn. 3-1}$$

A similar version of the FIGRA parameter based on cone calorimetry testing was developed for the present project based on the peak HRR per unit area of the material:

$$FIGRA_{cone} = \frac{HRRPUA_{peak}}{t_{peak}} \qquad \textbf{Eqn. 3-2}$$

where:

$FIGRA_{cone}$ = fire growth rate parameter derived from cone testing data (kW/m²s)

$HRRPUA_{peak}$ = peak HRR derived from cone testing data (kW/m²)

$t_{peak}$ = time to peak HRRPUA (s).

#### 3.1.4.3 Time to ignition method

The basis of Method 3 was simply to analyse the data by plotting the incident radiant heat flux, $\dot{q}''$, versus the ignition time, $t_{ig}$, and identifying any grouping of materials.

#### 3.1.4.4 Minimum heat flux for ignition method

For the purposes of Method 4, the minimum heat flux for ignition, as determined in section 3.1.3 was used.

#### 3.1.4.5 NZBC Group Number method

Group Numbers are a way of classifying internal wall and ceiling linings to meet specific performance requirements in the NZBC.

Verification Method C/VM2 Appendix A defines the calculation procedure for defining the Group Number when materials are tested in the cone calorimeter.

### 3.1.5 Clustering results

#### 3.1.5.1 Flux time product method

The experimental data was analysed in accordance with the procedure described in section 3.1.4.1. Table 27 provides a summary of the FTP dataset for each product.

Further clustering analysis was attempted but no additional insight was gained.

**Table 27. $\dot{q}''_{cr}$ deterimined by FTP method.**

| Product | $\dot{q}''_{cr}$ (kW/m²) | $FTP$ ((kW/m²)$^n$s) | $n$ (-) |
|---|---|---|---|
| A1 | 11.6 | 34299 | 2 |
| B1 | 9.2 | 41311 | 2 |
| B2 | 8.2 | 41469 | 2 |
| C1 | 13.4 | 8594 | 1.7 |
| D1 | 0.5 | 88173 | 2 |
| D2 | 1.5 | 66384 | 2 |
| D3 | 3.5 | 65306 | 2 |
| F1 | 7.5 | 42663 | 2 |
| F2 | 3.9 | 52436 | 2 |
| F3 | 9.9 | 12880 | 1.7 |
| F4 | 7.9 | 46621 | 2 |
| F5 | 7.8 | 37083 | 2 |
| F6 | 7.4 | 18558 | 1.8 |

The FTP dataset for the thickest product A1 (63 mm thick LVL, density ~ 575 kg/m³) was $\dot{q}''_{cr}$ = 11.6, $FTP$ = 34299 and $n$ = 2, while the corresponding best-fit parameters for the thinnest product B1 (7 mm thick plywood, density ~520 kg/m³) was $\dot{q}''_{cr}$ = 9.2, $FTP$ = 41311 and $n$ = 2. The comparison of these two datasets suggests that both products A1 and B1 are acting as thermally thick materials, which is not logical given their physical properties, whereas the best-fit parameters for product C1 (50 mm thick CLT, density ~458 kg/m³) was $\dot{q}''_{cr}$ = 13.4, $FTP$ = 8594 and $n$ = 1.7, indicating it is thermally thinner than the 7 mm plywood (product B1).

It is also considered that basing the FTP results solely on $R^2$ is unreliable. For example, it was considered highly unlikely that product D1 would have a critical heat flux of 0.5 kW/m². This is further supported by the cone testing results, which indicated that none of the products had a $\dot{q}''_{min}$ below 9.5 kW/m².

### 3.1.5.2 FIGRA method

The experimental data was analysed in accordance with the procedure described in section 3.1.4.2. The data was then plotted as shown in Figure 28.

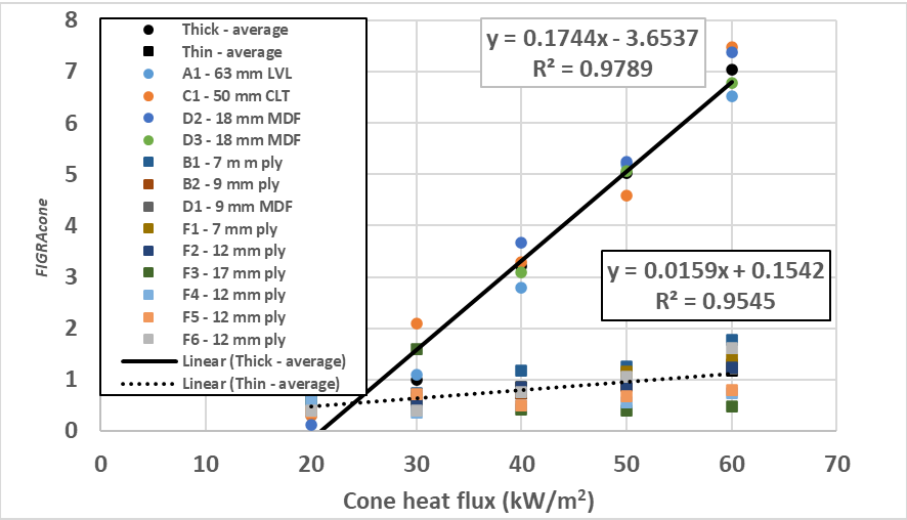


**Figure 28. FIGRA$_{cone}$ vs cone heat flux.**

The data was grouped into two clusters – nominally thick and thin – and a linear trendline fitted to each cluster. Products A1, C1 D2 and D3 were grouped into the thick cluster and the balance of products into the thin cluster. Method 2 was considered to be successful in grouping the materials into two distinctly different clusters (Figure 28).

### 3.1.5.3 Time to ignition method

The experimental data were analysed in accordance with the procedure described in section 3.1.4.3. The plotted data is shown in Figure 29.

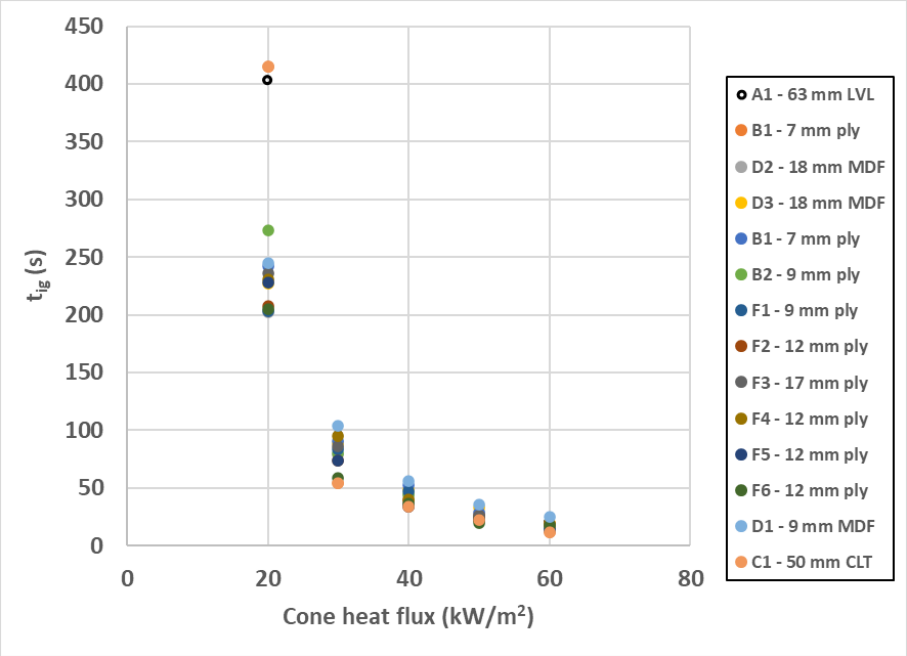


**Figure 29. $t_{ig}$ vs cone heat flux.**

Although Method 3 did differentiate product A1 and product C1 at the lowest heat flux setting, thereafter there were no discernible groupings. As such, Method 3 was not able to be used to cluster the different EWP products.

### 3.1.5.4 Experimental critical heat flux method

The experimental data were analysed in accordance procedure described in section 3.1.4.4. Table 28 provides a summary of the experimental minimum heat flux for ignition data for the different EWPs (excluding product D1).

Using Method 4 it is possible to group the products into two distinct clusters. The first cluster is the so-called thick cluster (products A1, C1, D2, D3 and F3), while the thin cluster is the balance of the products (and assuming product D1 is in this cluster). One limitation with Method 4, however, is that the difference between product F3 at the low end of the thick cluster and product F2 at the top end of the thin cluster is not large.

A second limitation is that the method does not appear to group product D2 ($\dot{q}''_{min}$ = 12.5 kW/m²) and D3 ($\dot{q}''_{min}$ = 17.5 kW/m²), which would be expected to give a similar result due to their physical similarity.

Bearing these limitations in mind, Method 4 was not considered as suitable to group the materials into clusters.

**Table 28. Summary of $\dot{q}''_{min}$ for all products.**

| Product | $\dot{q}''_{min}$ (kW/m²) |
|---|---|
| A1 | 13.5 |
| B1 | 9.5 |
| B2 | 9.5 |
| C1 | 13.5 |
| D1 | Not recorded |
| D2 | 12.5 |
| D3 | 17.5 |
| F1 | 9.5 |
| F2 | 10.5 |
| F3 | 12.5 |
| F4 | 9.5 |
| F5 | 9.5 |
| F6 | 9.5 |

### 3.1.5.5 NZBC Group Number method

The NZBC Group Numbers were calculated for each product at 50 kW exposure, as per Appendix A of C/VM2. The results are shown in Appendix C of this report.

All the products tested came out as Group 3, as expected, so the IQ1 and IQ2 values were used to see if any useful clusters could be established as shown in Figure 30. This revealed two main clusters – a small cluster containing products D2 and D3 (nominally very similar products) and the remaining products contained in the main cluster (with some outliers). This method was not considered a useful clustering tool.

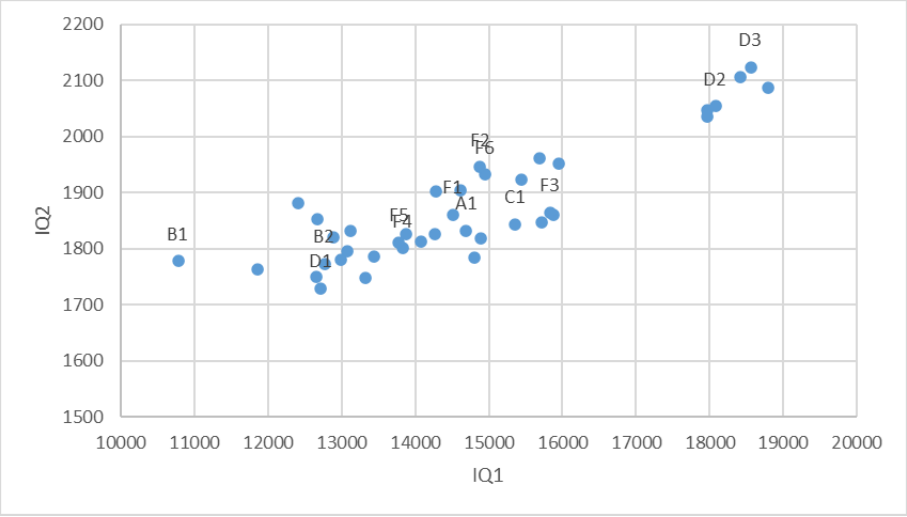


**Figure 30. IQ1 vs IQ2 cluster analysis.**

# 4. Room-scale testing

Following the clustering analysis, a material was selected from each of the thick and thin groups identified using the FIGRA analysis described in 3.1.5.2 and then tested at ISO 9705 room scale. It was decided that by selecting materials D1 (9 mm MDF) and D3 (18 mm MDF), from the same manufacturer, other experimental differences could be minimised. Pyrolysis parameters were also available for the MDF products for modelling purposes.

## 4.1 Lining configuration

The lining configurations chosen are shown in Table 29. Each configuration was tested with both material thicknesses, resulting in 14 experiments.

**Table 29. ISO 9705 room test configurations.**

| Experiment | Location of timber wall linings | Ceiling linings | Lower wall L (m²) | Upper wall U (m²) | Ceiling C (m²) | (Nominal) total lining area (m²) |
|---|---|---|---|---|---|---|
| 1810_1_9<br>1810_1_18 | Fully lined | Fully lined | 11.5 | 11.5 | 8.6 | 31.6 |
| 1810_2_9<br>1810_2_18 | None | Fully lined | - | - | 8.6 | 8.6 |
| 1810_3_9<br>1810_3_18 | Lower wall extending 3.6 m from burner corner | None | 8.6 | - | - | 8.6 |
| 1810_4_9<br>1810_4_18 | Upper wall extending 3.6 m from burner corner | None | - | 8.6 | - | 8.6 |
| 1810_6_9<br>1810_6_18 | Full-height wall extending 3.6 m from burner corner | None | 8.6 | 8.6 | - | 17.3 |
| 1810_7B_9<br>1810_7B_18 | Upper wall extending 2.4 m from burner corner, lower wall extending 1.2 m from burner corner | Fully lined | 2.9 | 5.8 | 8.6 | 17.3 |
| 1810_7D_9<br>1810_7D_18 | Upper wall extending 3.6 m from burner corner | Fully lined | - | 8.6 | 8.6 | 17.3 |

Moving away from the material used by both Peel and Baker et al. (7 and 12 mm thick plywood), it was considered that a fully lined configuration (Experiment 1) should be undertaken to provide a baseline comparison between the 7 mm and 12 mm plywood (with 15 mm calcium silicate backing) used by Peel and Baker et al., the 9 mm MDF and the 18 mm MDF in this research.

Configurations 2 and 4 matched the experiments by Peel and Baker et al., providing a comparison between 7 mm plywood, 12 mm plywood, 9 mm MDF and 18 mm MDF.

Configurations 3 and 6 again matched Peel, while 7B and 7D matched Baker et al.

## 4.2 Results

### 4.2.1 Heat release rate

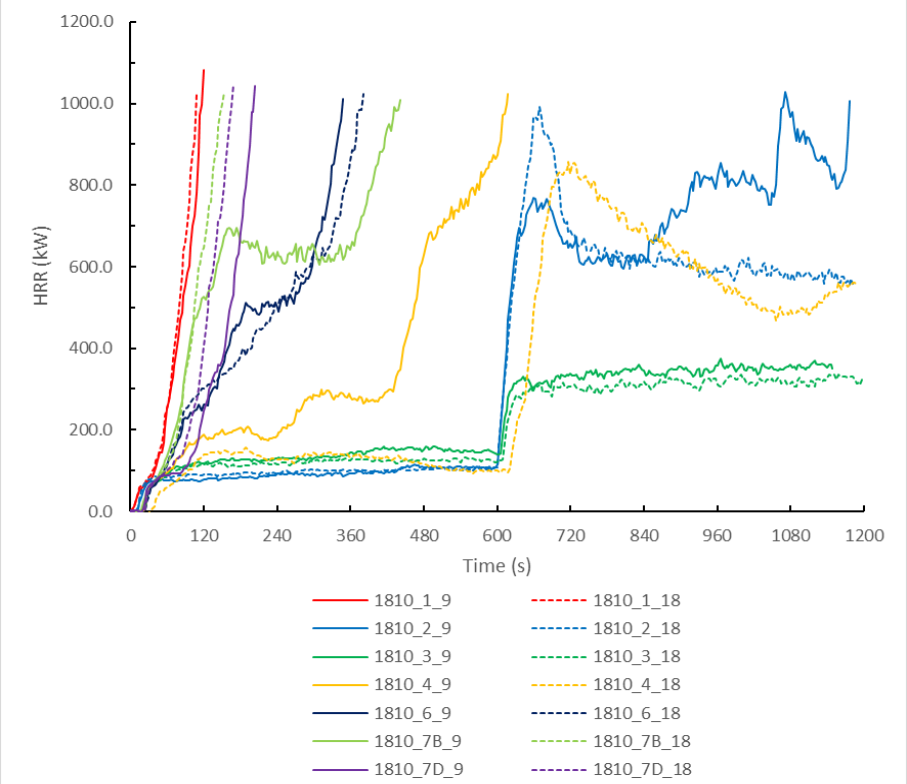


**Figure 31. HRR – all configurations.**

A comparison of results against Peel and Baker et al. was done for each configuration, where available.

#### 4.2.1.1 Experiment 1

All three materials performed very similarly up to 500 kW (Figure 32).

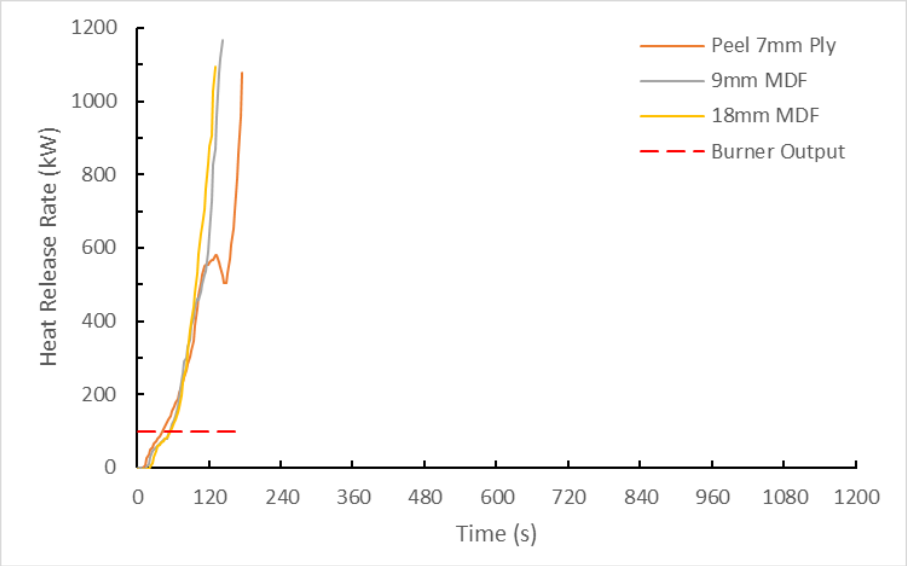


**Figure 32. Experiment 1 HRR comparison.**

At approximately 100 s, the 7 mm ply used by Peel shows a decrease in heat output, followed by an increase in output again at approximately 147 s before reaching flashover. It was considered this may have been the result of ply falling away.

The difference in the fire growth rate between the 9 mm and 18 mm MDF was negligible. With the room fully lined, both MDF products and the plywood product used by Peel achieve a Group 3 rating based on the criteria set out in Appendix A of C/VM2.

#### 4.2.1.2 Experiment 2

The 9 mm MDF, 18 mm MDF and 12 mm plywood materials contributed very little with the burner at 100 kW (Figure 34).

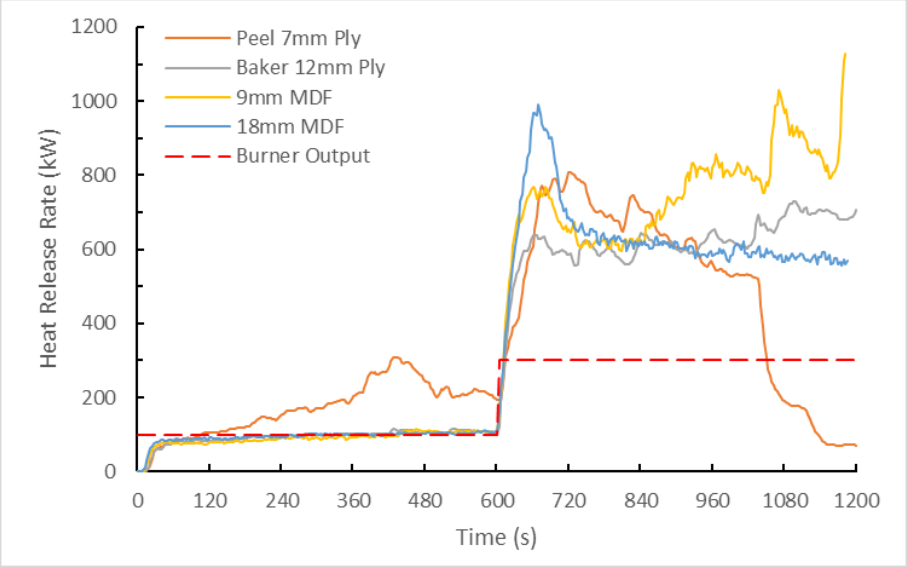


**Figure 33. Experiment 2 HRR comparison.**

After the burner output was increased to 300 kW, the 18 mm MDF came very close to the 1 MW limit (991 kW), but the output then reduced to a steady-state approximately 600 kW, achieving the equivalent of a Group 1 rating.

It is considered 9 kW is well within the expected margins of error (<1%) and might therefore have reached the 1 MW threshold and achieved only a Group 2 rating.

The 9 mm MDF had a lower peak after the burner output was increased to 300 kW. However, after dropping back down to approximately 600 kW, the same as the 18 mm MDF, the 9 mm MDF began to contribute more as the experiment continued, eventually exceeding the 1 MW threshold at 1,071 s, resulting in the equivalent of a Group 2 material.

When compared to the 7 mm plywood used by Peel (which achieved the equivalent of a Group 1), the 18 mm MDF was more closely matched to the plywood. This is contrary to the assumption that, based on the clustering analysis, the 7 mm ply would perform similarly to the 9 mm MDF and the 18 mm MDF would perform differently from both the 7 mm plywood and the 9 mm MDF. However, Peel conducted experiments with 15 mm thick calcium silicate backing (to represent being direct fixed), whereas these experiments were conducted with a cavity (to represent being batten fixed), so the 7 mm plywood used by Peel might have been expected to perform more closely to the 18 mm MDF than the clustering analysis suggested.

#### 4.2.1.3 Experiment 3

With just the lower part of the walls lined, both the 9 mm MDF and the 18 mm MDF performed similarly to the 7 mm plywood used by Peel, although the 7 mm plywood did appear to contribute slightly more and was continuing to become more involved towards the end of the experiment where the MDF was not (Figure 34).

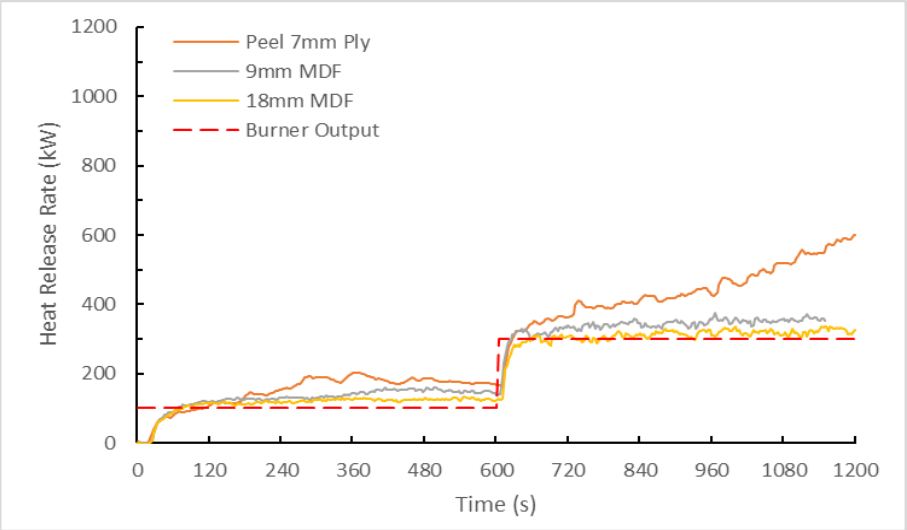


**Figure 34. Experiment 3 HRR comparison.**

This is possibly down to increased incident heat flux as a result of flaming combustion of the plywood compared to smouldering combustion of the MDF observed. All three products achieved the equivalent of a Group 1 material. As the MDF did not contribute much to the HRR with only the ceiling lined, it was considered that the potential difference in performance from a thick material (18 mm MDF) and thin material (9 mm MDF) as identified in the clustering analysis would not be noticeable.

#### 4.2.1.4 Experiment 4

With only the upper walls lined, the 7 mm plywood used by Peel almost reached the 1 MW threshold before dropping back down to around 600 kW (Figure 35).

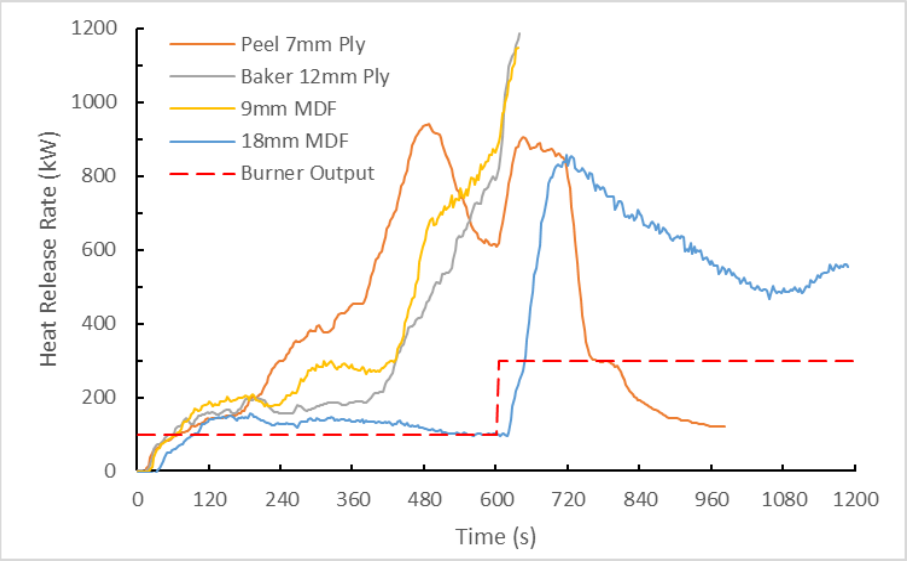


**Figure 35. Experiment 4 HRR comparison.**

At 600 s, the HRR goes back up as the burner output increased to 300 kW but again drops down significantly after 720 s, resulting in the equivalent of a Group 1 material.

Baker et al. (2017) hypothesised that the reason for not reaching the 1 MW threshold was that the available fuel had been largely expended and therefore undertook the same experimental configuration using 12 mm plywood (increasing the available fuel by approximately 70%). This exceeded the 1 MW threshold as predicted at around 615 s, giving the 12 mm ply the equivalent of a Group 2 material in this configuration and thus confirming the hypothesis.

The 9 mm MDF performed almost identically to the 12 mm plywood, exceeding 1 MW at 618 s and also achieving the equivalent of a Group 2 material.

The 18 mm MDF performed quite differently with very little contribution before the burner output increased to 300 kW and, even then, only reaching a peak of approximately 860 kW around 720 s before dropping back down. The 18 mm MDF in this configuration achieved the equivalent of a Group 1 material.

#### 4.2.1.5 Experiment 6

With both upper and lower walls lined 3.6 m from the burner corner, the 9 mm and 18 mm MDF performed very similarly to the 7 mm plywood used by Peel. All three materials reached the 1 MW threshold between 348 and 411 s, equivalent to a Group 3 material (Figure 36).

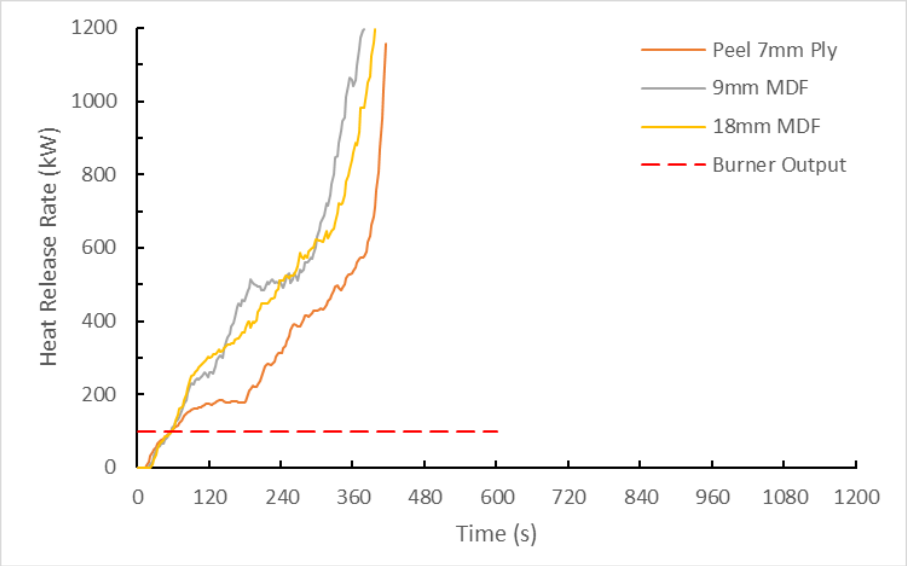


**Figure 36. Experiment 6 HRR comparison.**

This is again contrary to the hypothesis suggested by the clustering analysis, which would indicate that the 18 mm MDF should perform differently to the 7 mm plywood and the 9 mm MDF. The MDF products performed almost identically up to 600 kW, whereas the plywood used by Peel had a slightly slower growth rate. It is noted that the plywood rapidly increased to flashover at the same point as both the 9 mm and 18 mm MDF at around 600 kW.

#### 4.2.1.6 Experiment 7B

Experimental configuration 7B had the ceiling lined, the upper walls lined 2.4 m from the burner and the lower walls lined 1.2 m from the burner.

Given the plume shape and height from the burner, this is not significantly different from fully lining the room, the main difference being a slight reduction in fuel available in the hot upper layer from the upper walls. Up to 500 kW at around 105 s, both the 9 mm MDF and the 18 mm MDF performed identically to the 7 mm plywood used by Peel (Figure 37).

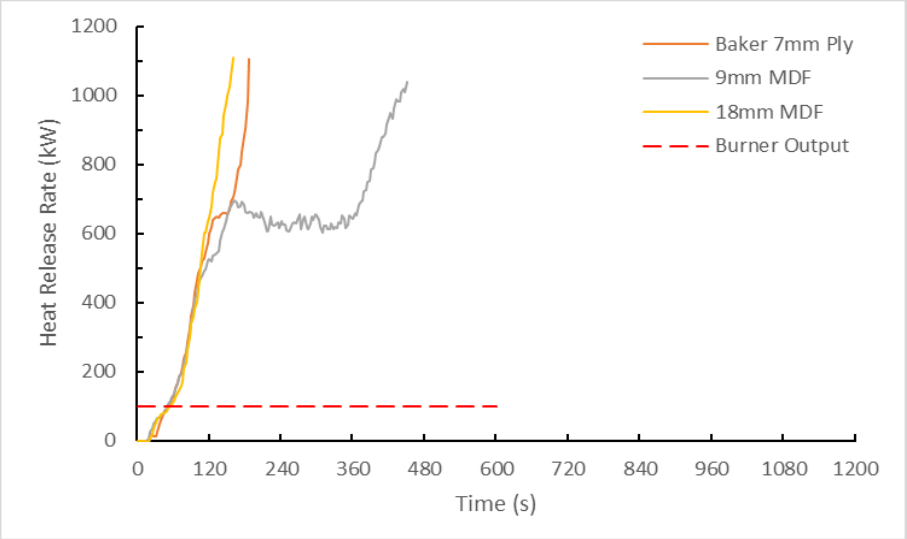


**Figure 37. Experiment 7B HRR comparison.**

After 105 s, the 18 mm MDF and the 7 mm plywood used by Baker et al. continued to contribute to the growth of the fire in the same way as a fully lined room. Both reached the 1 MW threshold at similar times to the fully lined room, giving them a Group 3 equivalent rating. The 9 mm MDF did perform differently from the fully lined room, plateauing at approximately 600 kW before increasing again at around 360 s, reaching 1 MW at 447 s. However, it still achieved the equivalent of a Group 3 rating.

This was a result of the 9 mm MDF char falling off (Figure 38) whereas in the fully lined room in Experiment 1810_1_9, there was no char fall off (Figure 39).

**Figure 38. Experiment 1810_7B_9 after extinguishment.**

**Figure 39. Experiment 1810_1_9 after extinguishment.**

The 18 mm MDF also stayed in place (Figure 40).

**Figure 40. Experiment 1810_7B_18 after extinguishment.**

#### 4.2.1.7 Experiment 7D

Experimental configuration 7D had the ceiling lined and the upper walls lined 3.6 m from the burner. This increased the fuel available in the hot upper layer compared to configuration 7B but removed the fuel between the burner and the upper walls.

However, the length of the burner plume is such that even at 100 kW, the flame was still able to impinge on the fuel on the upper walls.

All three materials performed almost identically as shown in Figure 41 and were very similar to the fully lined room, reaching the 1 MW threshold at similar times to the fully lined room and achieving a Group 3 equivalent.

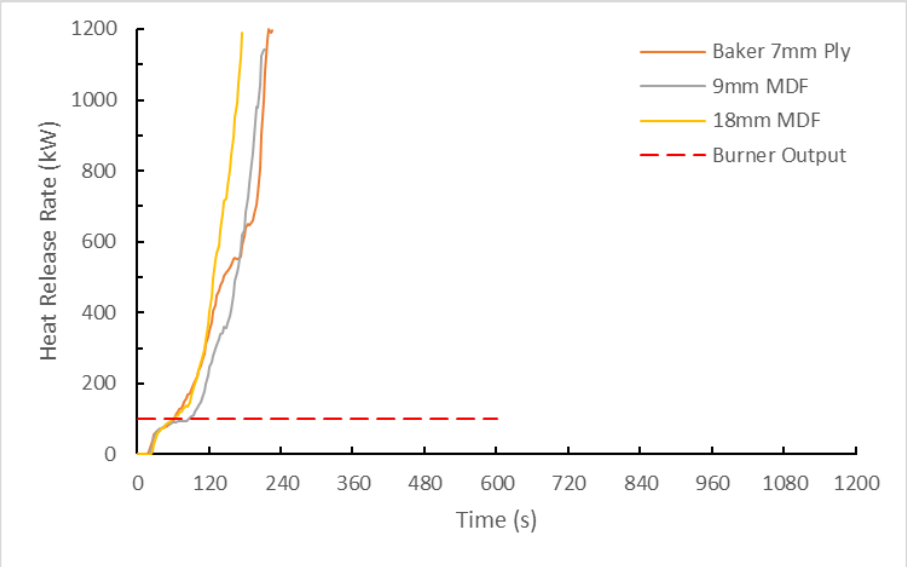


**Figure 41. Experiment 7D HRR comparison.**

### 4.2.2 Time to peak heat release rate

The time taken to reach flashover or the time to peak heat release rate if flashover did not occur was measured in order to calculate the $FIGRA_{RC}$ (Table 30).

**Table 30. Time to peak HRR for 9 mm and 18 mm thick MDF.**

| Experiment | Flashover | HRR | Time to peak HRR (s) | Burner HRR (kW) | Equivalent Group Number | $FIGRA_{RC}$ |
|---|---|---|---|---|---|---|
| 1_9 | Yes | >1 MW | 135 | 100 | 3 | 6.67 |
| 1_18 | Yes | >1 MW | 126 | 100 | 3 | 7.14 |
| 2_9 | Yes | >1 MW | 1071 | 300 | 2 | 0.65 |
| 2_18 | No | 991.5 kW | 669 | 300 | 1 | 1.03 |
| 3_9 | No | 375.8 kW | 966 | 300 | 1 | 0.08 |
| 3_18 | No | 336.6 kW | 1143 | 300 | 1 | 0.03 |
| 4_9 | Yes | >1 MW | 615 | 100 | 2 | 1.46 |
| 4_18 | No | 857.2 kW | 717 | 300 | 1 | 0.78 |
| 6_9 | Yes | >1 MW | 348 | 100 | 3 | 2.59 |
| 6_18 | Yes | >1 MW | 381 | 100 | 3 | 2.36 |
| 7B_9 | Yes | >1 MW | 441 | 100 | 3 | 2.04 |
| 7B_18 | Yes | >1 MW | 150 | 100 | 3 | 6.00 |
| 7D_9 | Yes | >1 MW | 204 | 100 | 3 | 4.41 |
| 7D_18 | Yes | >1 MW | 168 | 100 | 3 | 5.36 |

The 18 mm MDF would appear to have pyrolysed more fuel than the 9 mm MDF, resulting in flashover earlier in experimental configurations 1, 7B and 7D. It is suggested that this is a result of having the maximum fuel available in the location of the highest incident heat flux (i.e. where the burner flame was able to directly impinge on the MDF).

In experimental configuration 2 where only the ceiling was lined, at the lower 100 kW burner output, there was little contribution by either material.

It is proposed that the incident heat flux was not sufficient to cause ignition at the ceiling. Once the burner output was increased to 300 kW, the incident heat flux was sufficient to pyrolyse the area immediately above the burner causing an increase in heat release to a peak of 991 kW at 669 s but insufficient to cause ignition of the 18 mm MDF and therefore reducing towards the end of the experiment.

The 9 mm MDF was ignited, enabling a higher incident heat flux from the flaming combustion, causing a gradual increase in the HRR before reaching the 1 MW threshold at 1,071 s.

In experimental configuration 3 where only the lower walls were lined, neither material contributed much at either 100 kW or 300 kW burner output. Although the peak HRR measured for the 9 mm MDF was approximately 375 kW at 966 s, the general trend after the burner output increased to 300 kW was a gradual increase in heat release of approximately 77 W/s.

The same can be said for the 18 mm MDF. Although the peak was measured as 337 kW at 1,143 s, the trend after the burner output increased to 300 kW was a gradual increase in heat release of approximately 56 W/s. This is considered relevant when using $FIGRA_{RC}$ as a measure since the trend is likely more representative of the product performance, than a transient peak along the way.

Experimental configuration 4 performed quite differently from configurations 2 and 3, even though there was the same amount of fuel in the compartment. The fuel was located around the upper walls within the hot gas layer.

The thinner 9 mm MDF ignited after approximately 400 s. The increased heat flux from the flaming combustion caused the heat release to increase at approximately 1.9 kW/s. When the burner output was increased to 300 kW, the heat release jumped up and reached the 1 MW threshold at 615 s. It was considered that, even if the burner output had not been increased to 300 kW, the 9 mm MDF would have still exceeded the 1 MW threshold within 70 s if it had continued to grow at the same rate. The 18 mm MDF reached a peak of 857.2 kW at 717 s.

Experimental configuration 6 had just the upper and lower wall lined, extending 3.6 m from the burner location in the corner. The 9 mm MDF exceeded the 1 MW threshold at 348 s whereas the 18 mm MDF exceeded the threshold at 381 s. Both materials performed almost identically up to around 600 kW, at which point the rate of increase for the 9 mm MDF exceeded that of the 18 mm MDF.

### 4.2.3 Gas temperature

Gas temperatures within the ISO 9705 compartment were measured using a thermocouple tree located adjacent to the doorway with thermocouples at 260 mm, 670 mm, 970 mm, 1,270 mm, 1,420 mm, 1,570 mm, 1,720 mm, 1,910 mm and 2,100 mm above the floor level of the compartment.

For experimental configuration 1, at the point of flashover, the upper gas layer temperature for both materials was around 500–550°C and the boundary between the upper and lower gas layers was between 1,420 and 1,570 mm up from the compartment floor as shown in Figures 43 and 44.

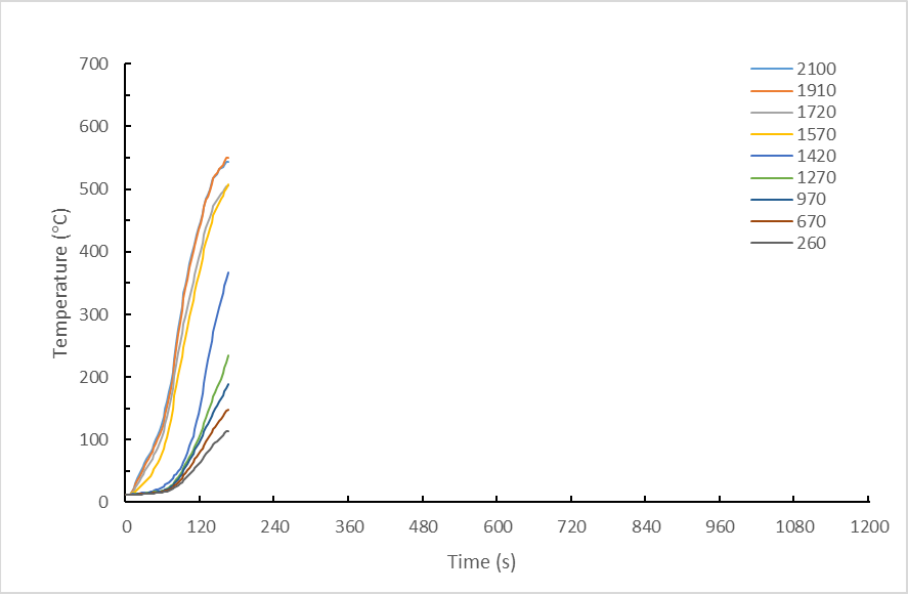


**Figure 42. Experiment 1_9 compartment temperatures.**

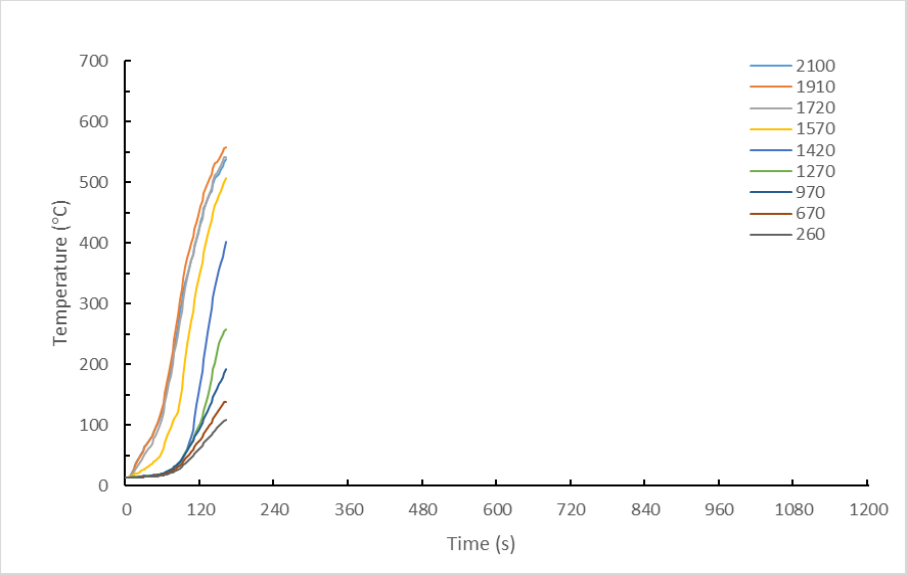


**Figure 43. Experiment 1_18 compartment temperatures.**

In experimental configuration 2 with the burner output at 100 kW, a hot layer developed between 150°C and 200°C, with the boundary between 1,570 mm and 1,720 mm from the floor of the compartment. At 600 s, the burner output was increased to 300 kW and the upper layer temperature was seen to go up to 500–500°C but the boundary remained at the same approximate height within the compartment.

With the 9 mm MDF, the temperature 1,570 mm above the floor increased initially after 600 s to around 440°C and continued to increase until the 1 MW threshold was reached at 1,074 s. The hot layer temperature also increased during this time, to between 550°C and 650°C (Figure 44). This is in line with the HRR measured.

With the 18 mm MDF, the temperature 1,570 mm above the floor increased initially after 600 s to around 440°C but then decreased over the remainder of the experiment to around 380°C at the end. This is in line with the decrease in HRR measured (in Figure 45).

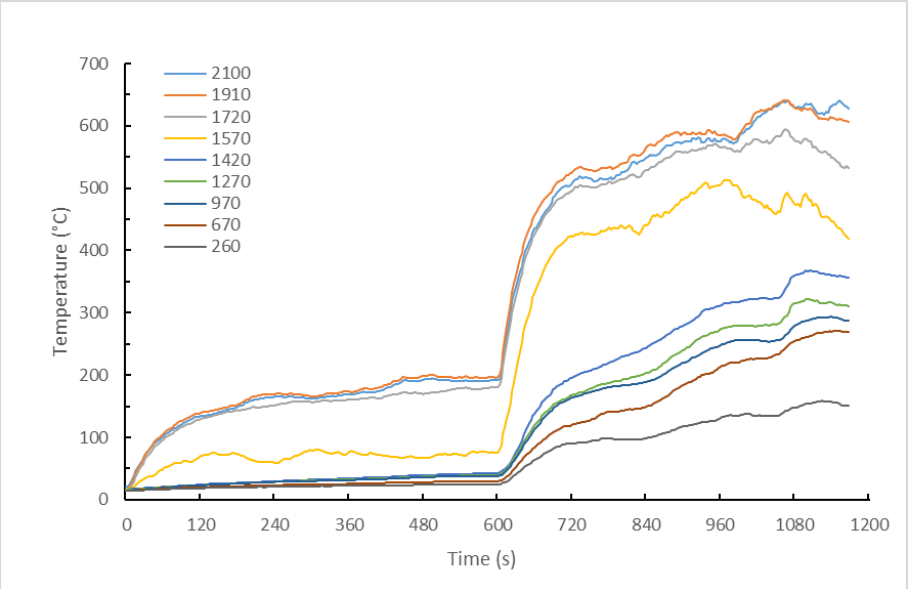


**Figure 44. Experiment 2_9 compartment temperatures.**

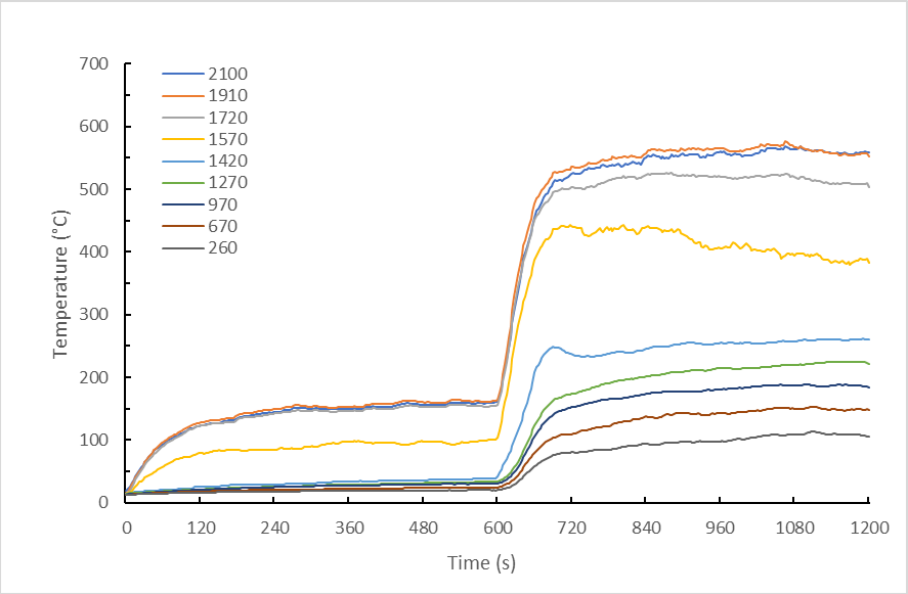


**Figure 45. Experiment 2_18 compartment temperatures.**

For experimental configuration 3, again the upper layer gas temperature was around 200°C at between 1,570 mm and 1,720 mm from the floor for both materials, when the burner output was 100 kW. When the output of the burner was increased to 300 kW at 600 s, the upper layer temperature increased to between 350 and 400°C for both materials, with no significant change in layer height.

For the 9 mm MDF, the temperature at 1,570 mm above the floor also rose from around 80°C and continued to rise (Figure 46), reaching over 350°C, indicating that the hot layer had descended to between 1,570 mm and 1,420 mm from the floor.

For the 18 mm MDF, the temperature at 1,570 mm above the floor rose from around 80°C to approximately 200°C after the burner output was increased to 300 kW (Figure 47). This is in line with the HRR measured, which indicated that the 18 mm MDF made little contribution in this scenario.

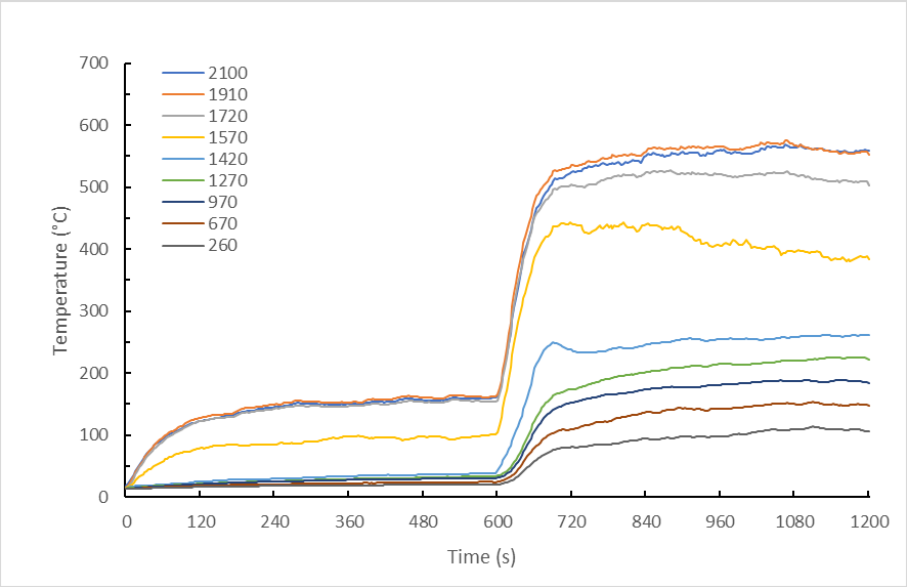


**Figure 46. Experiment 3_9 compartment temperatures.**

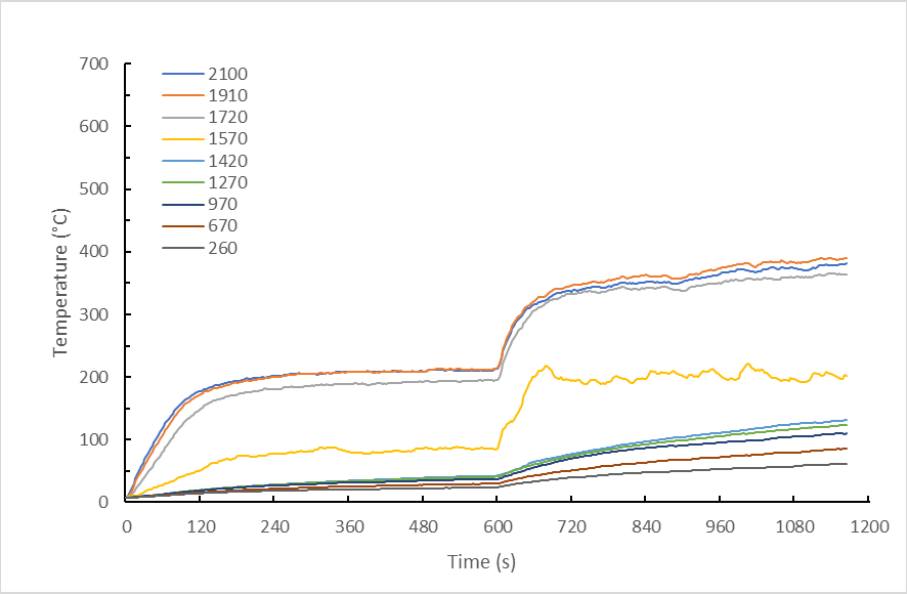


**Figure 47. Experiment 3_18 compartment temperatures.**

With experimental configuration 4, the first 180 s are almost identical in thermal profile. A hot layer begins to form at 250–300°C and 1,570–1,720 mm from the floor of the compartment.

The 9 mm MDF is ignited at this point and the temperature continues to rise, reaching between 600°C and 650°C (Figure 48). The hot layer also descends below 1,570 mm from the floor, shortly before the 1 MW threshold is reached at 615 s.

The 18 mm MDF hot layer remained stable from 180 s until the burner output is increased to 300 kW, at which time, the upper layer temperature increases to between 550°C and 650°C (Figure 49). The layer height also descends to between 1,270 mm and 1,420 mm from the floor of the compartment. The compartment temperature reaches a peak at around 800 s before reducing slightly by 1,080 s. This is in line with the HRR measured.

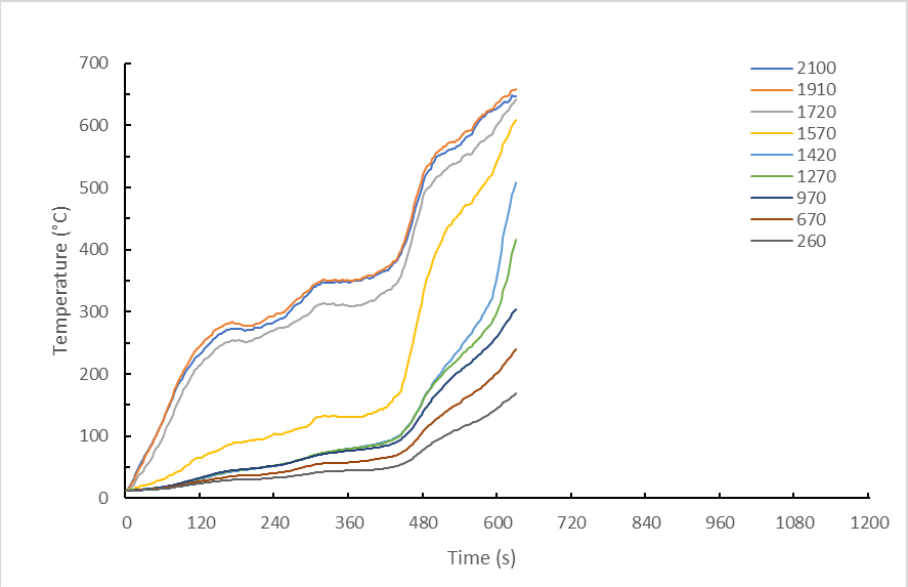


**Figure 48. Experiment 4_9 compartment temperatures.**

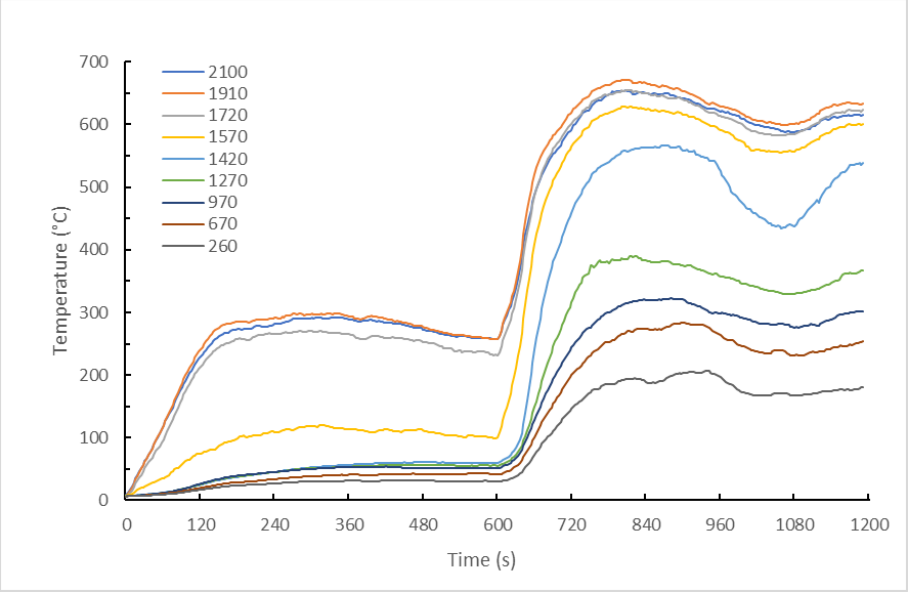


**Figure 49. Experiment 4_18 compartment temperatures.**

Experimental configuration 6 performed almost identically for both MDF products. A hot layer develops between 1,570 mm and 1,720 mm as shown in Figures 51 and 52. It continues to increase in temperature. By approximately 300 s, the layer height has dropped to between 1,420 mm and 1,570 mm from the floor and the temperature is still rising.

By the time the 1 MW threshold is exceeded (348 s for the 9 mm MDF and 381 s for the 18 mm MDF), the upper layer height had dropped to between 970 mm and 1,270 mm from the floor of the compartment. This is again in line with the HRR measured from both products.

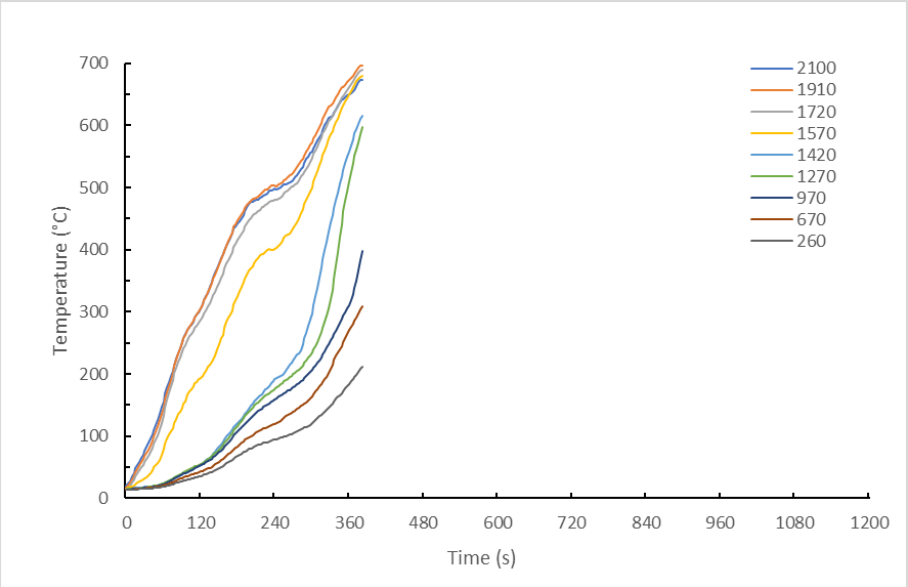


**Figure 50. Experiment 6_9 compartment temperatures.**

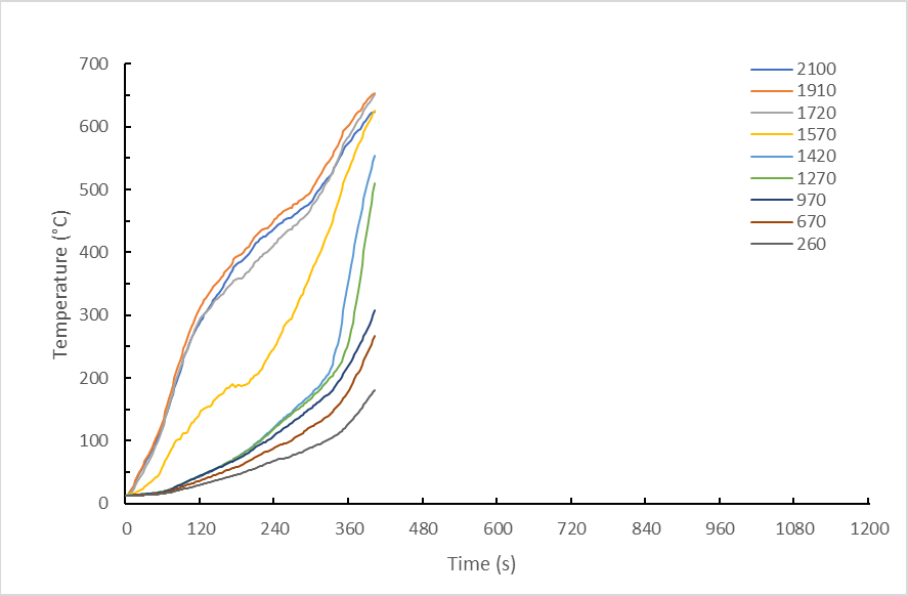


**Figure 51. Experiment 6_18 compartment temperatures.**

Experimental configuration 7B was considered very similar to the fully lined compartment, but with slightly less fuel around the upper walls, it was expected to take slightly longer to reach flashover.

For the first 100 s, the 9 mm MDF performed very similarly to the 18 mm MDF. However, after 100 s, the 9 mm MDF did not increase in temperature at the same rate, taking a further 260 s for the upper layer to reach 550–600°C (Figure 52). By the time the compartment exceeded the 1 MW threshold, the hot layer had descended below 1,420 mm and was approaching 1,270 mm above the floor of the compartment.

The delay in the 9 mm MDF reaching flashover was considered a result of the thin material and reduced coverage, resulting in insufficient fuel immediately available.

The 18 mm MDF did perform as expected – a hot gas layer quickly formed down to 1,720 mm above the floor (Figure 53). The temperature continued to rise and the layer height dropped further to 1,570 mm above the floor before reaching the 1 MW threshold at 153 s.

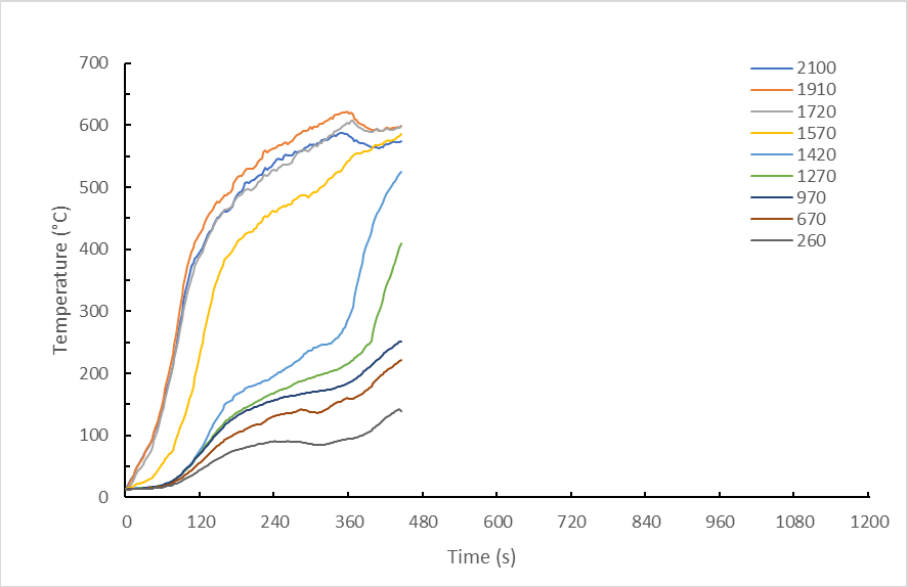


**Figure 52. Experiment 7B_9 compartment temperatures.**

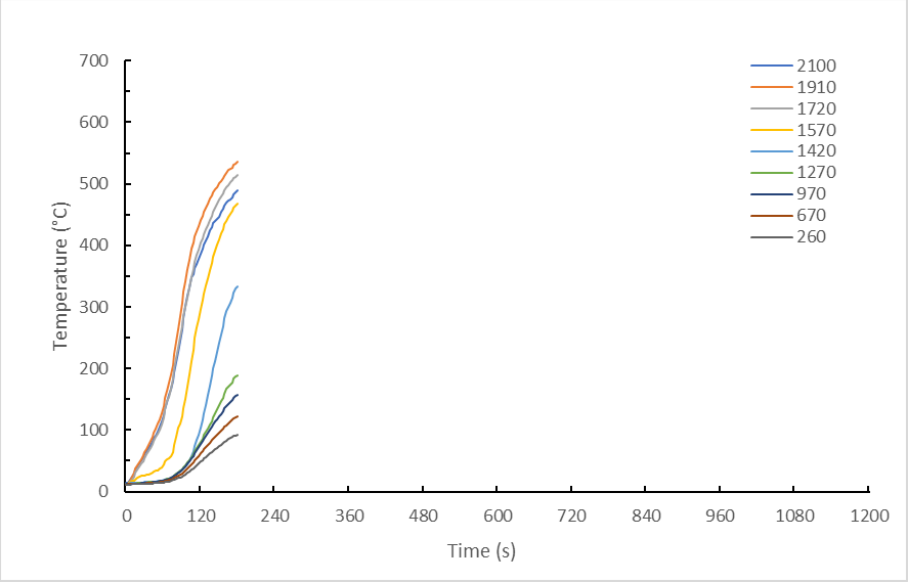


**Figure 53. Experiment 7B_18 compartment temperatures.**

Experimental configuration 7D was again expected to perform similarly to the fully lined room. However, with no fuel along the lower wall sections, it was expected that this configuration should take slightly longer to reach flashover.

Both materials performed very similarly. A hot layer down to 1,720 mm above the floor quickly formed, as shown in Figures 55 and 56, and continued to increase in temperature throughout the test. The layer descended to 1,570 mm above the floor shortly before the compartment exceeded the 1 MW threshold.

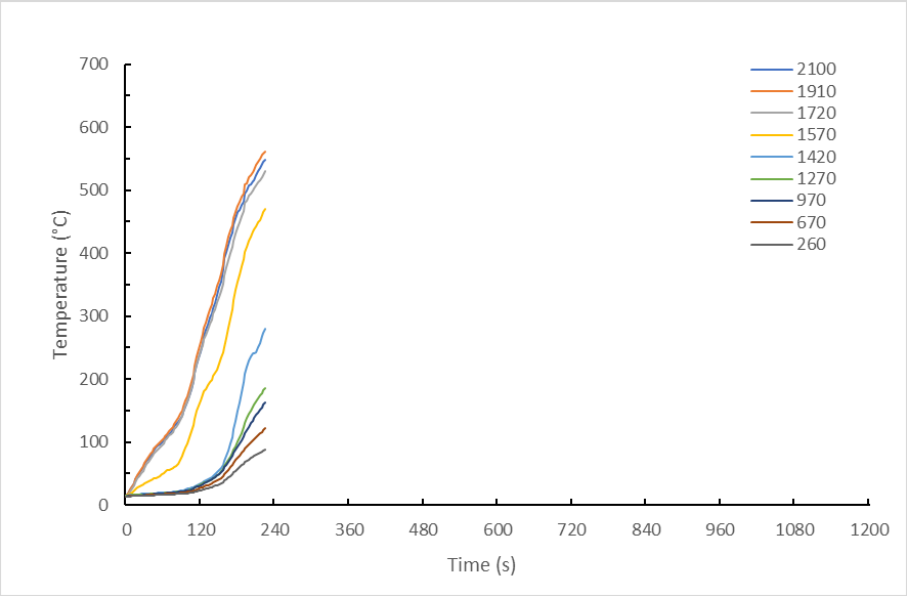


**Figure 54. Experiment 7D_9 compartment temperatures.**

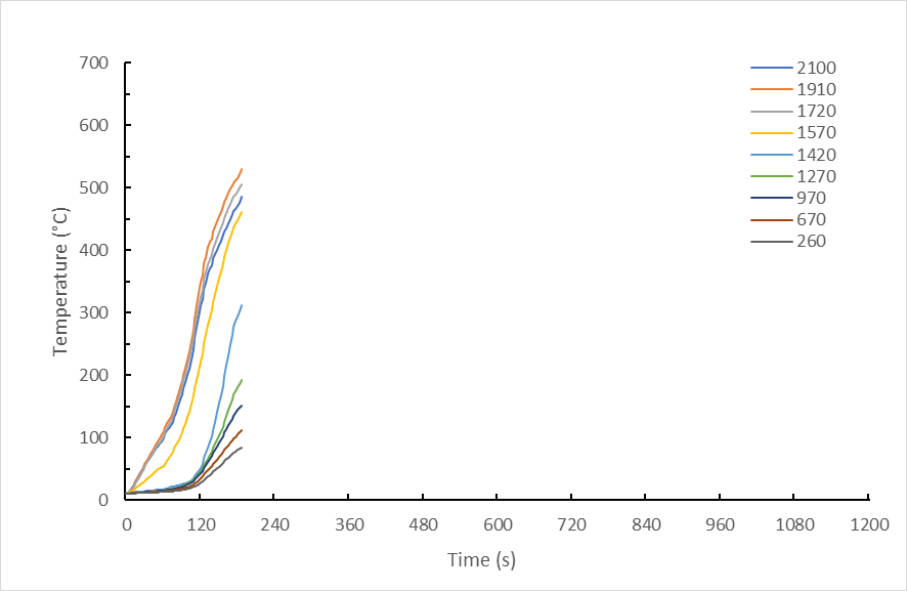


**Figure 55. Experiment 7D_18 compartment temperatures.**

### 4.2.4 Surface area burned

The end of each experiment was determined either by the HRR exceeding 1MW or a test time of 20 minutes, whichever was reached first. At the end of each experiment, a pole-mounted sprinkler was turned on to extinguish flaming and freeze the char pattern for later analysis.

Photographs were taken and an estimate of the burned surface area was made, based on the 100 mm grid drawn onto the MDF prior to the start of the test as shown in Figure 56.

**Figure 56. 100 mm grid prior to Experiment 4.**

Table 31 provides details of the surface area burned for each experimental configuration.

**Table 31. Experimental surface area burned.**

| Experiment | Area burned/total (m²) | | | % lined | % linings burned | Equivalent Group Number |
|---|---|---|---|---|---|---|
| | Ceiling (C) | Upper walls (U) | Lower walls (L) | | | |
| 1_9 | 8.6 / 8.6 | 8.5 / 11.5 | 0.6 / 11.5 | 100 | 56 | 3 |
| 1_18 | 8.6 / 8.6 | 8.5 / 11.5 | 0.6 / 11.5 | 100 | 56 | 3 |
| 2_9 | 8.6 / 8.6 | - | - | 27 | 100 | 2 |
| 2_18 | 8.6 / 8.6 | - | - | 27 | 100 | 1 |
| 3_9 | - | - | 0.75 / 8.6 | 27 | 9 | 1 |
| 3_18 | - | - | 0.75 / 8.6 | 27 | 9 | 1 |
| 4_9 | - | 8.6 / 8.6 | - | 27 | 100 | 2 |
| 4_18 | - | 8.6 / 8.6 | - | 27 | 100 | 1 |
| 6_9 | - | 8.6 / 8.6 | 5.4 / 8.6 | 54 | 81 | 3 |
| 6_18 | - | 8.6 / 8.6 | 5.4 / 8.6 | 54 | 81 | 3 |
| 7B_9 | 8.6 / 8.6 | 5.8 / 5.8 | 1.7 / 2.9 | 54 | 91 | 3 |
| 7B_18 | 8.6 / 8.6 | 3.6 / 5.8 | 0.6 / 2.9 | 54 | 74 | 3 |
| 7D_9 | 8.6 / 8.6 | 6.2 / 8.6 | - | 54 | 86 | 3 |
| 7D_18 | 8.6 / 8.6 | 6.2 / 8.6 | - | 54 | 86 | 3 |

The results from Table 31 were added to the datasets from Peel and Baker et al. and ranked based on lining coverage area and time to flashover (Table 32).From the combined data, it can be seen that, based on the four products tested at ISO 9705 room scale, the EWP type did not appear to play a big role in determining what Group Number would be achieved. This was also supported by the fact that they all achieve a Group 3 rating when tested in the cone calorimeter. Below 37% coverage, the location of fuel in the room also appeared to make little difference in the Group Number achieved.

**Table 32. Combined datasets.**

| Experiment | Material | Area lined (m²) | | | % lined | Time to flashover (s) | Equivalent Group Number |
|---|---|---|---|---|---|---|---|
| | | Ceiling (C) | Upper walls (U) | Lower walls (L) | | | |
| 1_18 | 18 mm MDF | 8.6 | 11.5 | 11.5 | 100 | 126 | 3 |
| 1_9 | 9 mm MDF | 8.6 | 11.5 | 11.5 | 100 | 135 | 3 |
| 1 | 7 mm Ply | 8.6 | 11.5 | 11.5 | 100 | 172 | 3 |
| 7C | 7 mm Ply | 8.6 | 8.6 | 2.9 | 64 | 179 | 3 |
| 7B_18 | 18 mm MDF | 8.6 | 5.8 | 2.9 | 54 | 150 | 3 |
| 7D_18 | 18 mm MDF | 8.6 | 8.6 | - | 54 | 168 | 3 |
| 7B | 7 mm Ply | 8.6 | 5.8 | 2.9 | 54 | 184 | 3 |
| 7D_9 | 9 mm MDF | 8.6 | 8.6 | - | 54 | 204 | 3 |
| 7D | 7 mm Ply | 8.6 | 8.6 | - | 54 | 210 | 3 |
| 6_9 | 9 mm MDF | - | 8.6 | 8.6 | 54 | 348 | 3 |
| 6_18 | 18 mm MDF | - | 8.6 | 8.6 | 54 | 381 | 3 |
| 7B_9 | 9 mm MDF | 8.6 | 5.8 | 2.9 | 54 | 441 | 3 |
| 7F | 7 mm Ply | 8.6 | - | 8.6 | 54 | 734 | 2 |
| 7E | 7 mm Ply | 8.6 | 2.9 | 2.9 | 46 | 347 | 3 |
| 7 | 7 mm Ply | 8.6 | 2.9 | 2.9 | 46 | 366 | 3 |
| 7H | 7 mm Ply | 5.8 | 2.9 | 2.9 | 37 | 624 | 2 |
| 5 | 7 mm Ply | - | 5.8 | 5.8 | 37 | 627 | 2 |
| 4B | 12 mm Ply | - | - | 8.6 | 27 | 614 | 2 |
| 4_9 | 9 mm MDF | - | 8.6 | - | 27 | 615 | 2 |
| 2_9 | 9 mm MDF | 8.6 | - | - | 27 | 1071 | 2 |
| 2_18 | 18 mm MDF | 8.6 | - | - | 27 | - | 1 |
| 3_9 | 9 mm MDF | - | - | 8.6 | 27 | - | 1 |
| 3_18 | 18 mm MDF | - | - | 8.6 | 27 | - | 1 |
| 4_18 | 18 mm MDF | - | 8.6 | - | 27 | - | 1 |
| 2B | 12 mm Ply | 8.6 | - | - | 27 | - | 1 |
| 7G | 7 mm Ply | 2.9 | 2.9 | 2.9 | 27 | - | 1 |
| 2 | 7 mm Ply | 8.6 | - | - | 27 | - | 1 |
| 3 | 7 mm Ply | - | - | 8.6 | 27 | - | 1 |
| 4 | 7 mm Ply | - | 8.6 | - | 27 | - | 1 |
| 7I | 7 mm Ply | 1.4 | 2.9 | 2.9 | 23 | - | 1 |
| 8A | 7 mm Ply | - | 2.9 | 2.9 | 18 | - | 1 |

The bold line indicates the boundary between Group 2 and Group 3 material performance.

# 5. Modelling tools

Modelling can be used in a number of ways to predict the performance of building designs.

Models can vary in complexity and therefore computational cost, ranging from hand calculations or spreadsheets to determine single parameters through to zone models requiring limited computation power and ultimately computational fluid dynamics (CFD) type models that require huge computational effort and cost.

## 5.1 CFD models

As the name suggests, CFD is used to model the flow of fluids. Early attempts by Lewis Fry Richardson to predict weather failed (Richardson, 1922). However, the calculations used formed the basis for further work at the Los Alamos National Laboratory, modelling 2D flows (Harlow, 1955). The first 3D flow model was published in 1967 by John Hess and Apollo Smith of Douglas Aerospace (Hess, 1967).

They work by breaking up a design into thousands/millions of discrete elements and then solve the Navier-Stokes equations for conservation of mass and momentum on each element for each time-step. The mesh size used determines the number of elements, with some models using a mesh where all of the elements are the same size, whereas others use a variable mesh with large elements in areas where there is little change or interaction between adjacent elements and smaller elements around details where the interactions between adjacent elements are greater.

The number of calculations being done on each element is dependent upon the application. Combined with the massive number of elements normally used, this drives the computer processor and memory requirements and therefore computational cost.

The Fire Dynamics Simulator (FDS), developed by the National Institute of Standards and Technology (NIST,2021) is one of the most commonly used CFD packages for modelling fire, including heat transfer and chemical reaction models.

### 5.1.1 FDS input file

An FDS user was engaged to undertake modelling of the experimental series based on their own experience and the cone data provided from the clustering analysis. An example FDS input file is shown in Appendix D.

### 5.1.2 FDS results

The same ISO 9705 room corner experimental configurations were modelled in FDS.

#### 5.1.2.1 Heat release rate

Even with a fully lined room, FDS predicted minimal contribution from the MDF linings. The 9 mm MDF did not even reach the 1 MW flashover criteria, indicating a Group 1 material, while the 18 mm MDF took more than 1,000 s to reach it, indicating a Group 2 material (Figure 57).

None of the other FDS models reached flashover, indicating a Group 1 performance, which is clearly not reflected in the experimental results.

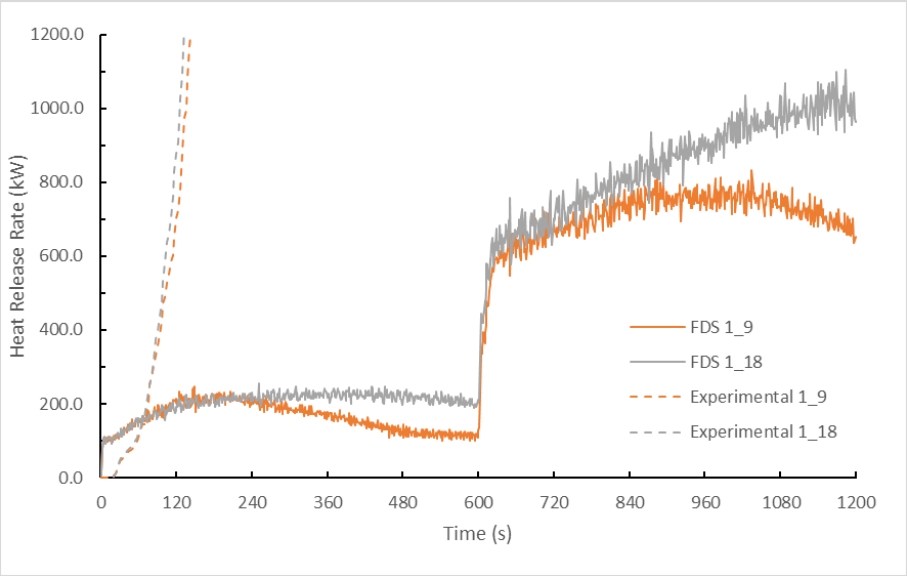


**Figure 57. FDS HRR vs experimental HRR.**

### 5.1.2.2 Compartment temperatures

The FDS model predicted a hot layer of 200–250°C to form between 1,420 mm and 1,570 mm above the floor up to 240 s (Figure 58). After 240 s, the layer was seen to rise to between 1,570 mm and 1,710 mm with the temperature dropping steadily to around 100–150°C at 1,570 mm. At 600 s when the burner output was stepped up to 300 kW, the compartment hot layer increased in temperature to 300–400°C and dropped to 1,270 mm from the floor.

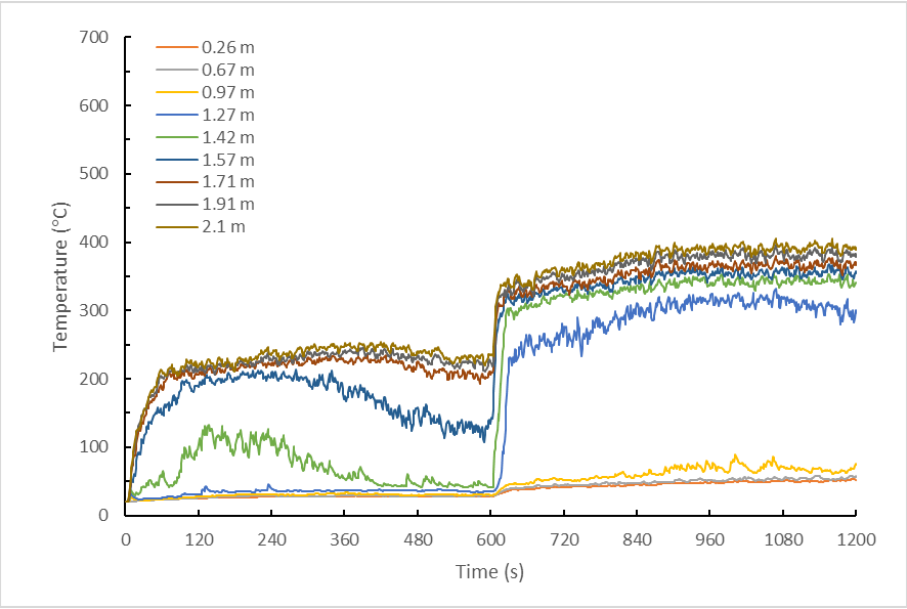


**Figure 58. FDS compartment temperatures for experimental configuration 1_9.**

Comparing the FDS results with the experimental results, it can be seen from Figure 59 that, although FDS predicts the temperature rise to occur earlier than the experimental results would suggest, the temperatures plateau at around 60 s with the hot upper layer only reaching approximately 200°C. The temperatures measured in the ISO room

experiment increased significantly after 60 s, reaching an upper layer temperature of 500–550°C before flashover.

Layer height can be seen to be reasonably consistent. FDS fairly closely matched the experiment, indicating an upper layer boundary height between 1,420 and 1,570 mm above the floor. For clarity, only temperatures over 1,000 mm above the floor are shown in Figure 59.

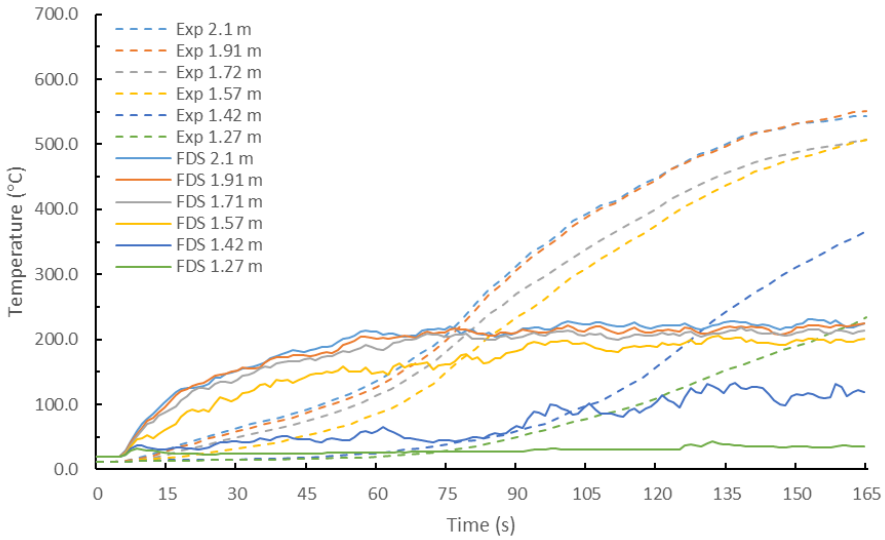


**Figure 59. Comparison of compartment temperatures up to flashover for experimental configuration 1_9.**

## 5.2 Zone models

Zone models are far less computationally intensive than CFD models. They work by splitting a compartment into at least two zones – a hot upper layer of combustion gases and a cooler lower layer. Conservation of mass and energy equations are then applied to each layer to determine temperature, pressure, volume and so on in much the same way as CFD models do. However, with only two volumes to consider, the calculations are completed much faster. Different submodels can also be applied – for example, plume and ceiling jet correlations.

As with CFD models, there are various zone models available, common ones being CFAST, developed by NIST, and B-RISK, developed by BRANZ.

### 5.2.1 B-RISK model

For this project, B-RISK version 2020.02 was used, with the partial combustible linings submodel developed by Wade for Peel.

Cone data from the earlier clustering analysis was used to provide the material properties and the 'use all cone calorimeter data provided and interpolate' setting in the Flame Spread Options

The area of coverage of the ceiling was selected by entering the percentage coverage in all cases. Where the lower wall was covered, the 'Pessimise combustible wall lining location' checkbox was deselected and the horizontal and vertical limits of coverage entered. Where the upper walls were covered, the 'Pessimise combustible wall lining location' checkbox was selected and the maximum percentage of wall covering was

entered. This is pessimistic as it considers all of the linings become involved up to the maximum percentage coverage, whereas in reality, some of the lower linings in the corner do not get consumed.

An example of a B-RISK input file is shown in Appendix E.

Because the B-RISK model was developed for more than just ISO 9705 simulation, flashover is determined by the upper layer temperature rather than the HRR reaching 1 MW as per the ISO 9705 standard. For this reason, the simulations were run to the ventilation limit (~1,150 kW) and then trimmed back to just over 1 MW or until the available fuel ran out (as with experimental configuration 3).

### 5.2.2 B-RISK results

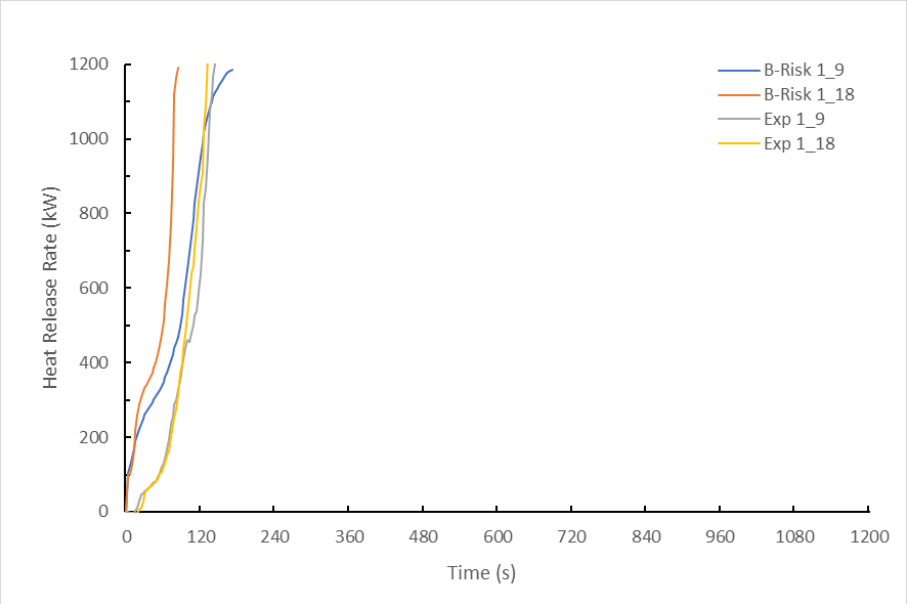


**Figure 60. Experimental configuration 1 – B-RISK vs experimental HRR.**

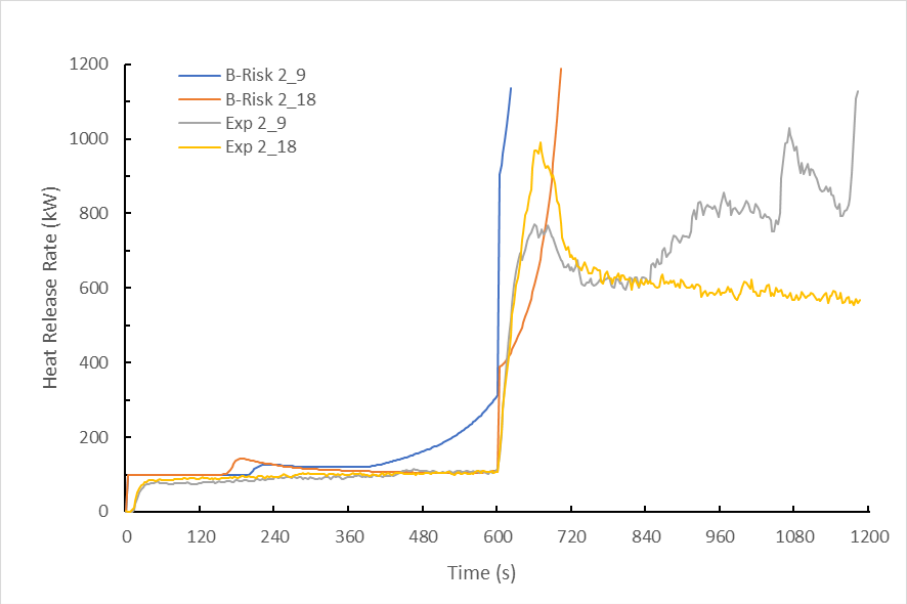


**Figure 61. Experimental configuration 2 – B-RISK vs experimental HRR.**

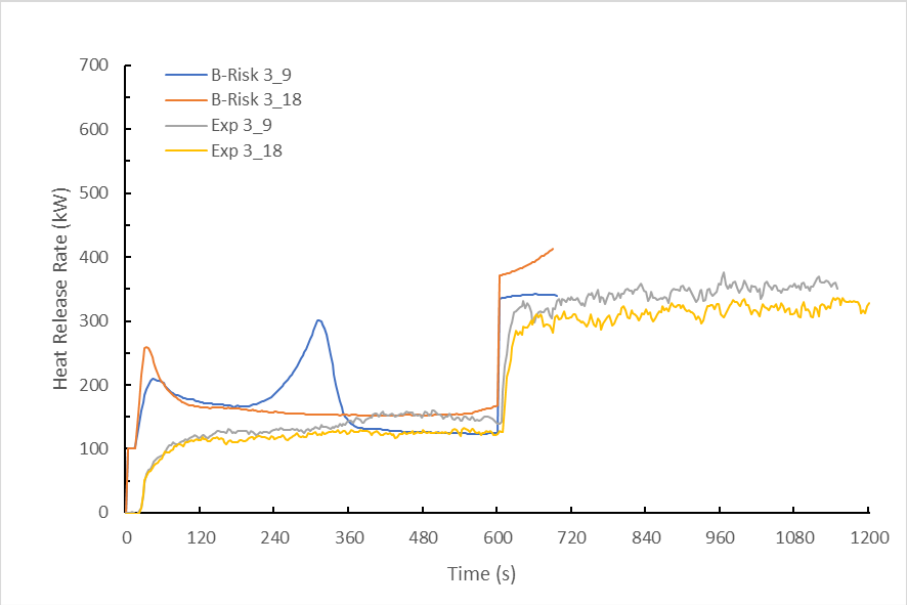


**Figure 62. Experimental configuration 3 – B-RISK vs experimental HRR.**

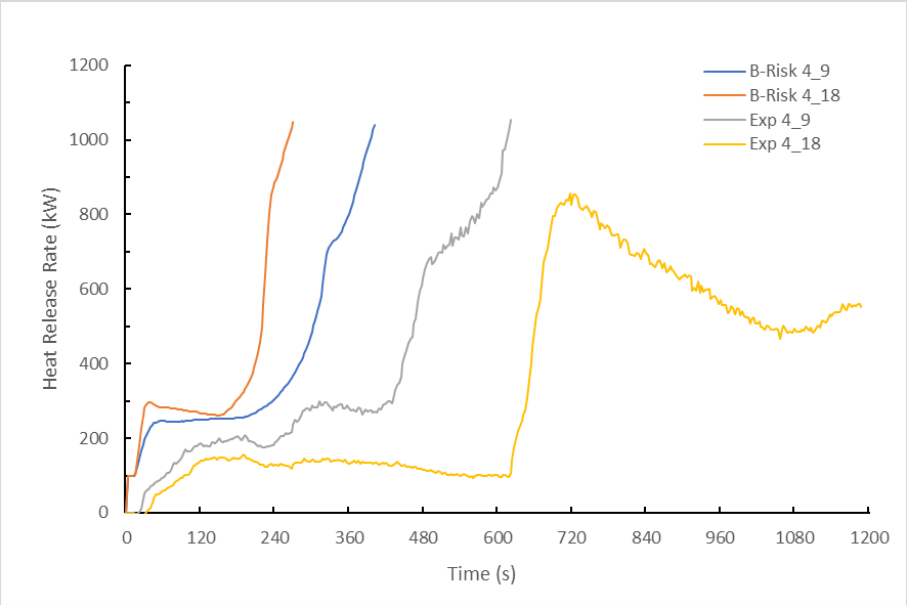


**Figure 63. Experimental configuration 4 – B-RISK vs experimental HRR.**

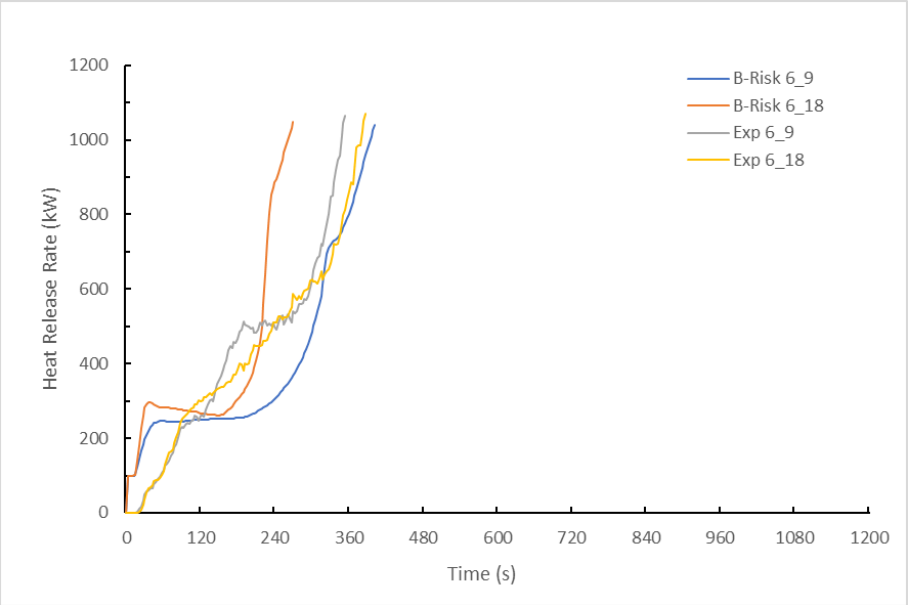


**Figure 64. Experimental configuration 6 – B-RISK vs experimental HRR.**

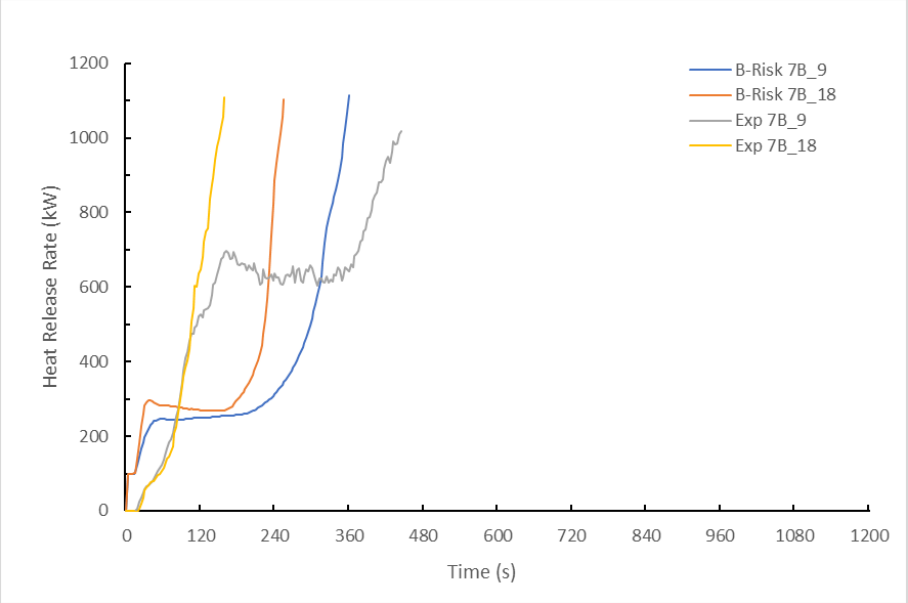


**Figure 65. Experimental configuration 7B – B-RISK vs experimental HRR.**

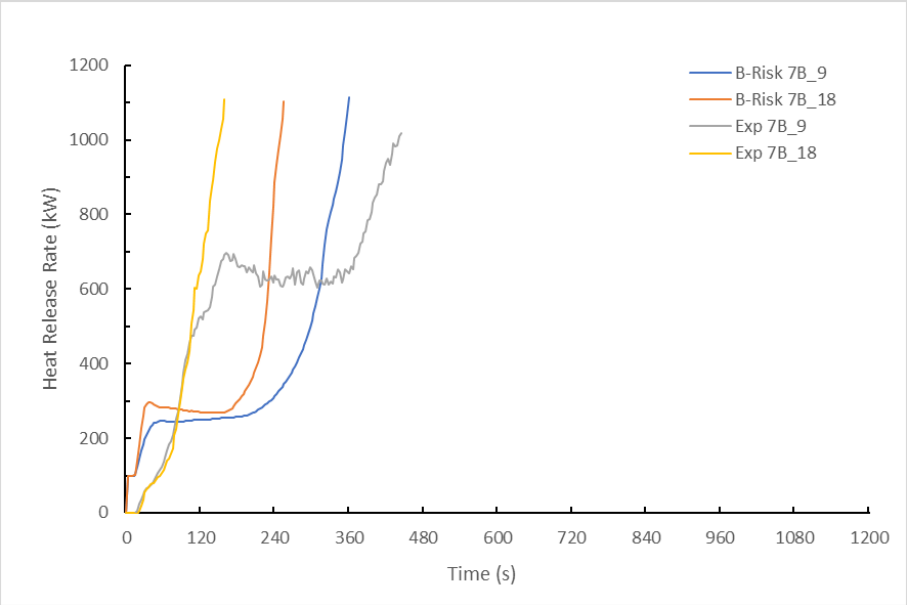


**Figure 66. Experimental configuration 7D – B-RISK vs experimental HRR.**

If the Group Number predicted by B-RISK is compared against the experimental output for each configuration, it can be seen than B-RISK accurately predicts the Group Number in most instances (10 out of 14 experiments) and where differences did occur, B-RISK predicted a more conservative value (Figure 67). For example, with configuration 2_18, B-RISK predicted a Group 2 material performance when the experimental performance was demonstrated at Group 1.

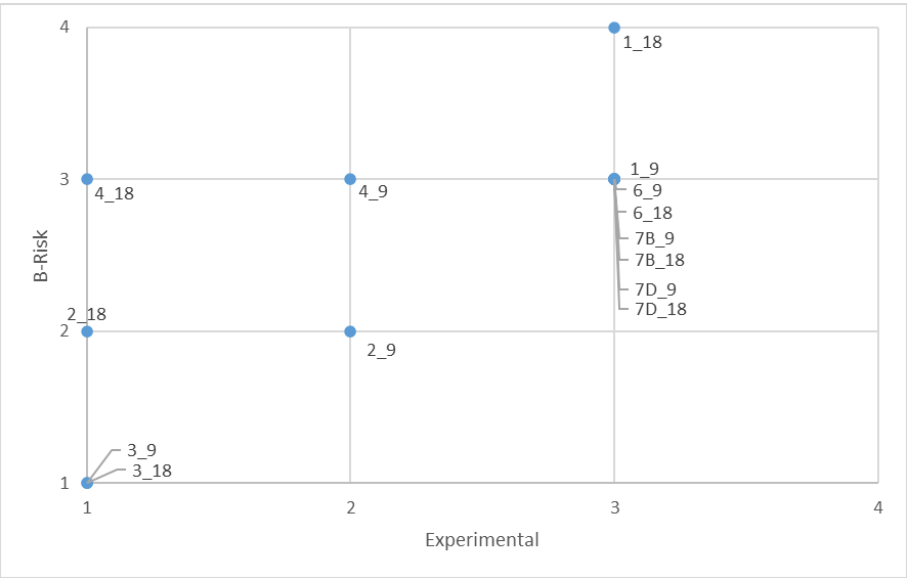


**Figure 67. B-RISK vs experimental Group Number.**

## 5.3 Risk ranking model

Baker et al.'s (2017) risk ranking model was used to see how accurately it could predict the performance of the products selected in order to determine if the model was generalised for all EWPs or tuned to the plywood used by Baker et al. and Peel. As can be seen from Table 33, not only does Baker et al.'s risk ranking model not give any

weighting to the lower wall area, it also does not distinguish between material thicknesses and therefore quantity of fuel in each area.

**Table 33. Baker et al. (2017) risk ranking modelling of experimental configurations.**

| Expt | Coverage area/weighting | | | Total area | Weighted total | Risk score | Rank | Experimental Group Number |
|---|---|---|---|---|---|---|---|---|
| | C / 1 | U / 1.42 | L / 0 | | | | | |
| 1_9 | 8.6 | 11.5 | 11.5 | 31.6 | 24.9 | 100.0 | 1 | 3 |
| 1_18 | 8.6 | 11.5 | 11.5 | 31.6 | 24.9 | 100.0 | 1 | 3 |
| 2_9 | 8.6 | 0 | 0 | 8.6 | 8.6 | 34.5 | 6 | 2 |
| 2_18 | 8.6 | 0 | 0 | 8.6 | 8.6 | 34.5 | 6 | 1 |
| 3_9 | 0 | 0 | 8.6 | 8.6 | 0 | 0.0 | 7 | 1 |
| 3_18 | 0 | 0 | 8.6 | 8.6 | 0 | 0.0 | 7 | 1 |
| 4_9 | 0 | 8.6 | 0 | 8.6 | 12.2 | 49.0 | 4 | 2 |
| 4_18 | 0 | 8.6 | 0 | 8.6 | 12.2 | 49.0 | 4 | 1 |
| 6_9 | 0 | 8.6 | 8.6 | 17.2 | 12.2 | 49.0 | 4 | 3 |
| 6_18 | 0 | 8.6 | 8.6 | 17.2 | 12.2 | 49.0 | 4 | 3 |
| 7B_9 | 8.6 | 5.8 | 2.9 | 17.3 | 16.8 | 67.5 | 3 | 3 |
| 7B_18 | 8.6 | 5.8 | 2.9 | 17.3 | 16.8 | 67.5 | 3 | 3 |
| 7D_9 | 8.6 | 8.6 | 0 | 17.2 | 20.8 | 83.5 | 2 | 3 |
| 7D_18 | 8.6 | 8.6 | 0 | 17.2 | 20.8 | 83.5 | 2 | 3 |

From the results in Table 33, it can be seen that ranks 1 to 3 do equate to Group 3 equivalent performance and ranks 6 and 7 equate to either Group 1 or 2 depending on material thickness. However, since there is a zero weighting on the lower wall area, experimental configurations 4 and 6 result in the same risk score at 49% of the fully lined room. This is clearly not reflected by the actual Group Numbers achieved during the ISO room testing. Configurations 6 achieving Group 3 and configuration 4, depending on thickness, achieving either Group 1 or Group 2.

## 5.4 Model discussions

### 5.4.1 FDS

CFD models such as FDS are complex, can be highly computationally expensive and require significant time to run. Often only a limited number of scenarios can be modelled within the budget and timeframe of many projects.

The experience of the modeller in being able select the right parameter values can significantly influence the model output. It is important to qualify 'right' in that there is no definitive right or wrong modelling approach, although there may be guidance provided by other users – in some cases, the model developers. Like most modelling, the goal is to gain useful insight to reality through a simulated simplified analogue. The purpose of the FDS modelling exercise in this research is to evaluate the ability of the model to provide this useful insight by testing it against known experimental observations for a similar case. This is a common approach taken in research. If successful, this exercise then builds trust in the ability of the model to represent other similar cases for which direct experimental information is not available. A pertinent example in this case would be using the model (in conjunction with other information) to verify if a building design maintains an adequate level of fire safety.

A key distinction should be drawn between a successfully validated simulation modelled a priori (with the model run prior to completing the lab fire experiment) or a posteriori (with the model run after completing the lab fire experiment). Insights from the experiment can affect the model input parameters chosen or allow the model to be tweaked to get the right result. In this case, the model was run a posteriori, but no further tweaking has been done.

In this modelling exercise, the output of the model (FDS) and chosen input parameters can be evaluated as to whether the experimental observations have been represented sufficiently for the intended purpose. In this case, the estimated heat release contribution from the lining was much less than was observed experimentally. If a building design was evaluated based on this model output, potential fire growth and spread would be underestimated and thus the fire safety of the building (time available for occupants to safely egress) likely overestimated. Following the modelling exercise, a review of the input files was undertaken. A number of observations were made of model input parameter decisions that could have influenced the simulated output including but not limited to the following.

A total of 16 meshes were defined, 14 of which using 50 mm cell size and two using 100 mm cell size. It was noted that the IJK values defined in the meshes did not all follow the recommendations set out in the FDS user manual:

> The pressure solver in FDS employs Fast Fourier Transforms (FFTs) in the y and z directions, and this algorithm works most efficiently if the number of cells in these directions (the J and K of IJK) can be factored into low primes, like 2, 3, and 5. The number of cells in the x direction (the I in IJK) is not affected by this restriction because the pressure solver does not use an FFT in the x direction. However, since the pressure solver uses less than 10 % of the total CPU time, the gains in using low prime dimensions are usually negligible. Experiment with different mesh dimensions to ensure that those that are ultimately used do not unduly slow down the calculation. (NIST, 2021, p. 34)

Although some of the JK values were not based on low primes, this is only considered to have a minor impact on computational speed.

The MDF products for the experiments were made of New Zealand-grown *Pinus radiata* with a phenol formaldehyde (PF) resin binder. A complex pyrolysis model was chosen with single reaction parameters given for each of the PF resin, cellulose, hemicellulose and lignin components of MDF. Kinetic parameters A and E have been specified for each, with formulae given in the FDS user manual for calculating values based on thermogravimetric analysis. However, it is also noted that, with the exception of cellulose, the reaction order (N_S) has also been specified with a non-unity value, which is contrary to the footnote contained in FDS user manual:

> These formulas have been derived from an analysis that considers a first-order reaction. When using the proposed method, do not specify non-unity value for the reaction order N_S on the MATL line. (NIST, 2021, p. 93)

It is unclear at this point what impact this may have had on the outcome of the simulation.

The overall results from the FDS modelling were highly inaccurate with much slower fire growth and heat release than shown in the experimental series resulting in a very non-conservative output.

This is a concern, where building consent authorities are increasingly being asked to approve designs based on far more complex modelling outputs than this experimental work. It is possible with different model parameters that FDS could be made to more accurately reflect the experimental outcomes. However, a posteriori model tweaks to improve the agreement of model output with experimental observations do not represent typical building fire safety analysis model. Another approach that can be taken to improve trust in the model is a sensitivity analysis where input parameters are varied to determine how sensitive model outputs are to changes in inputs. The computational expense of running CFD models may limit the amount of sensitivity analysis that can be done. More complex models such as CFD require greater experience and competency to evaluate input parameters by inspection alone. Ultimately, these findings demonstrate that relevant model validation and sensitivity studies should be included with building fire safety analysis. This becomes even more important for more complex models and provides a measure of confidence in both the model and the user-selected input parameters.

### 5.4.2 B-RISK

Although B-RISK showed reasonably good agreement with the experimental results, this is again in part due to the ability to run large numbers of simulations to fine tune the material parameters. In this case, the minimum temperature for flame spread was found to be the most crucial parameter.

Using the fully lined 9 mm MDF as a baseline, the minimum temperature for flame spread was adjusted until the growth rate of the fire was reasonably approximated to the experimental result by assessing the time to reach >1,000 kW by running the model to the ventilation limit ~1,150 kW.

Peel determined the minimum temperature for flame spread for the 7 mm plywood was 164 °C, so this was used as a starting point (Table 34 and Figure 68).

Peel's selection of 164°C was considered too conservative for the 9 mm MDF, reaching >1,000 kW by 105 s compared with the experimental result of 138 s, so the value was increased to 180°C. This pushed the time to exceed 1,000 kW out to 279 s, so was reduced in 5°C steps. It was noted that no difference in time to >1,000 kW was observed from 170–180°C and that 165°C and 166°C gave the same result.

Also of note was the fact that, irrespective of the minimum temperature for flame spread, up to 84 s into the simulations the HRR was identical, which implies there are other parameters at play.

A value of 167°C was used as it came close to the experimental flashover time (126 s compared to 138 s) while remaining on the conservative side. The same minimum temperature for flame spread value was used for both the 9 mm and the 18 mm MDF products tested.

As with the CFD modelling, this was only possible with the experimental dataset to validate against so is probably not extendable to other room geometries without further testing.

**Table 34. Minimum temperature for flame spread tuning.**

| Minimum temperature for flame spread (°C) | Time to >1,000 kW (s) |
|---|---|
| 164 | 105 |
| 180 | 279 |
| 175 | 279 |
| 170 | 279 |
| 165 | 108 |
| 166 | 108 |
| 167 | 126 |

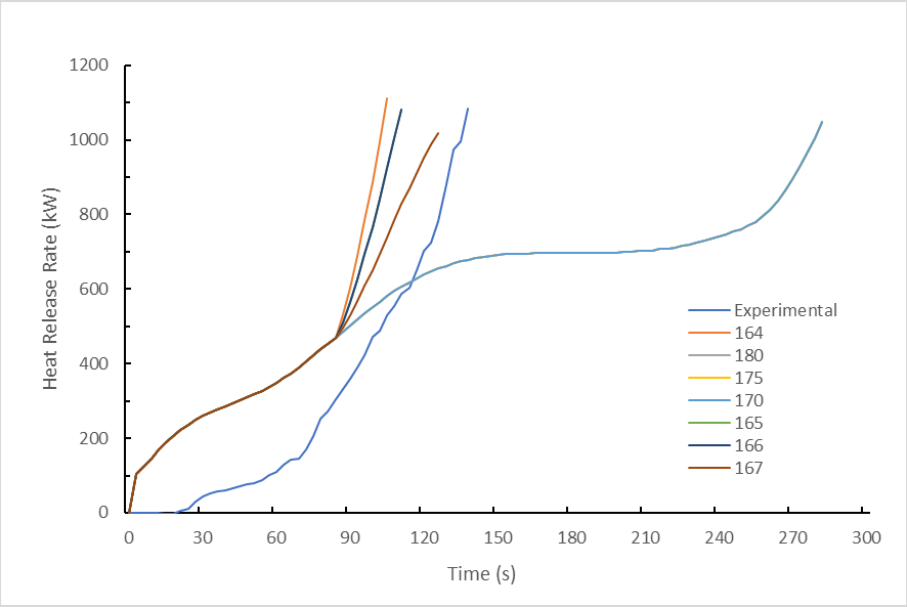


**Figure 68. B-RISK HRR vs minimum temperature for flame spread.**

Without the priori data, it also would be dependent on the experience of the engineer to ensure material parameters, plume correlations and so on are correctly selected. Although with less computational expense, with the ability to run multiple simulations in order to do a sensitivity analysis, a greater degree of confidence can be gained.

### 5.4.3 Modified risk model

Baker et al.'s model was further adapted using the full dataset from all three experimental series, factoring in the increased rate of growth provided by fuel in the lower wall area. The coverage areas were first normalised based on the maximum coverage area in each region. If fuel was located in the lower wall area, the upper wall area was increased by a factor of 1.5 rather than Baker et al.'s 1.42. The lower wall area, if present, was halved. This gives a maximum risk score of 3.0, unlike Baker et al.'s original model.

The results from the modified risk model are presented in Table 35. Although the modified risk model does not necessarily rank the experiments in the exact order of the experiments, it does indicate that configurations with a risk score over 1.5 would result in Material Group 3 performance while risk scores below 1.37 would result in Material Group 1 or 2. The model is less able to differentiate between configurations at the lower end, with some Group 1 configurations being ranked as Group 2 and vice versa.

**Table 35. Modified risk model.**

| Experiment | | Area lined (m²) | | | Time to flashover (s) | % lined | Material | Baker risk score | Baker risk rank | Lining thickness (mm) | Normalised area | | | | Total risk score | Rank | Equivalent Group Number |
|---|---|---|---|---|---|---|---|---|---|---|---|---|---|---|---|---|---|
| | | Ceiling (C) | Upper walls (U) | Lower walls (L) | | | | | | | Ceiling (C) | Upper walls (U) | Lower walls (L) | Weighted upper walls | | | |
| 1 | 1_18 | 8.6 | 11.5 | 11.5 | 126 | 100 | MDF | 24.9 | 1 | 18 | 1.00 | 1.00 | 1.00 | 1.50 | 3.00 | 1 | 3 |
| 2 | 1_9 | 8.6 | 11.5 | 11.5 | 135 | 100 | MDF | 24.9 | 1 | 9 | 1.00 | 1.00 | 1.00 | 1.50 | 3.00 | 1 | 3 |
| 3 | 7B_18 | 8.6 | 5.8 | 2.9 | 150 | 54 | MDF | 16.8 | 8 | 18 | 1.00 | 0.50 | 0.25 | 0.76 | 1.88 | 5 | 3 |
| 4 | 7D_18 | 8.6 | 8.6 | 0 | 168 | 54 | MDF | 20.8 | 4 | 18 | 1.00 | 0.75 | 0.00 | 0.75 | 1.75 | 8 | 3 |
| 5 | 1 | 8.6 | 11.5 | 11.5 | 172 | 100 | Ply | 24.9 | 1 | 7 | 1.00 | 1.00 | 1.00 | 1.50 | 3.00 | 1 | 3 |
| 6 | 7C | 8.6 | 8.6 | 2.9 | 179 | 64 | Ply | 20.8 | 4 | 7 | 1.00 | 0.75 | 0.25 | 1.12 | 2.25 | 4 | 3 |
| 7 | 7B | 8.6 | 5.8 | 2.9 | 184 | 54 | Ply | 16.8 | 8 | 7 | 1.00 | 0.50 | 0.25 | 0.76 | 1.88 | 5 | 3 |
| 8 | 7D_9 | 8.6 | 8.6 | 0 | 204 | 54 | MDF | 20.8 | 4 | 9 | 1.00 | 0.75 | 0.00 | 0.75 | 1.75 | 8 | 3 |
| 9 | 7D | 8.6 | 8.6 | 0 | 210 | 54 | Ply | 20.8 | 4 | 7 | 1.00 | 0.75 | 0.00 | 0.75 | 1.75 | 8 | 3 |
| 10 | 7E | 8.6 | 2.9 | 2.9 | 347 | 46 | Ply | 12.7 | 11 | 7 | 1.00 | 0.25 | 0.25 | 0.38 | 1.50 | 11 | 3 |
| 11 | 6_9 | 0 | 8.6 | 8.6 | 348 | 54 | MDF | 12.2 | 13 | 9 | 0.00 | 0.75 | 0.75 | 1.12 | 1.50 | 13 | 3 |
| 12 | 7 | 8.6 | 2.9 | 2.9 | 366 | 46 | Ply | 12.7 | 11 | 7 | 1.00 | 0.25 | 0.25 | 0.38 | 1.50 | 11 | 3 |
| 13 | 6_18 | 0 | 8.6 | 8.6 | 381 | 54 | MDF | 12.2 | 13 | 18 | 0.00 | 0.75 | 0.75 | 1.12 | 1.50 | 13 | 3 |
| 14 | 7B_9 | 8.6 | 5.8 | 2.9 | 441 | 54 | MDF | 16.8 | 8 | 9 | 1.00 | 0.50 | 0.25 | 0.76 | 1.88 | 5 | 3 |
| 15 | 4B | 0 | 0 | 8.6 | 614 | 27 | Ply | 0.0 | 28 | 12 | 0.00 | 0.00 | 0.75 | 0.00 | 0.37 | 28 | 1 |
| 16 | 4_9 | 0 | 8.6 | 0 | 615 | 27 | MDF | 12.2 | 13 | 9 | 0.00 | 0.75 | 0.00 | 0.75 | 0.75 | 23 | 1 |
| 17 | 7H | 5.8 | 2.9 | 2.9 | 624 | 37 | Ply | 9.9 | 18 | 7 | 0.67 | 0.25 | 0.25 | 0.38 | 1.18 | 16 | 2 |
| 18 | 5 | 0 | 5.8 | 5.8 | 627 | 37 | Ply | 8.2 | 24 | 7 | 0.00 | 0.50 | 0.50 | 0.76 | 1.01 | 17 | 1 |
| 19 | 7F | 8.6 | 0 | 8.6 | 734 | 54 | Ply | 8.6 | 19 | 7 | 1.00 | 0.00 | 0.75 | 0.00 | 1.37 | 15 | 2 |
| 20 | 2_9 | 8.6 | 0 | 0 | 1071 | 27 | MDF | 8.6 | 19 | 9 | 1.00 | 0.00 | 0.00 | 0.00 | 1.00 | 18 | 2 |
| 21 | 2_18 | 8.6 | 0 | 0 | - | 27 | MDF | 8.6 | 19 | 18 | 1.00 | 0.00 | 0.00 | 0.00 | 1.00 | 18 | 2 |
| 22 | 3_9 | 0 | 0 | 8.6 | - | 27 | MDF | 0.0 | 28 | 9 | 0.00 | 0.00 | 0.75 | 0.00 | 0.37 | 28 | 1 |
| 23 | 3_18 | 0 | 0 | 8.6 | - | 27 | MDF | 0.0 | 28 | 18 | 0.00 | 0.00 | 0.75 | 0.00 | 0.37 | 28 | 1 |
| 24 | 4_18 | 0 | 8.6 | 0 | - | 27 | MDF | 12.2 | 13 | 18 | 0.00 | 0.75 | 0.00 | 0.75 | 0.75 | 23 | 1 |
| 25 | 2B | 8.6 | 0 | 0 | - | 27 | Ply | 8.6 | 19 | 12 | 1.00 | 0.00 | 0.00 | 0.00 | 1.00 | 18 | 2 |
| 26 | 7G | 2.9 | 2.9 | 2.9 | - | 27 | Ply | 7.0 | 25 | 7 | 0.34 | 0.25 | 0.25 | 0.38 | 0.84 | 22 | 1 |
| 27 | 2 | 8.6 | 0 | 0 | - | 27 | Ply | 8.6 | 19 | 7 | 1.00 | 0.00 | 0.00 | 0.00 | 1.00 | 18 | 2 |
| 28 | 3 | 0 | 0 | 8.6 | - | 27 | Ply | 0.0 | 28 | 7 | 0.00 | 0.00 | 0.75 | 0.00 | 0.37 | 28 | 1 |
| 29 | 4 | 0 | 8.6 | 0 | - | 27 | Ply | 12.2 | 13 | 7 | 0.00 | 0.75 | 0.00 | 0.75 | 0.75 | 23 | 1 |
| 30 | 7I | 1.4 | 2.9 | 2.9 | - | 23 | Ply | 5.5 | 26 | 7 | 0.16 | 0.25 | 0.25 | 0.38 | 0.67 | 26 | 1 |
| 31 | 8A | 0 | 2.9 | 2.9 | - | 18 | Ply | 4.1 | 27 | 7 | 0.00 | 0.25 | 0.25 | 0.38 | 0.50 | 27 | 1 |

This modified risk model still does not take account of other material properties that might better distinguish between configurations. It was considered that other material properties such as thickness, density, critical heat flux and heat of combustion, which can be easily determined through small-scale experimentation, might provide a more accurate model. Further work will be required to see if this is the case.

It was considered that the ISO 9705 test is a benchmark for performance only. It is therefore proposed that the same logic could be applied to partially lined rooms or corridors to meet the same performance requirement for NZBC clause 3.4.

The boundary between the upper and lower walls was arbitrarily picked at the mid-height of the wall for the ISO 9705 room corner experiments. It is not known how varying the boundary height will affect the selectivity of the model and in fact whether the model would still work for different size compartments. However, if it was considered a benchmark only rather than being applied to a specific geometry such as a B-RISK or FDS model might be, it should remain valid.

### 5.4.4 MBIE C/VM2 modelling proposal

MBIE proposed an ultra-fast growth rate of 0.188t² (MBIE, 2017b) to account for the additional flame spread over internal linings as an alternative ASET/RSET calculation method for the Internal Spread (IS) scenario. None of the products tested performed worse than Material Group 3 in the cone calorimeter. The three products tested in a fully lined ISO 9705 room corner experiment also achieved Material Group 3 performance. The 0.188t² growth rate results in a Material Group 4 performance, exceeding the 1 MW threshold after only 73 s, and therefore might be considered a little too conservative, as even with a fully lined room, the growth rate was no worse than Material Group 3 (Figure 69). A growth rate of 0.069t² gives a worst-case Material Group 3 performance exceeding 1 MW just after 120 s.

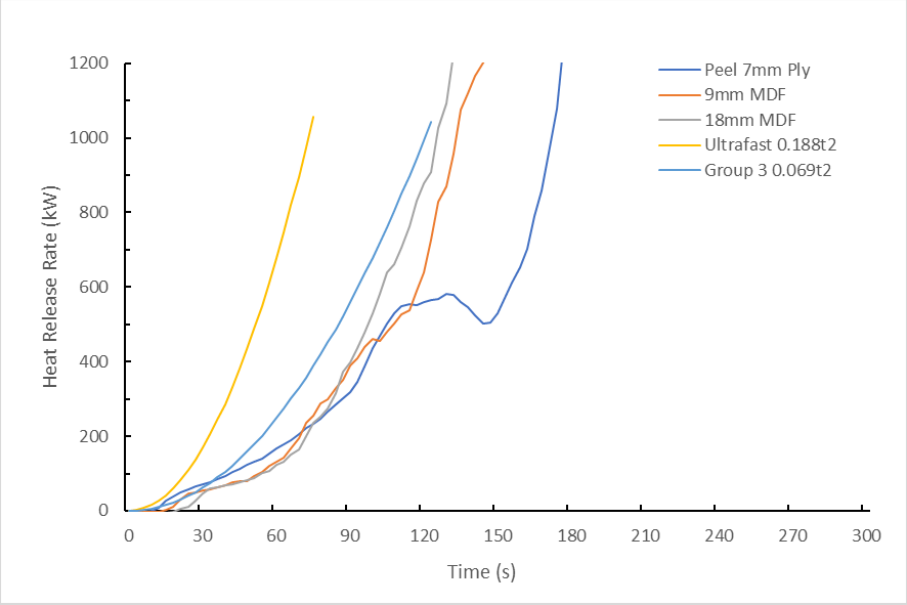


**Figure 69. Comparison between fully lined experimental growth rate and proposed MBIE ultra-fast 0.188t² and Material Group 3 0.069t² growth rate.**

# 6. Conclusions

Based on the combined results from Peel, Baker et al. and the experiments carried out for this project as shown in Table 32, the type of EWP does not appear to be a major factor. Across the full dataset, 16 products were tested in the cone calorimeter, and all achieved a Material Group 3 performance. Of the 13 products tested in this project, by most measures, they were largely indistinguishable by any physical means.

There were no distinguishable performance differences between the five products that were tested at ISO 9705 room-scale – Peel's 7 mm plywood, Baker et al.'s 7 mm and 12 mm plywood and the 9 mm and 18 mm MDF used in this series of experiments.

The greatest performance difference, as expected, was associated with the area of coverage of the lining material. Below 37% coverage, irrespective of EWP type or thickness, equivalent to a Material Group 2 or better was achieved.

A number of different models were used with varying success. FDS performed poorly, failing to adequately model the pyrolysis and flame spread, and although B-RISK was able to provide a reasonable and appropriately conservative result in all cases, this is considered to be largely a result of the fact that B-RISK has been validated over many years at ISO 9705 room scale and, even so, required tuning of the minimum temperature for flame spread in order to perform well.

The modified risk model (initially proposed by Baker) was also able to differentiate predicted performance based on the area coverage. Risk scores between 1.5 and 3.0 resulted in Material Group 3 performance, while those with a risk score below 1.37 resulted in either Material Group 2 or 1 performance. The model was less able to pick out the difference between Material Group 1 and Material Group 2, with three configurations predicted by the model to perform as Material Group 1 when experimentally they performed at Material Group 2.

The IS modelling approach proposed by MBIE is considered a reasonable one. However, the $0.188t^2$ growth rate is considered overly conservative. A growth rate of $0.069t^2$ would prove a challenging worst-case Material Group 3 growth rate.

Further work is required to validate the results at larger scale before the methods described in this report can be recommended for demonstrating compliance.

# References


Baker, G. B., Spearpoint, M. J., Fleischmann, C. M. & Wade, C. A. (2011). Selecting an ignition criterion methodology for use in a radiative fire spread submodel. *Fire and Materials, 35*(6), 367–381.

Baker, G. B., Wade, C. A. & Frank, K. (2017). Reaction-to-fire behaviour of partial quantities of timber surface linings in compartments. In D. Alvear (Ed.), *Research and advanced technology in fire safety* (pp. 331–346). Universidad de Cantabria.

BBC News. (2015, 31 October). *Bucharest nightclub fire leaves Romania stunned*. http://www.bbc.com/news/world-europe-34684973

DBH. (2011). *Compliance Document for New Zealand Building Code Clauses C1, C2, C3, C4 Fire Safety* (Amendment 9). Department of Building and Housing. https://www.building.govt.nz/assets/Uploads/building-code-compliance/c-protection-from-fire/asvm/Fire-Safety-C1-C4-amendment9-rp.pdf

DBH. (2012). *Extract from the New Zealand Building Code: Clauses C1-C6 Protection from Fire, Clause A3 Building Importance Levels.* Department of Building and Housing. https://www.building.govt.nz/assets/Uploads/building-code-compliance/c-protection-from-fire/asvm/c1-c6-protection-from-fire-a3.pdf

Drysdale, D. (1998). *An introduction to fire dynamics*. John Wiley & Sons Ltd.

Grosshandler, W., Bryner, N., Madrzykowski, D. & Kuntz, K. (2005). *Report of the technical investigation of The Station nightclub fire.* NIST NCSTAR 2: Vol. I. National Institute of Standards and Technology. https://tsapps.nist.gov/publication/get_pdf.cfm?pub_id=100988

Harlow, F. J. (1955). *A machine calculation method for hydrodynamic problems*. Los Alamos National Laboratory.

Hess, J. L. (1967). Calculation of potential flow about arbitrary bodies. *Progress in Aerospace Sciences*, *8*, 1–138. https://doi.org/10.1016/0376-0421(67)90003-6

ISO. (1993). *Fire tests – Full-scale room test for surface products* (ISO 9705:1993). International Organization for Standardization.

ISO. (2015). *Reaction-to-fire tests – Heat release, smoke production and mass loss rate – Part 1: Heat release rate (cone calorimeter method) and smoke producion rate* (ISO 5660-1:2015). International Organization for Standardization.

Karlsson, B. & Quintiere, J. G. (2000). *Enclosure fire dynamics*. CRC Press.

MBIE. (2015a). *Determination 2015/010 Regarding the authority's refusal to grant a modification of Clause C3.4(a) of the Building Code in respect of materials used for internal surface linings at a new school hall at 90-98 Blake Street, Greymouth*. Ministry of Business, Innovation and Employment. https://www.building.govt.nz/assets/Uploads/resolving-problems/determinations/2015/2015-010.pdf

MBIE. (2015b). *Determination 2015/022 Regarding the authority's refusal to grant a modification of Clause C3.4(a) of the Building Code in respect of materials used*

*for internal surface linings at a function centre at 75-79 Parker Avenue, New Lynn, Auckland*. Ministry of Business, Innovation and Employment. https://www.building.govt.nz/assets/Uploads/resolving-problems/determinations/2015/2015-022.pdf

MBIE. (2017a). *C/VM2 Verification Method: Framework for Fire Safety Design for New Zealand Building Code Clauses C1-C6 Protection from Fire* (Amendment 6). Ministry of Business, Innovation and Employment. https://www.building.govt.nz/assets/Uploads/building-code-compliance/c-protection-from-fire/asvm/cvm2-protection-from-fire-amendment-6.pdf

MBIE. (2017b). *Consultation on fire safety proposals, Changes to the Building Code, Amendments to Verification Method, Guidance for Acceptable Solutions*. Ministry of Business, Innovation and Employment. https://www.mbie.govt.nz/dmsdocument/27-consultations-on-fire-safety-proposals-pdf

MBIE. (2019). *C/AS2 Acceptable Solution for Buildings other than Risk Group SH* (Amendment 2). Ministry of Business, Innovation and Employment. https://www.building.govt.nz/assets/Uploads/building-code-compliance/c-protection-from-fire/asvm/cas2-2019-protection-from-fire-amendment-2.pdf

NIST. (2021). *Fire Dynamics Simulator users guide.* National Institute of Standards and Technology.

New Zealand Government. (2023). Schedule 1 The building code. In *Building Regulations 1992* (SR 1992/150). New Zealand Government. https://www.legislation.govt.nz/regulation/public/1992/0150/latest/whole.html#DLM162576

OFR Consultants. (2020). *Passive fire protection of cross-laminated timber*. BRANZ External Research Report ER68. BRANZ Ltd. https://www.branz.co.nz/pubs/research-reports/er68/

Peel, H. (2016). *Fire development in rooms partially lined with timber* [Master's thesis]. University of Canterbury. https://ir.canterbury.ac.nz/server/api/core/bitstreams/96e8fc96-c01c-4d4a-98fc-b5179c227689/content

Peel, H., Spearpoint, M. & Wade. C. (2016, 4–6 July). *Comparison of partially lined timber room experiments with the modified B-RISK flame spread capability* [Paper presentation]. International Conference and Exhibition on Fire Science and Engineering – Interflam 2016, Royal Holloway College, Windsor, UK. https://www.researchgate.net/publication/305983297_Comparison_of_partially_lined_timber_room_experiments_with_the_modified_B-RISK_flame_spread_capability

Richardson, L. F. (1922). *Numerical prediction by numerical process.* Cambridge University Press.

Shields, T. J., Silcock, G. W. & Murray, J. J. (1994). Evaluating ignition data using the flux time product. *Fire and Materials, 18*(4), 243–254.

Silcock, G. W. & Shields, T. J. (1995). A protocol for analysis of time-to-ignition data from bench scale tests. *Fire Safety Journal, 24*(1), 75–95.

Sundström, B. (2007). *The development of a European fire classification system for building products – test methods and mathematical modelling* [Doctoral thesis], Lund University, Sweden. https://lup.lub.lu.se/search/files/5444134/598792.pdf

The Telegraph. (2015, 3 June). *Brazil court convicts two firefighters in nightclub fire*. http://www.telegraph.co.uk/news/worldnews/southamerica/brazil/11650260/Brazil-court-convicts-two-firefighters-in-nightclub-fire.html

Wade, C. (2000). *BRANZFIRE technical reference guide*. BRANZ Study Report SR92. BRANZ Ltd. https://www.branz.co.nz/pubs/research-reports/sr92/

Wade, C. (2021). *Pyrolysis model for mass Timber: B-RISK theory.* BRANZ External Research Report ER67. BRANZ Ltd. https://www.branz.co.nz/pubs/research-reports/er67-pyrolysis-model-for-mass-timber-b-risk-theory/

# Appendix A: Cone calorimetry results

## Product A1

| Test | Heat flux (kW/m²) | Time to ignition (s) | Mean / SD | Peak HRR (kW/m²) | Mean / SD | Time to peak HRR (s) | Mean / SD | Time from ignition to peak HRR (s) | Average EHC (MJ/kg) | Mean / SD |
|---|---|---|---|---|---|---|---|---|---|---|
| A1 | 20 | 426 | 403 / 84 | 124.4 | 134 / 12 | 485 | 436 / 92 | 59 | 10.5 | 10.9 / 0.6 |
| A2 | | 310 | | 147.1 | | 330 | | 20 | 9.2 | |
| A3 | | 473 | | 129.5 | | 493 | | 20 | 10.6 | |
| A4 | 30 | 102 | 96 / 25 | 171.2 | 157 / 18 | 120 | 143 / 27 | 18 | 10.8 | |
| A5 | | 69 | | 136.2 | | 172 | | 103 | 11.1 | |
| A6 | | 118 | | 163.4 | | 136 | | 18 | 11.1 | |
| A7 | 40 | 51 | 46 / 14 | 170.9 | 168 / 3 | 67 | 60 / 15 | 16 | 11.0 | |
| A8 | | 30 | | 166.1 | | 42 | | 12 | 10.7 | |
| A9 | | 56 | | 167 | | 70 | | 14 | 11.0 | |
| A10 | 50 | 23 | 23 / 5 | 183.6 | 187 / 14 | 38 | 36 / 5 | 15 | 11.0 | |
| A11 | | 27 | | 202.1 | | 40 | | 13 | 11 | |
| A12 | | 18 | | 173.8 | | 30 | | 12 | 12.1 | |
| A13 | 60 | 15 | 20 / 8 | 201.4 | 209 / 8 | 26 | 32 / 7 | 11 | 10.9 | |
| A14 | | 16 | | 208.6 | | 31 | | 15 | 10.8 | |
| A15 | | 29 | | 218.3 | | 40 | | 11 | 11.4 | |

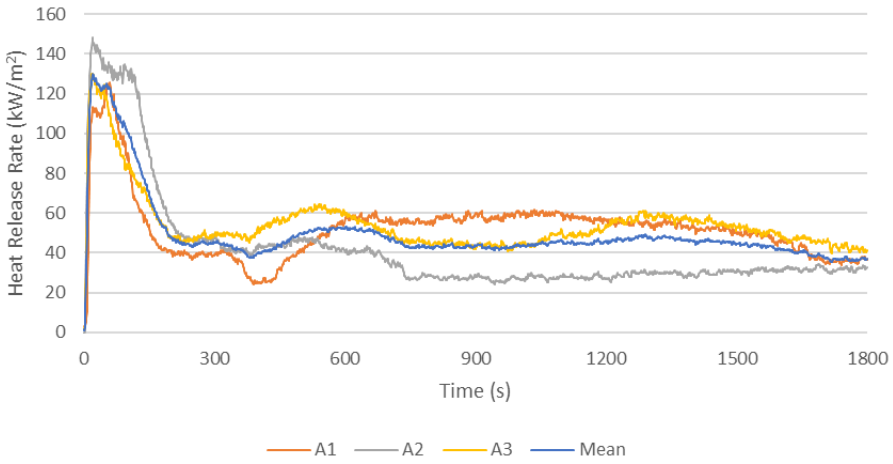


**Product A1 20 kW HRR after ignition.**

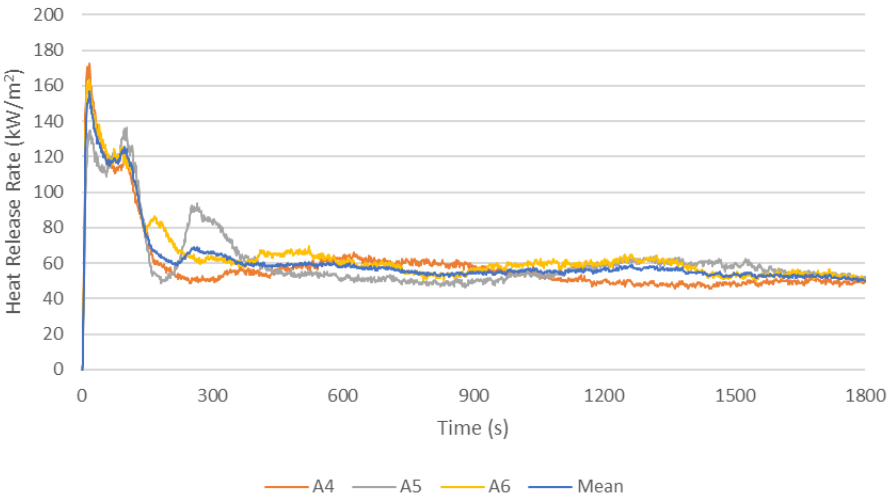


**Product A1 30 kW HRR after ignition.**

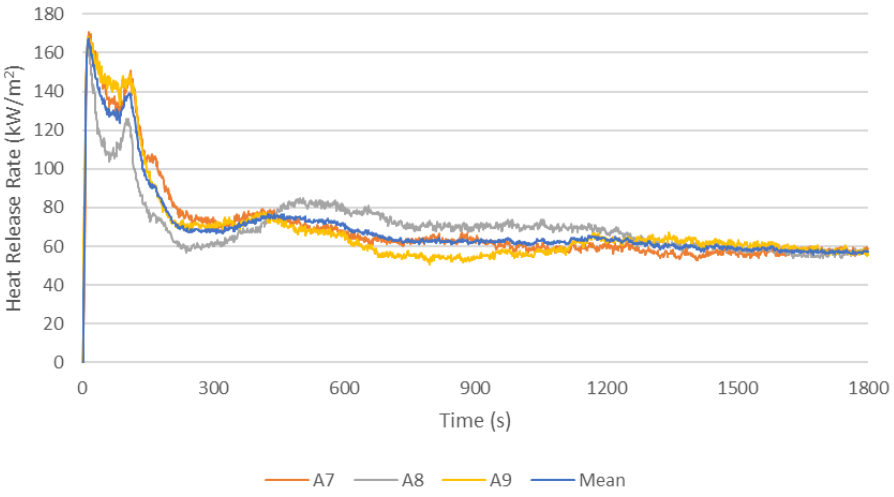


**Product A1 40 kW HRR after ignition.**

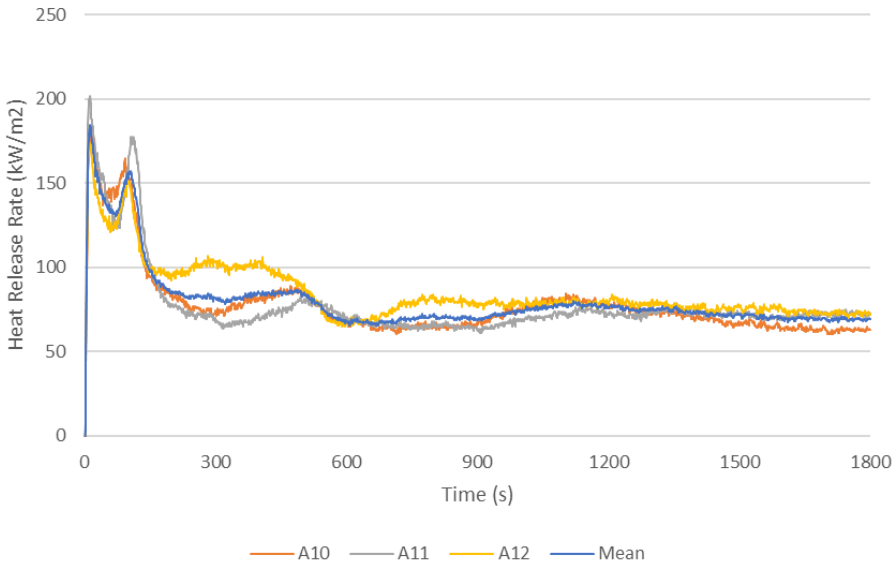


**Product A1 50 kW HRR after ignition.**

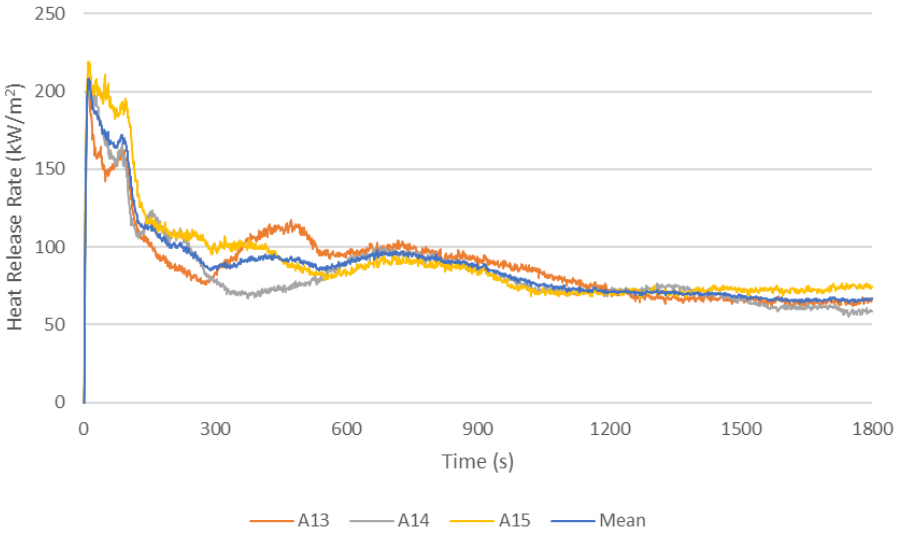


**Product A1 60 kW HRR after ignition.**

## Product B1

| Test | Heat flux (kW/m²) | Time to ignition (s) | Mean / SD | Peak HRR (kW/m²) | Mean / SD | Time to peak HRR (s) | Mean / SD | Time from ignition to peak HRR (s) | Average EHC (MJ/kg) | Mean / SD |
|---|---|---|---|---|---|---|---|---|---|---|
| B1 | 20 | 230 | 242 / 31 | 262.1 | 190 / 64 | 395 | 390 / 76 | 165 | 17.3 | 15.6 / 0.7 |
| B2 | | 277 | | 167.8 | | 464 | | 187 | 16.9 | |
| B3 | | 219 | | 139.1 | | 312 | | 93 | 14.7 | |
| B4 | 30 | 97 | 91 / 8 | 189.3 | 191 / 6 | 274 | 260 / 29 | 177 | 15.3 | |
| B5 | | 95 | | 185.4 | | 226 | | 131 | 14.7 | |
| B6 | | 83 | | 197.4 | | 279 | | 196 | 16.0 | |
| B7 | 40 | 60 | 53 / 10 | 302.4 | 267 / 51 | 234 | 227 / 11 | 174 | 16.0 | |
| B8 | | 46 | | 230.6 | | 219 | | 173 | 15.2 | |
| B9 | | 46 | | 217.1 | | 167 | | 121 | 15.0 | |
| B10 | 50 | 28 | 29 / 2 | 246.2 | 245 / 4 | 194 | 196 / 11 | 166 | 15.6 | |
| B11 | | 32 | | 248.1 | | 208 | | 176 | 15.4 | |
| B12 | | 28 | | 240.6 | | 186 | | 158 | 15.3 | |
| B13 | 60 | 14 | 15 / 0 | 308 | 290 / 45 | 161 | 164 / 3 | 147 | 15.8 | |
| B14 | | 15 | | 238.4 | | 167 | | 152 | 15.1 | |
| B15 | | 15 | | 322.2 | | 163 | | 148 | 15.6 | |

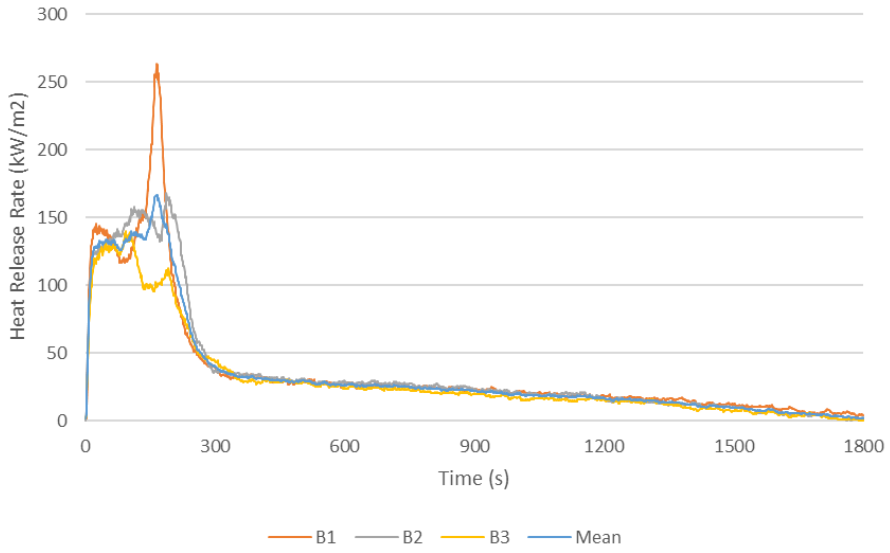


**Product B1 20 kW HRR after ignition.**

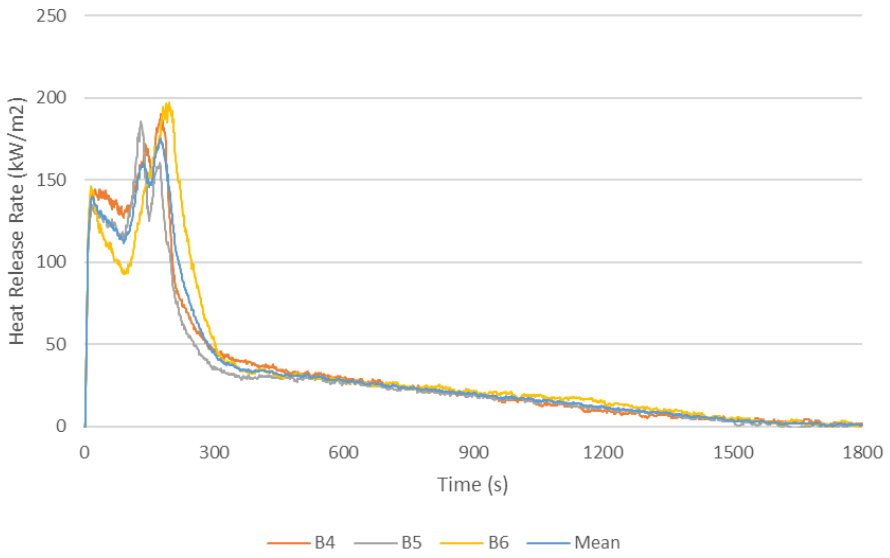


**Product B1 30 kW HRR after ignition.**

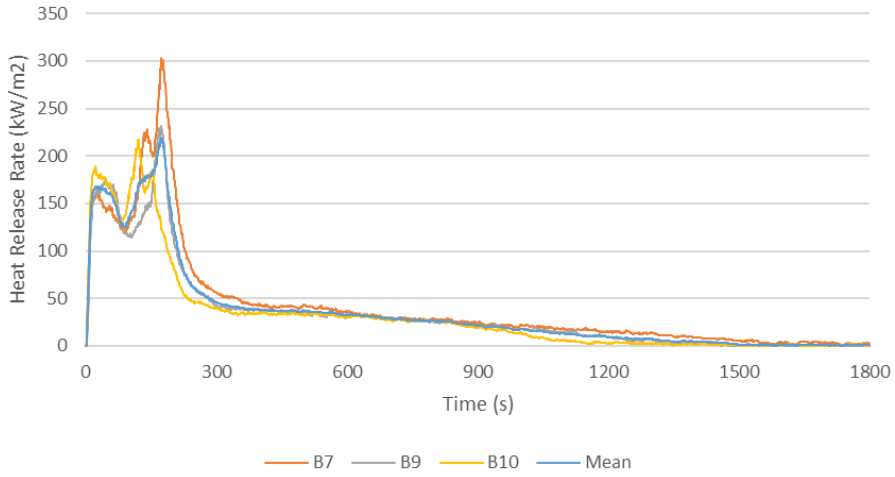


**Product B1 40 kW HRR after ignition.**

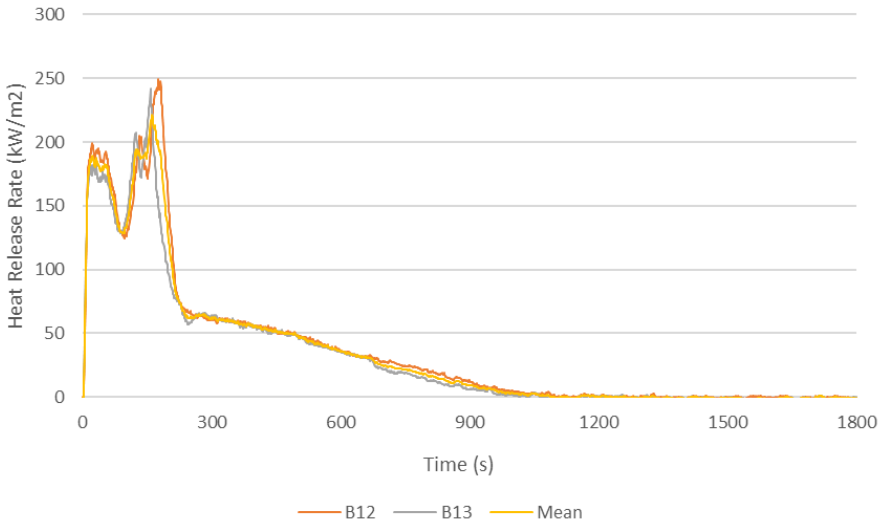


**Product B1 50 kW HRR after ignition.**

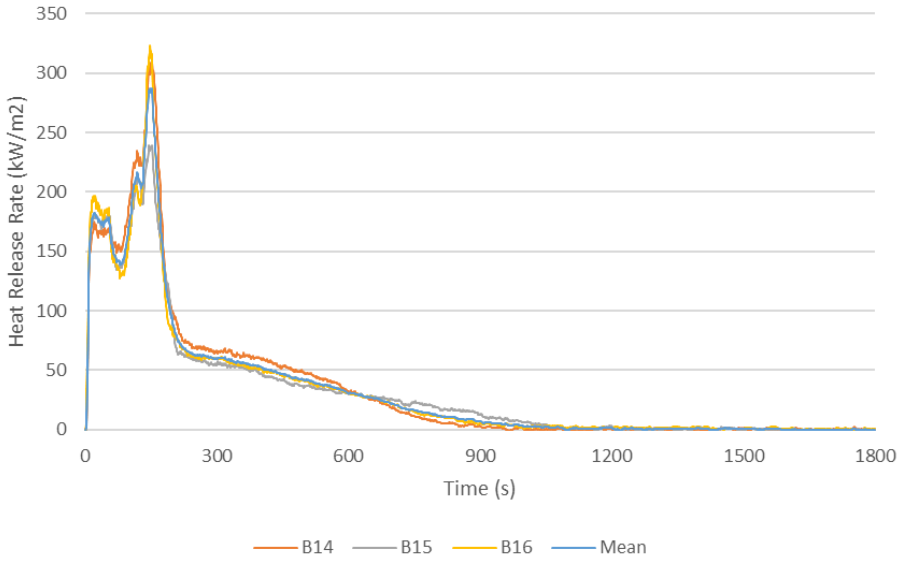


**Product B1 60 kW HRR after ignition.**

## Product B2

| Test | Heat flux (kW/m²) | Time to ignition (s) | Mean / SD | Peak HRR (kW/m²) | Mean / SD | Time to peak HRR (s) | Mean / SD | Time from ignition to peak HRR (s) | Average EHC (MJ/kg) | Mean / SD |
|---|---|---|---|---|---|---|---|---|---|---|
| B31 | 20 | 230 | 273 / 43 | 141.4 | 138 / 7 | 256 | 302 / 49 | 26 | 15.0 | 15.5 / 0.5 |
| B32 | | 315 | | 142 | | 354 | | 39 | 15.5 | |
| B33 | | 274 | | 129.7 | | 295 | | 21 | 15.3 | |
| B34 | 30 | 80 | 80 / 3 | 166.9 | 166 / 5 | 382 | 324 / 71 | 302 | 14.7 | |
| B36 | | 83 | | 161.3 | | 245 | | 162 | 14.6 | |
| B37 | | 77 | | 170.4 | | 344 | | 267 | 15.6 | |
| B38 | 40 | 41 | 45 / 4 | 197.4 | 220 /20 | 286 | 301 / 19 | 245 | 15.8 | |
| B39 | | 47 | | 233.4 | | 323 | | 276 | 15.1 | |
| B40 | | 47 | | 230 | | 294 | | 247 | 15.6 | |
| B41 | 50 | 23 | 25 /2 | 214.9 | 233 / 28 | 265 | 264 / 9 | 242 | 15.7 | |
| B42 | | 24 | | 265.7 | | 273 | | 249 | 15.9 | |
| B43 | | 27 | | 219.1 | | 255 | | 228 | 16.2 | |
| B44 | 60 | 14 | 15 / 2 | 271.8 | 305 / 31 | 232 | 234 /15 | 218 | 15.2 | |
| B45 | | 18 | | 332.9 | | 250 | | 232 | 15.8 | |
| B46 | | 14 | | 310.9 | | 221 | | 207 | 16.2 | |

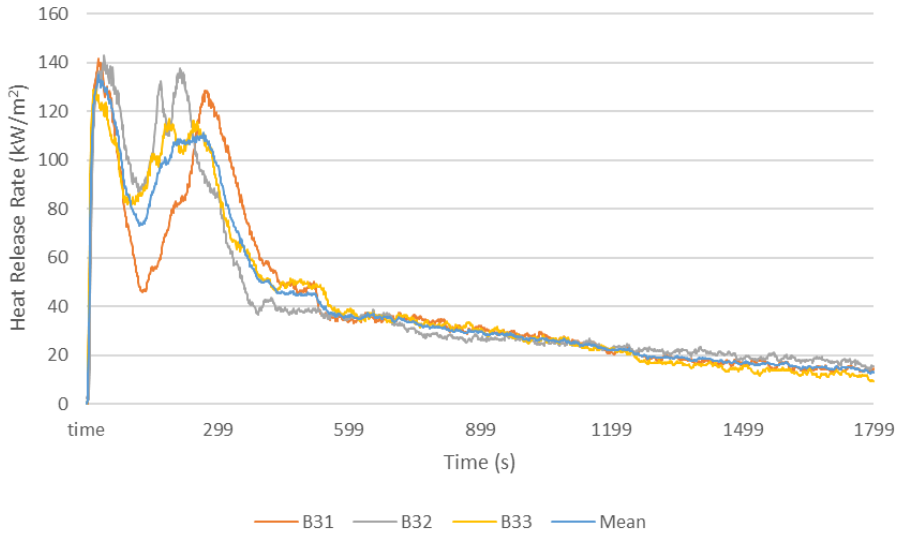


**Product B2 20 kW HRR after ignition.**

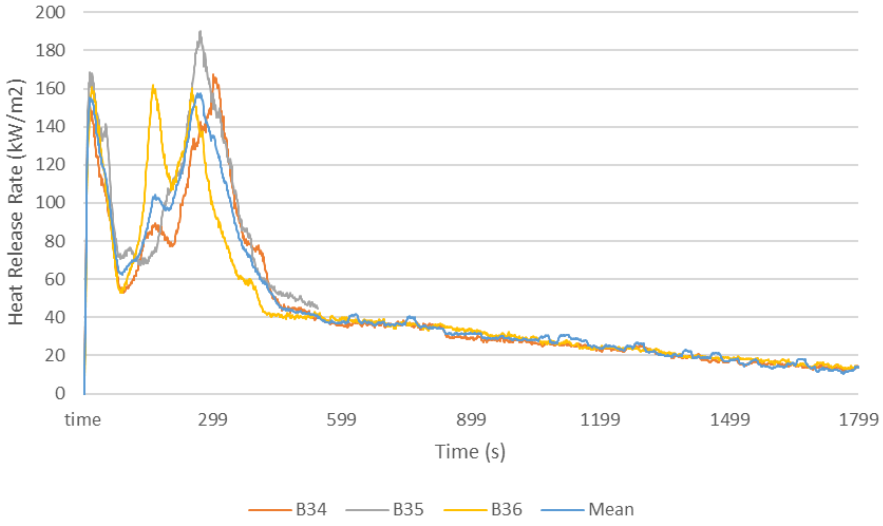


**Product B2 30 kW HRR after ignition.**

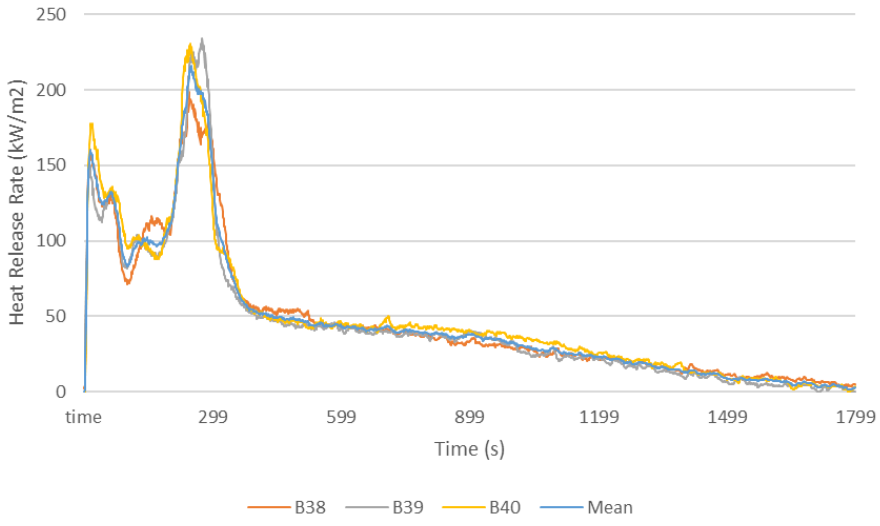


**Product B2 40 kW HRR after ignition.**

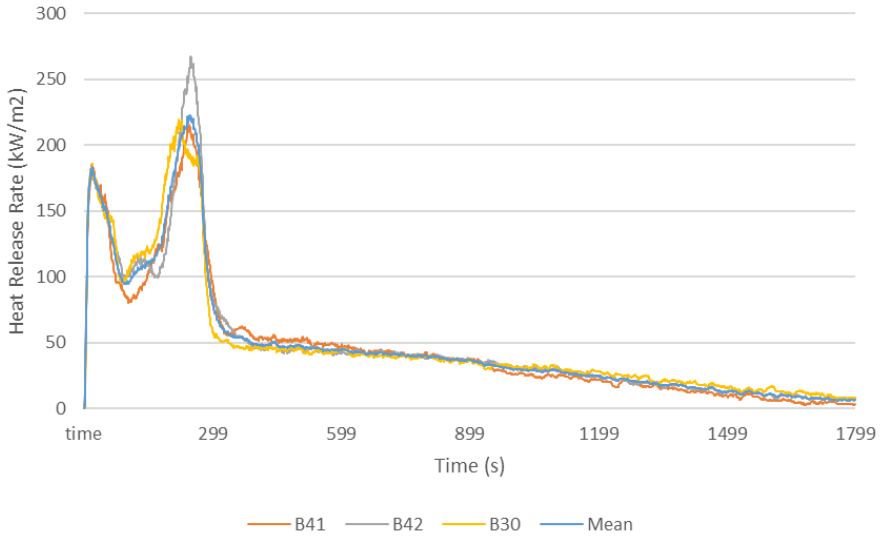


**Product B2 50 kW HRR after ignition.**

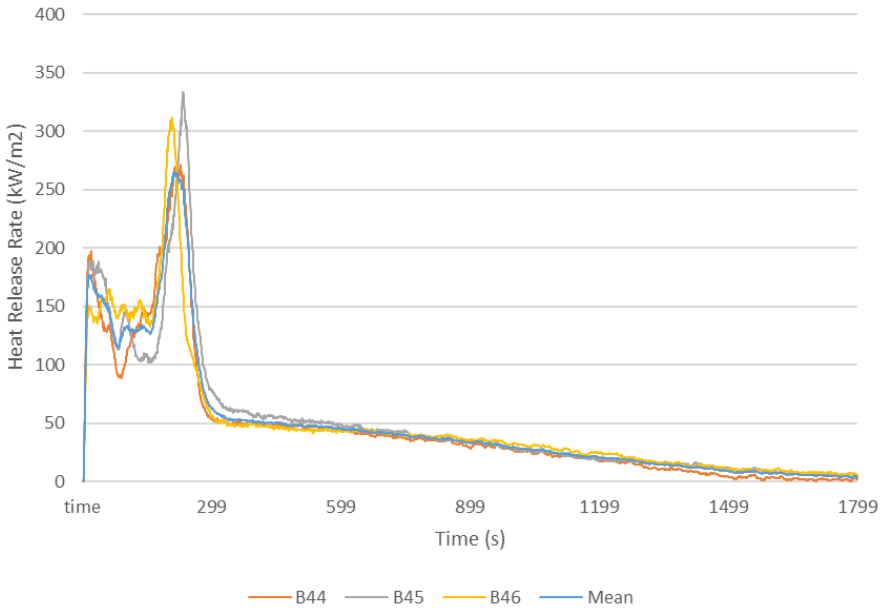


**Product B2 60 kW HRR after ignition.**

## Product C1

| Test | Heat flux (kW/m²) | Time to ignition (s) | Mean / SD | Peak HRR (kW/m²) | Mean / SD | Time to peak HRR (s) | Mean / SD | Time from ignition to peak HRR (s) | Average EHC (MJ/kg) | Mean / SD |
|---|---|---|---|---|---|---|---|---|---|---|
| C1 | 20 | 424 | 415 / 35 | 128.9 | 128 / 4 | 446 | 433 / 37 | 22 | 12.9 | 11.5 / 0.5* |
| C2 | | 375 | | 131.6 | | 392 | | 17 | 11.8 | |
| C3 | | 444 | | 124 | | 462 | | 18 | 7.8* | |
| C4 | 30 | 45 | 54 / 8 | 147 | 148 / 7 | 63 | 71 / 8 | 18 | 11.3 | |
| C5 | | 58 | | 156.1 | | 71 | | 13 | 10.8 | |
| C6 | | 59 | | 142 | | 79 | | 20 | 11.1 | |
| C7 | 40 | 27 | 34 / 7 | 150.0 | 165 / 14 | 41 | 50 / 8 | 14 | 11.3 | |
| C8 | | 40 | | 178.2 | | 57 | | 17 | 11.5 | |
| C9 | | 36 | | 167.1 | | 52 | | 16 | 11.4 | |
| C10 | 50 | 21 | 22 /2 | 183.5 | 189 / 9 | 35 | 39 / 5 | 14 | 11.7 | |
| C11 | | 21 | | 183.9 | | 37 | | 16 | 11.3 | |
| C12 | | 23 | | 168.7 | | 44 | | 21 | 11.1 | |
| C13 | 60 | 11 | 12 / 2 | 203.1 | 202 / 1 | 29 | 27 / 2 | 18 | 12.1 | |
| C14 | | 14 | | 202.0 | | 27 | | 13 | 11.3 | |
| C15 | | 12 | | 202.0 | | 25 | | 13 | 11.2 | |

* EHC is low. After 720 s after ignition, the HRR dropped down to ~20 kW, indicating no contribution from the product but combustion continued to the end of the test. Excluded from Mean/SD.

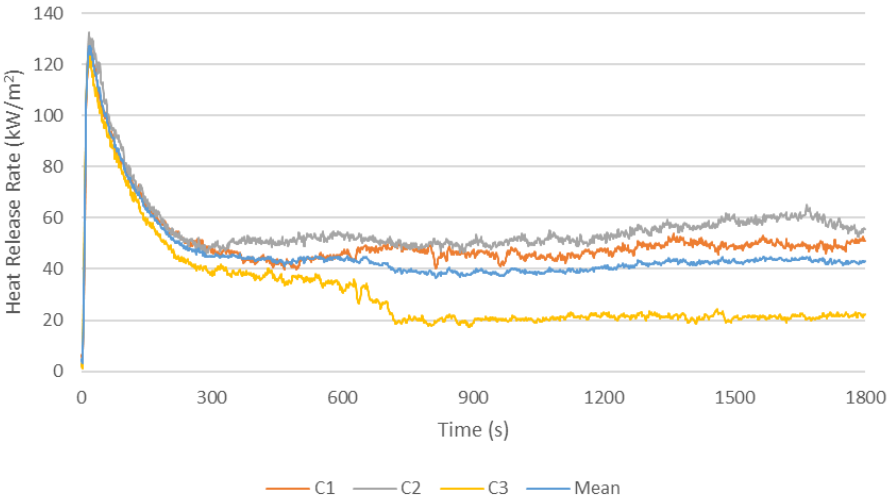


**Product C1 20 kW HRR after ignition.**

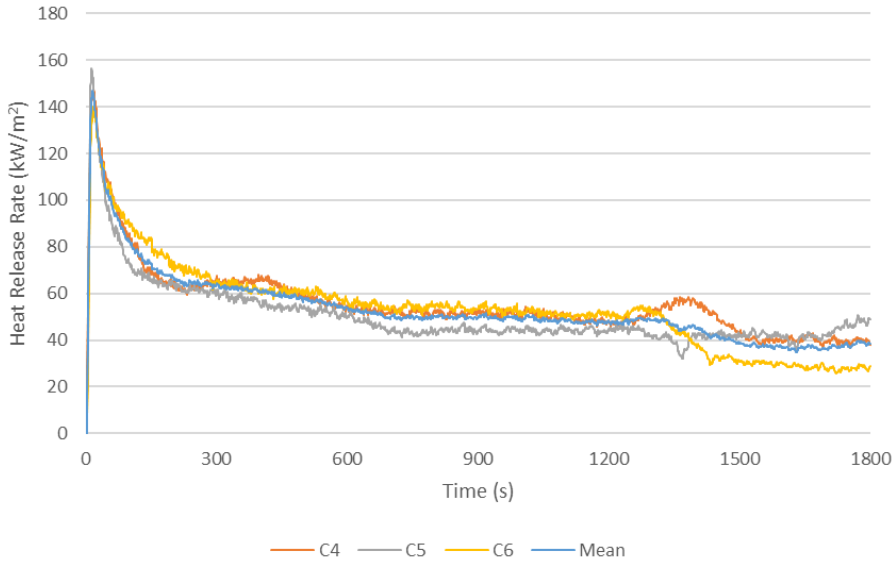


**Product C1 30 kW HRR after ignition.**

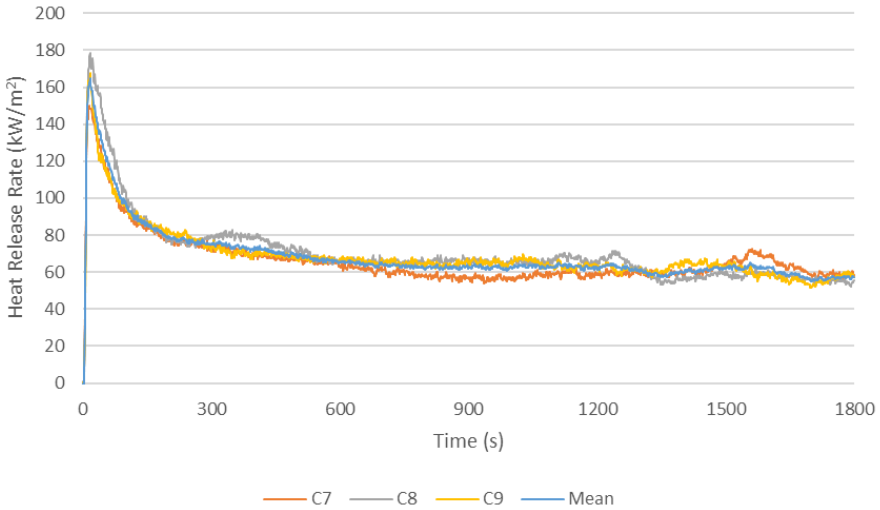


**Product C1 40 kW HRR after ignition.**

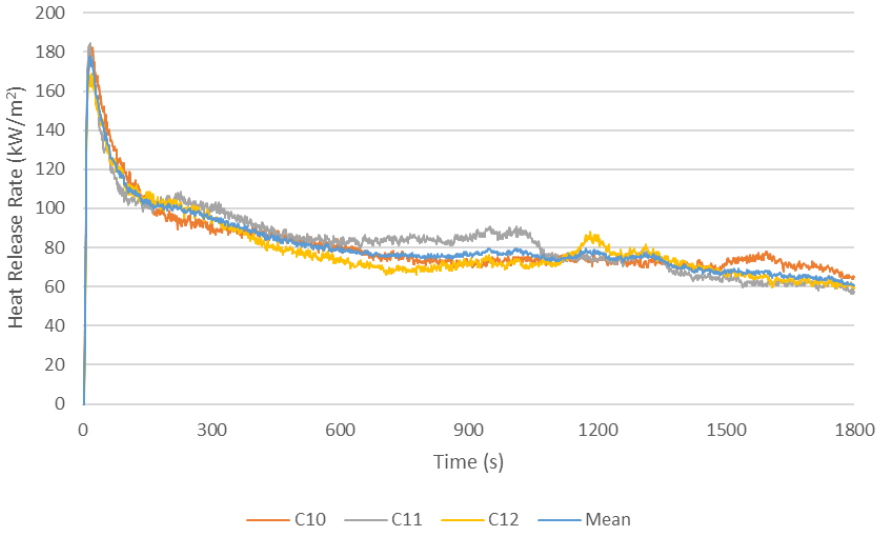


**Product C1 50 kW HRR after ignition.**

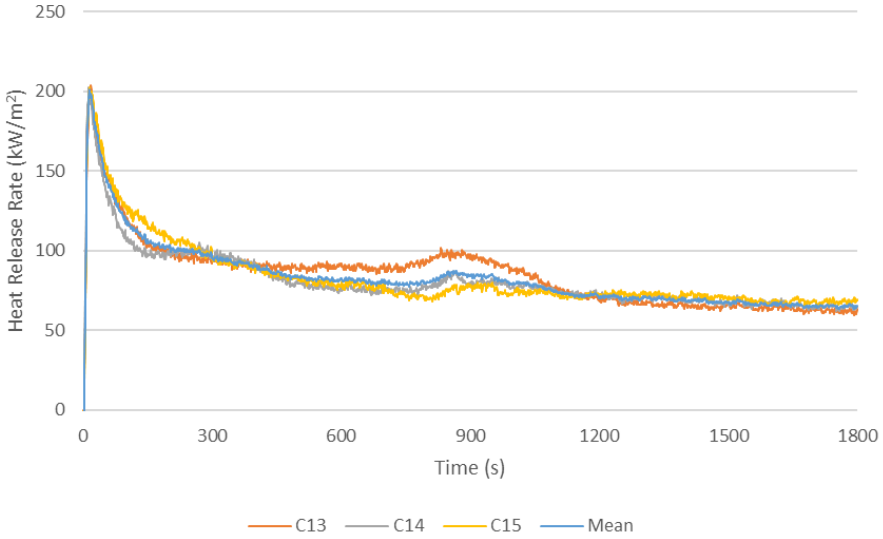


**Product C1 60 kW HRR after ignition.**

# Product D1

| Test | Heat flux (kW/m²) | Time to ignition (s) | Mean / SD | Peak HRR (kW/m²) | Mean / SD | Time to peak HRR (s) | Mean / SD | Time from ignition to peak HRR (s) | Average EHC (MJ/kg) | Mean / SD |
|---|---|---|---|---|---|---|---|---|---|---|
| D3 | 20 | 276 | 245 / 27 | 232.1 | 265 / 30 | 697 | 672 / 22 | 421 | 13.3 | 13.1 / 1.4 |
| D4 | | 230 | | 292.0 | | 659 | | 429 | 15.2 | |
| D5 | | 230 | | 270.8 | | 659 | | 429 | 17.5 | |
| D6 | 30 | 98 | 104 / 8 | 265.7 | 277 / 17 | 504 | 507 / 7 | 406 | 13.0 | |
| D7 | | 113 | | 269.0 | | 515 | | 402 | 12.9 | |
| D8 | | 101 | | 296.3 | | 501 | | 400 | 13.1 | |
| D10 | 40 | 55 | 56 / 1 | 331.7 | 338 / 19 | 430 | 406 / 25 | 375 | 12.4 | |
| D11 | | 57 | | 322.3 | | 381 | | 324 | 12.4 | |
| D12 | | 56 | | 359.1 | | 406 | | 350 | 12.2 | |
| D13 | 50 | 35 | 36 /2 | 417.3 | 394 / 21 | 349 | 352 / 3 | 314 | 12.3 | |
| D14 | | 35 | | 386.2 | | 354 | | 319 | 12.9 | |
| D15 | | 38 | | 378.2 | | 354 | | 316 | 12.3 | |
| D16 | 60 | 25 | 25 / 1 | 406.2 | 399 / 17 | 321 | 327 / 9 | 296 | 12.4 | |
| D17 | | 25 | | 410.2 | | 323 | | 298 | 12.1 | |
| D18 | | 26 | | 379.5 | | 338 | | 312 | 12.4 | |

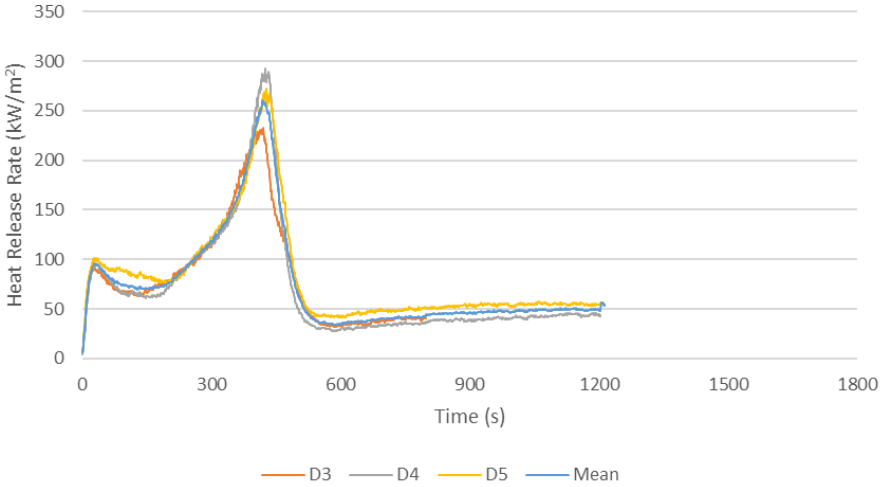


**Product D1 20 kW HRR after ignition.**

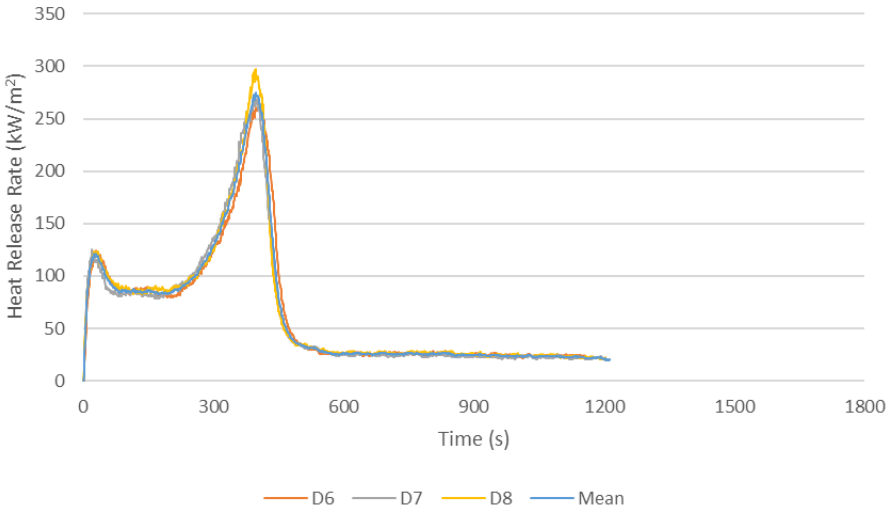


**Product D1 30 kW HRR after ignition.**

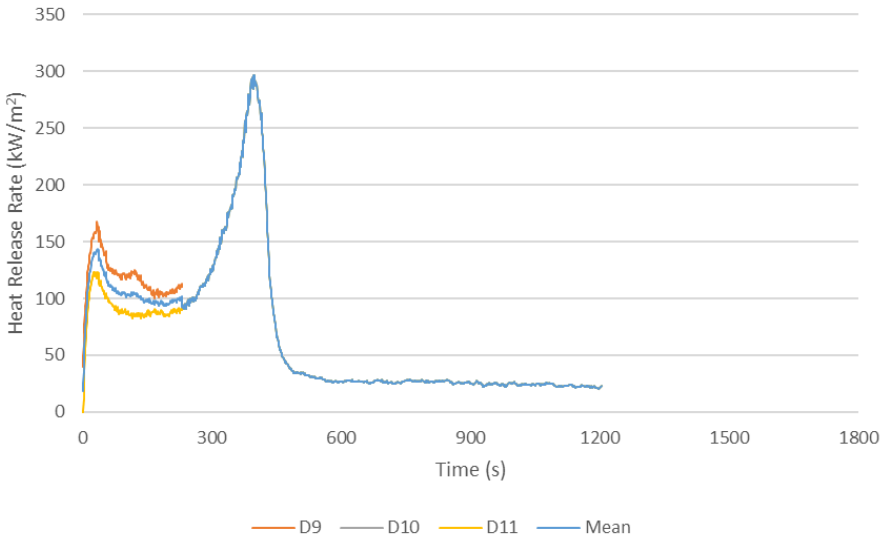


**Product D1 40 kW HRR after ignition.**

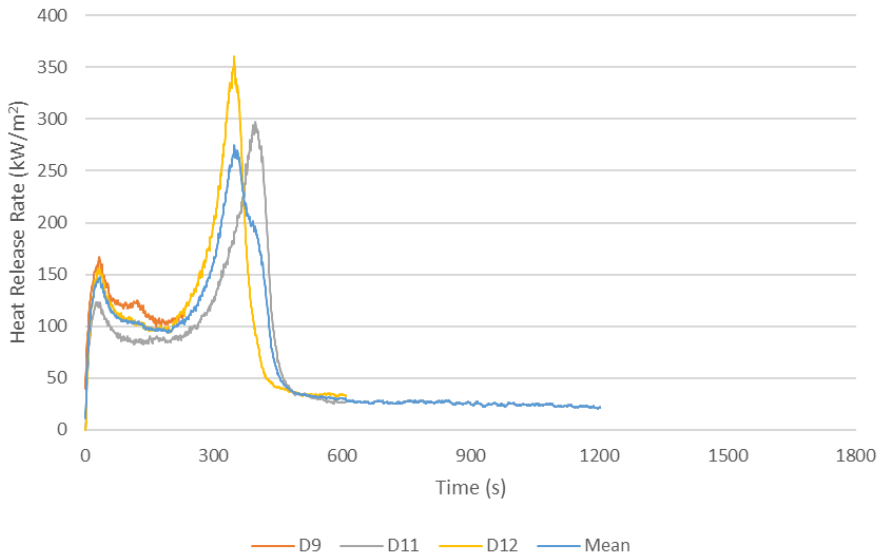


**Product D1 50 kW HRR after ignition.**

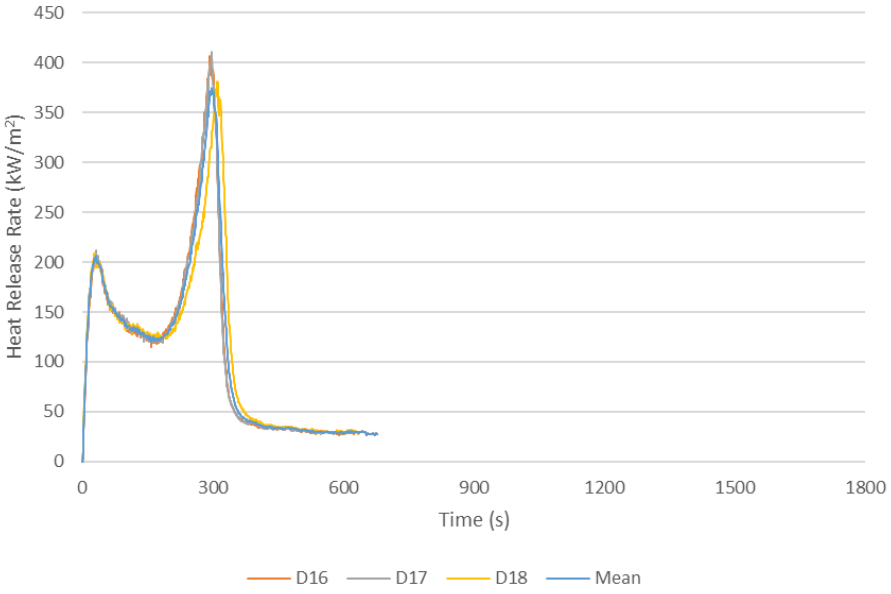


**Product D1 60 kW HRR after ignition.**

## Product D2

| Test | Heat flux (kW/m²) | Time to ignition (s) | Mean / SD | Peak HRR (kW/m²) | Mean / SD | Time to peak HRR (s) | Mean / SD | Time from ignition to peak HRR (s) | Average EHC (MJ/kg) | Mean / SD |
|---|---|---|---|---|---|---|---|---|---|---|
| D32 | 20 | 196 | 202 / 6 | 177.8 | 189 / 14 | 1542 | 1568 / 25 | 421 | 13.3 | 12.6 / 0.4 |
| D33 | | 209 | | 184.5 | | 1591 | | 429 | 15.2 | |
| D34 | | 202 | | 204.9 | | 1570 | | 429 | 17.5 | |
| D35 | 30 | 77 | 79 / 3 | 210.0 | 208 / 3 | 504 | 507 / 7 | 406 | 13.0 | |
| D36 | | 79 | | 210.6 | | 515 | | 402 | 12.9 | |
| D37 | | 82 | | 204.7 | | 501 | | 400 | 13.1 | |
| D38 | 40 | 43 | 44 / 2 | 240.1 | 246 / 5 | 430 | 406 / 25 | 375 | 12.4 | |
| D39 | | 46 | | 248.5 | | 381 | | 324 | 12.4 | |
| D40 | | 43 | | 250.2 | | 406 | | 350 | 12.2 | |
| D41 | 50 | 30 | 29 / 1 | 277.2 | 278 / 4 | 349 | 352 / 3 | 314 | 12.3 | |
| D42 | | 28 | | 275.2 | | 354 | | 319 | 12.9 | |
| D43 | | 30 | | 282.5 | | 354 | | 316 | 12.3 | |
| D44 | 60 | 18 | 19 / 1 | 309.1 | 310 / 2 | 321 | 327 / 9 | 296 | 12.4 | |
| D45 | | 20 | | 312.4 | | 323 | | 298 | 12.1 | |
| D46 | | 20 | | 308.8 | | 338 | | 312 | 12.4 | |

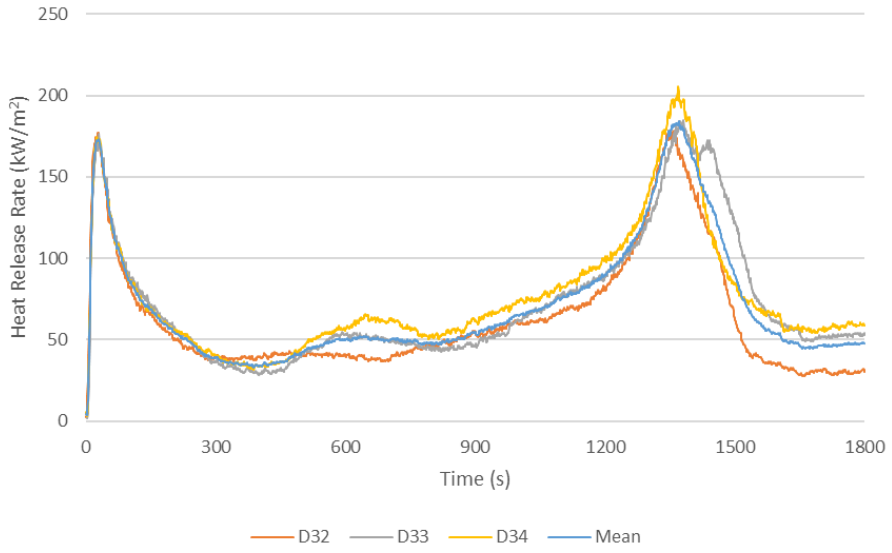


**Product D2 20 kW HRR after ignition.**

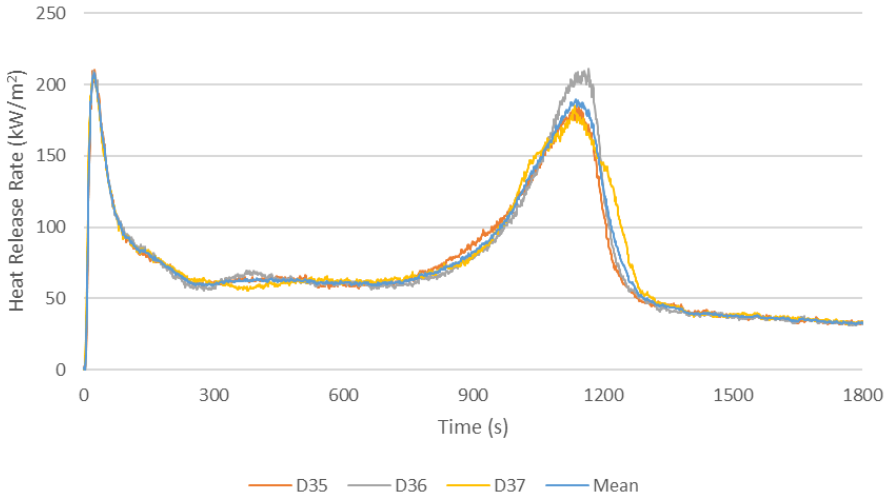


**Product D2 30 kW HRR after ignition.**

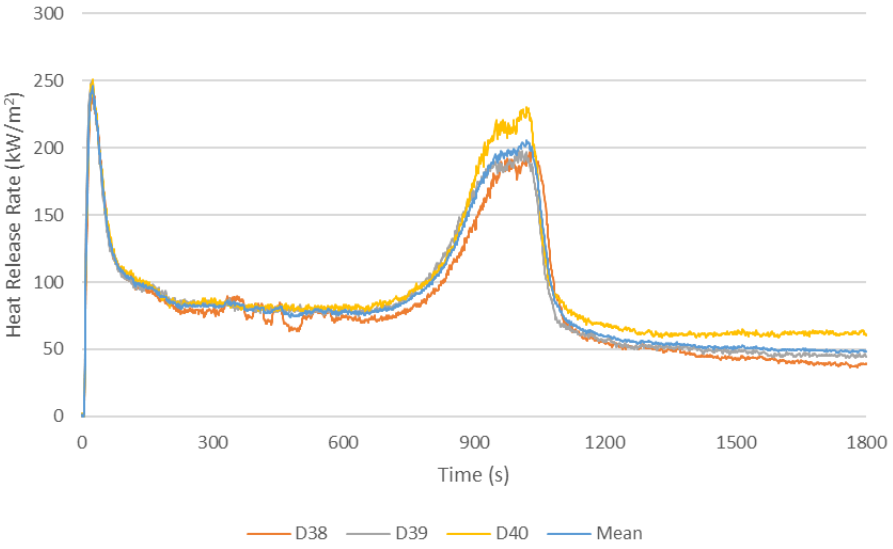


**Product D2 40 kW HRR after ignition.**

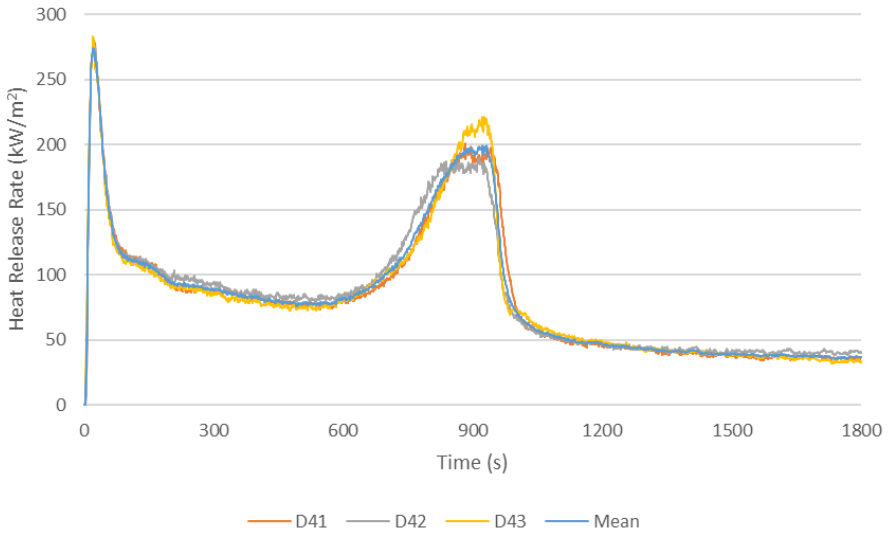


**Product D2 50 kW HRR after ignition.**

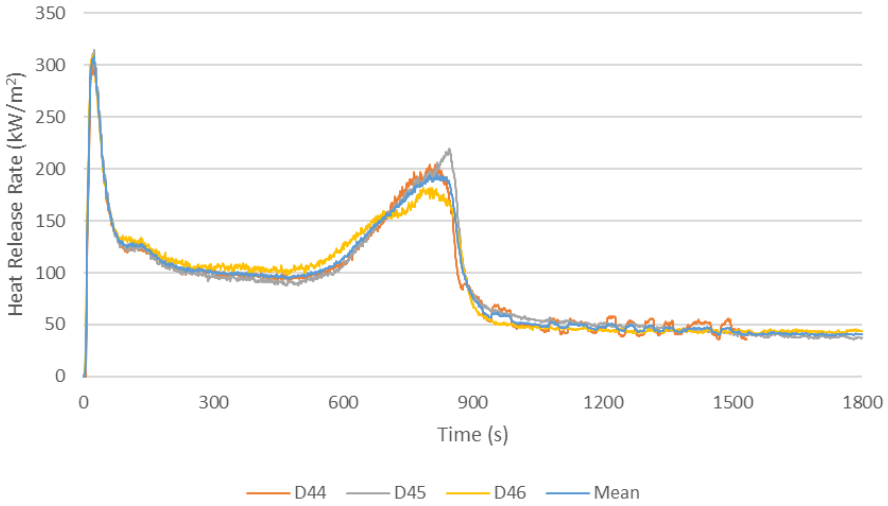


**Product D2 60 kW HRR after ignition.**

## Product D3

| Test | Heat flux (kW/m²) | Time to ignition (s) | Mean / SD | Peak HRR (kW/m²) | Mean / SD | Time to peak HRR (s) | Mean / SD | Time from ignition to peak HRR (s) | Average EHC (MJ/kg) | Mean / SD |
|---|---|---|---|---|---|---|---|---|---|---|
| D61 | 20 | 222 | 227 / 4 | 155.0 | 157 / 2 | 250 | 256 / 8 | 27.9 | 3.6* | 12.8 /1.2* |
| D62 | | 227 | | 155.5 | | 251 | | 23.7 | 3.6* | |
| D63 | | 232 | | 160.2 | | 267 | | 34.9 | 3.3* | |
| D64 | 30 | 89 | 89 / 2 | 191.0 | 194 / 2 | 107 | 110 / 2 | 17.7 | 11.3 | |
| D65 | | 86 | | 196.3 | | 110 | | 23.6 | 12.2 | |
| D66 | | 91 | | 195.7 | | 112 | | 20.7 | 11.2 | |
| D67 | 40 | 48 | 49 / 2 | 223.6 | 228 / 3 | 75 | 73 / 3 | 26.7 | 12.3 | |
| D68 | | 52 | | 229.9 | | 75 | | 23.0 | 12.1 | |
| D69 | | 48 | | 230.2 | | 69 | | 21.1 | 11.9 | |
| D70 | 50 | 34 | 33 / 1 | 274.6 | 268 / 5 | 54 | 53 / 1 | 19.6 | 12.9 | |
| D71 | | 32 | | 266.7 | | 51 | | 19.4 | 12.7 | |
| D72 | | 34 | | 263.6 | | 54 | | 19.8 | 14.0 | |
| D73 | 60 | 20 | 19 / 1 | 293.7 | 298 / 11 | 46 | 44 / 2 | 26.2 | 15.8 | |
| D74 | | 18 | | 288.0 | | 41 | | 22.6 | 12.9 | |
| D75 | | 20 | | 313.6 | | 45 | | 24.6 | 13.7 | |

* EHC is low, second peak evident with other samples was not observed. Excluded from Mean/SD.

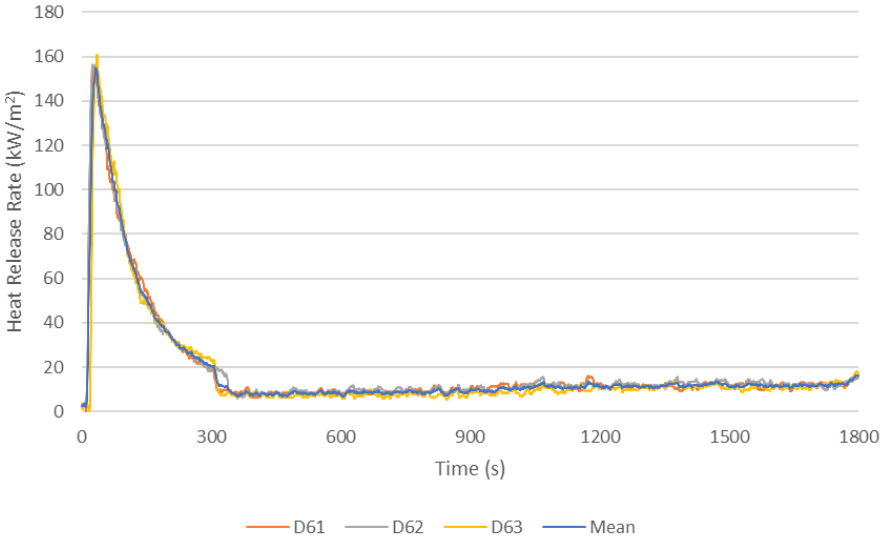


**Product D3 20 kW HRR after ignition.**

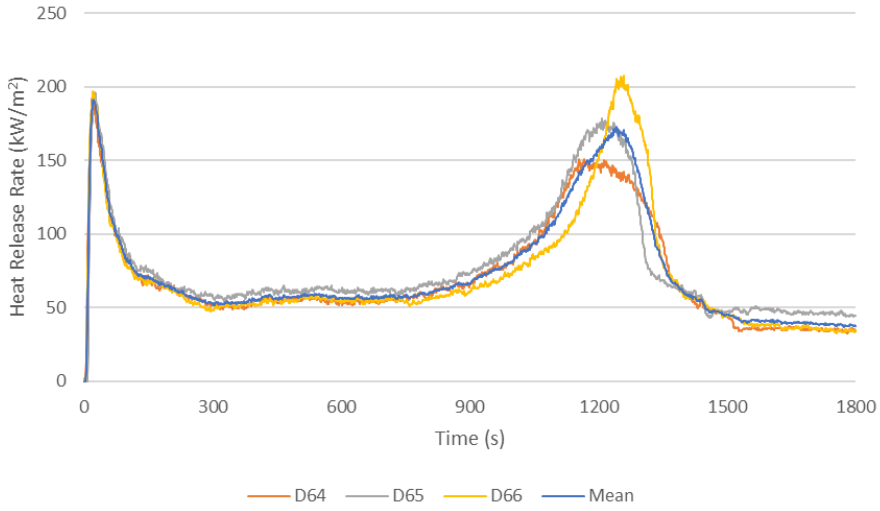


**Product D3 30 kW HRR after ignition.**

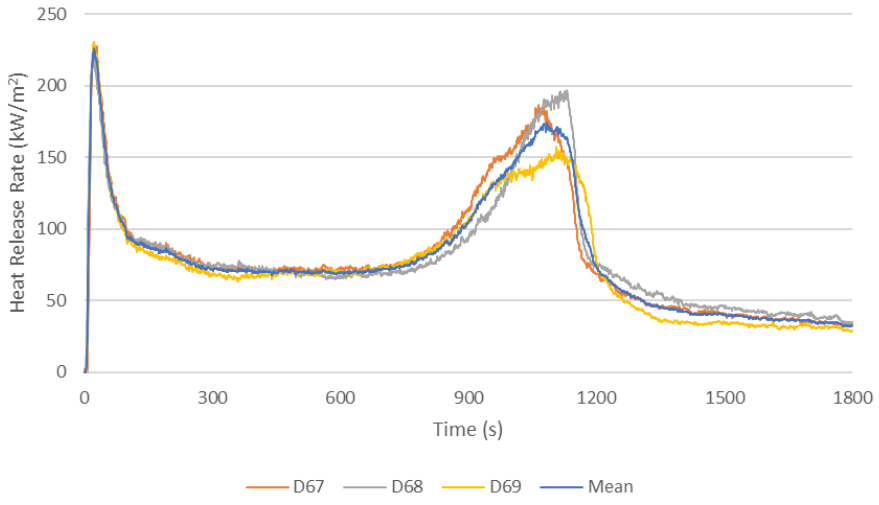


**Product D3 40 kW HRR after ignition.**

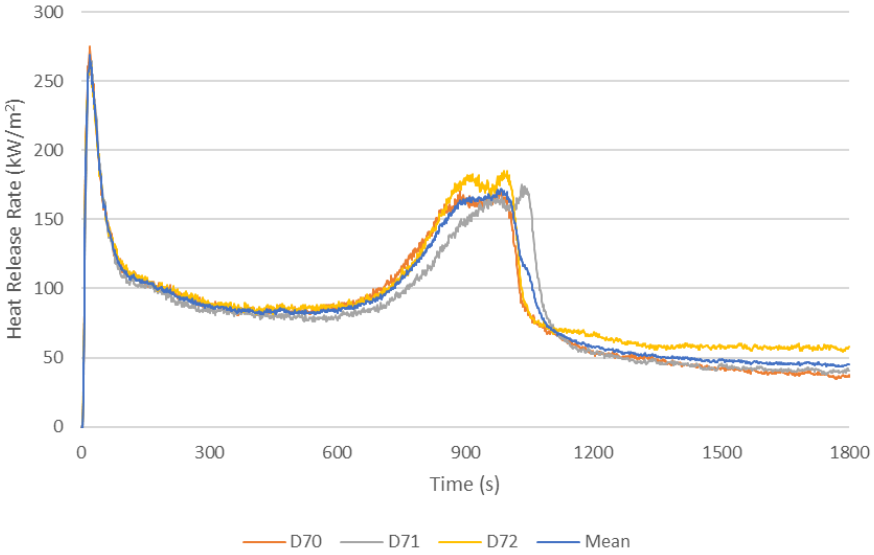


**Product D3 50 kW HRR after ignition.**

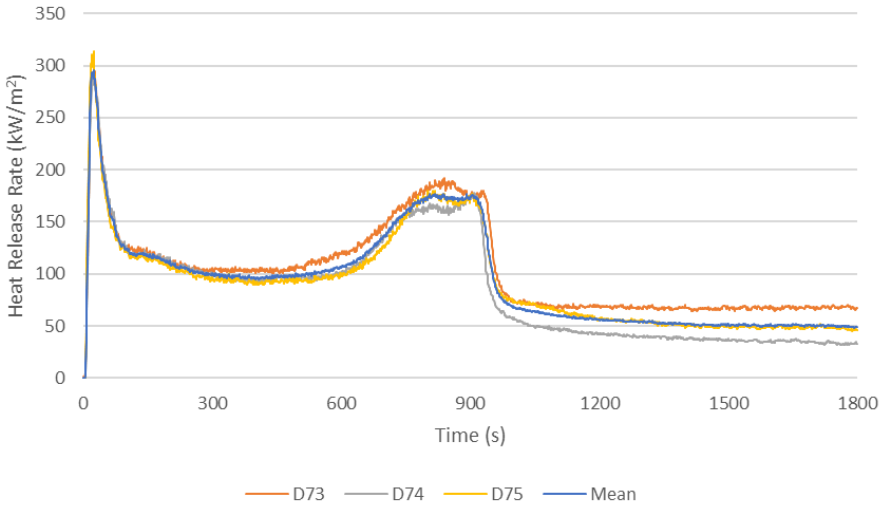


**Product D3 60 kW HRR after ignition.**

## Product F1

| Test | Heat flux (kW/m²) | Time to ignition (s) | Mean / SD | Peak HRR (kW/m²) | Mean / SD | Time to peak HRR (s) | Mean / SD | Time from ignition to peak HRR (s) | Average EHC (MJ/kg) | Mean / SD |
|---|---|---|---|---|---|---|---|---|---|---|
| F1 | 20 | 206 | 211/11 | 134.8 | 144/9 | 228/480* | 388/144 472/10* | 22/274* | 15.3 | 14.9/1.2 |
| F2 | | 226.2 | | 155.7 | | 479 | | 252.8 | 12.0 | |
| F3 | | 200.7 | | 140.6 | | 458 | | 257.3 | 16.2 | |
| F4 | 30 | 91.7 | 84/6 | 198.4 | 212/24 | 334 | 346/14 | 135.6 | 15.1 | |
| F5 | | 77.1 | | 191.5 | | 339 | | 147.5 | 15.3 | |
| F6 | | 82.4 | | 246.1 | | 365 | | 282.6 | 14.9 | |
| F7 | 40 | 41.7 | 47/4 | 221.3 | 246/24 | 287 | 287/1 | 245.3 | 15.1 | |
| F8 | | 47.9 | | 277.9 | | 286 | | 238.1 | 15.8 | |
| F9 | | 50.7 | | 238.2 | | 289 | | 238.3 | 15.8 | |
| F10 | 50 | 28.6 | 24/4 | 351.8 | 287/46 | 250 | 250/3 | 221.4 | 15.8 | |
| F11 | | 19.3 | | 254.5 | | 254 | | 234.7 | 14.9 | |
| F12 | | 24.6 | | 254.3 | | 247 | | 222.4 | 14.4 | |
| F13 | 60 | 15.5 | 15/0.4 | 368.1 | 322/36 | 234 | 232/8 | 218.5 | 15.7 | |
| F14 | | 14.6 | | 317.2 | | 241 | | 226.4 | 11.9 | |
| F15 | | 15.2 | | 280.9 | | 222 | | 206.8 | 15.1 | |

* The second peak, although slightly lower, occurred at 480 s which is consistent with the other specimens.

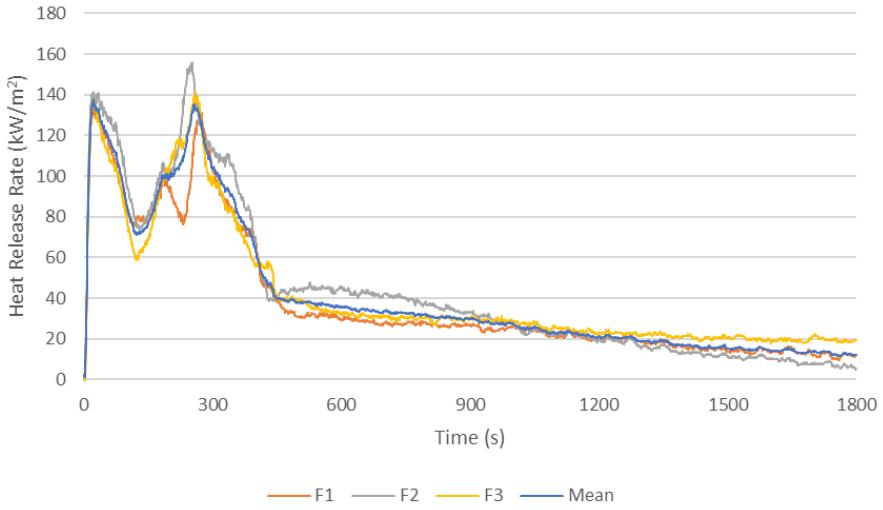


**Product F1 20 kW HRR after ignition.**

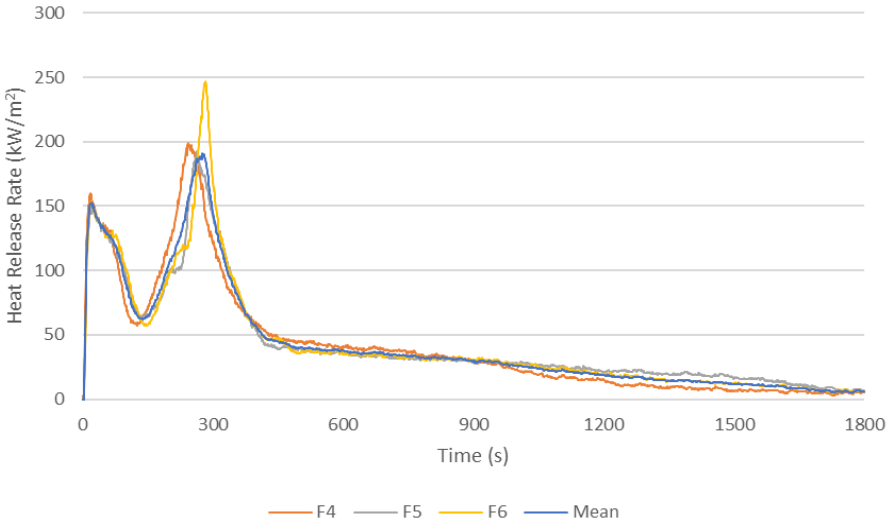


**Product F1 30 kW HRR after ignition.**

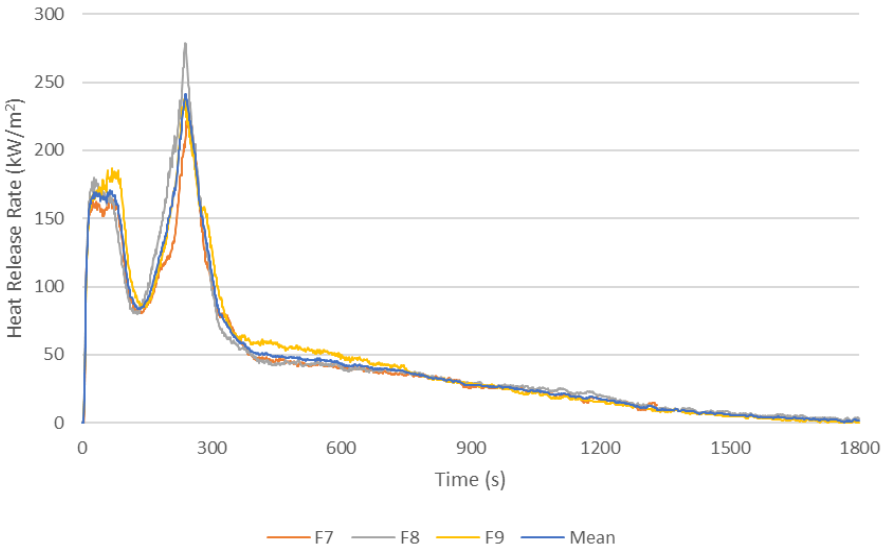


**Product F1 40 kW HRR after ignition.**

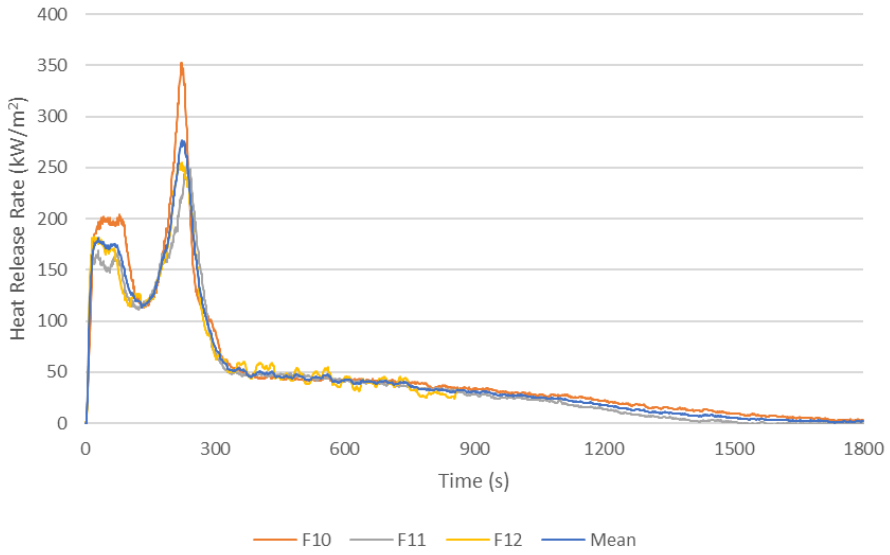


**Product F1 50 kW HRR after ignition.**

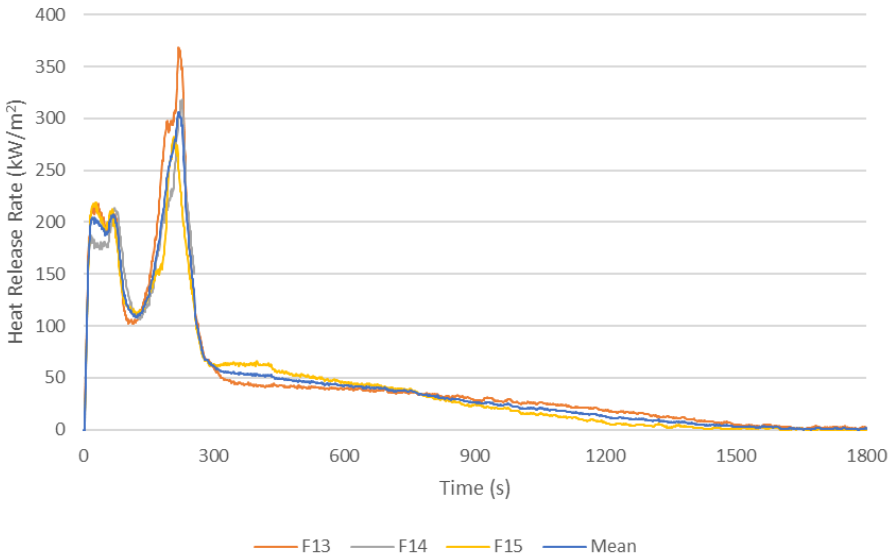


**Product F1 60 kW HRR after ignition.**

## Product F2

| Test | Heat flux (kW/m²) | Time to ignition (s) | Mean / SD | Peak HRR (kW/m²) | Mean / SD | Time to peak HRR (s) | Mean / SD | Time from ignition to peak HRR (s) | Average EHC (MJ/kg) | Mean / SD |
|---|---|---|---|---|---|---|---|---|---|---|
| F31 | 20 | 203.9 | 208/6 | 167.0 | 160/7 | 244 | 240/5 | 36.1 | 9.6 | 14.5/1.9 |
| F32 | | 203.3 | | 163.6 | | 243 | | 39.7 | 13.6 | |
| F33 | | 216.1 | | 150.6 | | 234 | | 17.9 | 13.2 | |
| F34 | 30 | 61.7 | 74/16 | 184.1 | 188/23 | 436 | 353/171 483/33* | 374.3 | 14.6 | |
| F35 | | 63.3 | | 217.3 | | 509 | | 445.7 | 14.7 | |
| F38 | | 96.9 | | 161.1 | | 115/503* | | 18.1/406.1* | 14.6 | |
| F39 | 40 | 41.4 | 39/2 | 174.0 | 185/26 | 57 | 172/166 54/2** | 15.6 | 14.8 | |
| F40 | | 35.8 | | 221.4 | | 54**/407 | | 18.2**/371.2 | 14.7 | |
| F43 | | 38.9 | | 160.1 | | 52 | | 13.1 | 11.3 | |
| F44 | 50 | 27.4 | 26/3 | 256.6 | 250/6 | 402 | 276/146 374/20* | 374.6 | 16.3 | |
| F45 | | 21.2 | | 243.2 | | 71/366* | | 49.8/344.8* | 15.9 | |
| F46 | | 28.9 | | 249.3 | | 356 | | 327.1 | 14.2 | |
| F47 | 60 | 24.0 | 19/4 | 306.4 | 307/1 | 72/343* | 247/124 337/9* | 48/319* | 16.4 | |
| F48 | | 13.5 | | 308.5 | | 325 | | 311.5 | 17.4 | |
| F49 | | 20.5 | | 306.3 | | 344 | | 323.5 | 16.1 | |

* Although the earlier peak was higher, the time to the second peak was more consistent with the other specimens.

** Although the second peak was higher, the time to the first peak was more consistent with the other specimens.

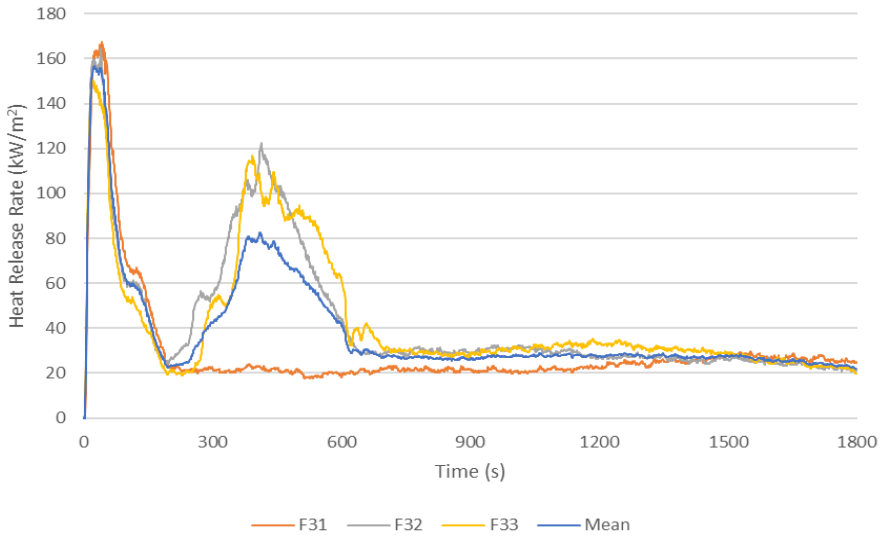


**Product F2 20 kW HRR after ignition.**

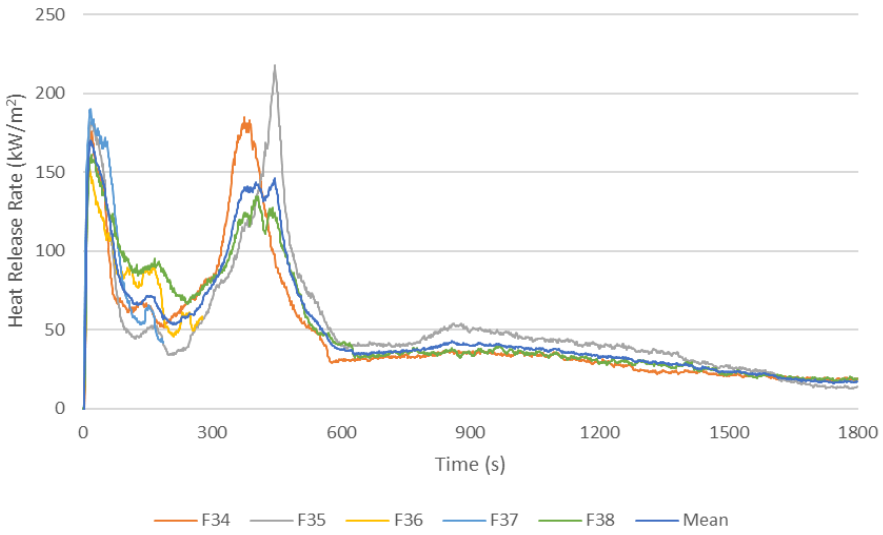


**Product F2 30 kW HRR after ignition.**

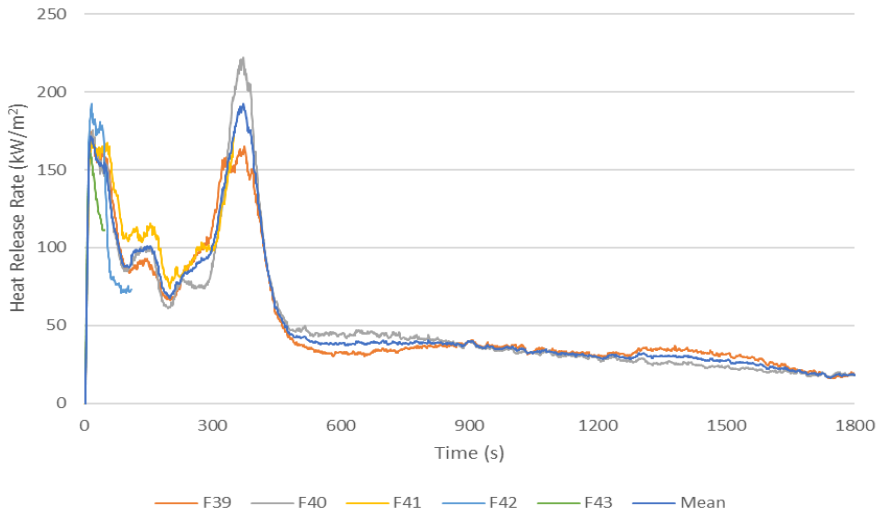


**Product F2 40 kW HRR after ignition.**

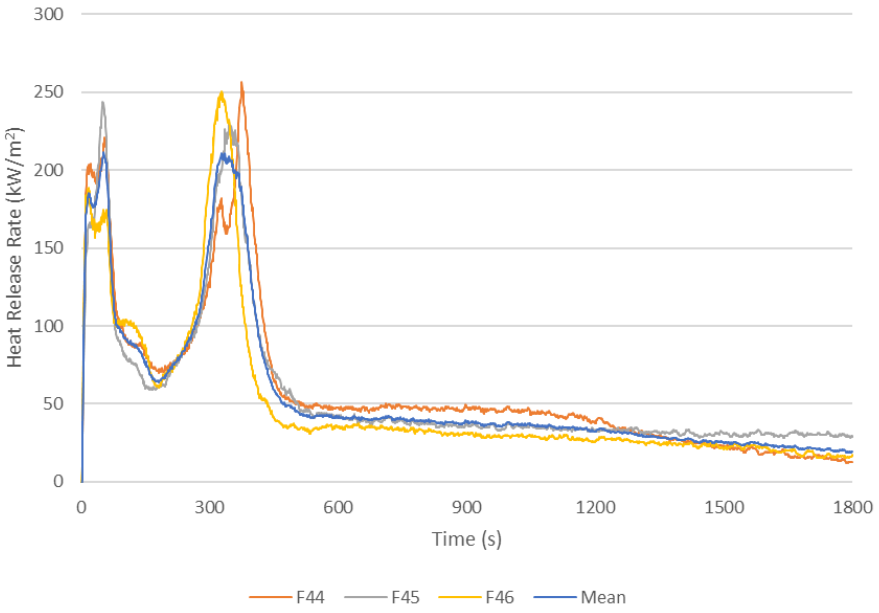


**Product F2 50 kW HRR after ignition.**

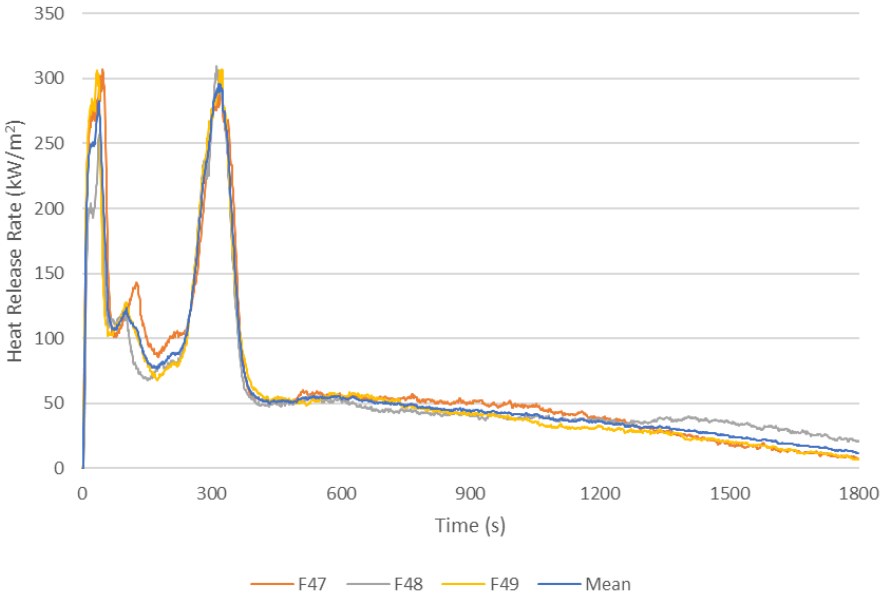


**Product F2 60 kW HRR after ignition.**

## Product F3

| Test | Heat flux (kW/m²) | Time to ignition (s) | Mean / SD | Peak HRR (kW/m²) | Mean / SD | Time to peak HRR (s) | Mean / SD | Time from ignition to peak HRR (s) | Average EHC (MJ/kg) | Mean / SD |
|---|---|---|---|---|---|---|---|---|---|---|
| F61 | 20 | 238.7 | 237/4 | 170.5 | 159/9 | 260 | 262/3 | 21.3 | 11.2 | 13.1/2.3 |
| F62 | | 230.9 | | 149.3 | | 266 | | 35.1 | 12.5 | |
| F63 | | 239.8 | | 155.8 | | 260 | | 20.2 | 5.5 | |
| F64 | 30 | 92.9 | 86/5 | 181.1 | 179/2 | 124 | 112/9 | 31.1 | 12.8 | |
| F65 | | 82.4 | | 177.4 | | 109 | | 26.6 | 12.9 | |
| F66 | | 82.2 | | 179.6 | | 102 | | 19.8 | 12.6 | |
| F67 | 40 | 38.6 | 36/3 | 197.4 | 205/5 | 679 | 482/286 688/7* | 640.4 | 14.9 | |
| F68 | | 32.1 | | 208.5 | | 690 | | 657.9 | 14.0 | |
| F69 | | 36.0 | | 208.0 | | 78/695* | | 42.0/659.0* | 12.9 | |
| F70 | 50 | 23.8 | 26/2 | 235.7 | 245/7 | 629 | 618/9 | 605.2 | 14.3 | |
| F71 | | 28.5 | | 245.0 | | 607 | | 578.5 | 14.2 | |
| F72 | | 26.2 | | 252.9 | | 619 | | 592.8 | 15.1 | |
| F73 | 60 | 15.9 | 17/1 | 251.7 | 262/7 | 533 | 558/18 | 517.1 | 14.3 | |
| F74 | | 17.1 | | 267.5 | | 568 | | 550.9 | 15.1 | |
| F75 | | 16.8 | | 265.7 | | 574 | | 557.2 | 14.7 | |

* Although the earlier peak was higher, the time to the second peak was more consistent with the other specimens.

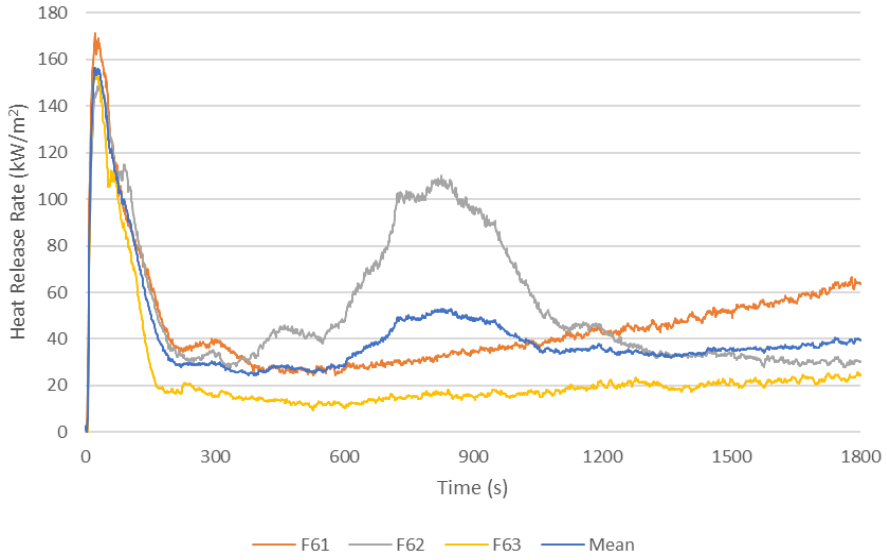


**Product F3 20 kW HRR after ignition.**

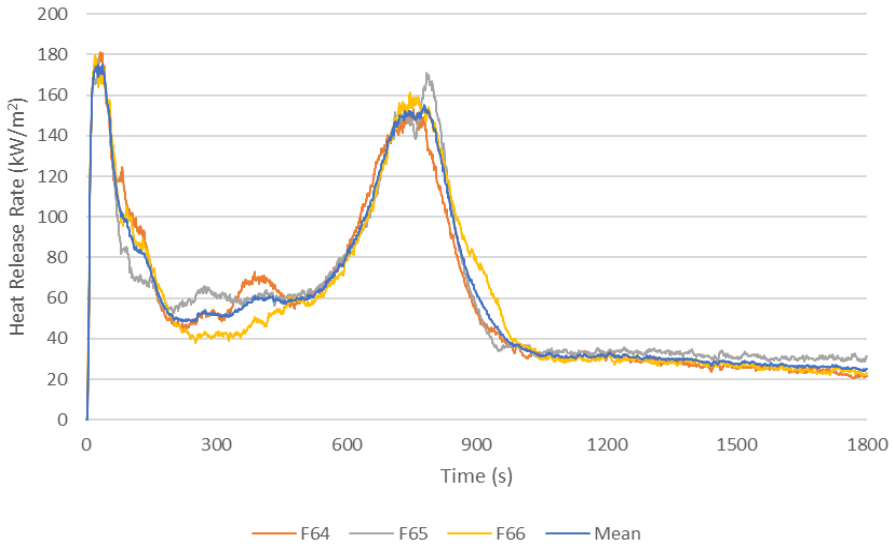


**Product F3 30 kW HRR after ignition.**

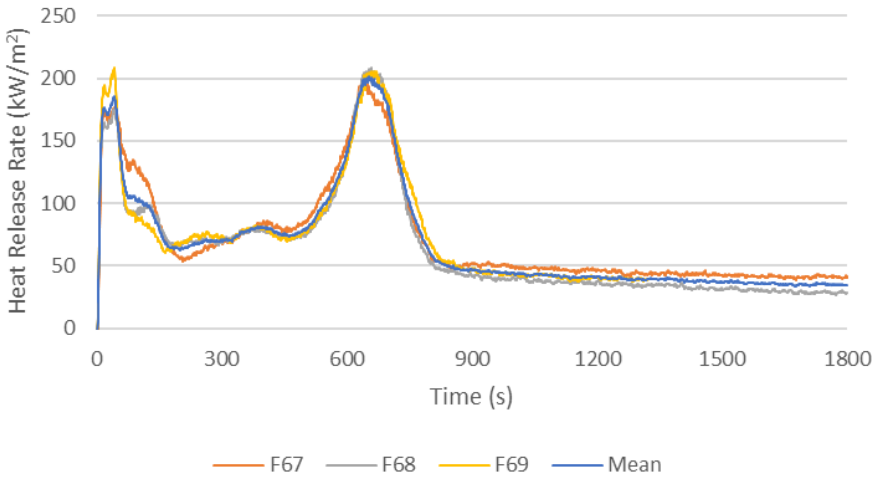


**Product F3 40 kW HRR after ignition.**

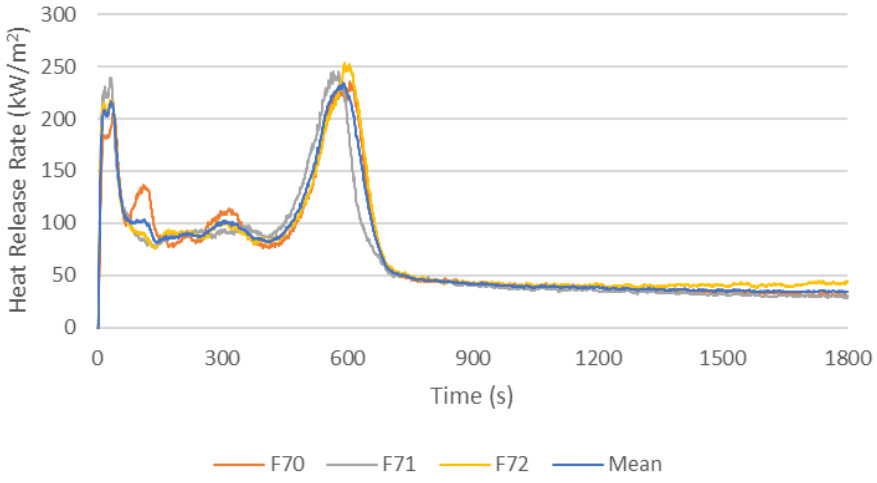


**Product F3 50 kW HRR after ignition.**

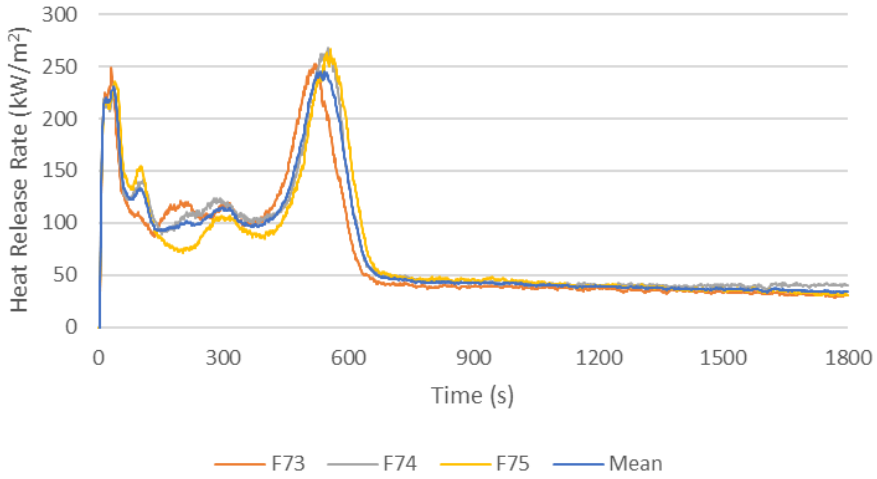


**Product F3 60 kW HRR after ignition.**

## Product F4

| Test | Heat flux (kW/m²) | Time to ignition (s) | Mean / SD | Peak HRR (kW/m²) | Mean / SD | Time to peak HRR (s) | Mean / SD | Time from ignition to peak HRR (s) | Average EHC (MJ/kg) | Mean / SD |
|---|---|---|---|---|---|---|---|---|---|---|
| F91 | 20 | 217.1 | 231/11 | 136.6 | 146/12 | 244 | 250/9 | 26.9 | 15.2 | 15.6/1.6 |
| F92 | | 244.3 | | 135.6 | | 262 | | 17.7 | 14.2 | |
| F93 | | 230.6 | | 161.3 | | 244 | | 17.4 | 20.7 | |
| F94 | 30 | 97.8 | 95/8 | 167.9 | 174/5 | 512 | 495/21 | 414.2 | 14.4 | |
| F95 | | 102.2 | | 173.2 | | 508 | | 405.8 | 14.4 | |
| F96 | | 83.7 | | 180.8 | | 465 | | 381.3 | 14.6 | |
| F97 | 40 | 36.9 | 40/3 | 275.3 | 221/40 | 455 | 437/13 | 418.1 | 15.5 | |
| F98 | | 43.2 | | 182.8 | | 430 | | 386.8 | 15.0 | |
| F99 | | 38.7 | | 204.7 | | 425 | | 386.3 | 17.8 | |
| F100 | 50 | 19.0 | 23/3 | 215.9 | 219/7 | 382 | 392/29 | 363.0 | 15.0 | |
| F101 | | 21.3 | | 211.9 | | 363 | | 341.7 | 16.4 | |
| F102 | | 27.1 | | 227.7 | | 431 | | 403.9 | 15.6 | |
| F103 | 60 | 17.1 | 18/1 | 281.2 | 270/16 | 393 | 366/20 | 375.9 | 15.3 | |
| F104 | | 18.0 | | 280.2 | | 355 | | 337.0 | 15.2 | |
| F105 | | 19.0 | | 247.5 | | 349 | | 330.0 | 15.4 | |

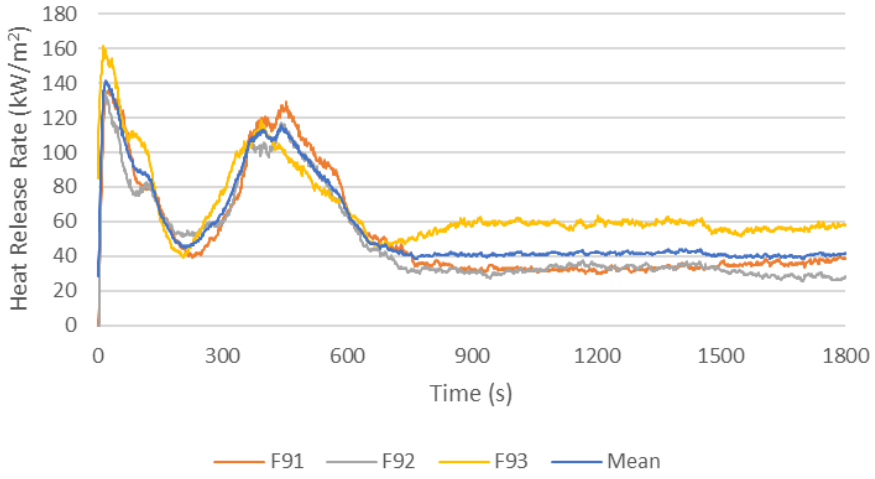


**Product F4 20 kW HRR after ignition.**

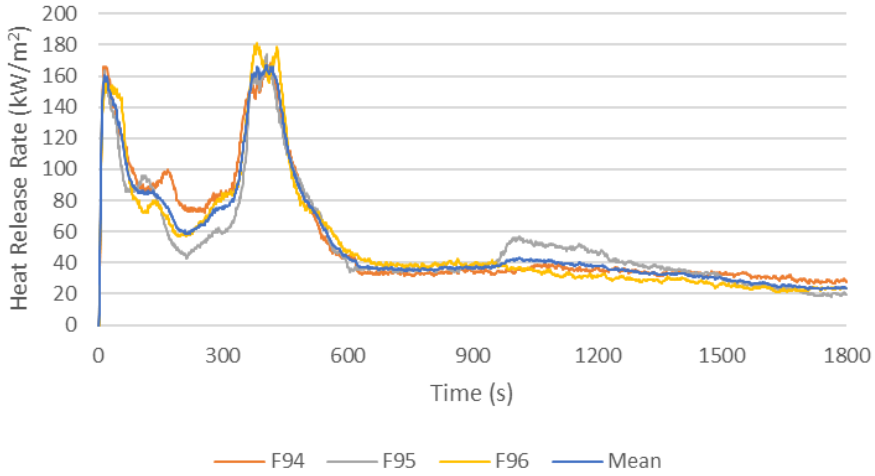


**Product F4 30 kW HRR after ignition.**

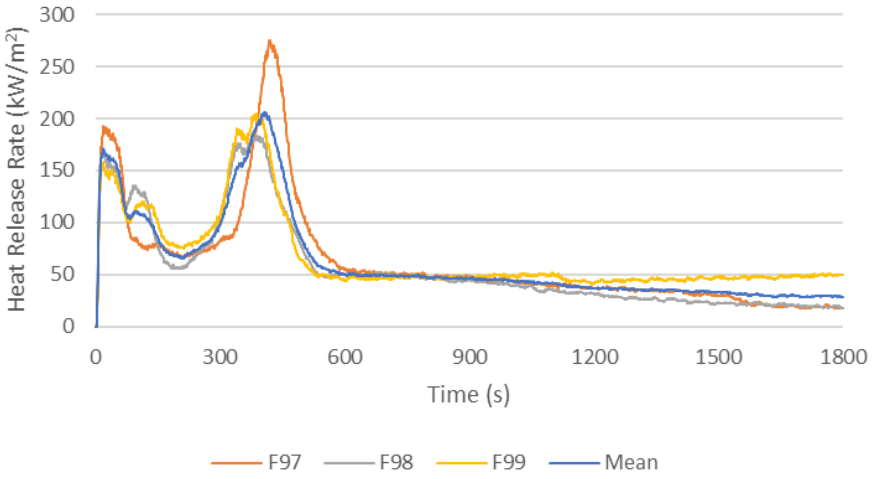


**Product F4 40 kW HRR after ignition.**

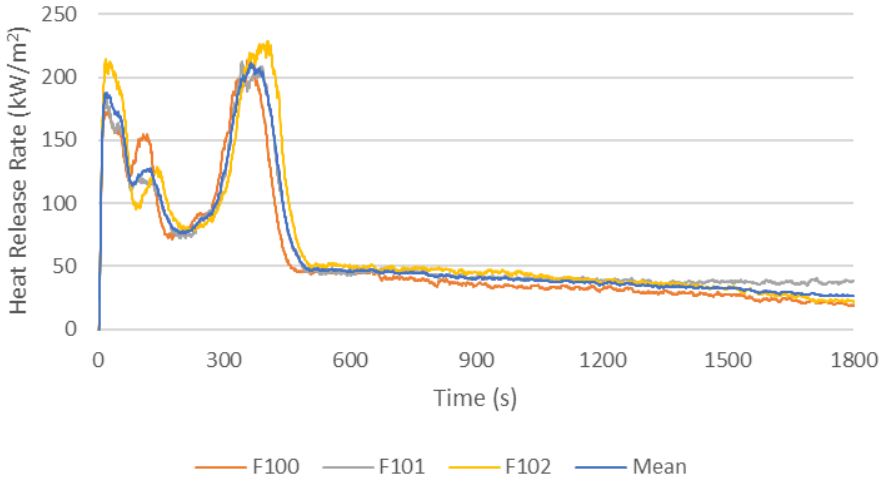


**Product F4 50 kW HRR after ignition.**

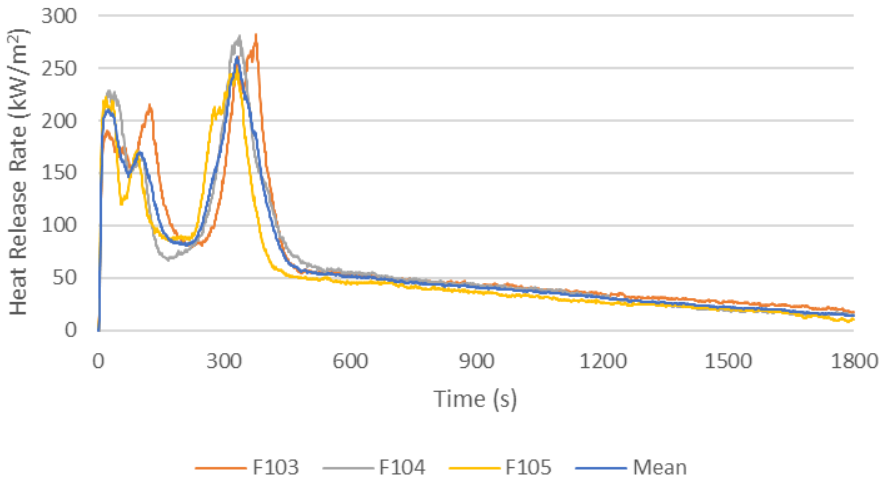


**Product F4 60 kW HRR after ignition.**

## Product F5

| Test | Heat flux (kW/m²) | Time to ignition (s) | Mean / SD | Peak HRR (kW/m²) | Mean / SD | Time to peak HRR (s) | Mean / SD | Time from Ignition to Peak HRR (s) | Average EHC (MJ/kg) | Mean / SD |
|---|---|---|---|---|---|---|---|---|---|---|
| F121 | 20 | 262.0 | 228/26 | 146.9 | 140/5 | 283/638* | 367/192 248/26* | 21.0/376.0* | 15.5 | 15.5/0.8 |
| F122 | | 221.8 | | 135.3 | | 242 | | 20.2 | 14.9 | |
| F123 | | 200.3 | | 138.1 | | 220 | | 19.7 | 14.9 | |
| F124 | 30 | 69.0 | 74/6 | 155.1 | 154/5 | 85 | 216/186 88/5* | 16.0 | 15.4 | |
| F125 | | 81.6 | | 158.2 | | 96/480* | | 14.4/398.4* | 14.6 | |
| F126 | | 71.4 | | 147.3 | | 84 | | 12.6 | 17.9 | |
| F127 | 40 | 30.9 | 34/4 | 180.8 | 196/16 | 376 | 389/18 | 345.1 | 15.7 | |
| F128 | | 39.7 | | 217.6 | | 414 | | 374.3 | 16.1 | |
| F129 | | 32.6 | | 190.7 | | 378 | | 345.4 | 15.2 | |
| F130 | 50 | 24.4 | 22/3 | 202.6 | 225/21 | 355 | 336/14 | 330.6 | 15.1 | |
| F131 | | 24.0 | | 253.3 | | 329 | | 305.0 | 15.9 | |
| F132 | | 18.8 | | 219.2 | | 324 | | 305.2 | 15.8 | |
| F133 | 60 | 11.2 | 14/2 | 249.5 | 243/26 | 310 | 302/14 | 298.8 | 15.0 | |
| F134 | | 14.2 | | 272.0 | | 314 | | 299.8 | 15.2 | |
| F135 | | 16.4 | | 208.5 | | 282 | | 265.6 | 15.9 | |

* Although the second peak was higher, the time to the first peak was more consistent with the other specimens.

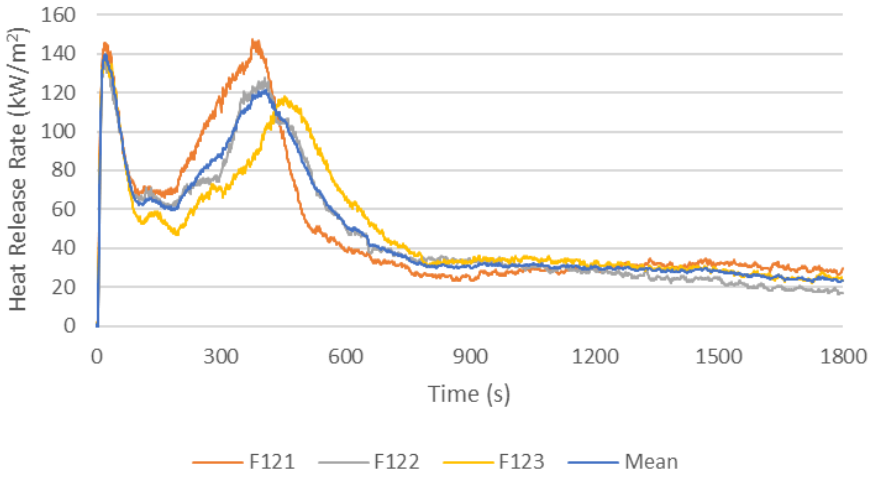


**Product F5 20 kW HRR after ignition.**

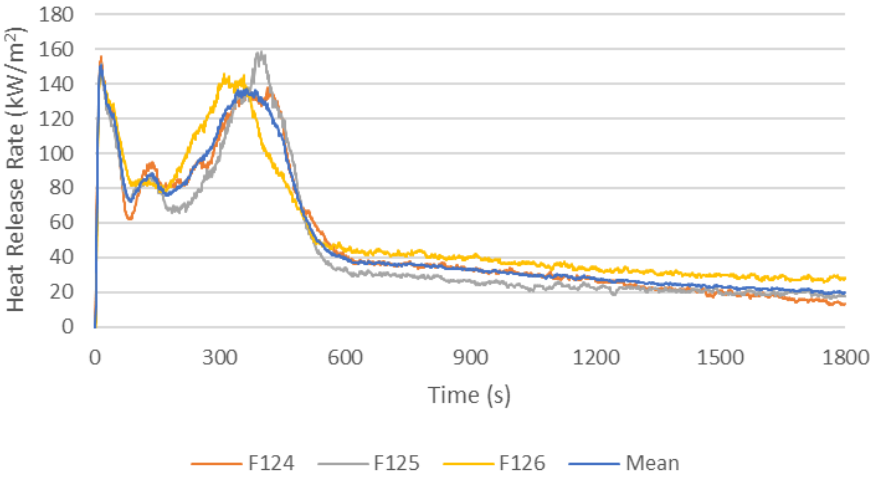


**Product F5 30 kW HRR after ignition.**

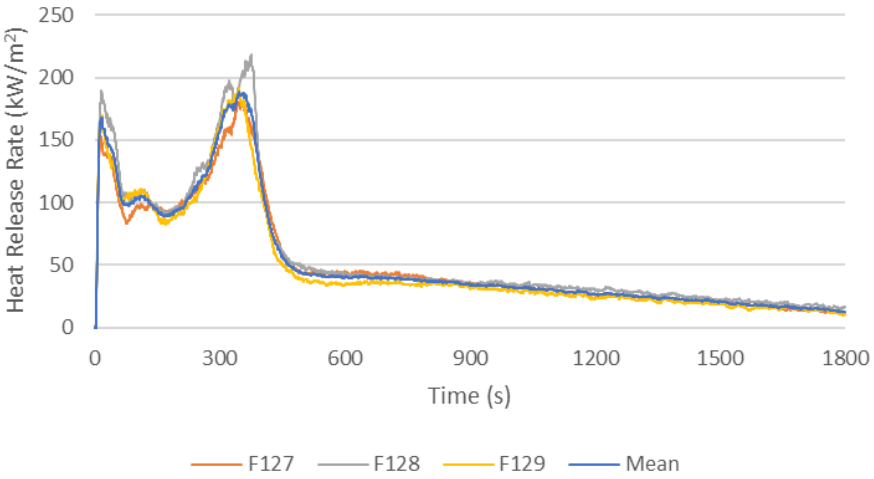


**Product F5 40 kW HRR after ignition.**

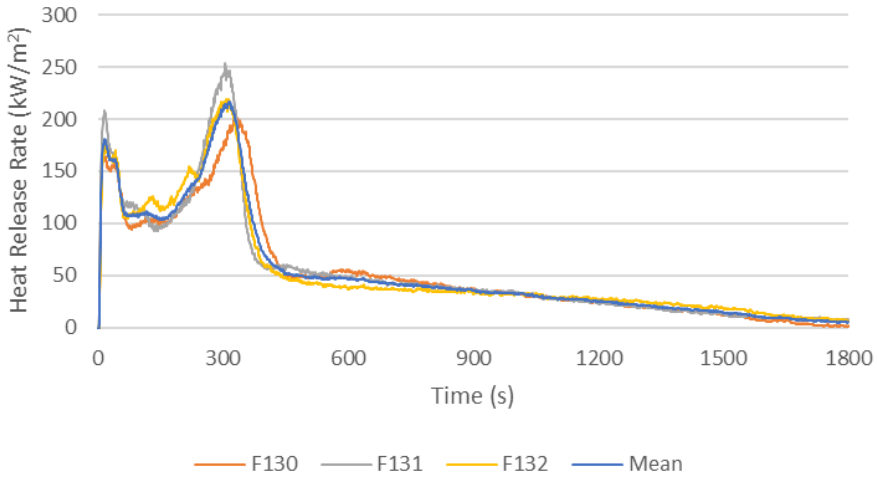


**Product F5 50 kW HRR after ignition.**

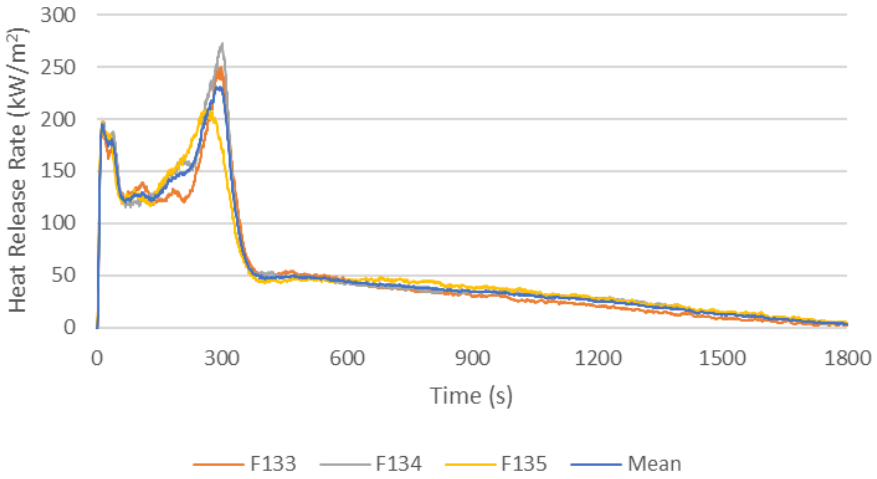


**Product F5 60 kW HRR after ignition.**

## Product F6

| Test | Heat flux (kW/m²) | Time to ignition (s) | Mean / SD | Peak HRR (kW/m²) | Mean / SD | Time to peak HRR (s) | Mean / SD | Time from ignition to peak HRR (s) | Average EHC (MJ/kg) | Mean / SD |
|---|---|---|---|---|---|---|---|---|---|---|
| F151 | 20 | 214.2 | 205/22 | 143.5 | 152/6 | 235 | 375/186<br>229/22** | 20.8 | 13.6 | 14.9/0.9* |
| F152 | | 225.5 | | 157.4 | | 252 | | 26.8 | 8.8* | |
| F153 | | 175.4 | | 153.7 | | 199/637** | | 23.6/461.6** | 12.7 | |
| F156 | 30 | 59.0 | 60/4 | 162.7 | 177/17 | 76/440*** | 335/184<br>457/20*** | 17.0/381.0*** | 14.4 | |
| F157 | | 56.0 | | 166.8 | | 445 | | 389.0 | 15.1 | |
| F158 | | 65.5 | | 200.3 | | 485 | | 419.5 | 14.5 | |
| F159 | 40 | 37.9 | 37/3 | 191.2 | 232/29 | 77/364*** | 303/160<br>398/29*** | 39.1/326.1*** | 14.3 | |
| F160 | | 33.6 | | 251.3 | | 434 | | 400.4 | 15.1 | |
| F161 | | 39.6 | | 253.4 | | 397 | | 357.4 | 14.8 | |
| F162 | 50 | 25.6 | 20/4 | 231.0 | 292/44 | 59/336*** | 278/155<br>371/25*** | 33.4/310.4*** | 15.4 | |
| F163 | | 17.5 | | 334.4 | | 382 | | 364.5 | 15.6 | |
| F164 | | 18.1 | | 310.8 | | 394 | | 375.9 | 15.3 | |
| F165 | 60 | 18.3 | 19/2 | 347.2 | 372/29 | 48/312*** | 231/130<br>319/7*** | 27.9/293.7*** | 15.7 | |
| F166 | | 15.7 | | 412.4 | | 317 | | 301.3 | 16.4 | |
| F167 | | 21.4 | | 357.2 | | 329 | | 307.6 | 15.3 | |

* EHC is low, second peak evident with other samples was not observed. Excluded from Mean/SD.

** Although the second peak was higher, the time to the first peak was more consistent with the other specimens.

*** Although the first peak was higher, the time to the second peak was more consistent with the other specimens.

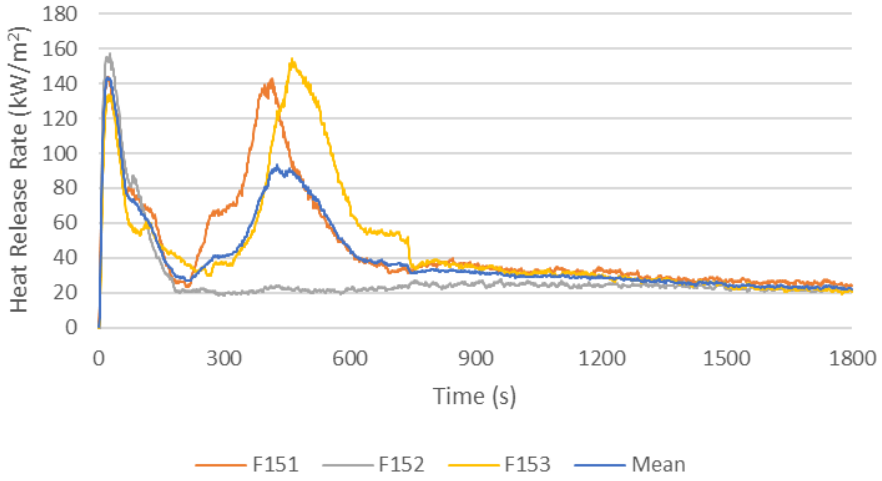


**Product F6 20 kW HRR after ignition.**

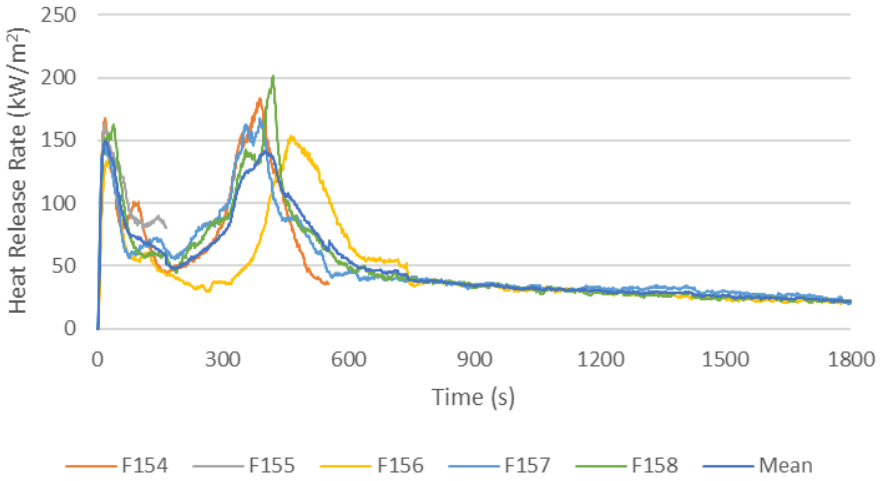


**Product F6 30 kW HRR after ignition.**

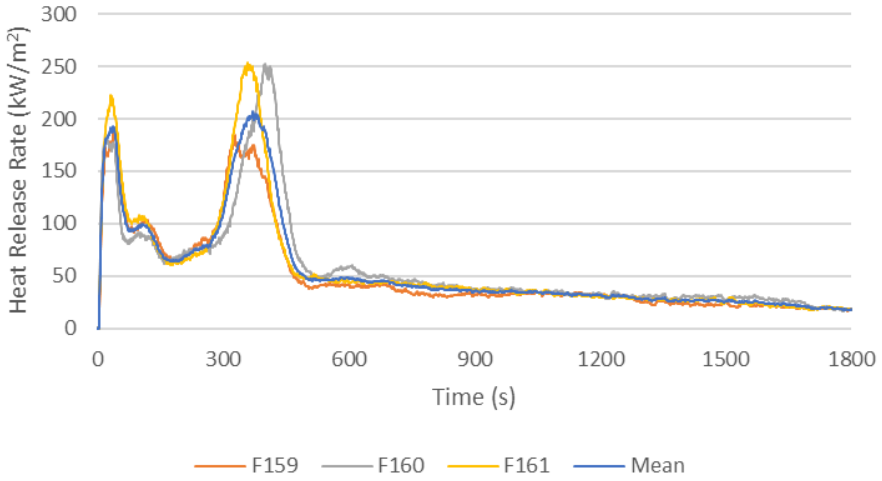


**Product F6 40 kW HRR after ignition.**

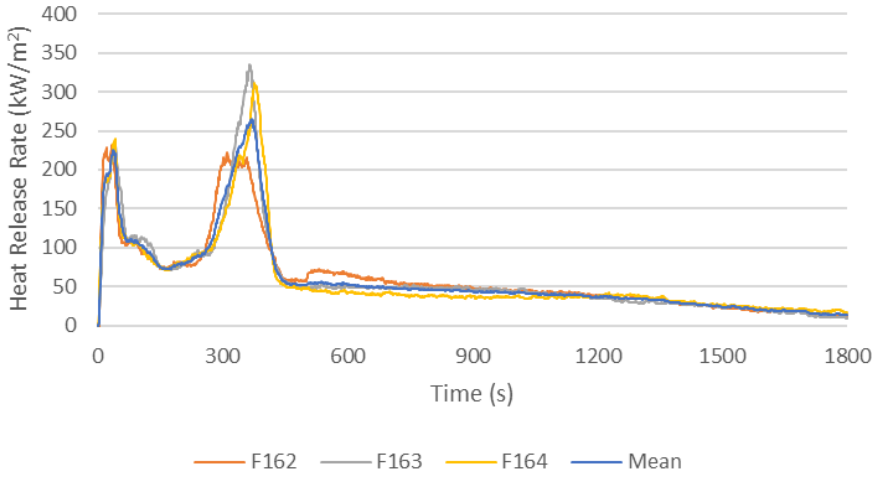


**Product F6 50 kW HRR after ignition.**

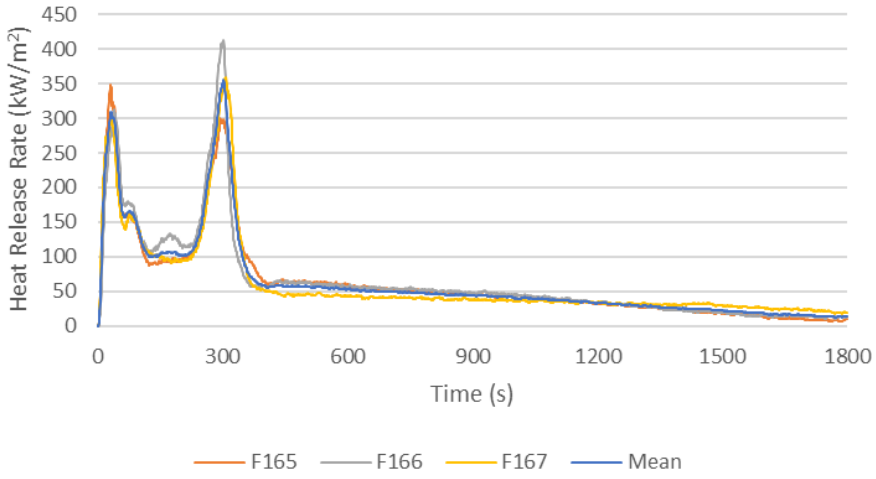


**Product F6 60 kW HRR after ignition.**

# Appendix B: Minimum heat flux for ignition measurements

NI = no ignition after 1,800 s exposure.

**Product B1 minimum heat flux ($\dot{q}''_{min}$).**

| Test number | Heat flux (kW/m²) | Time to ignition (s) | Minimum heat flux $\dot{q}''_{min}$ (kW/m²) |
|---|---|---|---|
| B17 | 15 | 349 | 9.5 |
| B18 | 14 | 517 | |
| B19 | 13 | 515 | |
| B20 | 12 | 647 | |
| B21 | 11 | 928 | |
| B22 | 10 | 1,041 | |
| B23 | 9 | NI | |
| B24 | | NI | |
| B25 | | NI | |

**Product B2 minimum heat flux ($\dot{q}''_{min}$).**

| Test number | Heat flux (kW/m²) | Time to ignition (s) | Minimum heat flux $\dot{q}''_{min}$ (kW/m²) |
|---|---|---|---|
| B47 | 15 | 540 | 9.5 |
| B48 | 14 | 557 | |
| B49 | 13 | 695 | |
| B50 | 12 | 836 | |
| B51 | 11 | 1,160 | |
| B52 | 10 | 1,105 | |
| B53 | 9 | NI | |
| B54 | | NI | |
| B55 | | NI | |

**Product C1 minimum heat flux ($\dot{q}''_{min}$).**

| Test number | Heat flux (kW/m²) | Time to ignition (s) | Minimum heat flux $\dot{q}''_{min}$ (kW/m²) |
|---|---|---|---|
| C16 | 15 | NI | 13.5 |
| C17 | 14 | 1,249 | |
| C18 | 13 | NI | |
| C19 | | NI | |
| C20 | | NI | |

**Product D2 minimum heat flux ($\dot{q}''_{min}$).**

| Test number | Heat flux (kW/m²) | Time to ignition (s) | Minimum heat flux $\dot{q}''_{min}$ (kW/m²) |
|---|---|---|---|
| D47 | 15 | 372 | 12.5 |
| D49 | 14 | 536 | |
| D50 | 13 | NI | |
| D51 | | 1,740 | |
| D52 | 12 | NI | |
| D53 | | NI | |
| D54 | | NI | |

**Product D3 minimum heat flux ($\dot{q}''_{min}$).**

| Test number | Heat flux (kW/m²) | Time to ignition (s) | Minimum heat flux $\dot{q}''_{min}$ (kW/m²) |
|---|---|---|---|
| D85 | 18 | NI | 17.5 |
| D86 | | 301 | |
| D82 | 17 | NI | |
| D83 | | NI | |
| D84 | | NI | |

**Product F1 minimum heat flux ($\dot{q}''_{min}$).**

| Test number | Heat flux (kW/m²) | Time to ignition (s) | Minimum heat flux $\dot{q}''_{min}$ (kW/m²) |
|---|---|---|---|
| F20 | 11 | 1077 | 9.5 |
| F21 | 10 | NI | |
| F22 | | NI | |
| F23 | | 1,183 | |
| F24 | 9 | NI | |
| F25 | | NI | |
| F26 | | NI | |

**Product F2 minimum heat flux ($\dot{q}''_{min}$).**

| Test number | Heat flux (kW/m²) | Time to ignition (s) | Minimum heat flux $\dot{q}''_{min}$ (kW/m²) |
|---|---|---|---|
| F50 | 15 | 609 | 10.5 |
| F51 | 14 | 766 | |
| F52 | 13 | NI | |
| F53 | 12 | 1,285 | |
| F54 | 11 | NI | |
| F55 | | 1,649 | |
| F56 | 10 | NI | |
| F57 | | NI | |
| F58 | | NI | |

**Product F3 minimum heat flux ($\dot{q}''_{min}$).**

| Test number | Heat flux (kW/m²) | Time to ignition (s) | Minimum heat flux $\dot{q}''_{min}$ (kW/m²) |
|---|---|---|---|
| F76 | 15 | 804 | 12.5 |
| F77 | 14 | 1,254 | |
| F78 | 13 | 1,607 | |
| F79 | 12 | NI | |
| F80 | | NI | |
| F81 | | NI | |

**Product F4 minimum heat flux ($\dot{q}''_{min}$).**

| Test number | Heat flux (kW/m²) | Time to ignition (s) | Minimum heat flux $\dot{q}''_{min}$ (kW/m²) |
|---|---|---|---|
| F106 | 15 | | 9.5 |
| F107 | 14 | | |
| F108 | 12 | | |
| F109 | 10 | | |
| F110 | 9 | NI | |
| F111 | | NI | |
| F112 | | NI | |

**Product F5 minimum heat flux ($\dot{q}''_{min}$).**

| Test number | Heat flux (kW/m²) | Time to ignition (s) | Minimum heat flux $\dot{q}''_{min}$ (kW/m²) |
|---|---|---|---|
| F136 | 15 | | 9.5 |
| F137 | 13 | | |
| F138 | 11 | | |
| F139 | 10 | | |
| F140 | 9 | NI | |
| F141 | | NI | |
| F142 | | NI | |

**Product F6 minimum heat flux ($\dot{q}''_{min}$).**

| Test number | Heat flux (kW/m²) | Time to ignition (s) | Minimum heat flux $\dot{q}''_{min}$ (kW/m²) |
|---|---|---|---|
| F168 | 15 | 356 | 9.5 |
| F169 | 13 | 515 | |
| F170 | 10 | NI | |
| F171 | 11 | 1,368 | |
| F172 | 10 | 1,093 | |
| F173 | 9 | NI | |
| F174 | | NI | |
| F175 | | NI | |

# Appendix C: Product NZBC Group Numbers

| Product | Specimen number | $t_{ig}$ | $I_{ig}$ | $IQ_{2min}$ | $IQ_{10min}$ | $IQ_{12min}$ | IQ1 | IQ2 | NZBC Group Number |
|---|---|---|---|---|---|---|---|---|---|
| A1 | A10 | 27.2 | 2.2 | 2111 | 5609 | 1286 | 14693 | 1832 | Group 3 |
| | A11 | 30.3 | 2.0 | 2148 | 5731 | 1323 | 14613 | 1905 | Group 3 |
| | A12 | 22.2 | 2.7 | 2029 | 5341 | 1204 | 15710 | 1847 | Group 3 |
| B1 | B10 | 51.2 | 1.2 | 2282 | 6167 | 1457 | 10776 | 1778 | Group 3 |
| | B11 | 31.5 | 1.9 | 2161 | 5771 | 1336 | 11852 | 1763 | Group 3 |
| | B12 | 37.9 | 1.6 | 2214 | 5945 | 1389 | 12403 | 1881 | Group 3 |
| B2 | B41 | 27.9 | 2.2 | 2120 | 5639 | 1295 | 12770 | 1773 | Group 3 |
| | B42 | 28.3 | 2.1 | 2125 | 5655 | 1300 | 13081 | 1795 | Group 3 |
| | B43 | 32.1 | 1.9 | 2167 | 5791 | 1342 | 13117 | 1832 | Group 3 |
| C1 | C10 | 25.2 | 2.4 | 2082 | 5514 | 1257 | 15356 | 1844 | Group 3 |
| | C11 | 25.7 | 2.3 | 2090 | 5539 | 1265 | 15873 | 1861 | Group 3 |
| | C12 | 29.1 | 2.1 | 2135 | 5687 | 1310 | 14888 | 1819 | Group 3 |
| D1 | D13 | 41.6 | 1.4 | 2237 | 6021 | 1412 | 12714 | 1729 | Group 3 |
| | D14 | 41.6 | 1.4 | 2237 | 6021 | 1412 | 13315 | 1747 | Group 3 |
| | D15 | 43.4 | 1.4 | 2247 | 6053 | 1422 | 12658 | 1749 | Group 3 |
| D2 | D41 | 35.1 | 1.7 | 2193 | 5877 | 1368 | 18083 | 2055 | Group 3 |
| | D42 | 35 | 1.7 | 2192 | 5874 | 1367 | 18420 | 2107 | Group 3 |
| | D43 | 34 | 1.8 | 2184 | 5847 | 1359 | 17970 | 2035 | Group 3 |
| D3 | D70 | 40.1 | 1.5 | 2228 | 5992 | 1403 | 18556 | 2124 | Group 3 |
| | D71 | 37.4 | 1.6 | 2210 | 5934 | 1385 | 17962 | 2048 | Group 3 |
| | D72 | 39.8 | 1.5 | 2226 | 5986 | 1401 | 18794 | 2087 | Group 3 |
| F1 | F10 | 35.5 | 1.7 | 2196 | 5887 | 1371 | 14510 | 1861 | Group 3 |
| | F11 | 25 | 2.4 | 2079 | 5504 | 1254 | 12986 | 1781 | Group 3 |
| | F12 | 30.8 | 1.9 | 2154 | 5748 | 1329 | 12662 | 1853 | Group 3 |
| F2 | F44 | 31.5 | 1.9 | 2161 | 5771 | 1336 | 14881 | 1946 | Group 3 |
| | F45 | 25.7 | 2.3 | 2090 | 5539 | 1265 | 13434 | 1786 | Group 3 |
| | F46 | 31.9 | 1.9 | 2165 | 5784 | 1340 | 12884 | 1821 | Group 3 |
| F3 | F70 | 28.4 | 2.1 | 2126 | 5659 | 1301 | 15829 | 1865 | Group 3 |
| | F71 | 32.3 | 1.9 | 2168 | 5797 | 1343 | 15691 | 1961 | Group 3 |
| | F72 | 30.6 | 2.0 | 2151 | 5741 | 1326 | 15948 | 1951 | Group 3 |
| F4 | F100 | 24.4 | 2.5 | 2069 | 5472 | 1244 | 13825 | 1801 | Group 3 |
| | F101 | 26.4 | 2.3 | 2100 | 5573 | 1275 | 14260 | 1827 | Group 3 |
| | F102 | 32.3 | 1.9 | 2168 | 5797 | 1343 | 15436 | 1923 | Group 3 |
| F5 | F130 | 29.4 | 2.0 | 2138 | 5698 | 1313 | 13777 | 1811 | Group 3 |
| | F131 | 28.2 | 2.1 | 2124 | 5651 | 1299 | 14284 | 1903 | Group 3 |
| | F132 | 23.6 | 2.5 | 2056 | 5427 | 1231 | 13872 | 1827 | Group 3 |
| F6 | F162 | 30.9 | 1.9 | 2155 | 5751 | 1330 | 14942 | 1932 | Group 3 |
| | F163 | 24.3 | 2.5 | 2068 | 5467 | 1243 | 14803 | 1784 | Group 3 |
| | F164 | 22.6 | 2.7 | 2037 | 5366 | 1212 | 14081 | 1812 | Group 3 |

# Appendix D: Example FDS input file

```
&HEAD CHID='MDF_1_9_05mm',TITLE='MDF_1_9_05mm'/

----------16 mesh----------------------------------------------------------------

&MESH ID='Mesh01', IJK=8,20,52, XB=-0.1,0.3,1.5,2.5,-0.1,2.5/     0.05m cell
&MESH ID='Mesh02', IJK=8,32,52, XB=-0.1,0.3,-0.1,1.5,-0.1,2.5/
&MESH ID='Mesh03', IJK=12,32,52, XB=0.3,0.9,-0.1,1.5,-0.1,2.5/
&MESH ID='Mesh04', IJK=12,20,52, XB=0.3,0.9,1.5,2.5,-0.1,2.5/
&MESH ID='Mesh05', IJK=6,52,52, XB=0.9,1.2,-0.1,2.5,-0.1,2.5/
&MESH ID='Mesh06', IJK=6,52,52, XB=1.2,1.5,-0.1,2.5,-0.1,2.5/
&MESH ID='Mesh07', IJK=6,52,52, XB=1.5,1.8,-0.1,2.5,-0.1,2.5/
&MESH ID='Mesh08', IJK=6,52,52, XB=1.8,2.1,-0.1,2.5,-0.1,2.5/
&MESH ID='Mesh09', IJK=6,52,52, XB=2.1,2.4,-0.1,2.5,-0.1,2.5/
&MESH ID='Mesh10', IJK=6,52,52, XB=2.4,2.7,-0.1,2.5,-0.1,2.5/
&MESH ID='Mesh11', IJK=6,52,52, XB=2.7,3.0,-0.1,2.5,-0.1,2.5/
&MESH ID='Mesh12', IJK=6,52,52, XB=3.0,3.3,-0.1,2.5,-0.1,2.5/
&MESH ID='Mesh13', IJK=4,52,52, XB=3.3,3.5,-0.1,2.5,-0.1,2.5/
&MESH ID='Mesh14', IJK=4,52,52, XB=3.5,3.7,-0.1,2.5,-0.1,2.5/     0.05m cell
&MESH ID='Mesh15', IJK=23,26,71, XB=3.7,6.0,-0.1,2.5,-0.1,7.0/    0.1m cell
&MESH ID='Mesh16', IJK=38,26,25, XB=-0.1,3.7,-0.1,2.5,2.5,5.0/    0.1m cell

&TIME TWFIN=1200.0 /                                  1200s simulation period
&DUMP DT_RESTART=300.0, DT_SL3D=0.25 /                save restart files every 300s
                                                      simulation time
----------TWO Reaction----------------------------------------------------------

&SPEC ID='NITROGEN',LUMPED_COMPONENT_ONLY = .TRUE. /
&SPEC ID='OXYGEN',LUMPED_COMPONENT_ONLY = .TRUE.   /
&SPEC ID='CARBON DIOXIDE',LUMPED_COMPONENT_ONLY = .TRUE.  /
&SPEC ID='WATER VAPOR'  /
&SPEC ID='SOOT',FORMULA='C', LUMPED_COMPONENT_ONLY = .TRUE. /

&SPEC ID = 'AIR',
SPEC_ID(1) = 'OXYGEN', VOLUME_FRACTION(1)=1,
SPEC_ID(2) = 'NITROGEN', VOLUME_FRACTION(2)=3.76,
BACKGROUND=.TRUE. /

&SPEC ID = 'PRODUCTS_1',
SPEC_ID(1) = 'CARBON DIOXIDE', VOLUME_FRACTION(1) = 3,
SPEC_ID(2) = 'WATER VAPOR', VOLUME_FRACTION(2) = 4,
SPEC_ID(3) = 'NITROGEN', VOLUME_FRACTION(3)=18.8/

&SPEC ID = 'PRODUCTS_2',
SPEC_ID(1) = 'CARBON DIOXIDE', VOLUME_FRACTION(1) = 3.2446,
SPEC_ID(2) = 'WATER VAPOR', VOLUME_FRACTION(2) = 3.1,
SPEC_ID(3) = 'SOOT', VOLUME_FRACTION(3)=0.1554,
SPEC_ID(4) = 'NITROGEN', VOLUME_FRACTION(4)=13.327696/

&SPEC ID='PROPANE' /
```

```
&SPEC ID='MDF', FORMULA = 'C3.4H6.2O2.5' /

&REAC FUEL='PROPANE', HEAT_OF_COMBUSTION=44715,
    SPEC_ID_NU='PROPANE','AIR','PRODUCTS_1'
    NU=-1,-5,1/

&REAC FUEL='MDF', HEAT_OF_COMBUSTION=12000,
    SPEC_ID_NU='MDF','AIR','PRODUCTS_2'
    NU=-1,-3.5446,1 /

&SURF ID='BURNER',
     COLOR='RED',
          SPEC_ID='PROPANE',
          MASS_FLUX(1)=0.23215,
          RAMP_MF(1)='fire_ramp' /

&RAMP ID='fire_ramp', T=0.0, F=0.0/
&RAMP ID='fire_ramp', T=1.0, F=0.333/
&RAMP ID='fire_ramp', T=600.0, F=0.333/
&RAMP ID='fire_ramp', T=601.0, F=1.0/
&RAMP ID='fire_ramp', T=1199.0, F=1.0/
&RAMP ID='fire_ramp', T=1200.0, F=0.0/

&OBST ID='Combustion source', XB=0.0,0.17,2.23,2.4,0.0,0.145,
SURF_IDS='BURNER','INERT','INERT'/
&OBST ID='Wall-Front', XB=0.0,3.6,-0.02,0.0,0.0,2.42,
SURF_ID6='INERT','INERT','INERT','MDF1','INERT','INERT'/
&OBST ID='Wall-Rear', XB=0.0,3.6,2.4,2.42,0.0,2.42,
SURF_ID6='INERT','INERT','MDF1','INERT','INERT','INERT'/
&OBST ID='Wall-Right', XB=3.6,3.62,-0.02,2.42,0.0,2.42, SURF_ID='INERT'/
&OBST ID='Wall-Left', XB=-0.02,0.0,-0.02,2.42,0.0,2.42,
SURF_ID6='INERT','MDF1','INERT','INERT','INERT','INERT'/
&OBST ID='Ceiling', XB=0.0,3.6,0.0,2.4,2.4,2.42,
SURF_ID6='INERT','INERT','INERT','INERT','MDF1','INERT'/
&OBST ID='Floor', XB=-0.02,3.62,-0.02,2.42,-0.02,0.0, SURF_ID='concrete'/

&HOLE ID='Door', XB=3.58,3.64,0.8,1.6,0.0,2.0/

&VENT ID='Mesh Vent: Mesh01 [XMIN]', SURF_ID='OPEN', XB=-0.1,-0.1,1.5,2.5,-
0.1,2.5, COLOR='INVISIBLE'/
&VENT ID='Mesh Vent: Mesh01 [YMAX]', SURF_ID='OPEN', XB=-0.1,0.3,2.5,2.5,-
0.1,2.5, COLOR='INVISIBLE'/
&VENT ID='Mesh Vent: Mesh01 [ZMIN]', SURF_ID='OPEN', XB=-0.1,0.3,1.5,2.5,-0.1,-
0.1, COLOR='INVISIBLE'/
&VENT ID='Mesh Vent: Mesh02 [XMIN]', SURF_ID='OPEN', XB=-0.1,-0.1,-0.1,1.5,-
0.1,2.5, COLOR='INVISIBLE'/
&VENT ID='Mesh Vent: Mesh02 [YMIN]', SURF_ID='OPEN', XB=-0.1,0.3,-0.1,-0.1,-
0.1,2.5, COLOR='INVISIBLE'/
&VENT ID='Mesh Vent: Mesh02 [ZMIN]', SURF_ID='OPEN', XB=-0.1,0.3,-0.1,1.5,-0.1,-
0.1, COLOR='INVISIBLE'/
```

&VENT ID='Mesh Vent: Mesh03 [YMIN]', SURF_ID='OPEN', XB=0.3,0.9,-0.1,-0.1,-0.1,2.5, COLOR='INVISIBLE'/
&VENT ID='Mesh Vent: Mesh03 [ZMIN]', SURF_ID='OPEN', XB=0.3,0.9,-0.1,1.5,-0.1,-0.1, COLOR='INVISIBLE'/
&VENT ID='Mesh Vent: Mesh04 [YMAX]', SURF_ID='OPEN', XB=0.3,0.9,2.5,2.5,-0.1,2.5, COLOR='INVISIBLE'/
&VENT ID='Mesh Vent: Mesh04 [ZMIN]', SURF_ID='OPEN', XB=0.3,0.9,1.5,2.5,-0.1,-0.1, COLOR='INVISIBLE'/
&VENT ID='Mesh Vent: Mesh05 [YMAX]', SURF_ID='OPEN', XB=0.9,1.2,2.5,2.5,-0.1,2.5, COLOR='INVISIBLE'/
&VENT ID='Mesh Vent: Mesh05 [YMIN]', SURF_ID='OPEN', XB=0.9,1.2,-0.1,-0.1,-0.1,2.5, COLOR='INVISIBLE'/
&VENT ID='Mesh Vent: Mesh05 [ZMIN]', SURF_ID='OPEN', XB=0.9,1.2,-0.1,2.5,-0.1,-0.1, COLOR='INVISIBLE'/
&VENT ID='Mesh Vent: Mesh06 [YMAX]', SURF_ID='OPEN', XB=1.2,1.5,2.5,2.5,-0.1,2.5, COLOR='INVISIBLE'/
&VENT ID='Mesh Vent: Mesh06 [YMIN]', SURF_ID='OPEN', XB=1.2,1.5,-0.1,-0.1,-0.1,2.5, COLOR='INVISIBLE'/
&VENT ID='Mesh Vent: Mesh06 [ZMIN]', SURF_ID='OPEN', XB=1.2,1.5,-0.1,2.5,-0.1,-0.1, COLOR='INVISIBLE'/
&VENT ID='Mesh Vent: Mesh07 [YMAX]', SURF_ID='OPEN', XB=1.5,1.8,2.5,2.5,-0.1,2.5, COLOR='INVISIBLE'/
&VENT ID='Mesh Vent: Mesh07 [YMIN]', SURF_ID='OPEN', XB=1.5,1.8,-0.1,-0.1,-0.1,2.5, COLOR='INVISIBLE'/
&VENT ID='Mesh Vent: Mesh07 [ZMIN]', SURF_ID='OPEN', XB=1.5,1.8,-0.1,2.5,-0.1,-0.1, COLOR='INVISIBLE'/
&VENT ID='Mesh Vent: Mesh08 [YMAX]', SURF_ID='OPEN', XB=1.8,2.1,2.5,2.5,-0.1,2.5, COLOR='INVISIBLE'/
&VENT ID='Mesh Vent: Mesh08 [YMIN]', SURF_ID='OPEN', XB=1.8,2.1,-0.1,-0.1,-0.1,2.5, COLOR='INVISIBLE'/
&VENT ID='Mesh Vent: Mesh08 [ZMIN]', SURF_ID='OPEN', XB=1.8,2.1,-0.1,2.5,-0.1,-0.1, COLOR='INVISIBLE'/
&VENT ID='Mesh Vent: Mesh09 [YMAX]', SURF_ID='OPEN', XB=2.1,2.4,2.5,2.5,-0.1,2.5, COLOR='INVISIBLE'/
&VENT ID='Mesh Vent: Mesh09 [YMIN]', SURF_ID='OPEN', XB=2.1,2.4,-0.1,-0.1,-0.1,2.5, COLOR='INVISIBLE'/
&VENT ID='Mesh Vent: Mesh09 [ZMIN]', SURF_ID='OPEN', XB=2.1,2.4,-0.1,2.5,-0.1,-0.1, COLOR='INVISIBLE'/
&VENT ID='Mesh Vent: Mesh10 [YMAX]', SURF_ID='OPEN', XB=2.4,2.7,2.5,2.5,-0.1,2.5, COLOR='INVISIBLE'/
&VENT ID='Mesh Vent: Mesh10 [YMIN]', SURF_ID='OPEN', XB=2.4,2.7,-0.1,-0.1,-0.1,2.5, COLOR='INVISIBLE'/
&VENT ID='Mesh Vent: Mesh10 [ZMIN]', SURF_ID='OPEN', XB=2.4,2.7,-0.1,2.5,-0.1,-0.1, COLOR='INVISIBLE'/
&VENT ID='Mesh Vent: Mesh11 [YMAX]', SURF_ID='OPEN', XB=2.7,3.0,2.5,2.5,-0.1,2.5, COLOR='INVISIBLE'/
&VENT ID='Mesh Vent: Mesh11 [YMIN]', SURF_ID='OPEN', XB=2.7,3.0,-0.1,-0.1,-0.1,2.5, COLOR='INVISIBLE'/
&VENT ID='Mesh Vent: Mesh11 [ZMIN]', SURF_ID='OPEN', XB=2.7,3.0,-0.1,2.5,-0.1,-0.1, COLOR='INVISIBLE'/
&VENT ID='Mesh Vent: Mesh12 [YMAX]', SURF_ID='OPEN', XB=3.0,3.3,2.5,2.5,-0.1,2.5, COLOR='INVISIBLE'/

```
&VENT ID='Mesh Vent: Mesh12 [YMIN]', SURF_ID='OPEN', XB=3.0,3.3,-0.1,-0.1,-0.1,2.5, COLOR='INVISIBLE'/
&VENT ID='Mesh Vent: Mesh12 [ZMIN]', SURF_ID='OPEN', XB=3.0,3.3,-0.1,2.5,-0.1,-0.1, COLOR='INVISIBLE'/
&VENT ID='Mesh Vent: Mesh13 [YMAX]', SURF_ID='OPEN', XB=3.3,3.5,2.5,2.5,-0.1,2.5, COLOR='INVISIBLE'/
&VENT ID='Mesh Vent: Mesh13 [YMIN]', SURF_ID='OPEN', XB=3.3,3.5,-0.1,-0.1,-0.1,2.5, COLOR='INVISIBLE'/
&VENT ID='Mesh Vent: Mesh13 [ZMIN]', SURF_ID='OPEN', XB=3.3,3.5,-0.1,2.5,-0.1,-0.1, COLOR='INVISIBLE'/
&VENT ID='Mesh Vent: Mesh14 [YMAX]', SURF_ID='OPEN', XB=3.5,3.7,2.5,2.5,-0.1,2.5, COLOR='INVISIBLE'/
&VENT ID='Mesh Vent: Mesh14 [YMIN]', SURF_ID='OPEN', XB=3.5,3.7,-0.1,-0.1,-0.1,2.5, COLOR='INVISIBLE'/
&VENT ID='Mesh Vent: Mesh14 [ZMIN]', SURF_ID='OPEN', XB=3.5,3.7,-0.1,2.5,-0.1,-0.1, COLOR='INVISIBLE'/
&VENT ID='Mesh Vent: Mesh15 [XMAX]', SURF_ID='OPEN', XB=6.0,6.0,-0.1,2.5,-0.1,7.0, COLOR='INVISIBLE'/
&VENT ID='Mesh Vent: Mesh15 [XMIN]', SURF_ID='OPEN', XB=3.7,3.7,-0.1,2.5,5.0,7.0, COLOR='INVISIBLE'/
&VENT ID='Mesh Vent: Mesh15 [YMAX]', SURF_ID='OPEN', XB=3.7,6.0,2.5,2.5,-0.1,7.0, COLOR='INVISIBLE'/
&VENT ID='Mesh Vent: Mesh15 [YMIN]', SURF_ID='OPEN', XB=3.7,6.0,-0.1,-0.1,-0.1,7.0, COLOR='INVISIBLE'/
&VENT ID='Mesh Vent: Mesh15 [ZMAX]', SURF_ID='OPEN', XB=3.7,6.0,-0.1,2.5,7.0,7.0, COLOR='INVISIBLE'/
&VENT ID='Mesh Vent: Mesh15 [ZMIN]', SURF_ID='OPEN', XB=3.7,6.0,-0.1,2.5,-0.1,-0.1, COLOR='INVISIBLE'/
&VENT ID='Mesh Vent: Mesh16 [XMIN]', SURF_ID='OPEN', XB=-0.1,-0.1,-0.1,2.5,2.5,5.0, COLOR='INVISIBLE'/
&VENT ID='Mesh Vent: Mesh16 [YMAX]', SURF_ID='OPEN', XB=-0.1,3.7,2.5,2.5,2.5,5.0, COLOR='INVISIBLE'/
&VENT ID='Mesh Vent: Mesh16 [YMIN]', SURF_ID='OPEN', XB=-0.1,3.7,-0.1,-0.1,2.5,5.0, COLOR='INVISIBLE'/
&VENT ID='Mesh Vent: Mesh16 [ZMAX]', SURF_ID='OPEN', XB=-0.1,3.7,-0.1,2.5,5.0,5.0, COLOR='INVISIBLE'/

&MATL ID='CONCRETE',
      FYI='NBSIR 88-3752 - ATF NIST Multi-Floor Validation',
      SPECIFIC_HEAT=1.04,
      CONDUCTIVITY=1.8,
      DENSITY=2280.0/

&SURF ID='concrete',
      RGB=146,202,166,
      BACKING='VOID',
      MATL_ID(1,1)='CONCRETE',
      MATL_MASS_FRACTION(1,1)=1.0,
      THICKNESS(1)=0.02/

----------MDF PANEL----------------------------------------------------------------
```

```
&MATL ID = 'PF resin'
      SPECIFIC_HEAT_RAMP          = 'c_wood'
      CONDUCTIVITY_RAMP           = 'k_wood'
      DENSITY                     = 730
      N_REACTIONS                 = 1
      NU_MATL                     = 0.2
      NU_SPEC                     = 0.80
      SPEC_ID                     ='MDF'
      A                           = 544577633073245
      E                           = 149272.53
      N_S                         = 3.50E+00
      MATL_ID                     ='CHAR'
      HEAT_OF_REACTION            = 1100.0
      HEAT_OF_COMBUSTION          = 12000.0 /

&MATL ID = 'Hemicellulose'
      SPECIFIC_HEAT_RAMP          = 'c_wood'
      CONDUCTIVITY_RAMP           = 'k_wood'
      DENSITY                     = 730
      N_REACTIONS                 = 1
      NU_MATL                     = 0.2
      NU_SPEC                     = 0.80
      SPEC_ID                     ='MDF'
      A                           = 6.08E11
      E                           = 151640.88
      N_S                         = 2.07
      MATL_ID                     ='CHAR'
      HEAT_OF_REACTION            = 0.0
      HEAT_OF_COMBUSTION          = 12000.0 /

&MATL ID = 'Cellulose'
      SPECIFIC_HEAT_RAMP          = 'c_wood'
      CONDUCTIVITY_RAMP           = 'k_wood'
      DENSITY                     = 730
      N_REACTIONS                 = 1
      NU_MATL                     = 0.2
      NU_SPEC                     = 0.80
      SPEC_ID                     ='MDF'
      A                           = 48262676179898.5
      E                           = 189531.68
      N_S                         = 1.0
      MATL_ID                     ='CHAR'
      HEAT_OF_REACTION            = 150.0
      HEAT_OF_COMBUSTION          = 12000.0 /    115, 2.5

&MATL ID = 'Lignin'
      SPECIFIC_HEAT_RAMP          = 'c_wood'
      CONDUCTIVITY_RAMP           = 'k_wood'
      DENSITY                     = 730
      N_REACTIONS                 = 1
      NU_MATL                     = 0.2
      NU_SPEC                     = 0.80
```

```
      SPEC_ID                    ='MDF'
      A                          = 69115300406244.7
      E                          = 199971.84
      N_S                        = 6.1
      MATL_ID                    ='CHAR'
      HEAT_OF_REACTION           = 0.0
      HEAT_OF_COMBUSTION         = 12000.0 /

&MATL ID = 'WATER'
      EMISSIVITY                 = 0.8
      DENSITY              = 730.
      CONDUCTIVITY               = 0.58
      SPECIFIC_HEAT              = 4.19
      N_REACTIONS                = 1
      A                                = 9.5712677e+22
      E                          = 135663.11
      N_S                        = 3.3119154
      NU_SPEC                    = 1
      SPEC_ID                    = 'WATER VAPOR'
      HEAT_OF_REACTION           = 2410./

&MATL ID = 'CHAR'
EMISSIVITY                       = 1.0
ABSORPTION_COEFFICIENT  = 1
DENSITY                          = 150.
CONDUCTIVITY_RAMP                = 'k_char'
SPECIFIC_HEAT_RAMP               = 'c_char'/ Char properties

&RAMP ID='k_wood', T= 20., F=0.103498 / 0.103498
&RAMP ID='k_wood', T= 100., F=0.111198 / 0.111198
&RAMP ID='k_wood', T= 200., F=0.122198 / 0.122198
&RAMP ID='k_wood', T= 500., F=0.155198 / 0.155198
&RAMP ID='k_wood', T= 700., F=0.177198 / 0.177198
&RAMP ID='k_wood', T= 900., F=0.199198 / 0.199198

&RAMP ID='c_wood', T= 20., F=1.130 /
&RAMP ID='c_wood', T=900., F=3.330 /

&RAMP ID='c_char', T= 20., F=0.6306338 /
&RAMP ID='c_char', T= 100., F=0.9065698 /
&RAMP ID='c_char', T= 200., F=1.1830898 /
&RAMP ID='c_char', T= 500., F=1.5566498 /
&RAMP ID='c_char', T= 700., F=1.4256898 /
&RAMP ID='c_char', T= 900., F=0.9907298 /

&RAMP ID='k_char', T= 20., F=0.09 /0.09 0.054
&RAMP ID='k_char', T= 100., F=0.1404 /0.1404 0.08424
&RAMP ID='k_char', T= 200., F=0.2034 /0.2034 0.12204
&RAMP ID='k_char', T= 500., F=0.3924 /0.3924 0.23544
&RAMP ID='k_char', T= 700., F=0.5184 /0.5184 0.31104
&RAMP ID='k_char', T= 900., F=0.6444 /0.6444 0.38664
```

```
&SURF ID            = 'MDF1'
MATL_ID(1,1:5) =  'PF resin','Hemicellulose','Cellulose','Lignin','WATER'
     MATL_MASS_FRACTION(1,1:5)                                                    =
0.070698082,0.245062297,0.283486641,0.142413099,0.022937942
MATL_ID(2,1:5) =  'PF resin','Hemicellulose','Cellulose','Lignin','WATER'
     MATL_MASS_FRACTION(2,1:5)                                                    =
0.075691034,0.262369476,0.303507486,0.152470824,0.024557902
MATL_ID(3,1:5) =  'PF resin','Hemicellulose','Cellulose','Lignin','WATER'
     MATL_MASS_FRACTION(3,1:5)                                                    =
0.08079938,0.280076644,0.323991035,0.162760994,0.026215301
MATL_ID(4,1:5) =  'PF resin','Hemicellulose','Cellulose','Lignin','WATER'
     MATL_MASS_FRACTION(4,1:5)                                                    =
0.085919214,0.297823638,0.344520654,0.173074307,0.027876427
MATL_ID(5,1:5) =  'PF resin','Hemicellulose','Cellulose','Lignin','WATER'
     MATL_MASS_FRACTION(5,1:5)                                                    =
0.090915082,0.315140925,0.364553191,0.183137906,0.029497333
MATL_ID(6,1:5) =  'PF resin','Hemicellulose','Cellulose','Lignin','WATER'
     MATL_MASS_FRACTION(6,1:5)                                                    =
0.095626603,0.33147257,0.383445543,0.192628718,0.031025982
MATL_ID(7,1:5) =  'PF resin','Hemicellulose','Cellulose','Lignin','WATER'
     MATL_MASS_FRACTION(7,1:5)                                                    =
0.095626603,0.33147257,0.383445543,0.192628718,0.031025982
MATL_ID(8,1:5) =  'PF resin','Hemicellulose','Cellulose','Lignin','WATER'
     MATL_MASS_FRACTION(8,1:5)                                                    =
0.090915082,0.315140925,0.364553191,0.183137906,0.029497333
MATL_ID(9,1:5) =  'PF resin','Hemicellulose','Cellulose','Lignin','WATER'
     MATL_MASS_FRACTION(9,1:5)                                                    =
0.085919214,0.297823638,0.344520654,0.173074307,0.027876427
MATL_ID(10,1:5) =  'PF resin','Hemicellulose','Cellulose','Lignin','WATER'
     MATL_MASS_FRACTION(10,1:5)                                                   =
0.08079938,0.280076644,0.323991035,0.162760994,0.026215301
MATL_ID(11,1:5) =  'PF resin','Hemicellulose','Cellulose','Lignin','WATER'
     MATL_MASS_FRACTION(11,1:5)                                                   =
0.075691034,0.262369476,0.303507486,0.152470824,0.024557902
MATL_ID(12,1:5) =  'PF resin','Hemicellulose','Cellulose','Lignin','WATER'
     MATL_MASS_FRACTION(12,1:5)                                                   =
0.070698082,0.245062297,0.283486641,0.142413099,0.022937942

     RGB           = 165,42,42
     BACKING       ='EXPOSED'
     STRETCH_FACTOR=1
     CELL_SIZE_FACTOR=0.5
     THICKNESS(1)     = 0.000750
     THICKNESS(2)     = 0.000750
     THICKNESS(3)     = 0.000750
     THICKNESS(4)     = 0.000750
     THICKNESS(5)     = 0.000750
     THICKNESS(6)     = 0.000750
     THICKNESS(7)     = 0.000750
     THICKNESS(8)     = 0.000750
     THICKNESS(9)     = 0.000750
     THICKNESS(10)     = 0.000750
```

```
      THICKNESS(11)     = 0.000750
      THICKNESS(12)     = 0.000750

 /                9mm    solid MDF properties

&DEVC ID='01', QUANTITY='THERMOCOUPLE', XYZ=3.58,0.4,0.26/
&DEVC ID='02', QUANTITY='THERMOCOUPLE', XYZ=3.58,0.4,0.67/
&DEVC ID='03', QUANTITY='THERMOCOUPLE', XYZ=3.58,0.4,0.97/
&DEVC ID='04', QUANTITY='THERMOCOUPLE', XYZ=3.58,0.4,1.27/
&DEVC ID='05', QUANTITY='THERMOCOUPLE', XYZ=3.58,0.4,1.42/
&DEVC ID='06', QUANTITY='THERMOCOUPLE', XYZ=3.58,0.4,1.57/
&DEVC ID='07', QUANTITY='THERMOCOUPLE', XYZ=3.58,0.4,1.72/
&DEVC ID='08', QUANTITY='THERMOCOUPLE', XYZ=3.58,0.4,1.91/
&DEVC ID='09', QUANTITY='THERMOCOUPLE', XYZ=3.58,0.4,2.10/

&BNDF QUANTITY='WALL TEMPERATURE' /
&BNDF QUANTITY='INCIDENT HEAT FLUX' /

&TAIL /
```

# Appendix E: Example B-RISK input file

```
<?xml version="1.0" encoding="utf-8"?>
<!--Created by B-RISK Version 2020.02-->
<!--Input File B-RISK DESIGN FIRE TOOL 2020.02 - RISK SIMULATOR MODE (+ DEVELOPER
MODE ENABLED)-->
<simulation>
  <general_settings>
    <version>2020.02</version>
    <user_mode>False</user_mode>
    <evacnz>False</evacnz>
    <file_type>montecarlo</file_type>
    <description />
    <number_iterations>1</number_iterations>
    <output_interval>5</output_interval>
    <vent_clearance>0</vent_clearance>
    <grid_size>0.1</grid_size>
    <dfg_fixitem1>False</dfg_fixitem1>
    <dfg_windspeed>0</dfg_windspeed>
    <dfg_winddir>0</dfg_winddir>
    <base_name>basemodel_1_9</base_name>
    <spr_num_prob
      sprnum1="1"
      sprnum²="0"
      sprnum3="0"
      sprnum4="0" />
    <simulation_duration>300</simulation_duration>
    <display_interval>10</display_interval>
    <ceiling_nodes>20</ceiling_nodes>
    <wall_nodes>20</wall_nodes>
    <floor_nodes>20</floor_nodes>
    <enhance_burning>False</enhance_burning>
    <job_number />
    <excel_interval>3</excel_interval>
    <time_step>1</time_step>
    <error_control>0.1</error_control>
    <error_control_ventflows>0.001</error_control_ventflows>
    <fire_dbase>fire.mdb</fire_dbase>
    <mat_dbase>thermal.mdb</mat_dbase>
    <ceiling_jet>0</ceiling_jet>
    <vent_logfile>True</vent_logfile>
    <LE_Solver>LU Decomposition</LE_Solver>
    <no_wall_flow>True</no_wall_flow>
    <sprink_mode>0</sprink_mode>
    <auto_populate>False</auto_populate>
    <calc_sprdist>False</calc_sprdist>
    <calc_sddist>False</calc_sddist>
    <ignite_secitems>False</ignite_secitems>
    <firstitem>1</firstitem>
    <storage_height>1</storage_height>
    <powerlaw_T2fire>True</powerlaw_T2fire>
    <powerlaw_designfire>False</powerlaw_designfire>
    <compartment_effects>False</compartment_effects>
    <autosavepdf>False</autosavepdf>
    <autosaveXL>True</autosaveXL>
  </general_settings>
```

```
<rooms
 number_rooms="1"
 fire_room="1">
 <room
  id="1"
  ceilingslope="False">
  <width>2.4</width>
  <length>3.6</length>
  <max_height>2.4</max_height>
  <description>ISO 9705</description>
  <min_height>2.4</min_height>
  <floor_elevation>0</floor_elevation>
  <abs_X>0</abs_X>
  <abs_Y>0</abs_Y>
  <two_zones>True</two_zones>
  <wall_lining>
   <description>MDF 9mm</description>
   <thickness>9</thickness>
   <conductivity>0.12</conductivity>
   <specific_heat>2580</specific_heat>
   <density>728</density>
   <emissivity>0.88</emissivity>
   <cone_file>D1_MDF.txt</cone_file>
   <min_temp_spread>440</min_temp_spread>
   <flame_spread_parameter>13</flame_spread_parameter>
   <eff_heat_of_combustion>12.5</eff_heat_of_combustion>
   <soot_yield>0.015</soot_yield>
   <CO2_yield>1.09</CO2_yield>
   <H20_yield>0.442</H20_yield>
   <HCN_yield>0</HCN_yield>
  </wall_lining>
  <wall_substrate
   present="False" />
  <ceiling_lining>
   <description>MDF 9mm</description>
   <thickness>9</thickness>
   <conductivity>0.12</conductivity>
   <specific_heat>2580</specific_heat>
   <density>728</density>
   <emissivity>0.88</emissivity>
   <ceiling_cone_file>D1_MDF.txt</ceiling_cone_file>
   <eff_heat_of_combustion>12.5</eff_heat_of_combustion>
   <soot_yield>0.015</soot_yield>
   <CO2_yield>1.09</CO2_yield>
   <H20_yield>0.442</H20_yield>
   <HCN_yield>0</HCN_yield>
  </ceiling_lining>
  <ceiling_substrate
   present="False" />
  <floor_lining>
   <description>concrete</description>
   <thickness>100</thickness>
   <conductivity>1.2</conductivity>
   <specific_heat>880</specific_heat>
   <density>2300</density>
   <emissivity>0.5</emissivity>
   <floor_cone_file>null.txt</floor_cone_file>
```

```
      <min_temp_spread>0</min_temp_spread>
      <flame_spread_parameter>0</flame_spread_parameter>
      <eff_heat_of_combustion>0</eff_heat_of_combustion>
      <soot_yield>0</soot_yield>
      <CO2_yield>0</CO2_yield>
      <H20_yield>0</H20_yield>
      <HCN_yield>0</HCN_yield>
    </floor_lining>
    <floor_substrate
     present="False" />
  </room>
</rooms>
<flamespread
 algorithm="2">
 <suppress_ceiling_hrr>False</suppress_ceiling_hrr>
 <flame_area_constant>0.0065</flame_area_constant>
 <flame_length_power>1</flame_length_power>
 <burner_width>0.3</burner_width>
 <wall_heat_flux>45</wall_heat_flux>
 <ceiling_heat_flux>35</ceiling_heat_flux>
 <ignite_next_room>False</ignite_next_room>
 <one_cone_curve>False</one_cone_curve>
 <ign_correlation>0</ign_correlation>
 <pessimise_comb_wall>True</pessimise_comb_wall>
 <wall_percent>100</wall_percent>
 <ceiling_percent>100</ceiling_percent>
 <HFS_limit>0</HFS_limit>
 <VFS_limit>0</VFS_limit>
</flamespread>
<tenability>
 <FEDCO_toxicity_model>True</FEDCO_toxicity_model>
 <monitor_height>2</monitor_height>
 <activity_level>Light</activity_level>
 <endpoint_radiation>0.3</endpoint_radiation>
 <endpoint_temp>873</endpoint_temp>
 <endpoint_visibility>10</endpoint_visibility>
 <endpoint_FED>0.3</endpoint_FED>
 <endpoint_convect>626</endpoint_convect>
 <illumination>False</illumination>
 <FEDpath_1_starttime>0</FEDpath_1_starttime>
 <FEDpath_1_endtime>600</FEDpath_1_endtime>
 <FEDpath_1_room>1</FEDpath_1_room>
 <FEDpath_2_starttime>0</FEDpath_2_starttime>
 <FEDpath_2_endtime>0</FEDpath_2_endtime>
 <FEDpath_2_room>0</FEDpath_2_room>
 <FEDpath_3_starttime>0</FEDpath_3_starttime>
 <FEDpath_3_endtime>0</FEDpath_3_endtime>
 <FEDpath_3_room>0</FEDpath_3_room>
</tenability>
<postflashover
 post="False"
 fluxcriteria="False"
 calcFRR="False"
 modGER="False">
 <fuel_thickness>0.05</fuel_thickness>
 <stick_spacing>0.05</stick_spacing>
 <crib_height>0.8</crib_height>
```

```
    <excess_fuel_factor>1.3</excess_fuel_factor>
    <CLT_model>False</CLT_model>
    <CLT_ceil_percent>100</CLT_ceil_percent>
    <CLT_wall_percent>100</CLT_wall_percent>
    <CLT_chartemp>300</CLT_chartemp>
    <integral_model>False</integral_model>
    <Lamella_depth>20</Lamella_depth>
    <CLT_Qcrit>0</CLT_Qcrit>
    <CLT_flameflux>0</CLT_flameflux>
    <CLT_latentheatofgasification>0</CLT_latentheatofgasification>
    <CLT_ignitiontemp>0</CLT_ignitiontemp>
    <CLT_calibration>0</CLT_calibration>
    <CLT_debondtemp>2000</CLT_debondtemp>
    <kinetic_model>False</kinetic_model>
    <kinetic_hemi_Ei>164000</kinetic_hemi_Ei>
    <kinetic_hemi_Ai>32500000000000</kinetic_hemi_Ai>
    <kinetic_hemi_ni>2.1</kinetic_hemi_ni>
    <kinetic_hemi_mf>0.37</kinetic_hemi_mf>
    <kinetic_cell_Ei>198000</kinetic_cell_Ei>
    <kinetic_cell_Ai>351000000000000</kinetic_cell_Ai>
    <kinetic_cell_ni>1.1</kinetic_cell_ni>
    <kinetic_cell_mf>0.44</kinetic_cell_mf>
    <kinetic_lig_Ei>152000</kinetic_lig_Ei>
    <kinetic_lig_Ai>84100000000000</kinetic_lig_Ai>
    <kinetic_lig_ni>5</kinetic_lig_ni>
    <kinetic_lig_mf>0.09</kinetic_lig_mf>
    <kinetic_wat_Ei>100000</kinetic_wat_Ei>
    <kinetic_wat_Ai>10000000000000</kinetic_wat_Ai>
    <kinetic_wat_ni>1</kinetic_wat_ni>
    <kinetic_wat_mf>0.1</kinetic_wat_mf>
    <kinetic_cell_charyield>0.13</kinetic_cell_charyield>
    <kinetic_hemi_charyield>0.13</kinetic_hemi_charyield>
    <kinetic_lig_charyield>0.13</kinetic_lig_charyield>
    <CLT_moisturecontent>0.1</CLT_moisturecontent>
    <thermal_props>1</thermal_props>
  </postflashover>
  <chemistry>
    <nC>0.95</nC>
    <nH>2.4</nH>
    <nO>1</nO>
    <nN>0</nN>
    <fueltype>wood</fueltype>
    <hcn_calc>False</hcn_calc>
    <soot_alpha>2.5</soot_alpha>
    <soot_epsilon>1.2</soot_epsilon>
    <emission_coefficient>0.8</emission_coefficient>
    <stoichiometric_air_fuel_ratio>6.1</stoichiometric_air_fuel_ratio>
    <post_CO>0.4</post_CO>
    <post_soot>0.14</post_soot>
    <CO_mode>False</CO_mode>
    <soot_mode>False</soot_mode>
  </chemistry>
  <fires />
</simulation>
```